Effects of climate change on the immune defenses and disease susceptibility of amphibian hosts

by

Veronica Saenz Calderon

B.S., Pontificia Universidad Católica del Ecuador, 2011

Master's degree, Tulane University, 2015

Submitted to the Graduate Faculty of

the Dietrich School of Arts and Sciences in partial fulfillment

of the requirements for the degree of

Doctor of Philosophy

University of Pittsburgh

2021

UNIVERSITY OF PITTSBURGH

DIETRICH SCHOOL OF ARTS AND SCIENCES

This dissertation was presented

by

Veronica Saenz Calderon

It was defended on

June 15, 2021

and approved by

Anne Carlson, Assistant Professor, Department of Biological Sciences

Jon P Boyle, Associate Professor, Department of Biological Sciences

Kevin Kohl, Assistant Professor, Department of Biological Sciences

Louise Rollins-Smith, Associate Professor, Department of Biological Sciences, Vanderbilt University

Dissertation advisor: Corinne Richards-Zawacki, Professor, Department of Biological Sciences

Effects of climate change on the immune defenses and disease susceptibility of amphibian hosts

Veronica Saenz Calderon, Ph.D.

University of Pittsburgh, 2021

Effects of climate change on immunity could affect wildlife disease risk. Climate change is predicted to alter conditions in ephemeral ponds, which many amphibians threatened by the disease chytridiomycosis require for larval development. Environmental stressors like early pond drying and elevated temperature are known to accelerate larval development and metamorphosis in some amphibians, allowing them to escape harsh aquatic conditions faster. However, little is known about how these stressors may impact the development of immune defenses. In this dissertation, I investigated how pond drying and an increase in pond temperature impact the development of immune defenses and susceptibility to *Batrachochytrium dendrobatidis* (*Bd*), the fungus that causes chytridiomycosis, in North American leopard frogs. To better understand the dynamics and spread of *Bd,* I also conducted a field study comparing infection among amphibian communities that breed in permanent versus ephemeral ponds. Exposure to pond drying and elevated temperatures resulted in froglets that were smaller at metamorphosis. Both stressors also had direct and indirect carry-over effects on the post-metamorphic immune system. Frogs that developed under different drying and temperature treatments differed in many immune parameters. The innate and adaptive immune systems tended to respond differently, suggesting that both branches should be considered when evaluating the potential impacts of climate change. Upon exposure to *Bd,* pathogen load did not differ among frogs from different climate

treatments. However, mortality was greater in frogs that developed in faster drying and higher temperature treatments. This suggests that climate stressors experienced during early development can impact how tolerant hosts are to infection later in life. In my field study, I found a large amount of genetic variation in the *Bd* sampled from amphibian hosts. *Bd* prevalence and load were lower on hosts from ephemeral ponds than permanent ponds early in the breeding season. Interestingly, some ephemeral pond breeders emerged from terrestrial hibernation sites infected with *Bd,* suggesting that transmission from permanent ponds is not required to bring *Bd* to ephemeral ponds each year. My findings in this amphibian disease system suggest that impacts on immunity may be an important yet overlooked consequence of global climate change.

Table of contents

List of tables

List of figures

Preface

First and foremost, I would like to thank my advisor and mentor, Dr. Cori Richards-Zawacki, for taking me into her lab two times. Thank you for your continuous support of my Ph.D., for your patience, motivation, and all your knowledge. Your guidance helped me during my research and writing of this thesis. I would also like to thank you for your friendship during these eight years. You have not only made me a better scientist, but also made me a kinder and more open human being.

To my committee members, Dr. Anne Carlson, Dr. Jon Boyle, Dr Kevin Kohl and Dr Louise Rollins Smith, thank you for the guidance and advice during all the years of my dissertation. To Dr. Michel Ohmer, thank you for guiding me in R, for always answering the hard questions patiently, and for all the collaboration in the three chapters of my dissertation. Also, thank you for your great friendship.

To Dr. Tali Hammond, thank you for teaching me R and for all your friendship and fun moments in the field and lab.

To Dr. Laura Brannelly and Dr. Karie Altman, thank you for all the help in the field and for the collaboration in the SERDP project.

To my field and lab assistants, thank you for all the late hours in the field and for taking care of all the tadpoles inside the chambers.

To all the collaborators in the SERDP project, thank you for helping me in the immune assays and analyzing the data that was outside my knowledge in the project.

Thank you to my advisor, the University of Pittsburgh, SERDP, the Pymatuning Lab of Ecology, and Senescyt for funding my research.

To Chris Davis, Jessica Barabas and Nick Mihailoff, thank you for all the help during my long stay over four summers at PLE.

To all the current and previous members of the RZ lab, thank you for your support and friendship.

To my parents, thank you for always supporting my choice of research and for helping me by calling me online every day.

To my fiancé, thank you for supporting me in the long-distance relationship and for calling me every day.

1.0 Effects of hydroperiod on the immune defenses and *Bd* susceptibly of northern leopard frog

The part up until the Bd infection experiment occurred has already been published in Brannelly, L. A., Ohmer, M. E., Saenz, V., & Richards-Zawacki, C. L. (2019). Effects of hydroperiod on growth, development, survival and immune defences in a temperate amphibian. Functional Ecology, 33(10), 1952-1961

1.1 Introduction

Climate change is predicted to alter air and water temperatures, precipitation, and humidity (Easterling *et al.* 2000). The global mean air temperature is projected to increase by 0.3°C to 0.7°C between 2016 and 2035 (IPCC 2014). In general, precipitation is predicted to decrease in the middle latitudes and subtropical dry regions (IPCC 2014). With these predicted changes will come increased rates of evapotranspiration (water lost to the atmosphere from land surfaces and via transpiration from plants), meaning that human activities like agriculture will require increasing volumes of freshwater to maintain the same area of cultivated land (Peterson and Keller 1990). This, coupled with increased rates of evaporation, suggests that dramatic changes are in store for North American freshwater ecosystems. More streams may become ephemeral or remain dry for longer periods (Schindler *et al.* 1996), and water availability in ponds is predicted to decrease as well (Peterson and Keller 1990, Wilk and Hughes 2002). Organisms that depend on these small bodies of freshwater to complete their life cycles will be

negatively impacted by these changes (Deutsch *et al.* 2008, IPCC 2014). In addition to its direct negative effects, climate change may impact the susceptibility of animals to disease outbreaks. The potential for this sort of interaction, however, remains poorly understood.

Climate change is likely to influence the dynamics of many infectious disease systems. The consistent and expected pattern of seasonal outbreaks exhibited by many exclusively human pathogens provides a clear example of how climate can impact host-pathogen systems. Influenza and *Pneumococcus* infections are most prevalent in winter, measles cases usually peak in the spring, and risk of contracting polio is greatest in the Summer (Dowell 2001). Explanations for these phenomena have been attributed to three interrelated seasonal drivers: (1) pathogen appearance and disappearance, (2) environmental changes, and (3) host behavior changes (Dowell 2001). For aquatic vertebrates, the same factors may drive seasonal patterns of infectious disease. Many parasites, viruses and bacteria that infect these hosts are known to have an optimal temperature for growth and reproduction (McArthur 2006). Changes in precipitation can also modify the balance between hosts and their parasites, leading to outbreaks (Adlard *et al.* 2015).

Climate change has the potential to push hosts and/or pathogens outside of their optimal thermal conditions. One way that organisms can rapidly adapt to such changes is through phenotypic plasticity. Phenotypic plasticity is the ability of an organism to produce different phenotypes in response to stimuli or inputs from the environment (Pigliucci *et al.* 2006). Changes in developmental timing (*e.g.*, a shorter generation time; Altizer *et al.* 2013) are a common form of phenotypic plasticity that hosts and pathogens exhibit in response to climate stressors. For example, warmer temperatures generally accelerate development (but they can also

reduce life span; Harvell *et al.* 2002). The problem for hosts is that their pathogens may adapt more quickly than they do (Raffel *et al.* 2013).

While studies aimed at understanding the impact of climate change on disease risk remain few, several illustrate why this is an important topic. For example, elevated water temperatures increase the virulence of the pathogen *Vibrio coralliilyticus* (Burge *et al.* 2014) and also reduce the fitness of its coral host, *Pocillopora damicornis*, such that the coral is not able to effectively resist infection (Ben-Haim *et al.* 2003). This host-pathogen interaction provides a useful case study of increased virulence in the face of warming ocean temperatures driven by anthropogenic climate change. Effects of climate change have also been documented in freshwater and terrestrial host-pathogen systems. For example, in birds, there is evidence that disease and climate change may be interacting to affect species distributions. The avian malaria parasite (*Plasmodium relictum*), which was introduced into Hawaii, caused marked declines in endemic forest birds. Malaria's impact is most intense in mid-elevation forests where conditions that support the mosquito that vectors this disease and endemic birds have the greatest overlap (Liao *et al.* 2017). Malaria currently poses the least risk to birds at high elevations where mosquito populations and disease transmission are limited by cool temperatures. Models predict that with climate change, the mosquito vector will expand its range upward in elevation reducing or eliminating the high elevation refuge some endemic bird species depend on for their survival (Liao *et al.* 2017). And finally, in Pacific chorus frogs (*Pseudacris regilla*), infection with a pathogenic trematode parasite (*Ribeiroia ondatrae*) appears to hinder the tadpole's ability to speed metamorphosis and escape a drying pond. Tadpoles experiencing accelerated pond drying were twice as likely to metamorphose early if they were not infected with the parasite (Koprivnikar *et al.* 2014).

Amphibians are an ideal taxon for studies that aim to understand the potential impact of climate change on disease dynamics in freshwater ecosystems. Many amphibians require aquatic habitats to reproduce and complete larval development. They are also a group known to exhibit plasticity in developmental timing in response to conditions in the aquatic environment. This type of plasticity has been documented in at least 20 species representing 12 amphibian genera (Ruthsatz *et al.* 2018). For example, accelerated metamorphosis has been documented in wood frog (*Rana sylvatica)* and Western spadefoot toad (*Scaphiopus hammondii*) tadpoles exposed to simulated pond drying. In both species, larvae that develop under simulated drying not only have shorter larval periods but are also smaller in size at metamorphosis than animals from control (non-drying) treatments (Denver *et al.* 1998, Gervasi and Foufopoulos 2008). Tradeoffs like these, between growth and development, have been observed in many amphibian species (Edge *et al.* 2016, Tejedo *et al.* 2010). Faster development is clearly beneficial for larvae seeking to escape from desiccation (or predation, or competition) that might occur before they are equipped to survive on land. However, beginning the next life stage a smaller size may represent an important fitness tradeoff.

It is well-established that the environment that is experienced early in life can affect the expression of traits in later life stages and different habitats (O'Connor *et al.* 2014, Moore and Martin 2019). Little is known about how the developmental plasticity an animal exhibits in response to climate early on may affect its ability to withstand threats later in life. Given the threat that diseases pose to wildlife, one of the ways we can assess the effects of developing under stressful conditions is by measuring immune function. A good example of such a study comes from tree swallows (*Tachycineta bicolor*). Nestlings that were incubated as eggs in experimentally cooled nests had lower body mass and reduced constitutive innate immunity, as

reflected in a reduced ability of B-cells to kill a strain of *E. coli* (Ardia *et al.* 2010). Only a few studies have examined the effects of accelerated development on amphibian immune function, and these suggest that individuals with accelerated development in response to a stressor tend to invest less in costly immune defenses, and hence be more prone to infections (Gervasi & Foufopoulos 2008, Johnson *et al.* 2012, Brannelly *et al.* 2019). For example, juvenile wood frogs that were exposed to simulated pond drying as larvae have weaker cellular immune responses to the T-cell mitogen phytohemagglutinin (PHA) and lower leukocyte numbers in the blood than animals that developed under non-drying conditions (Gervasi and Foufopoulos 2008). How common this sort of trade-off between development and immune function is, and its potential impact on disease dynamics, remains poorly understood.

Infectious disease threatens amphibian diversity. In particular, chytridiomycosis, the disease caused by the chytrid fungus *Batrachochytrium dendrobatidis* (*Bd*), has been linked to amphibian declines worldwide (Berger *et al.* 1998; Scheele *et al.* 2019). The effects of *Bd* on its hosts differs among species and populations (Schloegel *et al.* 2006). For example, some species like *Rana catesbeiana* (American bullfrog) and *Xenopus laevis* (African clawed frog) appear to tolerate infection well. They carry and spread *Bd* rarely suffer mortality when infected or even develop clinical signs of chytridiomycosis (Daszak *et al.* 2004). In other amphibians infected with *Bd*, the intensity of infection (i.e., pathogen load) can increase exponentially, causing a breakdown in proper cutaneous functioning that leads to mortality (Voyles *et al.* 2009). There is evidence that *Bd* evades some amphibian immune defenses. For example, it has been shown that *Bd* can inhibit the proliferation, and induce apoptosis of, amphibian lymphocytes, limiting the potential for an adaptive immune response (Fites *et al.* 2013). However, there is evidence for adaptation of amphibian hosts to this pathogen as well. For example, some species that

experienced *Bd*-associated population declines during an epizootic were found, decades later, to be surviving and even rebounding despite the continued presence and virulence of the *Bd* pathogen (Knapp *et al.* 2016, Voyles *et al.* 2018). Evidence suggests that adaptations in innate immune defenses of amphibian hosts are playing a role in this recovery (Voyles *et al.* 2018). Elements of the adaptive and innate immune responses, as well as cutaneous microbial communities, appear to contribute to the amphibian response to *Bd* (reviewed in Rollins-Smith and Woodhams 2012). Cutaneous antimicrobial peptides (AMPs) are an essential component of an amphibian's innate immunity to *Bd* (Rollins-Smith 2009). AMPs are natural cationic amphipathic helical peptides that are secreted by granular glands at the surface of the skin (Rollins-Smith 2009). Amphibian AMPs are active against Gram positive and Gram negative bacteria, fungi, protozoa, and viruses (Narayana and Chen 2015). Members of four families of AMPs (ranatuerin, temporin, brevinin and esculetin) have been shown to inhibit *Bd* growth *in vitro* (Rollins-Smith *et al.* 2006, Rollins-Smith and Conlon 2005, Rollins-Smith 2009). Besides AMPs, other components of the mucosal layer on the amphibian skin also appear to kill *Bd*. Collectively, the AMPs and other defenses found in skin mucus have been termed the mucosome (Woodhams *et al.* 2014). The mucosome contains secondary metabolites, AMPs, lysozymes, mucosal antibodies, and alkaloids (Woodhams *et al.* 2014). In one study, in which four host species were raised from field collected eggs in outdoor mesocosms through metamorphosis then exposed to *Bd*, a greater capacity of the mucosome to inhibit *Bd* growth was found to be correlated with a lower *Bd* load (Woodhams *et al.* 2014). An amphibian's skin also harbors symbiotic resident microbes which constitute a line of defense that is not directly host-produced but interacts with the innate immune system (Harris *et al.* 2009). Amphibians also have a complex adaptive immunity, with similar immune cell types and functions (including

lymphocytes, neutrophils, monocytes, basophils, and eosinophils) to mammals (Hadji-Azimi *et al.* 1987). The extent of the adaptive immune system's involvement in defense against *Bd* remains unclear, though Ramsey *et al.* (2010) found that some frogs (*Xenopus laevis*) possess antibodies that bind to *Bd* and inhibit infection. Clearly, amphibians have a suite of potential defenses against *Bd* that could be contributing to the endemic coexistence of these hosts with the *Bd* pathogen.

In general, low temperatures favor *Bd* over its amphibian hosts because *Bd* is cold-tolerant (growing from ~4 – 25 °C; Woodhams *et al.* 2008, Voyles *et al.* 2012), and amphibian immune defenses are often sluggish at low temperatures (Robak *et al.* 2019). In nature, declines due to *Bd* have been largely limited to areas with at least seasonally cool climates, including temperate and mid- to high-elevation areas of the tropics (Berger *et al.* 2004, Kriger *et al.* 2007). Given this, an increase in mean environmental temperatures, as is predicted with global climate change, may be favorable to amphibians, decreasing the likelihood of *Bd* outbreaks and declines (Stevenson *et al.* 2013). However, an increase in temperature variability, as is also predicted under global climate change, could impair amphibian defenses and increase the risk of *Bd* epidemics, the pathophysiology of *Bd*, or both (Rohr and Raffel 2010, Raffel *et al.* 2011, Raffel *et al.* 2013). The mechanisms linking climate variation to the occurrence and severity of chytridiomycosis outbreaks remain unclear. Recently metamorphosed frogs are usually more vulnerable than older frogs to chytridiomycosis, in part because their immune systems are often immature (Rachowicz & Vredenburg, 2004). More rapid development in nutrient limited conditions, as may occur more frequently in a warmer and less predictable climate, may result in metamorphs with underdeveloped AMP repertoires (Holden *et al.* 2015) and fewer lymphocytes (Rollins-Smith, 1988). Additional studies are needed to understand how plasticity in

developmental timing, in response to climate change affects immune development. Here, I examine specifically how the climate change stressor of pond drying, alone, and in combination with *Bd* exposure, affect the development and the immune system of one North American amphibian host, the Northern leopard frog (*Rana pipiens*).

Rana pipiens has a broad distribution in Eastern North America and relies on flooded grasslands and permanent ponds to breed (Noland and Ultsh 1981). In northwest Pennsylvania, where my study was conducted, *R. pipiens* had the highest springtime *Bd* load of any amphibian species surveyed (Richards-Zawacki, *unpublished data*). The aim of this study was to determine whether developing in a stressful larval environment impacts the availability of key immune defenses against *Bd* post-metamorphosis. My focal climate stressor was hydroperiod, the length of time an ephemeral wetland holds water (Babbitt, 2005), as this is predicted to decrease with climate change. I hypothesized that if Northern leopard frogs exhibit developmental plasticity, those that develop in fast-drying ponds will have shorter larval periods, will be smaller at metamorphosis, and will have higher mortality than frogs that develop in slower-drying and non-drying ponds. I also hypothesized that frogs that develop under drying conditions would exhibit carry over effects that increase their susceptibility to *Bd* infections and chytridiomycosis. Specifically, I predicted that *Bd* infection would have the greatest negative impacts on survival and body condition in frogs that developed as larvae under drying conditions. I also predicted that both *Bd* exposure and development under drying conditions would lead to decreases in the immune function of juvenile frogs.

To test these predictions, I conducted a mesocosm experiment in which I allowed *R. pipiens* to develop as larvae under three drying treatments (fast, moderate, and no drying). I first tested for direct effects of pond drying on development up to and right after metamorphosis.

Then, beginning when the frogs were five weeks post-metamorphosis, I conducted a 12- week *Bd* exposure experiment during which I measured *Bd* load, probability of infection, and survival among frogs from the three larval drying treatments. This allowed me to test for direct effects of pond drying on susceptibility to *Bd*. However, I also tested for indirect effects of post-metamorphic growth rate and mass on the outcomes of *Bd* exposure. After the exposure experiment, I compared the total number of antimicrobial peptides (AMPs), their diversity, and the ability of mucosome to inhibit *Bd* growth among frogs from the three drying and two exposure (*Bd* and sham) treatments. These results of this study will help us better understand the effects of drying, an important climate change stressor for freshwater species, on immune function before and after exposure to a pathogen.

1.2 Methods

1.2.1 Egg collection

In early April 2016, I collected four *Rana pipiens* egg masses from wetlands near Linesville, PA for study at the Donald S. Wood Field Lab at the Pymatuning Lab of Ecology's (PLE) in Crawford County, PA. I reared each egg mass in a separate green plastic kiddie pool (89 cm x 89 cm x 15 cm) containing 150 L aged well water until embryos reached the free-swimming stage (stage 25 of Gosner 1960, 18-20 days from egg mass collection). I used DNA sequencing to verify that the collected egg masses were from *R. pipiens* (as opposed to *R. sylvatica*, which often breeds concurrently and has similar-looking egg masses). To do this, I sacrificed one egg per clutch, placing it in 95% ethanol at -20ºC prior to DNA extraction. I

extracted genomic DNA from each egg using the Qiagen DNeasy Blood and Tissue kit following the protocol for animal tissue extraction and amplified a portion of the 16s rDNA gene using 16Spip-L forward and 16Saa reverse primers (Hillis and Wilcox 2005) and reaction condidtions described in Brannelly *et al.* (2019). The PCR products were then Sanger sequenced and a BLAST search in Genbank (Benson *et al.* 2013) was used to confirm that the sequences from our eggs were a match for *R. pipiens*.

1.2.2 Mesocosm set up

The experiment took place in twenty-one 770 L cattle tanks (1.6 m diameter, 0.6 m height), which I cleaned with 13% bleach, rinsed twice, and left outside to dry for five days prior to use. I added 600 L (a 41 cm depth) of well water, 200 g of dry leaf litter, and 15 g of rabbit chow to each cattle tank to provide the initial food and substrate for periphyton growth and covered the tanks with black 50% shade cloth (Turner and Chislock, 2007). Six days after adding the leaf litter and rabbit chow, I added 0.5 L of water collected from a local pond to provide a source of algae and zooplankton. Before seeding the mesocosms I tested our pond water samples for *Bd* using an environmental DNA protocol (Lacoursière-Roussel *et al.* 2016). I filtered 1 liter of water and extracted genomic DNA from the filter following the "animal tissue" protocol and the Qiagen DNeasy Blood and Tissue Kit. I used a quantitative polymerase chain reaction (qPCR) assay (Boyle *et al.* 2004) to ensure that no *Bd* DNA was detected in the filtered sample. One day after adding the pond water, and when the larvae were free swimming (Gosner stage 25, Gosner 1960), I added 40 *R. pipiens* tadpoles (10 from each of the four egg masses) to each cattle tank. I added 5 g of rabbit chow to each cattle tank 75 days after the tadpoles were added to ensure they had sufficient food.

1.2.3 Experimental design

Our experiment included three treatments: fast, medium, and no drying (control) regimes, each with seven replicates (840 total tadpoles). To simulate drying, I removed water from mesocosms in our fast and medium drying treatments. In the control treatment, mesocosm water levels were allowed to fluctuate naturally in response to local precipitation and evaporation. I removed 43.6 L (3 cm) of water from fast-drying mesocosms and 29.1 L (2 cm) of water from our medium-drying mesocosms every five days (Figure 1.1) using dedicated 10L buckets, each fit with a screen mesh top to prevent the accidental removal tadpoles and large organic material.

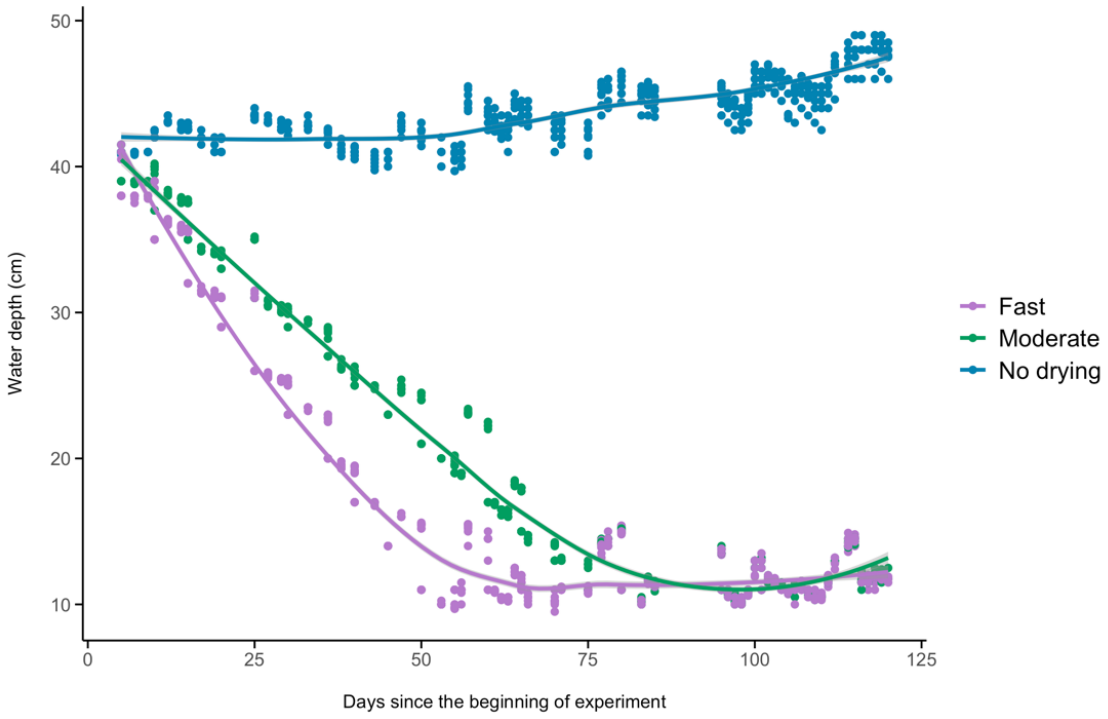

Figure 1.1 Water height in the mesocosms over the course of the experiment.
Each point represents the average of the seven mesocosms in that treatment on a specific day, the lines represent lines of smoothed lines of best fit to the average water depth per treatment.

Water in no-drying (control) mesocosms was disturbed using a bucket on the same day as the other mesocosms but no water was taken from it unless the level was higher than 50 cm. In this case, I removed water until the depth reached 50 cm. This resulted in drying to 10 cm depth (150 L) by 50 and 75 days after the start of the experiment in the fast- and medium-drying mesocosms, respectively. After this point, water was added to or removed from fast- and medium-drying mesocosms every five days to maintain a 10 cm depth. I chose these drying regimes based on the knowledge that *Rana pipiens* takes from 60 – 90 days to develop from a free-swimming tadpole through metamorphosis (Kendell, 2002).

I checked the mesocosms daily and removed individuals when their forelimbs emerged (Gosner stage 42), placing them individually into 2.12 L Ziploc plastic containers with 1.5 cm of filtered well water. I tilted one end of these containers to allow the froglets access to a dry habitat and provided each with an inverted plastic cup with a hole cut in one side, which was used as a hide. Water was changed twice per week and animals were fed crickets two or three times a week (5-10 crickets per frog per feeding). Following completion of metamorphosis (Gosner stage 46), I measured the frogs (mass and snout-vent length, hereafter SVL) using a 0.01 g scale and a dial caliper. I assigned them to immune assay treatments (details below) using a randomized block design, to make sure I had similar animal numbers for each experimental condition.

1.2.4 *Bd* exposure

I exposed a subset (N = 120) of the newly metamorphosed *R. pipiens* from our mesocosms (N = 40 fast-drying, N = 41 medium-drying, N = 39 no-drying treatment) to zoospores of *Bd* every two weeks for 12 weeks (Table 1.1). To prepare the inocula, I used a

culture of the "Rio Maria" isolate of *Bd*, isolated from a *Pristimantis cruentus* frog from Panama by Jamie Voyles in 2012, which had been passaged 14 times prior to this experiment. I used two-week-old liquid TGhL broth (16 g tryptone, 4 g gelatin hydrolysate, 2 g lactose, 1000 ml distilled water; Longcore *et al.* 1999; Boyle *et al.* 2003) cultures to grow *Bd* on agar plates. The inverted plates grew for one week before I flooded them with DI water to collect zoospores for inoculation. Frogs were exposed to *Bd* for the first time ~ 5-6 weeks after metamorphosis. I exposed them to differing quantities of *Bd* zoospores ranging from 500,000-5,000,000 per inoculation (Table 1.1). For the first one and last three inoculations the frogs were exposed to *Bd* by individual baths in 60 ml containers containing 5 ml of a zoospore solution in DI for eight hours. For the second and third inoculations the frogs were again inoculated using 5 ml of DI water containing *Bd* zoospores, but these times the inoculum was put directly on each frog's skin and was allowed to run off its back and into its enclosure (a 2.12 L Ziplock container which contained 400 ml of water) before the animal was returned to this enclosure. The enclosures were cleaned two days after each exposure. Another subset of frogs (N = 40 fast-drying, N = 41 medium-drying, N = 38 no-drying treatment) of the same age were sham-exposed and served as a control group. I exposed these control frogs following the protocol and schedule described above but made our sham inoculum by flooding blank (no *Bd*) agar plates with of DI water.

Table 1.1 Inoculation procedure by week for the Bd-exposure experiment

Week	Zoospores	Volume of inoculum (ml)	Inoculation method
2	500,000	5	cup
4	5,000,000	400	tank
6	5,000,000	400	tank
8	250,000	5	cup
10	250,000	5	cup
12	250,000	5	cup

I swabbed, measured, and weighed the frogs seven days after each inoculation using a 0.01 g scale and a dial caliper. I checked the frogs daily for clinical signs of chytridiomycosis (Berger *et al.* 1999) and I measured mass, snout-vent length and infection intensity every two weeks. To estimate infection intensity, I swabbed each frog five times on each of the dorsal surface, ventral surface, each side of the body and each limb, making sure to rotate the swab while taking the samples. DNA was extracted from each swab using the "animal tissue" protocol and the Qiagen Dneasy Extraction Kit with a final elution volume of 200 µl. I then ran a qPCR assay (Boyle *et al.* 2004) using a QuantStudio™ 3 Real Time PCR system. I used 25 µl reactions containing 12.5 µl of 2x SensiFast probe Lo-Rox Mix, PCR primers at a concentration of 900 nM, the MGB probe at 240 nM, 400 ng/µl BSA, 3 µl water per well and 5 µl of template DNA (diluted 1:10 in DI water). The negative controls had the same master mix but with water added instead of a DNA template. The default QuantStudio amplification (V.1.4) software conditions (2 min at 50°C and 10 min at 95°C, followed by 50 cycles of 15 s at 95°C and 1 min at 60°C) were used to amplify a portion of the ITS-3 and 5.8S rDNA genes (Boyle *et al.* 2004; Hyatt *et al.*

2007). Each swab sample was run once and each qPCR run contained a positive and negative control, and a series of plasmid dilution standards (Pisces Molecular, CO).

1.2.5 Mucosome collection

I collected skin mucus from a subset of *Bd*-exposed and sham-exposed frogs from each drying treatment after the *Bd* exposure experiment to test for differences in the ability of the "mucosome" (Woodhams *et al.* 2014), which includes secondary metabolites, AMPs, lysozymes, mucosal antibodies, and alkaloids, to inhibit *Bd* growth *in vitro*. To collect the mucosome, each frog was rinsed in 10 ml of molecular grade water for one hour in a 50 ml conical tube. The frog was then returned to its enclosure and the rinse water was immediately passed through a 0.22 μm filter to remove live bacterial cells. The filtered samples were then stored at -20 °C prior to growth challenge assays (described below). The mucosome collection occurred after 14 weeks of exposure (or sham exposure) to *Bd* zoospores, when the frogs were 19 – 20 weeks post-metamorphosis. I collected mucus from sham-exposed frogs from fast- (N = 8), medium- (N = 10), and no-drying treatments (N = 7), and *Bd*-exposed frogs from fast- (N = 7), medium- (N = 9), and no-drying (N = 9) treatments.

1.2.6 Collection of peptides secreted onto the skin

One hour after sampling their mucosomes, I collected skin secretions from the same subset of *Bd*-exposed and sham-exposed frogs as described above in order to compare the AMPs they produced. I collected the secretions using a modification of the protocol outlined in Rollins-Smith *et al.* (2002). I began by weighing each frog and then giving an injection (in the dorsal-

plicae) of norepinephrine (40 nmol/g body weight in 0.01 ml/g body weight), a hormone that stimulates the secretion of skin peptides (Ramsey *et al.* 2010). After injection, I placed frogs individually in 50 ml conical tubes containing 15 ml high performance liquid chromatography (HPLC) grade water for 15 minutes to collect secretions. After returning the frogs to their enclosures, I acidified the water in the 50 ml conicals with HCl (Sigma) to a final concentration of 1 % HCl to inactivate endogenous peptidases that might also have been secreted. These peptide samples were stored at -20°C and shipped frozen to Vanderbilt University for enrichment and mass-spectrometry.

At Vanderbilt University, my collaborators in the Rollins-Smith lab activated the C18 Sep Pak cartridges (Waters Corp, Milford, MA) with 10 ml of 100% HPLC grade methanol then washed them with 10 ml of Buffer A (0.1% triflouroacetic acid in HPLC grade water). Next, they passed the thawed skin secretion samples over the activated Sep Pak cartridges then washed the Sep Paks again with Buffer A. They then eluted the Sep Paks in 11 ml of Buffer B (0.1% triflouroacetic acid, 70% acetonitrile, 29.9% HPLC water). One ml of the eluted material was removed to quantify total peptides in the skin secretion (see below) and the remaining volume (10 ml) they then spun under vacuum until dry in preparation for mass spectrometry (see below).

1.2.7 Quantification of total peptides

Peptides were quantified, by my collaborators in the Rollins-Smith lab at Vanderbilt University, in a 1 ml sample of skin secretion using a Micro BCA™ Protein Assay Kit (Pierce Biotechnology, Rockford, IL). The protocol for this followed Rollins-Smith *et al.* (2002) but used bradykinin instead of BCA (bovine serum albumin) as a standard as it is more similar in size to the peptides I was hoping to detect. A standard curve was run at the following bradykinin

concentrations: 200 μg/ml, 40 μg/ml, 20 μg/ml, 10 μg/ml, 5 μg/ml, 2.5 μg/ml, 1.0 μg/ml, 0.5 μg/ml. Using a 96 well microtiter plate, they added 100 μl of the peptide or standard sample to 100 μg of the working reagent. All standards and samples were run in triplicate. The working reagent is supplied with the kit and was diluted according to the manufacturer's instructions. The plate was incubated at 37 °C for 2 hours. They then measured absorbance at 570 nm on a Biotek Elx808 spectrophotometer using Gen5 2.01 software for analysis.

1.2.8 Mass spectrometry

Peptides were examined by mass spectrometry by my collaborators in the Rollins-Smith lab at Vanderbilt University. They first resuspended the dried peptide samples to a concentration of 1 mg/ml in HPLC water then spotted them onto a Matrix Assisted Laser Desorption/Ionization (MALDI) plate at a 1:1 ratio with matrix [10 mg/ml α-cyano-4-hydroxycinnamic acid (Sigma, St. Louis, MO), 60% acetonitrile, 39.6% HPLC-grade water, and 0.4% trifluoroacetic acid (v/v/v)]. An Ultraflex III time-of-flight mass spectrometer (Bruker Daltonics, Billerica, MA) was used and calibrated using the following standards (Sigma, St. Louis, MO): bradykinin fragment 1-7 (m/z 757.3997), human angiotensin II (m/z 1046.5423), $P_{14}R$ synthetic peptide (m/z 1533.8582), adrenocorticotropic hormone fragment 18-39 (m/z 2464.1989), and bovine oxidized insulin chain B (m/z 3494.6513). For each standard and peptide sample, 250 laser shots were collected (following Woodhams *et al.* 2006). They analyzed the spectra with Data Explorer v4.4 software (Applied Biosystems, Foster City, CA). The nineteen most common AMPs in *R. pipiens* skin secretions have been previously described (Tennessen *et al.* 2009). I used the Tennessen *et al.* (2009) peptide list and their reported peptide centroid masses to determine the presence/absence and relative intensities of these common AMPs in our samples. I created a data

matrix that listed the relative intensity for each peptide detected. I used zeros to denote non-detection of peptides and removed rows/columns with (a) individual (frog) samples for which no or only one peptide was detected and (b) peptides that were only detected in one frog. I did this because rows or columns with only one non-zero cell are uninformative for the multivariate analyses I used.

1.2.9 *Bd* growth assays

To test for differences in the abilities of the skin secretions of frogs from our drying and *Bd*-exposure treatments to inhibit the growth of *Bd*, I used *in vitro* growth (for AMP enriched samples, following Bell *et al.* 2013) and viability (for whole mucosome samples, (Woodhams *et al.* 2014) assays. To begin each assay, I harvested *Bd* zoospores by filtering the *Bd* grown in TGhL broth through a cone shaped filter funnel (8 mL, 10 μm pore size, Chemrus Inc.). This removes the larger sporangia but allows the smaller zoospores to pass through. I then diluted the filtered broth solution to our desired concentration and added a standard volume of this zoospore solution to wells of a 96 well optical plate (Costar, 3799). Skin secretion samples (either whole mucosome or AMP enriched) were then added to these wells in triplicate, as described below. Each plate contained samples from all treatment groups and samples were randomly ordered in 96 well plates. Each plate also contained replicated positive (containing no skin secretion sample) and negative (containing heat-killed *Bd*: a *Bd* zoospore solution heated to 60 – 80 ºC for 10 – 30 min) control wells. Plates were incubated at 21 °C and growth or viability of *Bd* was compared among wells using a plate reader.

To assess the inhibition of *Bd* growth by AMPs, I quantified the concentration of a five-day old culture of *Bd* isolate "Rio Maria" (passage 22) using a hemocytometer and diluted a

sample to a concentration of 555,555 zoospores/ml. I put 90 µl of this zoospore solution into each sample well for a starting concentration of ~50,000 zoospores/well. I diluted the concentration of our peptide samples (originally at 1 mg/ml in HPLC water) to 0.5 mg/ml using HPLC water and added 10 µl of each diluted sample to three replicate wells containing 90 µl of the zoospore solution to reach a final volume of 100 µl and peptide concentration of 50 µg/ml. Each plate contained three positive control and four negative control wells. The positive control wells contained 90 µl of *Bd* solution + 10 µl of HPLC water. The negative control wells contained 90 µl of heat killed *Bd* plus 10 µl of HPLC water. The perimeter wells of the plate were designated as blanks and contained 10 µl HPLC water and 90 µl of broth. The optical density of each well at 490 nm was measured immediately after the plate set-up was complete (day 0) and at day 3, 5 and 7 using an Epoch™ Biotek spectrophotometer. For each sampling day, I first calculated the mean of the daily absorbance values for all replicates of each type of control and experimental sample. Then, to remove baseline absorbance, I subtracted the mean negative control value on each day from each of the mean sample and positive control values on that day, to obtain corrected absorbance values. Optical density (OD) readings were transformed using equation: ln(OD/(1-OD)) (Becker *et al*. 2015). A linear regression was then used to estimate the growth rate of *Bd* in the presence of each peptide sample, using only the linear part of the growth curve. To calculate *Bd* inhibition, an average slope was calculated for each set of triplicate samples. I then divided this by the average growth rate of the positive control and subtracted from 1 to yield positive values representing proportional growth above that of the positive control and negative values that represent proportional growth inhibition.

To assess the effect of whole mucosome on zoospore viability I used an assay that quantifies cell proliferation by ATP detection. To begin, I lyophilized each mucosome sample

until completely dry and resuspended it in 1 ml of sterile molecular grade water. I quantified the concentration of a 4-day old culture of *Bd* isolate "Rio Maria" (passage 32) using a hemocytometer and diluted a sample to a concentration of 10^6 zoospores/ml. Each sample was run in triplicate wells containing *Bd* plus media and in duplicate wells containing sterile media to facilitate background correction (due the potential for ATP presence in water and media). For each sample, 25 µl of *Bd* solution (or sterile medium) and 25 µl of the mucosome sample were added to each well. Each plate contained 6 positive control wells (25 µl of *Bd* solution + 25 µl of sterile MilliQ water) and 6 negative control wells (25 µl of heat killed *Bd* + 25 µl of sterile MilliQ water). Triplicate nutrient background wells (to account for ATP in the water and media) were also included on each plate by adding 25 µl of media and 25 µl of sterile MilliQ water to each well. After setup was complete, I incubated each plate for 1 hour at 21 ºC, then in a dark room, I added 50 µl of Cell Titer Glo Reagent (Promega) to each well to make a 1:1 solution and covered the plate with a foil sealing film. I placed the plates on a shaker for 3 minutes at 200 rpm and then removed the plates and incubated them at 21 ºC for 15 min to lyse the cells and release ATP. Plates were then read using a luminescent channel of a POLARstar Omega microplate reader. To calculate percent zoospore viability, I first subtracted the average media control (media + MilliQ) luminescent reading value from each positive and negative control, and from each of the triplicate samples. I then averaged the background luminescent reading (containing media + mucosome) for each sample and subtracted this value from each sample replicate that contained mucosome and *Bd*. I averaged the replicates for the negative control wells, and subtracted this value from each of the other wells (mucosome and positive controls) to remove the ATP value of dead *Bd*. Finally, I averaged the resulting values for the positive control replicates and divided the background-corrected sample well values by the average positive

control value to get a proportional cell viability. These proportional cell viability values were then averaged for each sample prior to statistical analysis.

1.2.10 Statistical analysis

All statistical analyses were performed using R Studio 2017 (RStudio Team 2017) and R version 1.1.383 (R Core Team 2017). Additional details for analyses of tadpole metamorphosis time, survival and size at metamorphosis are described in Brannelly *et al.* (2019). Tables describing the statistical models and their outputs can be found in Appendix A (Tables A1-A19).

Larval period – To compare larval period, here defined as the time between when tadpoles were placed in mesocosms and when tail absorption (Gosner stage 46) occurred, across drying treatments I used a linear mixed-effects model (LMM) with larval period as the dependent variable, drying treatment as the fixed effect and mesocosm as the random effect (package: 'nlme', function: 'lme': Pinheiro *et al.* 2017).

Survival – In order to compare whether survival to metamorphosis differed between drying treatments, I concatenated two numbers per mesocosm; 1) the number of animals that successfully completed metamorphosis and 2) the number of animals remaining as tadpoles in each mesocosm on day 120. I compared survival across drying treatments using a generalized linear mixed model (GLME) with a binomial error structure (package: 'lme4', function: 'glmer'). I also tested for differences in survival from metamorphosis until day 42 post-metamorphosis, when animals began entering immune assay treatments. To do this, I used the Cox proportional hazards model (package: 'survival', function: 'coxph'), with drying treatment, body size (SVL, mm) and their interaction as factors, clustered by mesocosm.

Size at metamorphosis – In order to compare size at metamorphosis between drying treatments, I compared SVL and mass (log-transformed) at metamorphosis across the three drying treatments using a linear mixed model (LMM) with drying treatment and larval period as interactive fixed effects and mesocosm as a random effect.

Infection and disease indicators- To examine the relationship between growth rate and infection probability, I calculated growth in mass (g/day) using mass before each exposure minus mass previous to each exposure divided by the age in days at the second time point. I centered or scaled days post exposure, mass at metamorphosis and growth in mass by using (package: 'stats', function: 'scale'). I then ran a generalized linear mixed model (package: 'lme4', function: 'glmer') with binomial distribution. The response variable was infection probability, the interaction between drying treatment and days post exposure was the independent variable, the covariates were mass at metamorphosis and growth in mass, and the random effect was frog ID. To measure infection load, quantified as the log number of zoospores detected on each swab, I ran a linear mixed model (package: 'lme4', function: 'lmer') (LMM) with infection load as the dependent variable and drying treatment was the independent variable. The covariates used were mass at metamorphosis and growth in mass. I also included the interaction between treatment and days post exposure, and the random effect was frog ID. To compare survival between naïve and exposed frogs after exposure I used a Cox proportional hazards model (package: 'survival', function: 'coxph'), in exposed and naïve frogs. I included mesocosm as a cluster effect and the time-dependent covariate developmental time in the model, which was time transformed using the tt function (package: coxph). To compare survival between all combinations of drying treatments and exposure group, I used the same cox regression but included an interaction term (Drying treatment * Exposure group). To compare scaled mass index (a measure of body

condition) among temperature treatments I used the R package "23mart", following Peig and Green (2009). The Peig and Green (2009) method accounts for the covariation between body size and body mass by calculating a score that standardizes body mass at a fixed value of a linear body measurement based on the scaling relationship between mass and length (Kelly *et al.* 2014). I used the animal's mass just before the first exposure as a reference for the slope. I ran a linear mixed effect model (package nlme, lme function). Log-transformed SMI was the dependent variable and the three-way interaction between drying treatment, *Bd* exposure group, and days post exposure were the independent variables. The random effects were mesocosm and frog ID. I tested for differences in mass and SVL across groups using the same linear mixed effect model structure, but the dependent variables were log mass and log SVL, respectively.

Total mucosal peptides – The total concentration of skin peptides recovered after Sep-Pak separation was determined by Micro BCA protein Assay Kit. To test for a difference in peptide concentrations among frogs from different drying treatments and between sham- and *Bd*-exposed frogs, I used a linear model (LM), function: 'lm' with BCA as the dependent variable and exposure group, drying group and their interaction as main effects.

Peptide growth challenge assay – To test for a difference in *Bd* growth inhibition by AMPs collected from sham- and *Bd*-exposed frogs and frogs from the three drying treatments I also ran a linear model (LM) with exposure and drying treatments and their interaction as main effects and *Bd* growth as the dependent variable with time to metamorphosis as a covariate.

Antimicrobial peptide compositions – To test for differences in the composition of previously described skin antimicrobial peptide samples among *Bd* exposure groups and drying regimes, I used a non-metric multidimensional scaling (NMDS) ordination to compare the Bray–Curtis distance (a metric of difference in relative abundance) among samples, using the

"metaMDS" command (Vegan package in R). I then used the "Adonis" function in the Vegan package (Oksanen *et al.* 2013) to carry out a permutation-based multivariate analysis of variance (PERMANOVA) in R (R-Core-Team 2013). PERMANOVA tests were run using the Bray–Curtis distance comparisons of peptide relative abundances among samples, using 9,999 permutations. When the PERMANOVA suggested differences between treatment groups, I then used SIMPER (Similarity Percentage) to determine which peptides are primarily responsible for those observed differences (Clarke 1993). In this case, I used SIMPER to assess differences between *Bd*-exposed and sham-exposed and frogs in both the presence/absence and relative intensity of secreted peptides. In order to know the difference between peptide counts, I counted the number of known antimicrobial skin peptides of *R. pipiens* per frog and compared these counts among treatment groups. I did a generalized linear model (GLM) with exposure, drying treatments and their interaction as main effects and peptide counts as the dependent variable with a quasi-Poisson distribution. To ask which treatment had greater peptide diversity I calculated the Shannon index between naïve and exposed frogs using the relative peptide intensity. I did an ANOVA with the diversity index as the dependent variable Shannon diversity is a measure of biodiversity which accounts for richness and evenness (Shannon, 1948).

Mucosome Bd inhibition assay – To test for a difference in *Bd* viability when exposed to mucosome samples collected from sham- and *Bd*-exposed frogs and frogs from our three drying treatments I ran a linear mixed model (LMM). I subtracted viability from 100 to calculate inhibition. *Bd* inhibition was the dependent variable, exposure the independent variable, log mass at metamorphosis was a covariate and mesocosms ID were the random effects. To see if there was correlation between higher loads and better *Bd* inhibition I ran an LMM with *Bd* inhibition

as the dependent variable *Bd* load in the last week of exposure was the independent variable mesocosms ID was the random effect.

1.3 Results

Tables describing all statistical models and their outputs for this chapter can be found in Appendix A (Tables A1-A19).

Differences in water height levels – There were significant differences between drying treatments in the water heights in the mesocosms, including between medium and fast drying treatments (LMM: $\chi^2 \leq 15833$, $p \leq 0.001$), suggesting that our manipulations were successful in creating different drying environments among the three treatments.

Larval period – Larval period ranged from 62 to 127 d, with a mean and standard deviation of 85.58 ± 16.27 d. (Figure 1.2A). There was no significant difference in larval period among drying treatments (LMM: $\chi^2 = 0.650$, $p = 0.722$).

Survival - The proportion of animals that successfully metamorphosed per mesocosm did not differ significantly across drying treatments (GLME: $\chi^2 = 0.388$, $p = 0.824$, Figure 1.2A). However, survival from metamorphosis until day 42 post-metamorphosis did differ among treatments (: $\chi^2 = 6.042$, $p = 0.049$; Figure 1.2B). Survival was higher in the no drying treatment (mean, 95% CI = 0.952, 0.914 – 0.974; COXPH: $\beta = -0.803$, $p = 0.018$) (Figure 1.2B) than in the fast drying treatment but there was no difference in survival between the moderate (mean, 95% CI = 0.890, 0.855 – 0.933) and fast drying treatments (0.890, 0.856 – 0.936; COXPH: $\beta = -0.107$, $p = 0.685$). Body size (SVL, in mm) was also a significant predictor of survival probability after

metamorphosis (COXPH: $\chi^2 = 5.856$, $\beta = -0.247$, $p = 0.016$), with larger frogs being more likely to survive than smaller frogs.

Body size – Neither body mass (in g; LMM= $\chi^2_2 = 1.571$, $p = 0.455$) nor body size (SVL in mm; LMM: $\chi^2 = 5.477$, $p = 0.064$) at metamorphosis differed significantly among drying treatments. However, the animals in the fast and medium drying treatments were, on average, 17.08% smaller in mass (mean ± SD = 0.73 ± 0.17 g) than animals in the no drying treatment (0.86 ± 0.21 g) and slope of the regression for fast vs. no drying treatment was significantly different (LMM no drying: $\beta = -0.048$ $p = 0.374$). Likewise, animals in the fast and medium drying treatments were, on average, 4.94% smaller in SVL (mean ± SD = 21.71 ± 1.69 mm) at metamorphosis than animals in the no drying treatment (22.78 ± 1.75 mm) and the comparison between fast and no drying treatment was again significant (LMM: $\beta = -0.043$, $p = 0.034$). There were significant interactions between larval period and drying treatment on the mass (LMM: $\chi^2 = 10.774$, $p = 0.005$) and SVL (LMM: $\chi^2_2 = 15.163$, $p = 0.001$) at metamorphosis such that both measures of size increased with larval period more rapidly in the no drying treatment (mass LMM no drying: $\beta = 0.001$ $p = 0.012$, Figure 1.2C; SVL LMM no drying: $\beta = 0.001$ $p < 0.001$, Figure 1.2D).

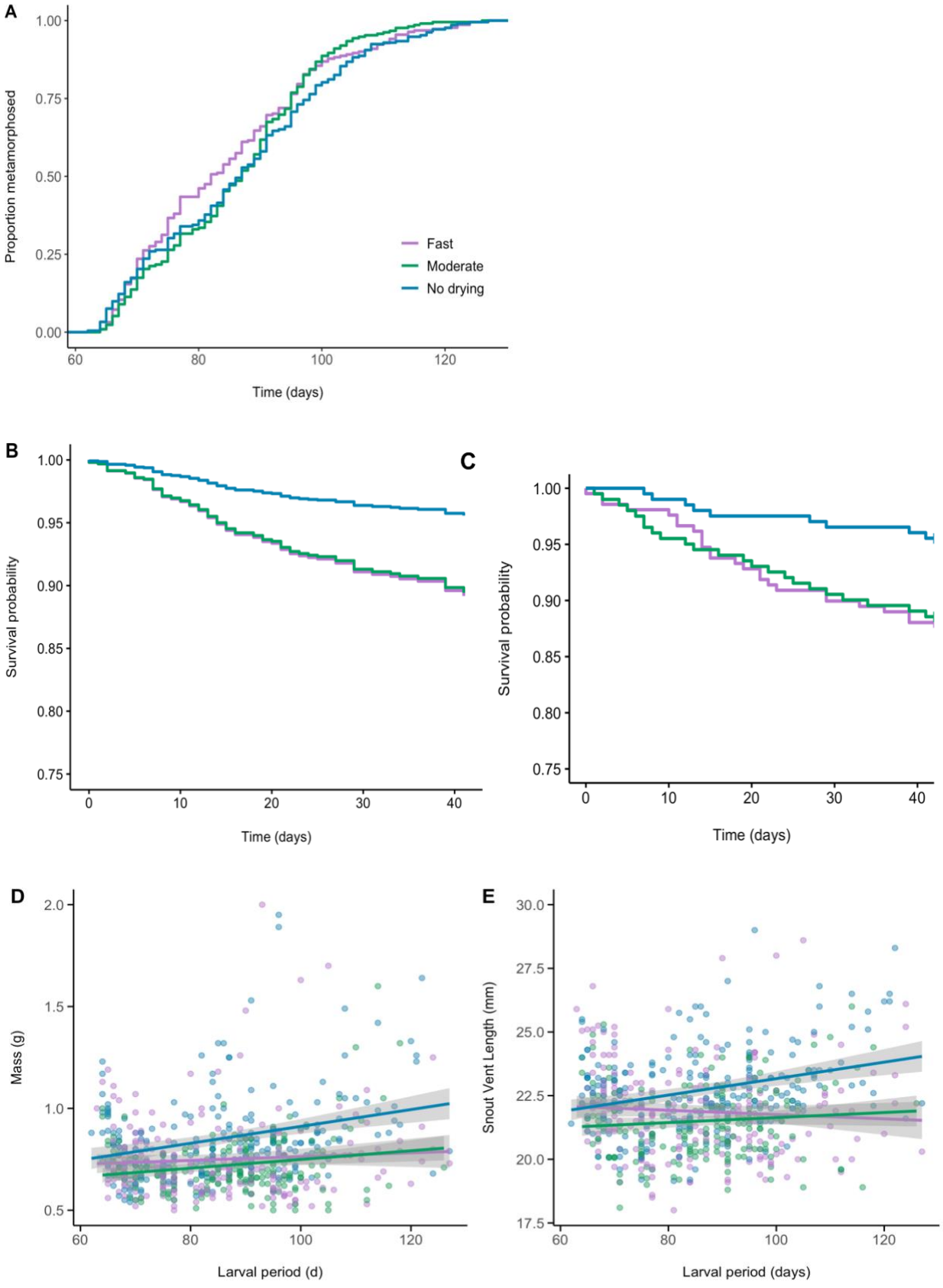
A
Proportion metamorphosed
1.00
0.75
0.50
0.25
0.00
60
80
100
120
Time (days)
Fast
Moderate
No drying
B
Survival probability
1.00
0.95
0.90
0.85
0.80
0.75
0
10
20
30
40
Time (days)
C
Survival probability
1.00
0.95
0.90
0.85
0.80
0.75
0
10
20
30
40
Time (days)
D
Mass (g)
2.0
1.5
1.0
0.5
60
80
100
120
Larval period (d)
E
Snout Vent Length (mm)
30.0
27.5
25.0
22.5
20.0
17.5
60
80
100
120
Larval period (days)

Figure 1.2 Comparisons of leopard frog survival and development across drying treatments.

A) The proportion of individuals (that entered the mesocosms on day 0) that successfully metamorphosed (i.e., survived to tail-absorption, Gosner stage 46) by day and drying treatment. The shortest time to tail-absorption was 62 days after tadpoles were placed in the mesocosms. B) Size-adjusted (using gg-adjusted curves, taking into account animal size at metamorphosis and clustered by mesocosm) survival rate from metamorphosis until day 42 after metamorphosis in the three drying treatments. C) Un-adjusted survival curve (using ggsurvplot). D) Mass (g) of each frog at tail-absorption from the three drying treatments. Shaded areas are 95% confidence intervals. E) Body size, measured as SVL (mm) of each frog at tail-absorption from the three drying treatments. In D) and E), each point represents an individual, and the lines represent the linear relationships between the y-variable and larval period (time from start of experiment to tail-absorption) for each drying treatment. Shaded areas are 95% confidence intervals.

Infection and disease indicators – I hypothesized that frogs that developed under drying conditions would exhibit carry-over effects that increase their susceptibility to *Bd* infections and chytridiomycosis. However, for frogs exposed to *Bd* in our exposure experiment, I did not find a significant main effect of drying treatment on whether the animal became infected (infection probability, GLME: $\chi^2 = 4.708$, $p = 0.095$). However, post-metamorphic growth rate (GLME: $\chi^2 = 4.191$, $\beta = 0.301$, $p = 0.041$, Figure 1.3), the interaction between time since first exposure and drying treatment (GLME: $\chi^2 = 7.889$, $p = 0.019$) were significant predictors of probability of infection for *Bd*-exposed frogs; frogs that grew faster after metamorphosis, from all drying treatments, were more likely to become infected upon exposure and as the experiment progressed, frogs from the no drying treatment were less likely to be infected while frogs from the moderate drying treatment were more likely to become infected ($\beta = 0.589$, $p = 0.006$, Figure 1.4). While the interaction between drying treatment and mass at metamorphosis was not a significant predictor across all drying treatments (GLME: $\chi^2 = 4.807$, $p = 0.090$), there was significant positive relationship between mass at metamorphosis and infection for frogs from the

fast drying treatment (GLME: $\beta = 0.490$, $p = 0.040$, Figure 1.5); frogs with greater mass at metamorphosis were more likely to become infected after exposure to *Bd* if they were reared in the fast drying treatment, but in the no drying treatment frogs with greater mass at metamorphosis had lower probability of getting infected. The main effects of time post exposure, mass at metamorphosis, and the interactions between drying treatment and mass at metamorphosis and drying treatment and growth rate were not significant (GLME: $\chi^2 \leq 3.194$, $p \geq 0.074$).

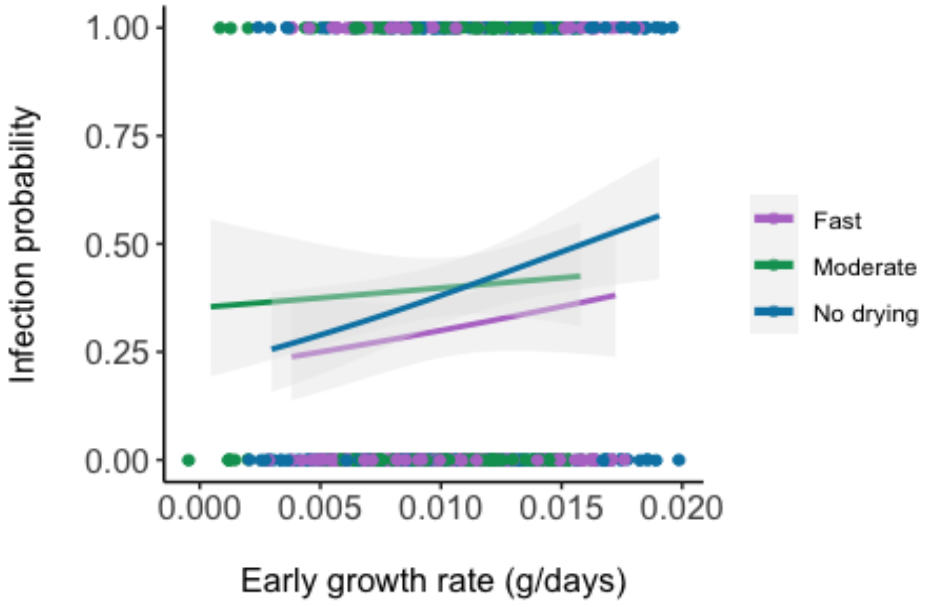

Figure 1.3 Relationship between the probability of becoming infected with Bd after exposure and post-metamorphic growth rate (g/day) in the three drying treatments.

The lines represent the logistic regressions between infection probability and growth rate. The shaded areas are 95% confidence intervals.

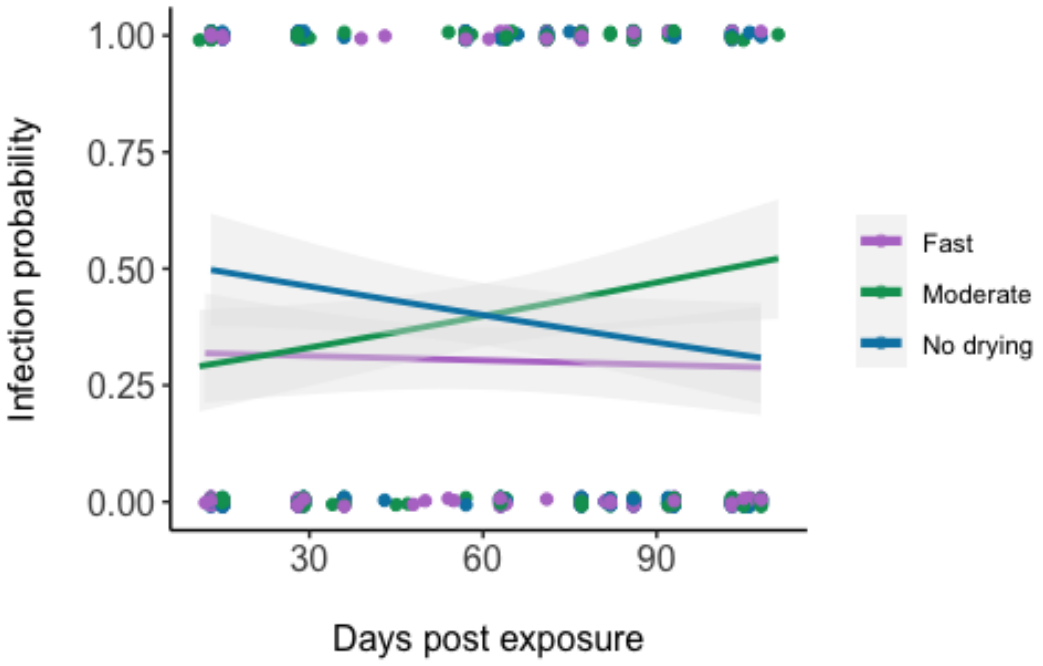

Figure 1.4 Relationship between the probability of becoming infected with Bd after exposure and time since first exposure in the three drying treatments.

The lines represent the logistic regressions between infection probability and days since first *Bd* exposure and the shaded areas are 95% confidence intervals.

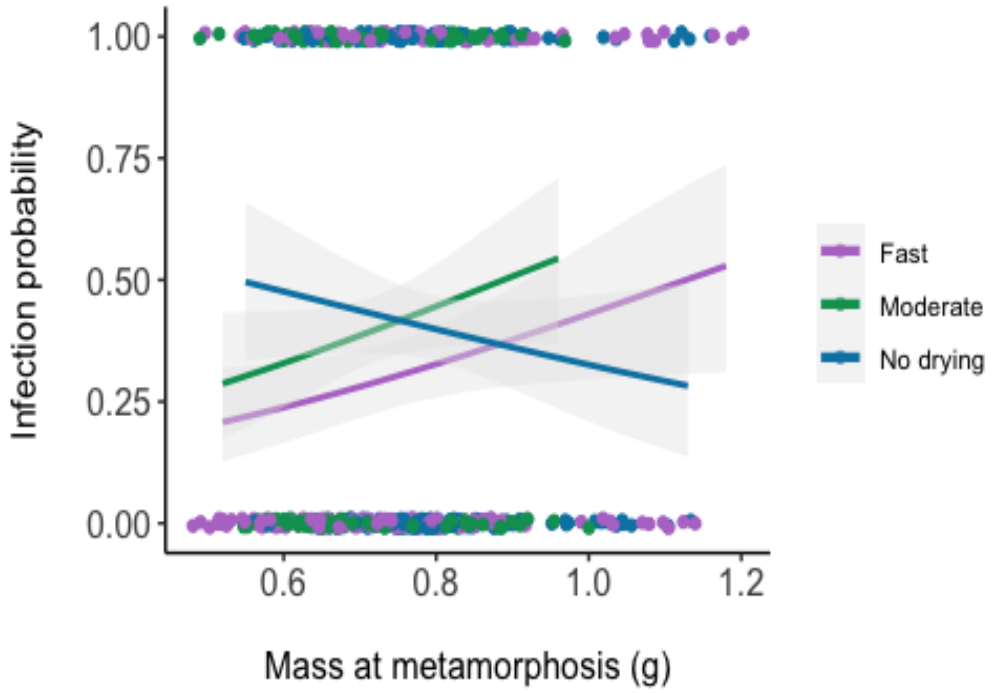

Figure 1.5 Relationship between the probability of becoming infected with Bd after exposure and mass at metamorphosis (g) for frogs reared in the three drying treatments.

The lines represent the logistic regressions between infection probability and growth rate. The shaded areas are 95% confidence intervals.

I did not find a significant effect of drying treatment on *Bd* load after exposure doing a linear mixed model (LMM: $\chi^2 = 1.465$, $p = 0.481$). However, *Bd* load was significantly correlated with time since first exposure (LME: $\chi^2 = 4.771$, $p = 0.031$) and body mass just prior to the first exposure (LMM: $\chi^2 = 9.870$, $p = 0.002$). Animals with lower mass tended to develop greater infection loads ($\beta = 0.242$, Figure 1.6). There was also a significant interaction between drying treatment and days since first *Bd* exposure (LMM: $\chi^2_2 = 6.949$, $p = 0.031$) on infection load such that *Bd* load decreased faster in frogs reared in the drying treatments than in frogs from the no drying treatment (Figure 1.7). There was not a significant main effect of growth rate on *Bd* load (LMM: $\chi^2 = 0.512$, $p = 0.223$).

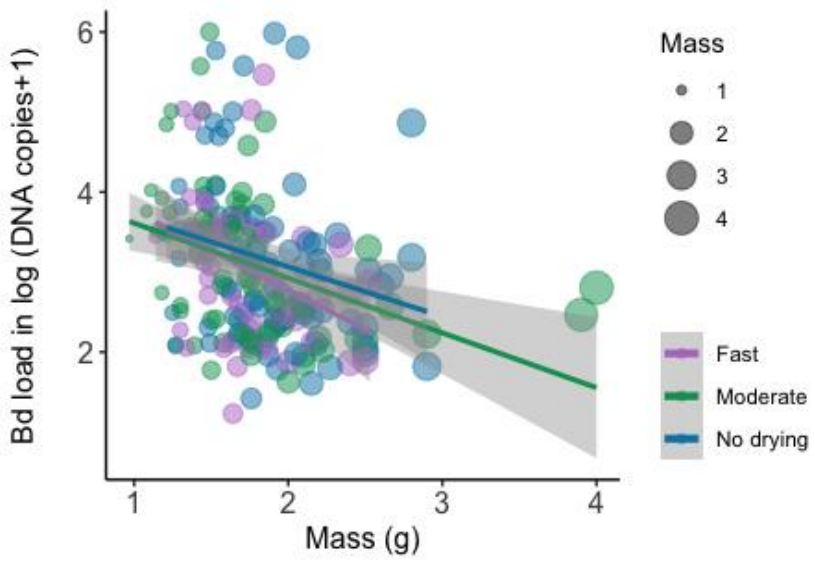

Figure 1.6 Relationship between body mass just prior to the first exposure and Bd infection load in Bd-exposed animals from the three drying treatments.

The lines represent the linear regression, and the shaded areas are 95% confidence intervals. The larger the marker size the larger the mass

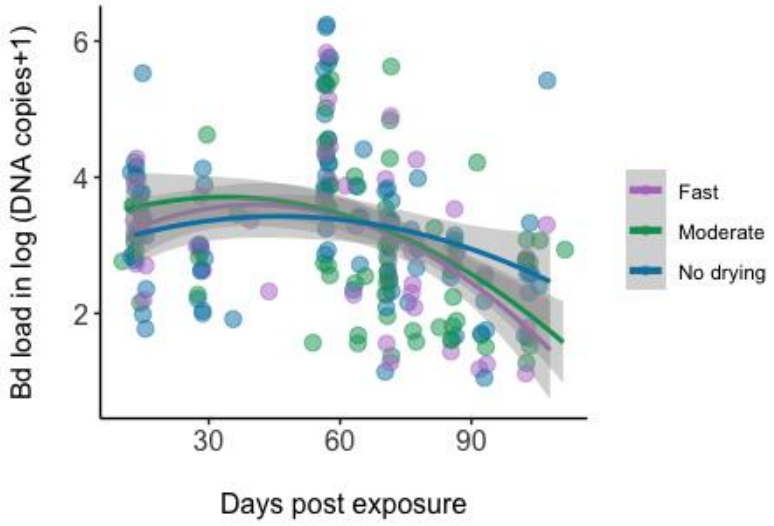

Figure 1.7 Relationship between days since first Bd exposure and Bd infection load in the three drying treatments.

The lines represent the smoothed quadratic model fit between days post exposure and *Bd* load and the shaded areas are 95% confidence intervals.

When I considered body condition (measured as scaled mass index, or SMI) over the course of the exposure experiment, I did not find significant main effects of drying treatment or exposure group (*Bd* vs. sham). The interactions between these two factors, the interaction between drying treatment and time since first exposure, and the three-way interaction between exposure group, drying treatment, and time since first exposure were also not significant (LMM: all $\chi^2 \leq 4.0851$, $p \geq 0.077$). However, time since first exposure had a significant main effect on body condition (LMM: $\chi^2 = 8.763$, $p = 0.003$) and there was a significant interaction between exposure group and days post exposure (LME: $\chi^2 = 37.562$, $p < 0.001$) such that sham infected (control) frogs gained body condition over the course of the experiment while *Bd*-exposed frogs declined in body condition (Figure 1.8).

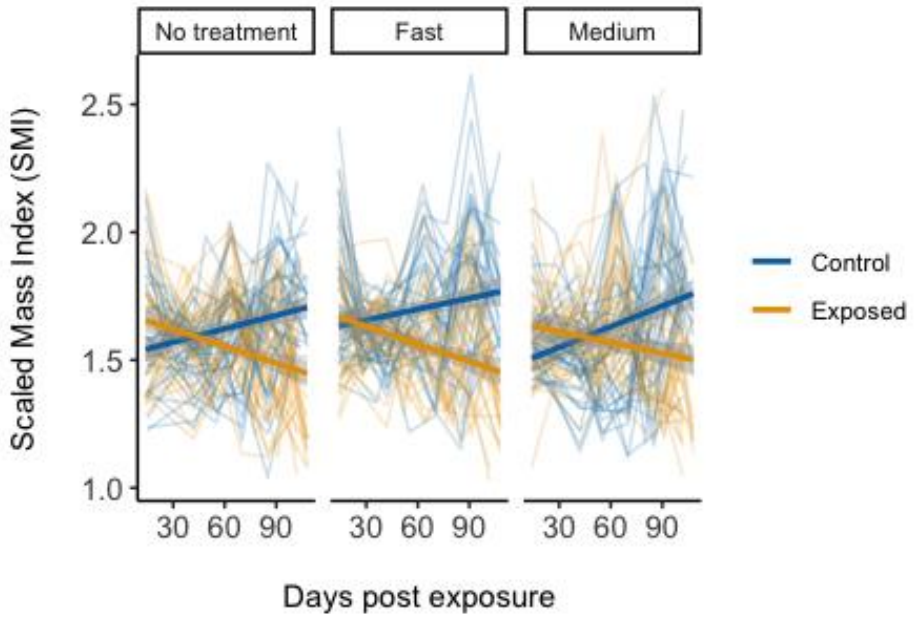

Figure 1.8 Relationship between body condition (measured as scaled mass index, or SMI) and days since first Bd exposure in frogs from control (sham infected) and Bd-exposed treatment groups.

Thick lines represent linear regressions and thin lines show changes in SMI over time for individual frogs.

When considering survival to three months post-exposure as the dependent variable, I found a significant interaction between drying treatment and exposure group (COXPH: χ^2_5 = 11.061, p = 0.050). The *Bd*-exposed frogs in the fast-drying treatment (COXPH: β = 1.803, z = 2.475, p = 0.013) and in the moderate drying treatment (COXPH: β = 1.572, z = 2.061, p = 0.040) had a lower survival probability than the *Bd*-exposed frogs in the no drying control (Figure 1.9). There was no significant difference in survival among control (sham exposed) frogs reared in the different drying treatments (COXPH: β = ≤ 0.676, z ≤ 1.650, p ≥ 0.318).

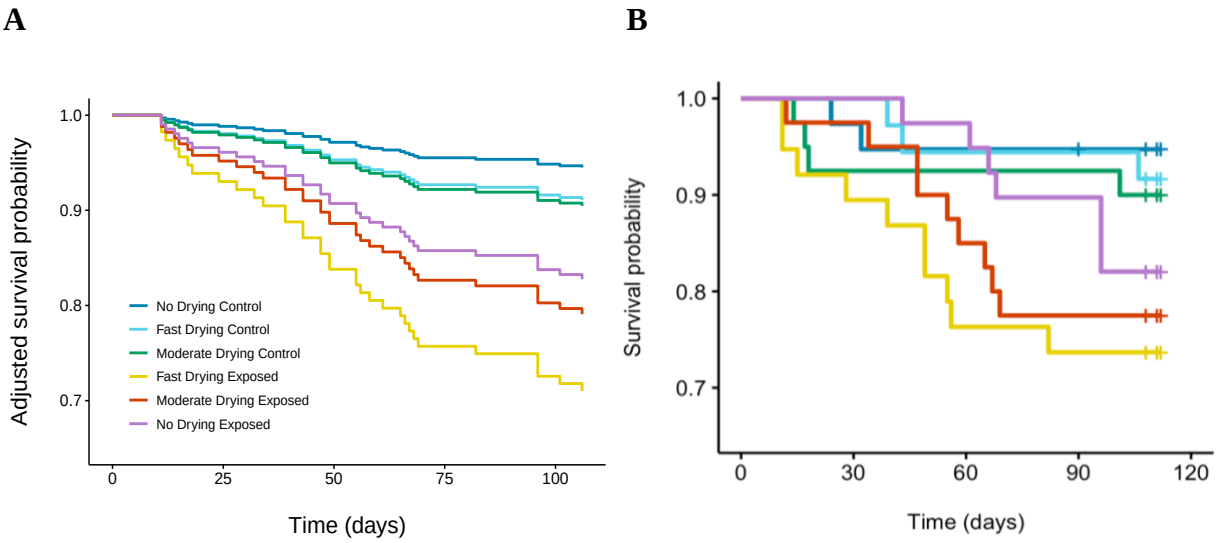

Figure 1.9 Survival curves for control (sham infected) and Bd-exposed frogs reared under the different drying treatments.

A) Adjusted survival curves (using gg-adjusted curves, taking into account animal size at metamorphosis and clustered by mesocosm). B) Un-adjusted survival curves (using ggsurvplot).

Total mucosal peptides - There was no significant main effect of drying treatment (LM: $F_{2,52}$ = 2.225, p = 0.118) or exposure group (LM: $F_{1,52}$ = 0.691, p = 0.410) on the total quantity of peptides secreted. There was also no significant interaction between drying treatment and

exposure group on peptide quantity (LM: $F_{1,52} = 1.721$, $p = 0.189$). The mean mass of mucosal peptides secreted by all *Bd* exposed frogs was 107.021 µg/gbw (range: 15.161 to 284.243 µg/gbw) and for sham-exposed frogs, the mean was 121.936 µg/gbw (range: 10.939 to 286.585 µg/gbw).

Bd growth challenge assay with mucosal peptides - Across all drying treatments and exposure groups there were some AMP samples that enhanced (positive growth index values) and others that inhibited (negative growth index values) growth of *Bd*. There was no significant difference in *Bd* growth in the presence of AMP samples collected from frogs in the different drying treatments (LM: $F_{2,42} = 0.258$, $p = 0.773$) or from *Bd*- and sham-exposed frogs (LM: $F_{1,42} = 0.258$, $p = 0.721$). Nor was there a significant interaction between drying treatment and exposure group on *Bd* growth in the presence of mucosal peptides (LM: $F_{2,42} = 0.046$, $p = 0.830$). The mean of *Bd* growth inhibition index after *Bd* exposure was 0.003 (range: -2.928 to 0.978).

AMP composition – After the exposure experiment (18 weeks post-metamorphosis), frogs were found to have secreted 18 of the 19 previously described peptides for *R. pipiens* (Tennessen *et al*., 2009), the majority of which were from the family of Brevinins. The PERMANOVA considering antimicrobial peptide presence/absence only showed differences between the AMP communities in secretions collected from *Bd*-exposed and naïve (sham exposed) frogs (Bray–Curtis distance: $F_{1,48} = 14.087$, $R^2 = 0.228$ $p < 0.001$, Figure 1.10) with the naïve frogs secreting a greater number of AMPs than the exposed frogs (GLM: $\chi^2 = 6.326$, $p = 0.021$, Figure 1.11). However, I did not find a significant difference in AMP communities in the secretions collected from frogs that developed in the different drying treatments (Bray–Curtis distance: $F_{2,48} = 0.972$, $R^2 = 0.032$, $p = 0.426$).

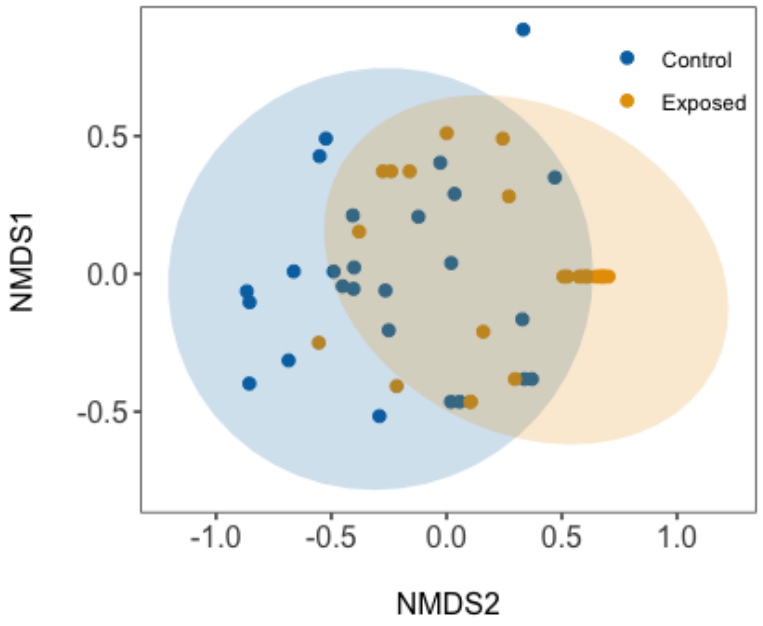

Figure 1.10 Non-multidimensional scaling (NMDS) plot of Bray–Curtis distances based on presence/absence of AMPs detected by MALDI in control (sham exposed) and Bd-exposed frogs.

Blue dots are samples from control and yellow are samples from *Bd*-exposed frogs. The ellipses represent 95% confidence intervals.

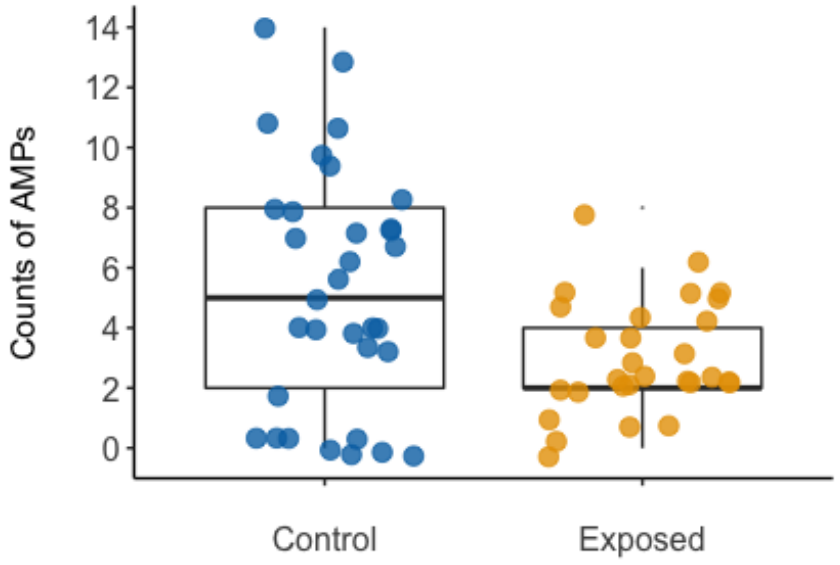

Figure 1.11 Boxplots showing counts of AMPs secreted by control (sham exposed) and Bd-exposed animals after the Bd-exposure experiment.

The middle line corresponds to the median. The lower and upper hinges correspond to the first and third quartiles (the 25th and 75th percentiles). The upper whisker extends from the hinge to the largest value no further than 1.5 times the inter-quartile range.

I did the same analysis but with relative peptide intensities instead of just presence/absence for each peptide and found similar results. The PERMANOVA comparing relative peptide intensities showed that *Bd*- and sham-exposed frogs had different peptide communities (Bray–Curtis distance: $F_{1,43} = 7.160$, $R^2 = 0.134$, $p < 0.001$, Figure 1.12). However, I did not find a significant difference between drying treatments (Bray–Curtis distance: $F_{2,43} = 0.709$, $R^2 = 0.026$, $p = 0.629$). The Shannon index indicated that the sham-exposed frogs have a greater diversity of AMP community than the *Bd*-exposed frogs (ANOVA: $F_{1,43} = 14.935$, $p < 0.001$) (Fig 1-13).

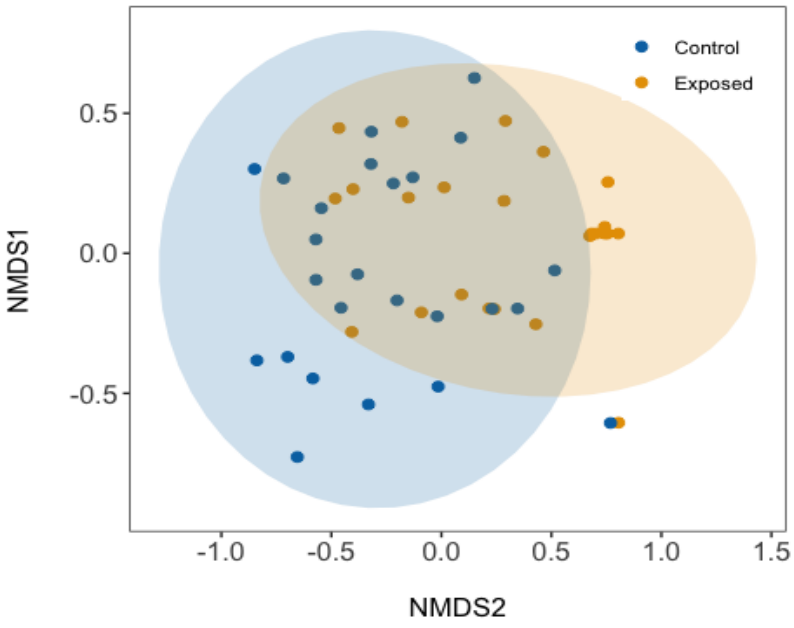

Figure 1.12 Non-multidimensional scaling (NMDS) plot based on Bray–Curtis distances on relative intensities of antimicrobial peptides (AMPs) detected by MALDI in control (sham exposed) and Bd-exposed frogs.

Blue dots represent the peptides present in control frogs and yellow dots represent the peptides in the *Bd*-exposed frogs. The ellipses are 95% confidence intervals.

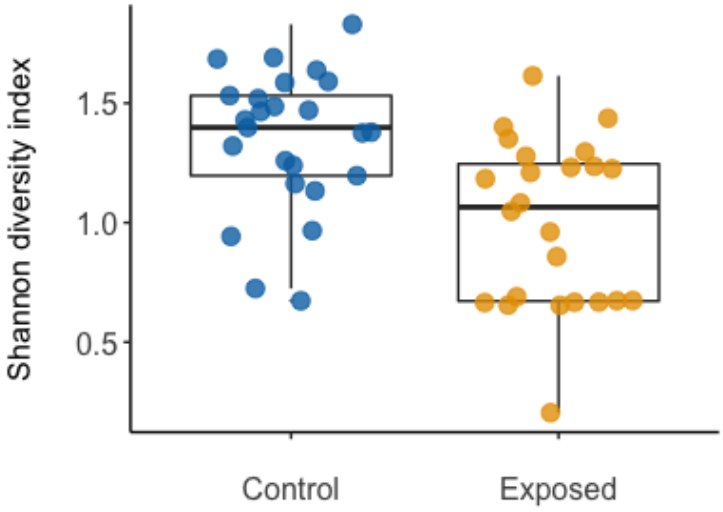

Figure 1.13 Boxplots of Shannon index of diversity showing differences in AMP communities secreted by control (sham-exposed) and Bd-exposed frogs from the exposure experiment.

Each point represents one individual. The middle line corresponds to the median. The lower and upper hinges correspond to the first and third quartiles (the 25th and 75th percentiles). The upper whisker extends from the hinge to the largest value no further than 1.5 times the inter-quartile range.

Using a SIMPER analysis, I assessed which peptides were primarily responsible for the observed differences between *Bd*- and sham-exposed frogs. For the presence/absence analysis, six peptides drove the differences between naïve and exposed frogs (brevinin 1Pa, brevinin 1Pb, brevinin 1Pc, brevinin 1Pd, brevinin 1Pe, brevinin 1Pla). For the peptide intensity analysis, three peptides were found to be driving the difference (brevinin 1Pg, brevinin 1Pk, brevinin 1Pe).

Bd growth challenge assay with mucosome – After the exposure experiment, the ability of mucosome samples to inhibit the growth of *Bd* did not differ among *Bd*-exposed and sham exposed frogs or between the frogs in the three drying treatments and the interaction between exposure group and drying treatment was also non-significant (LME all: $\chi^2 \leq 1.969$, $p \geq 0.374$). However, there was significant effect of mass at metamorphosis on *Bd* growth inhibition (LME: $\chi^2 = 7.146$, $p = 0.013$, Figure 1.14). The frogs that metamorphosed at a smaller size had mucosome that was less effective at inhibiting *Bd* growth. Contrary to what I expected, I didn't find a correlation between higher *Bd* inhibition and lower *Bd* loads (LME: $\chi^2_1 = 0.006$, $p = 0.930$).

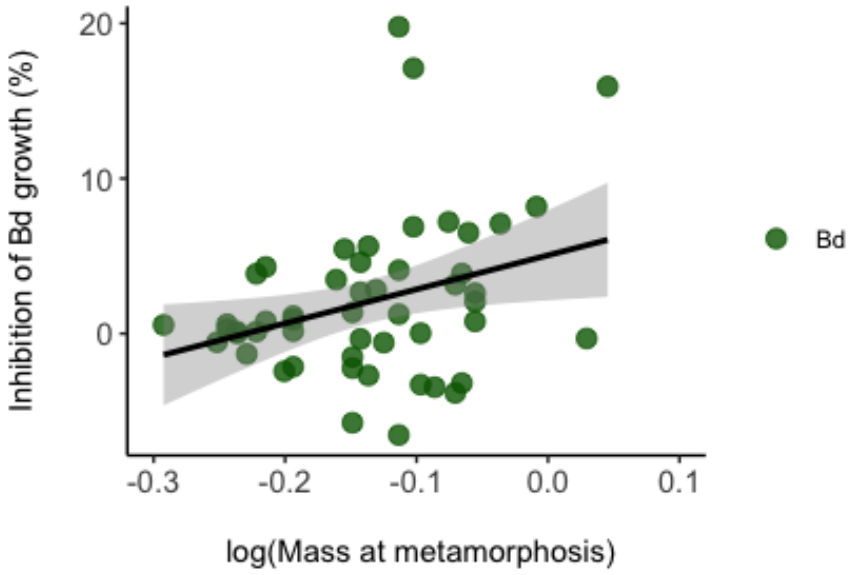

Figure 1.14 Scatterplot showing the percent inhibition of Bd growth by mucosome samples versus log-transformed mass of frogs at metamorphosis.

Each point represents one individual, and the linear relationship between mucosome inhibition and log (mass) metamorphosis is represented with the line and 95% confidence interval (shaded area).

1.4 Discussion

1.4.1 Simulated pond drying conditions did not induce developmental plasticity

Most amphibian species rely on humid to aquatic environments for reproduction and are more active during wet periods. To cope with the unpredictable availability of such conditions, many amphibians exhibit developmental plasticity. For example, many anurans that develop as larvae in ephemeral water bodies and can accelerate metamorphosis to escape a drying pond (Denver *et al.*1998, Loman and Claesson, 2003). The endocrine stress axis modulates the timing of metamorphosis in amphibians in response to pond desiccation and other

environmental cues such as predators, and food resources (Kikuyama *et al.* 1993, Crespi and Warne, 2013). Specifically, the developmental response to environmental stimuli in amphibians is regulated by the hypothalamus–pituitary–interrenal (HPI) axis and is driven by plasma corticosterone levels. However, not all amphibians that develop in unpredictable aquatic habitats show plasticity in development in response to drying (Amburgey *et al.* 2012). Here I found that, contrary to my predictions, the larval period of northern leopard frog (*Rana pipiens*), a species that often breeds in the calm water of lakes, ponds, canals, and streams (Stebbins 2003), did not respond to drying by accelerating development to shorten the aquatic larval period. The animals in my drying treatments did, however, experience other physiological and immunological costs of developing in a drying habitat.

1.4.2 Effects of drying conditions on survival and growth

The animals that experienced the fast and medium drying treatments during their larval period had lower survival to, and size at metamorphosis. Reduced survival to metamorphosis is a clear indication of a fitness cost of developing in a drying pond. However, small size at metamorphosis may also be detrimental as for many anurans, larger juveniles have greater survival in the terrestrial habitat and grow to be larger adults whereas smaller juveniles take longer to reach sexual maturity and lay smaller egg masses (Berven, 1990, Rowe and Ludwig 1991, Reques and Tejedo 1997, Cabrera-Guzmán *et al.* 2013). Anurans that are larger at metamorphosis can also exhibit greater resistance to parasites (Rohr *et al.* 2009) and can build up larger energy stores before hibernation (Reading and Clarke 1999). There are numerous anuran species in which size at metamorphosis, through one or more of the mechanisms listed above, has been shown to affect fitness later in life (*e.g.*, *Hyla pseudopuma*, Crump, 1989; *Spea*

intermontana, *Pseudacris regilla*, and *Rana aurora*, O'Regan *et al.* 2013). Taken together, this strongly suggests that even though I did not see a plastic response to drying in terms of developmental timing in *R. pipiens*, there were costs associated with developing in our drying mesocosms.

1.4.3 Effects of pond drying on development of immune defenses

While changes in developmental timing and growth due to the stress of a drying pond have been well studied in anurans, the potential impacts of drying on other aspects of physiology has received less attention. In particular, the impact that developing in a drying pond may have on immune development has received little attention even though infectious disease (namely chytridiomycosis caused by *Bd*) ranks among the top threats to amphibian populations globally (Scheele *et al.* 2019). One study by Gomez-Mestre *et al.* (2013) showed that accelerated development in response to pond desiccation in the Andean frog *Pristimantis curtipes* resulted in smaller juveniles with proportionately shorter limbs, and an increase in activity of the antioxidant enzymes catalase, superoxide dismutase, and gluthathione peroxidase. However, more studies that investigate the impacts of drying on immune function and disease are needed to understand the potential threat that climate change induced shifts in the availability of aquatic breeding and developmental poses for amphibians.

1.4.4 Lower survival after *Bd* exposure

Regardless of in which drying treatments they developed in as larvae, the juvenile leopard frogs in this study appeared to be somewhat resistant to *Bd* infection. Despite being

exposed multiple times, I rarely saw clinical signs of chytridiomycosis, I only detected *Bd* infections in ~ 50% of animals at any given time point in our experiment, and infection loads decreased over time in animals from all three drying treatments. However, survival was lower in the frogs exposed to *Bd* than in the sham-exposed control frogs, and *Bd*-exposed frogs lost body condition over the course of the study while the body condition of sham-exposed frogs increased, suggesting that even in animals that are able to resist infections and do not show signs of disease there can be costs associated with fighting infection.

1.4.5 Indirect effects of drying and *Bd* exposure

The *Bd*-exposed frogs that experienced fast drying during development had the lowest survival and developed the largest difference in body condition (as compared with sham-exposed controls) over the course of the exposure experiment. These results suggest that developing in a drying pond has indirect effects on susceptibility to *Bd* that act through differences in size and growth rate after metamorphosis, rather than through differences in developmental timing as I had predicted. A similar outcome was observed in tadpoles of the gray treefrog (*Hyla versicolor*), which co-occur in temporary and permanent ponds with a snail (*Pseudosuccinea columella*) that is frequently infected with trematodes (*Telorchis* sp.) whose cercariae can infect *H. versicolor* tadpoles. When these tadpoles were exposed to the infected snails in drying ponds their survivorship decreased by 30%, and mass at metamorphosis was reduced by 40% as compared with permanent ponds (Kiesecker and Skelly 2001). While developing in a drying environment did not appear to directly affect infection loads or the probability that a *Bd*-exposed frog would become infected in this study, body mass at metamorphosis, which was affected by my drying treatment, was a significant predictor of the infection load a *Bd*-exposed frog would

develop, with animals that were larger at metamorphosis having lower infection loads. Furthermore, individuals that experienced a faster growth rate post-metamorphosis, as many frogs from our drying treatments did, had a greater probability of developing a *Bd* infection after exposure. This may have resulted from undersized froglets preferentially investing more energy into growth and less into their immune defenses. Also, despite drying treatment not having direct effects on the probability or load of infection, frogs that developed in our drying treatments before being exposed to *Bd* had significantly lower survival.

1.4.6 Antimicrobial peptides after drying treatment and exposure to *Bd*

I hypothesized that, due to stress and/or the need to accelerate growth and metamorphosis, animals that developed as larvae in our drying treatments would secrete lower quantities of peptides and a less diverse cocktail of AMPs than frogs from our no drying treatment. This hypothesis is also consistent with previous work suggesting an evolutionary trade-off between larval period and AMP production in anurans, with species with longer larval periods having more secreting quantities of AMPs (Woodhams *et al.* 2016). Thus, I predicted I may see a similar effect within species, with individuals that experienced longer larval periods secreting more AMPs after metamorphosis. However, in the juvenile leopard frogs in this study, I found no evidence for an effect of exposure to drying during development on the quantity of peptides secreted, the identities or relative intensities of AMPs, or the ability of secreted peptides to inhibit *Bd* growth. Perhaps because the tadpoles developed at a similar rate across the drying treatments they also developed their peptide repertoires on a similar schedule. Or, since I collected peptides 19 weeks post-metamorphosis, it is also possible that frogs that initially had less-developed peptides had already ‘caught up’ with their peers by that point in development.

AMPs appear to be an important part of the defense against *Bd.* For example, frogs from populations that are recovering from *Bd* epizootics in Panama were found to have mucosal peptides than were more effective against *Bd* than did animals from those same populations prior to the pathogen's arrival (Voyles *et al.* 2018). In Southern leopard frogs (*R. sphenocephala*), Robak *et al.* (2019) also showed that AMPs are renewed more slowly by *Bd*-infected animals (than by sham-exposed animals). Hence, I hypothesized that the frogs exposed to *Bd* in this study would secrete different quantities and/or communities of peptides than sham-exposed frogs and that these differences would be related to the peptides' abilities to inhibit *Bd* growth. Twenty AMPs have been identified in *R. pipiens*: 15 from the brevinin family, four from ranateurin family, and one each in the esculetin and temporin families (Tennessen *et al.* 2009). Of these 20 peptides, brevinines are the most common peptides expressed, and they have been shown to inhibit *Bd* growth (Tennessen *et al.* 2009). I also found that the brevinins are the most common peptides expressed in my study population of *R. pipiens* from Pennsylvania. The peptides that were most abundant in both *Bd*-exposed and *Bd*-naïve frogs were brevinins Pk, Pg and Pe. These peptides do inhibit *Bd* growth when purified, but not to the extent that other brevinin peptides have been shown to (Rollins-Smith *et al.* 2002). In this study, on average, the purified peptides from neither sham-exposed nor *Bd*-exposed frogs were able to inhibit *Bd* growth *in vitro*. After the end of our exposure experiment, the *Bd*-exposed frogs in our study secreted similar quantities of total peptides to the sham exposed frogs. However, the *Bd*-exposed frogs secreted lower quantities of antimicrobial peptides, and fewer peptide types than *Bd*-naive frogs. This suggests that either the *Bd*-exposed frogs were using up more of their store of AMPs (but somehow not depleting total peptide stores) to fight *Bd* infection, *Bd* exposure impacted the production of AMPs, or both. In a previous experiment with *R. sphenocephala*, a sister species to *R. pipiens*,

Bd infection was shown impaired the capacity of juvenile frogs to produce and secrete AMPs (Robak *et al.* 2019). Given that I found fewer AMPs but not smaller overall quantities of hydrophobic peptides secreted by *Bd*-exposed *R. pipiens*, specific inhibition of AMP production by *Bd* infection seems the most likely explanation for the pattern I saw as well. However, in the field, in the lowland population of Australian frog *Litoria genimaculata,* heavier *Bd* infections were correlated with lower intensities of total AMPs (Woodhams *et al.* 2010).

1.4.7 Mucosome after drying treatment and exposure to *Bd*

While I did not see effects of my drying treatments on AMP secretion, the effects of developing in a drying pond appear to have impacted the juvenile leopard frogs' skin mucus in other ways. It has been shown previously that mucosome's function against *Bd* is predictive of infection risk in natural amphibian populations and of survival in laboratory exposure experiments (Woodhams *et al.* 2014). In my experiment, the mucosome of frogs that were larger in mass at metamorphosis, which was more often the case when they developed in our no drying treatment, was more effective at inhibiting *Bd* growth *in vitro*. In *Xenopus*, it has been shown that the size of the granular glands in the skin, which hold and secrete AMPs, increase as the animal grows (Flucher *et al.* 1986). Larger leopard frogs in our study may have larger granular glands that can hold more AMPs. If so, this may have resulted in more concentrated mucosome samples coming from these larger frogs, which could explain the relationship I found between body mass and *Bd*-growth inhibition by mucosome. In nature, larger frogs that can secrete more mucus containing AMPs may also be able to fight *Bd* better, but the relationship between body size and mucosome efficacy against *Bd* has not yet been studied *in vivo*. In our experiment, neither being previously exposed to *Bd* nor experiencing drying during development reduced the

ability of the mucosome to inhibit *Bd* growth. Antifungal function is often primarily attributed to innate defenses like AMPs, but to understand this result it will likely be necessary to quantify other components of the mucus, including microbial products, some of which have been shown to have antifungal properties (Woodhams *et al*. 2020).

Taken together, my results suggest that the combined threats of drought and infectious disease across life stages may interact to put amphibians at a greater risk of mortality than would be expected from one of these threats alone. This work demonstrates that developing under the stress of a drying pond can have complex effects on amphibians. Although development in drying conditions impacted some fitness-related traits (*e.g.*, size at metamorphosis), it did not seem to have effects on the timing of metamorphosis or the development of immune defenses directly. Instead, drying indirectly impacted susceptibility to *Bd* via impacts on size at metamorphosis and juvenile growth rate. Smaller sizes at metamorphosis, and larger (likely compensatory) growth rates in juvenile frogs appear to result in lower mucosal defenses and greater susceptibility to *Bd*. The amphibian immune system is complex (Rollins-Smith, 1998; Rollins-Smith & Woodhams, 2012) and the impacts of stressors on some elements of the immune system might be more pronounced than others. I have shown that the environmental stress of a reduced hydroperiod during development can impact post-metamorphic size, growth rate, and survival. These carry over effects of a stressful larval environment impacted the immune function and disease susceptibility of frogs post-metamorphosis, demonstrating that the effects of these combined stressors, even if not experienced at the same time, may be detrimental to wildlife populations.

2.0 Impacts of elevated temperature and *Bd* exposure on immune function

2.1 Introduction

A clearer understanding of how climate affects host-pathogen interactions is needed to predict and mitigate the effects of wildlife diseases. Ecoimmunology is a field that examines how host immune systems and pathogens interact in different environments (Demas and Nelson, 2012). An important component of this is understanding how environmental change may influence disease susceptibility (Downs and Stewart, 2014). For ectotherm hosts, the effects of temperature on immunity, and the ability to regulate immune activity in conjunction with other physiological demands, could play important roles in shaping disease risk. For example, exposing the blue mussel, *Mytilus edulis*, to elevated temperatures and cadmium had a significant negative effect on hemocyte (phagocytic cells in invertebrates) counts and no effects on lysozymes (cells that disrupt the bacterial cell membranes) at 5, 10 and 20 °C (Beaudry *et al.* 2016). In the tortoise *Gopherus polyphemus*, the heterophil (a leukocyte) to lymphocyte ratio in the blood was found to be significantly reduced as a result of rapid warming in winter. This created a lag in immunity, which may make the species more susceptible to infectious diseases (Goessling *et al.* 2017). These examples illustrate that climate change can affect the immune system and how well a host can defeat a pathogen.

As infectious diseases emerge with increasing frequency and impact wildlife populations, it becomes increasingly critical to understand the links between environment, host-pathogen biology, and disease dynamics (Raffel *et al*. 2013). Fungal pathogens, like the ones linked to white nose syndrome in bats (Foley *et al.* 2011), colony collapse disorder in bees (Bromenshenk

et al. 2010), and chytridiomycosis in amphibians (Berger *et al*. 1998), have driven recent wildlife declines and appear to be particularly sensitive to changes in climate (Fisher and Garner 2020). For example, for white nose syndrome in bats, replication of the causal fungus (*Geomyces destructans*) and transmission among hosts peak in early winter when the temperatures are cooler and bats begin hibernating (Langwig *et al*. 2015). By contrast, the rabies virus, generally pauses transmission and/or decelerates disease progression while bats are hibernating (Streicker *et al*. 2012). Similarly, chytridiomycosis in amphibians, caused by the fungal pathogen *Batrachochytrium dendrobatidis* (*Bd*), has caused mass mortality events on several continents, and differences in *Bd* infection load and prevalence within and among host species have been attributed to environmental conditions (Phillott *et al*. 2013, Simpkins *et al.* 2017, Cohen *et al.* 2019). Temperature, in particular, is an important factor in the distribution of *Bd* (Kriger *et al.* 2007, Xie *et al.* 2016) and its impacts on hosts (Robak and Richards-Zawacki 2019, Sonn *et al.* 2019). These examples clearly illustrate how interactions between climate, host, and pathogen seem to be driving the emergence and spread of infectious fungal diseases.

The interaction between *Bd* and its amphibian hosts provides a good study system for understanding how climate change may impact host-pathogen interactions. As a moderate carbon fuel emission scenario (RCP4.5), climatologists project a rise in mean air temperature from 1990 to 2100 of 1.1°C to 2.6°C (IPCC 2014, Houghton *et al*. 2007) along with shifts in water temperature, precipitation, and humidity (Zhang *et al.* 2017). While climate change impacts diverse taxonomic groups, amphibians are particularly at risk of adverse effects because their body temperatures are modulated by environmental temperatures (Angilletta and Angilletta 2009) and because susceptibility to *Bd* also appears to be temperature dependent (Sonn *et al*. 2017, 2019, 2020). Temperature is known to affect the amphibian immune response to *Bd*

(Robak *et al*. 2018, 2019), suggesting that the rapid fluctuations and extreme conditions that are projected to result from human-induced climate change may impact the ability of these hosts to effectively defend themselves from *Bd* and other pathogens (Rohr *et al*. 2013).

Amphibians have many forms of defense against pathogens, including both adaptive and innate immune responses and cutaneous microbial communities. The innate immune response is activated as soon as a pathogen is detected and players in this response include antimicrobial peptides (AMPs), the complement pathway, and non-specific leukocytes (Carey *et al*. 1999). In amphibians, antimicrobial peptides are an important component of the innate immune response. These host-produced peptides are secreted from granular glands in the skin into the mucus layer that surrounds the body from granular glands in the skin and represent the first line of defense against pathogens (Rollins-Smith 2009). They can kill a variety of microorganisms, including bacteria, yeast, and fungi (Nicolas and Mor, 1995). The 'mucosome', a term used to holistically describe the contents of amphibian skin mucus (Woodhams 2014), contains AMPs, lysozymes and other small organic molecules, such as alkaloids, which may also play a role in defense (Rollins-Smith, 2020). The adaptive immune response requires time to be activated following the body's detection of a pathogen. Amphibian immune systems have T- and B-lymphocytes (Baldwin and Cohen, 1981) that have cell surface receptors that recognize and bind to certain pathogens and regulate antibody production. Amphibians also have two important lymphoid organs: the thymus and the spleen. The thymus is the site of T cell development (Jurd, 1994) while the spleen is in charge of antigen processing and development of immune T and B cell responses (Kanakambika and Muthukkaruppan, 1972) and production of some new blood cells (Zapata *et al*. 1981). Thus, amphibians have a suite of defenses against pathogens, though our understanding of how they may be impacted by climate change remains poor.

Physiological processes are governed by temperature in ectotherms, and accordingly, many aspects of the immune system of amphibians are also known to exhibit temperature dependence (Rollins-Smith and Woodhams 2012). Some studies have shown detrimental effects of sudden increases or decreases in temperature on the amphibian immune system. Lymphocytes, eosinophils, complement proteins, and antibodies generally remain at low levels when environmental temperatures are low and take a while to recover after temperatures are increased. For example, in northern leopard frogs (*Rana pipiens*), the serum complement activity took 7-9 days to recover following an increase in air temperature from 5 to 22ºC degrees (Maniero and Carey, 1997). Another study showed that immunoglobulin Y (IgY) antibodies recovered from southern leopard frogs (*Rana sphenocephala*) that had previously been exposed to the *Bd* pathogen at 14ºC had greater binding activity to that pathogen at 14ºC than at 26ºC (Robak 2016). Few studies have examined the role of increased environmental temperature on innate defenses. However, one study found that southern leopard frogs held at 26°C produced more AMPs than frogs at 14°C after peptide secretion (Robak *et al.* 2019).

Stressors experienced early in development, such as harsh environmental conditions or poor nutrition, can have impacts on the health and fitness of individuals much later in life. Extreme temperatures, like those predicted to occur more frequently under global climate change, are known to have effects on developmental timing that carry over to affect fitness later in life (Groner *et al.* 2013, Martin *et al.* 2010). For example, in the relict leopard frog (*Rana onca*), time to metamorphosis was faster for tadpoles reared at 25°C (their optimal temperature) than for tadpoles reared at 20 or 30°C (Goldstein *et al*. 2017, Ruthsatz *et al*. 2018). Usually, ectotherms that develop as larvae in warmer temperatures develop faster, but at the cost of a smaller body size at metamorphosis (Harkey and Semlitsch 1988). These differences can be

important because in many species of amphibians, both size and age at metamorphosis directly affect factors like survival rate, reproductive output, and dispersal ability later in life (Riha and Berven 1991, Freitas *et al*. 2017, Brannelly *et al*. 2019). The development of immune defenses is also energetically costly and an organism that experiences stress during development might not have the resources it needs to devote to this, leaving it susceptible to infection (Schmid-Hempel 2005). Lower immune function as a result of developmental stress could be particularly detrimental to species threatened by infectious disease, like amphibians. Here I test the hypothesis that elevated temperatures, when experienced during the larval period, affect amphibian development, immunity, and susceptibility to the fungal pathogen *Bd*.

Researchers disagree as to whether climate change will ease or worsen the impact of *Bd* on amphibian populations. Some have hypothesized that climate change will worsen *Bd*'s effects, based on the idea that increasing variability of temperatures and precipitation may change the host-pathogen dynamics (Yeh *et al.* 2009). Others have predicted the opposite, that climate change will lessen the impact of *Bd* on its hosts given that *Bd* is a cold-adapted fungus and warmer temperatures are associated with faster amphibian immune responses (Rohr and Raffel 2010). To test the hypothesis that elevated environmental temperatures during the larval period negatively affect the ability of newly-metamorphosed froglets (the life stage most susceptible to chytridiomycosis; Rollins-Smith 1998) to defend themselves against the *Bd* fungus, I experimentally raised larvae from two populations of each of two species (northern leopard frog *Rana pipiens* and southern leopard frog *Rana sphenocephala*) under either their current or simulated future local pond temperatures. I then tested whether exposure to warmer temperatures during development, as predicted under global climate change, impacts later-life fitness and the development of the amphibian immune system.

I tested for direct effects of temperature treatment on growth and development to metamorphosis in all frogs. Then, I tested for direct and indirect effects of temperature on different measures of the innate immune system in the same subset of frogs (including both temperature treatments) at one- and two-months post-metamorphosis. Another subset of frogs from both temperature treatments was used for measurements of the adaptive immune system at one and two months post-metamorphosis. Finally, when another subset of frogs reached one to two weeks post-metamorphosis, I exposed them to *Bd.* I measured *Bd* load and probability of becoming infect during the eight weeks that followed. After infection, I compared splenocyte counts and the mucosome's ability to inhibit *Bd* among frogs from both temperature treatments and both (*Bd* and sham) exposure groups (Figure 2.2). I predicted that frogs that developed under future (warmer) climate conditions would have lower survival, a smaller size at metamorphosis, reduced immune function, and greater susceptibility to *Bd* relative to those developing under current (cooler) climate conditions. The results of this study bring us closer to understanding how climate change will impact amphibian populations, particularly those that are threatened with emerging pathogens such as *Bd*. Given the potential impact of climate change on disease dynamics, studies of this nature may be critical in developing strategies to promote the long-term health of threatened wildlife.

2.2 Methods

2.2.1 Temperature treatment design

To design current and future temperature regimes for each leopard frog population, I used the microclimate model of the Niche Mapper^{LLC} package (Kearney and Porter, 2017) to model water temperatures in the ponds where the egg masses were collected, including both daily and monthly variation, across the time period when leopard frogs would be undergoing embryonic and larval development. The Niche Mapper model uses meteorological variables, soil properties and terrain characteristics to predict the local microclimate (Kearney *et al.* 2014). To model water temperature in Niche Mapper, I started by collecting air temperature information for the current climate and a predicted future climate scenario from each egg collection site. For current climate, I used 30-year-average air temperatures for the years 1960-1990 from WorldClim (Fick and Hijmans 2005, 30 s or ~ 1 km^2 resolution). For future climate, I used air temperatures averages for the years 2061-2080. These were downscaled IPCC5 data, also at 30 s resolution, that were calibrated using the WorldClim 1.4 database. Specifically, I used the HadGEM2-ES global climate model (Collins *et al.* 2011) from IPCC5 with representative concentration pathway 60 (an intermediate gas emission scenario). Under this model, global temperatures are predicted to increase by an average of 1 to 2.5 °C between 2010 and 2070 (Collins *et al*. 2013). For each egg collection site, I set the properties of the substrate (thermal conductivity, density, and specific heat) to the values for fresh water at each month's average air temperature using the online applications Presto (v. 0.255, https://prestodb.io) and Niche Mapper (http://niche-mapper.com/). I set the percent of the substrate that acts like a free water surface to 100 % since I was modelling water temperature, and I set the substrate reflectivity to 12 %, which is the

average reflectivity of fresh water at an incident angle of 25 ° (Kirk, 1984). I used the monthly average minimum and maximum relative humidity and wind speed values recorded in 2017 at the nearest weather station (Figure B1, Appendix B) for both current and future climate models. The distances between the ponds where eggs were collected, and these weather stations are provided in Figure B1, Appendix B. The end result of our model was an average predicted 24 h temperature profile for each pond for each month under both current and predicted future climate scenarios.

I programmed environmental chambers (Conviron, model BDR16 and A1000 accurate to ± 0.5 °C) hour by hour so that the air temperature inside would fluctuate to match our predicted water temperature values for one egg collection site and temperature treatment (current vs. future). In each chamber, the temperature program was set to cycle from the average daily high-water temperature (which occurred at 18:00) to the average daily low water temperature (which occurred at 8:00) for a given month and back again within a 24 h period. Lights inside the chamber provided a photoperiod of 12 hours of light (600 - 1800 h) and 12 hours of dark. Throughout the experiment I had two temperature data-loggers inside each environmental chamber, one measuring water temperature in a volume of water equivalent to that in the tadpoles' enclosures (HOBO pendant temp/alarm one channel data loggers UA-001-08, accurate to ± 0.53 °C, Onset Computer Corporation, Bourne, MA). Another logger was suspended in the chamber to measure air temperature (HOBO Pro v2 Temperature/Relative Humidity U23-002 accurate to ± 0.21 °C, Onset Computer Corporation, Bourne, MA). The differences between measured air and water temperatures throughout the experiment can be found in (Table 2.1).

Following the predictions from our model, the difference in water temperature programs between current and future climate chambers (measured using data loggers) differed by egg

collection site. The minimum difference between the two treatments at any given time was 1.14 °C and the maximum was 4.29 °C. Under this model, the average temperature difference for all sites was 2.277 °C. The same temperature regime was applied each day for one month before switching to the temperature regime representative of the next month. The only exceptions to this occurred for the larvae from our Vermont and Pennsylvania collection sites, where the temperatures in both current and future climate treatments were maintained at modeled August pond temperatures for longer than one month (174 days for PA and 200 for VT). For these populations, the August temperatures were used until the end of the experiment because the larvae were developing so slowly, even at warm August temperatures, that I worried dropping temperatures to mimic September and later fall conditions would prohibit animals from metamorphosing at all.

Table 2.1 Modelled and measured water temperatures for each temperature treatment for each egg collection locality and month of the experiment.

Locality	Temperature treatment	Modelled month	Modelled daily min. (ºC)	Modelled daily max. (ºC)	Mean diff. (ºC)	SD (ºC)	SE (ºC)	Max Diff. (ºC)	Min Diff. (ºC)
LA	Future	February	8.89	10.96	-	-	-	-	-
LA	Future	March	12.5	15.21	-	-	-	-	-
LA	Future	April	16.64	19.68	-	-	-	-	-
LA	Future	May	21.74	24.96	0.55408	0.1287262	0.0252638	0.802	0.458
LA	Future	June	25.18	27.9	0.97327	0.1041491	0.0175301	0.522	1.022
LA	Future	July	26.1	29.33	1.36907	0.0263625	0.001533	1.27	1.652
LA	Future	August	27.06	29.49	-	-	-	-	-
LA	Current	February	6.77	8.67	-	-	-	-	-
LA	Current	March	10.34	12.81	-	-	-	-	-
LA	Current	April	13.79	16.55	-	-	-	-	-
LA	Current	May	18	20.86	-	-	-	-	-
LA	Current	June	21.87	24.34	-	-	-	-	-
LA	Current	July	22.62	25.46	-	-	-	-	-
LA	Current	August	23.03	25.19	-	-	-	-	-
TN	Future	March	4.92	8.01	-	-	-	-	-
TN	Future	April	9.81	12.12	-	-	-	-	-
TN	Future	May	15.51	18.64	0.33675	0.1487597	0.0345975	0.595	0.323
TN	Future	June	20.55	23.26	0.74783	0.1131538	0.0216457	0.831	1.363
TN	Future	July	23.48	25.96	0.32476	0.0437979	0.0077416	-0.248	2.865
TN	Future	August	23.49	25.99	0.12417	0.109788	0.0216637	0.023	2.017
TN	Current	March	4.15	7.11	-	-	-	-	-

Table 2.1 (continued)

TN	Current	April	8.47	11.93	-	-	-	-	-
TN	Current	May	13.58	16.47	0.59639	-0.0721425	-0.021617	0.519	0.466
TN	Current	June	18.44	20.81	0.26844	0.1002015	0.0215999	0.431	0.229
TN	Current	July	20.58	23.34	0.62573	0.0474237	0.0077818	0.24	1.763
TN	Current	August	19.92	22.41	0.75778	0.0434347	0.0065228	1.169	2.445
VT	Future	May	12.05	15.49	-	-	-	-	-
VT	Future	June	17.16	19.53	-0.41004	-0.0926854	-0.0199463	-0.229	0.2
VT	Future	July	20.57	23.99	0.19983	-0.1708824	-0.0369414	-0.168	1.873
VT	Future	August	19.1	22.76	-0.95001	-0.0188113	0.0009103	-1.398	-1.038
VT	Current	May	9.06	12.64	-	-	-	-	-
VT	Current	June	13.61	17.03	-0.40727	0.1426242	0.0341224	2.794	-0.06
VT	Current	July	17.16	19.53	0.47656	0.5869134	0.1271003	2.809	-1.059
VT	Current	August	18.16	15.77	-0.34603	0.0439915	0.0150092	-0.3	-1.607
PA	Current	June	10.23	12.28	-13.92542	-0.6266126	-0.1679171	-15.08	-13.02
PA	Current	July	15.33	17.21	-0.58618	-0.0046647	0.001604	-1.18	-0.633
PA	Current	August	17.67	19.77	-1.11211	-0.5658614	-0.122357	-5.824	0.279
PA	Current	September	16.7	18.49	-0.71055	-0.0991379	-0.0201326	-1.356	-0.43
PA	Future	June	12.64	14.59	0.71465	0.0294448	0.0110203	-0.298	-0.538
PA	Future	July	17.76	19.62	0.50577	0.0074583	-0.0001616	0.562	2.234
PA	Future	August	20.66	22.74	0.52222	-0.098195	-0.0233177	0.068	1.504
PA	Future	September	20.31	22.21	0.4649	-0.2590353	-0.0632313	-0.382	3.065

The absolute value mean (Mean diff.), standard error (SE), standard deviation (SD), maximum (Max Diff.) and minimum (Min Diff.) temperature differences between modeled water temperatures and water temperatures measured from within each environmental chamber are provided for each chamber and month where iButton temperature sensors were used to measure temperatures within the chamber

2.2.2 Animals

To begin this experiment, I collected naturally deposited egg masses from two populations of northern leopard frogs (*Rana pipiens*) and two populations of southern leopard frogs (*R. sphenocephala*) during the 2018 breeding season. The locations of these populations were chosen to represent different latitudes within each species' range (Figure 2.1). For *R. pipiens*, I collected egg masses on April 25th from near the Pymatuning Lab of Ecology in northwest Pennsylvania (PA: 41.672 °N, 80.513 °W) and on May 1st from just north of Burlington, Vermont (VT: 44.494 °N, 73.243 °W). For *R. sphenocephala*, the egg masses were collected on February 18th from Arnold Air Force Base in central Tennessee (TN: 35.450 °N, 86.070 °W) and on January 14th from Fort Polk Wildlife Management Area in central Louisiana (LA: 31.127 °N, 93.014 °W). The eggs from each location came from two different clutches and were shipped to the University of Pittsburgh (Pittsburgh, Pennsylvania, USA) in plastic containers or Ziplock bags. I held each egg mass at room temperature (measured as mean 18.3 and range 16 - 20 °C) in a separate 11 L (36.8 cm L x 22.2 W x 24.8 H) plastic tank filled with 7 L aged tap water until larvae hatched and reached the free-swimming stage (stage 21 of Gosner, 1960, 8 - 10 days after eggs were received).

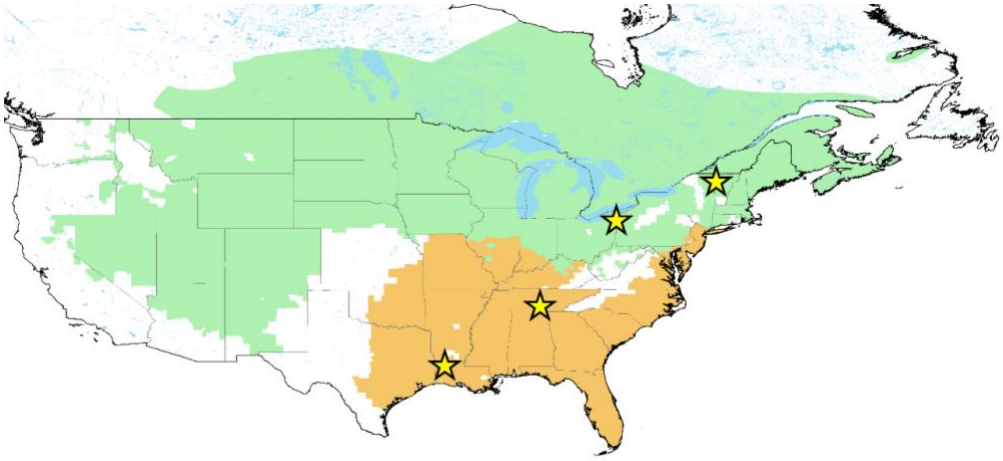

Figure 2.1 Map showing the four different locations where the egg masses were collected for the experiment (stars) and the ranges of R. pipiens (green shading) and R. sphenocephala (orange shading).

From north to south: Vermont *R. pipiens*, Pennsylvania *R. pipiens*, Tennessee *R. sphenocephala*, Louisiana *R. sphenocephala*. Blue shading indicates water areas, gray lines are U.S. state boundaries and black lines are U.S. and Canadian national boundaries. Species ranges are from the IUCN Red List of Threatened Species, Version 2020-3, https://www.iucnredlist.org, Downloaded on 24 February 2020.

When they reached the free-swimming stage (stage 25 of Gosner 1960), I moved the tadpoles to individual housing in 1 L plastic cups filled with 0.9 L aged tap water. Half of all tadpoles from each population were then assigned haphazardly to a "current" temperature treatment and the remaining tadpoles to a "future" temperature treatment. The plastic cups, each containing 1 tadpole, were then placed in an environmental chamber where the air temperature was gradually shifted (by 1 °C every 3 h) from room temperature to the maximum daily temperature of the tadpole's assigned population-specific current or future temperature regime (described above). Tadpoles remained in these environmental chambers until metamorphosis (Gosner stage 45). At the point when tadpoles entered their temperature treatments there were N = 135 - 190 tadpoles per treatment group (see Table 2.2 for details).

Table 2.2 Sample sizes for each treatment group for each experiment and assay performed.

	Louisiana		**Pennsylvania**		**Vermont**	
Temperature treatments	Current	Future	Current	Future	Current	Future
Temperature groups	135	145	190	184	152	148
Metamorphosis time	153-241	127-169	206-262	145-207	182-321	141-259
Immune Assays of Newly-metamorphosed Froglets						
Skin peptide collection (1 mo.)	11	9	7	11	5	7
Skin peptide collection (2 mo.)	12	5	7	11	5	7
AMPS (1 mo.)	-	-	3	4	5	3
AMPS (2 mo.)	-	-	4	6	5	3
Thymocytes	19	21	16	24	11	15
Splenocytes						
B-cell proliferation	9	10	10	12	5	9
T-cell proliferation	7	6	6	12	5	6
White blood cell counts	17	15	10	24	9	13
Exposure Experiment and Subsequent Immune Assays						
(*Bd*) or sham (S) exposure	*Bd* S	*Bd* S	*Bd* S	*Bd* S	*Bd* S	*Bd* S
Exposure groups	16 16	16 16	15 15	15 15	10 8	15 8
Splenocyte counts	9 12	13 9	13 14	11 14	7 7	14 7
Mucosome inhibition	8 7	7 8	4 8	7 9	9 7	6 8

From the time they reached the free-swimming stage until metamorphosis was complete, each tadpole was fed *ad libidum* with TetraMin Complete Diet Tropical Tablets (Tetra, Germany) dissolved in tap water three times a week. I did full water changes once a week and one half of the water was changed two more times each week such that the water was at least partially changed approximately every other day. I monitored survival and tadpole development daily, and when the forelimbs emerged (Gosner stage 42), each animal was moved to an individual 2.12 L (9.32 x 30.48 x 22 cm) rectangular plastic container filled to a depth of 1 cm with aged tap water. These containers were placed back into the same environmental chamber so that they continued to experience the same temperature treatment as they had previously. I tilted one end of each container to create a dry side to the habitat and provided a small plastic dome as a hide. At completion of metamorphosis (Gosner stage 45), I calculated larval period as the time between when tadpoles were placed in the chambers (Gosner stage 21) and when tail absorption occurred (Gosner stage 45) and recorded each animal's mass (using a scale accurate to 0.01 g), and snout-vent length (SVL, using dial caliper). At metamorphosis, frogs were removed from the environmental chambers and most were housed at room temperature. A subset of frogs were housed at 16 °C after metamorphosis and prior to *Bd* exposure (see Figure 2.2). After metamorphosis, water was changed twice per week and frogs were fed 5 - 10 crickets (3 – 4 mm in size) *ad libidum* three times a week.

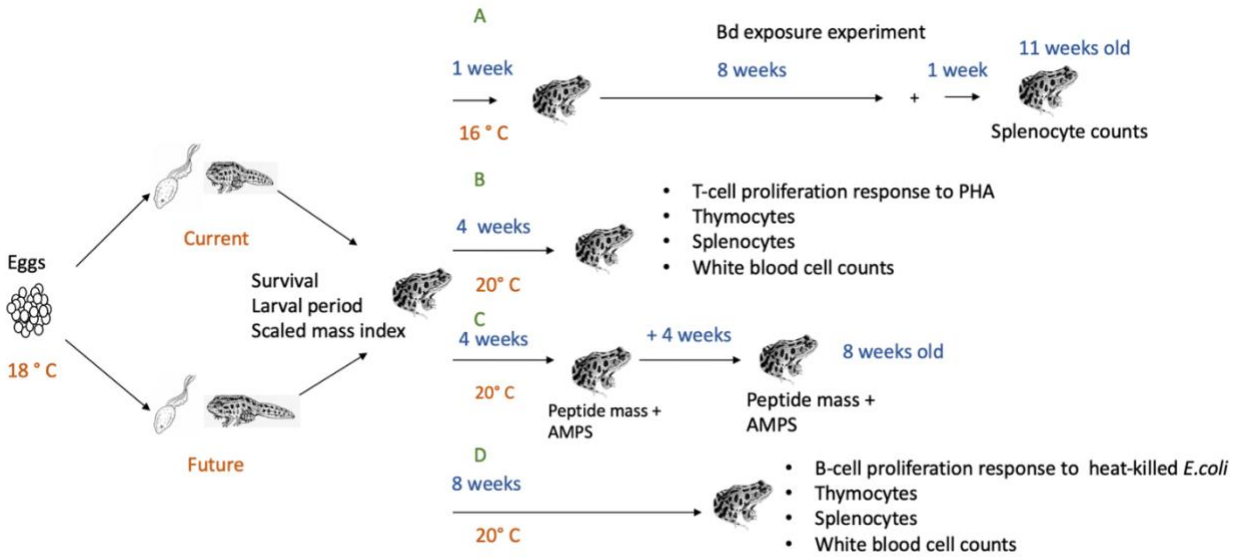

Figure 2.2 Experimental design indicating when each experiment took place.

In orange I show the temperatures at which the experiment took place and in blue the age of the frogs: A. *Bd* exposure experiment, which began at one week post-metamorphosis; B. Immune experiments that took place at four weeks post-metamorphosis; C. Immune experiments, which took place at four or eight weeks post-metamorphosis using a separate set of frogs than in B and D; D. Immune experiments that took place eight weeks post-metamorphosis using a separate set of frogs than in B and C.

2.2.3 Statistical analyses for comparisons of larval survival, growth and development

All statistical analyses were performed using R Studio 2019 (RStudio Team 2019) and R version 1.1.383 (R Core Team 2019). For each analysis, I used a separate statistical model for animals from each locality to compare survival, growth and development between animals that developed under current vs. future temperature scenarios. Statistical model results tables can be found in Appendix B (Tables B1-B79)

I compared tadpole survival, from the day animals were placed into their temperature regimes to the point of metamorphosis, among temperature groups using a Cox proportional

hazards model (package: ‘survival’, function: ‘coxph’), with days surviving as the dependent variable and temperature treatment as a factor. To compare larval period between temperature treatments I used a Cox proportional hazards model (package: ‘survival’, function: ‘coxph’), with larval period as the dependent variable and temperature treatment as a factor.

To compare body size (SVL) and mass at metamorphosis among temperature treatments I ran separate linear models (package ‘nlme’, function ‘lm’). If needed to meet the assumption of normality, I ran the models with either mass, or mass and SVL log transformed. I used mass and SVL as the dependent variables and temperature treatment (current vs. future) as a factor in each model.

2.2.4 Post-metamorphic treatments

After metamorphosis, I haphazardly assigned frogs to one of three treatment groups such that each group contained an approximately equal number of animals from each locality and temperature treatment group and also contained animals that spanned the range of developmental timing (i.e., time to metamorphosis) I observed in this study (Table 2.2, Figure 2.2). Using two of these groups, I conducted a variety of immune assays on *Bd*-naïve (never exposed or sham-exposed to *Bd*) juveniles, to assess the impact of exposure to current and simulated future temperatures on immune development, at one- and two-months post-metamorphosis. These two groups were shipped to Vanderbilt University, where the assays took place, when the frogs were one to three weeks post-metamorphosis. Using the third group of frogs, I ran a *Bd* exposure experiment (which began when the frogs were one to two weeks post-metamorphosis) and subsequently performed another set of immune assays to assess the combined impacts of developmental temperatures and *Bd* (vs. sham) exposure on immune development. At the end of

the experiment, all frogs were euthanized by bath in 1 % buffered tricaine methanosulfonate (MS-222, Sigma-Adrich, St Louis, Missouri, USA).

2.2.5 Immune assays of newly metamorphosed froglets

Statistical analyses for the immune assays described below often involved comparisons between models containing different sets of main effects. All models included temperature treatment (current vs. future) as a main effect. I also ran models that included the additional effects of mass at metamorphosis, growth rate (calculated as mass at one or two months old minus mass at metamorphosis divided by the number of days between the two time points), time to metamorphosis, and interactions between these variables and temperature on the dependent variables. The model with the lowest Akaike information criterion (AIC, an estimator of prediction error) is reported in the results. When the difference in AIC between two models was ≤ 2, I reported results from the simpler of the two models.

2.2.6 Skin peptide collection and quantification

The skin peptide sample collection was done at Vanderbilt University. Samples were collected from 5 - 12 animals (Table 2.2) per treatment at both one month and two months post-metamorphosis. Each frog was injected (in the dorsal lymph sac region) with norepinephrine (NE) bitartrate dissolved in amphibian phosphate buffered saline (APBS; 6.6 g of NaCl, 1.15 g of Na_2HPO_4, and 0.2 g of KH_2PO_4/liter of distilled water). For the one-month group, the frogs were injected with 10 nmol per gram body weight (gbw) NE and for the two months group, 20 nmol/gbw NE was used. After injection, the frogs were individually placed into 50 ml conical

tubes containing 10 ml HPLC grade water for 15 min to collect secretions before returning the frogs to their enclosures. Because froglets were quite small, the conical tubes allowed for movement and breathing air but also ensured that the water level covered the dorsum. After returning the frogs to their enclosures, the water was acidified in the 50 ml conical tubes with Trifluoracetic acid (TFA, added to achieve a 1% concentration). These samples were then stored at -80 °C prior to analysis.

The C18 Sep Pak cartridges were activated (Waters Corp, Milford, MA) with 10 ml of 100 % HPLC grade methanol, then washed them with 10 ml of Buffer A (0.1 % triflouroacetic acid in HPLC grade water) to prepare them. The skin secretion samples were dried under vacuum at 70 °C as they thawed (following Rollins-Smith *et al*. 2002). Next, the thawed skin secretion samples were passed over the activated Sep Paks, then washed the Sep Paks again with Buffer A. Then they were eluted in 11 ml of Buffer B (0.1 % triflouroacetic acid, 70 % acetonitrile, 29.9 % HPLC water). This resulted in concentrated skin secretion samples enriched for hydrophobic peptides. One ml of the eluted material was then used to quantify total peptides in the skin secretion and the remaining volume (10 ml) was sedimented under vacuum until dry in preparation for mass spectrometry (see below).

To quantify the total mass of peptides in a 1 ml sample of skin secretion, the Micro BCA™ Protein Assay Kit (Pierce Biotechnology, Rockford, IL) was used. The protocol in Rollins-Smith *et al.* (2002) was used with six bradykinin standards instead of BCA (bovine serum albumin) standards as bradykinin is more similar in size to the peptides I was measuring than BCA. A standard curve was run at the following concentrations: 200 µg/ml, 40 µg/ml, 20 µg/ml, 10 µg/ml, 5 µg/ml, 2.5 µg/ml, 1.0 µg/ml, and 0.5 µg/ml bradykinin. Using a 96-well microtiter plate, 100 µl of the peptide or standard sample was added to 100 µl of the working

reagent (supplied with the kit and diluted according to the manufacturer's instructions). All standards and samples were run in triplicate. Plates were incubated at 37 °C for 2 h, and absorbance was measured at 570 nm on a BioTek Elx808 spectrophotometer, using Gen5 2.01 software for analysis.

Mass spectrometry was used to identify, and obtain an approximate quantification of, antimicrobial peptides (AMPs) from the skin secretion samples. The dried peptide samples were resuspended at a concentration of 1 mg/ml in HPLC water and spotted them onto a Matrix Assisted Laser Desorption/Ionization (MALDI) plate at a 1:1 ratio with matrix [10 mg/ml α-cyano-4-hydroxycinnamic acid (Sigma, St. Louis, MO), 60 % acetonitrile, 39.6 % HPLC-grade water, and 0.4 % trifluoroacetic acid (v/v/v)]. An Ultraflex III time-of-flight mass spectrometer (Bruker Daltonics, Billerica, MA) was used and calibrated using the following standards (Sigma, St. Louis, MO): bradykinin fragment 1-7 (m/z 757.3997), human angiotensin II (m/z 1046.5423), $P_{14}R$ synthetic peptide (m/z 1533.8582), adrenocorticotropic hormone fragment 18-39 (m/z 2464.1989), and bovine oxidized insulin chain B (m/z 3494.6513). For each standard and peptide sample, 250 laser shots were collected (following Woodhams *et al.* 2006). Spectra were analyzed with Data Explorer v4.4 software (Applied Biosystems, Foster City, CA). The 19 most common AMPs in *R. pipiens* and closely related species secretions have been previously described (Tennessen *et al*. 2009), although only 7 were previously reported for *R. pipiens* in Vermont. For *R. sphenocephala*, there have only been 4 peptides described (Holden *et al*. 2015; Colon *et al.* 2003). I used the Tennessen *et al.* (2009) and the Holden *et al.* (2015) peptide list and their reported peptide centroid masses to determine the presence/absence and relative intensities of these common AMPs. As a more conservative approach, I also analyzed the data using only the AMPs previously described for *R. pipiens* from Vermont to compare more specifically

differences in peptides from the Vermont and Pennsylvania *R. pipiens* in this study as the AMPs in *R. pipiens* from Pennsylvania have not been described. In data matrices representing relative intensities of AMPs I used zeros to denote non-detection of individual peptides.

2.2.7 Skin peptide analyses

To test for differences in the total secreted peptides, corrected for body weight (μg/gbw), among animals from different temperature treatments, I log transformed these values, as measured from frogs at one month and two months post-metamorphosis to meet the assumption of normality. I then ran separate linear models (package 'nlme', function 'lm'), with peptide concentration as the response variable, for frogs at one- and two-months post-metamorphosis.

To test for differences in the composition and intensities of skin peptide samples collected from frogs that developed as larvae in the different temperature treatments, I used a non-metric multidimensional scaling (NMDS) ordination to compare the Bray-Curtis distance (a metric of compositional dissimilarity) among samples, using the 'metaMDS' command ('Vegan' package). I then used the 'Adonis' function in the Vegan package (Oksanen *et al.* 2013) to carry out a permutation-based multivariate analysis of variance (PERMANOVA). PERMANOVA tests were run using the Bray-Curtis distance comparisons of peptide presence/absence and peptide relative abundances among temperature treatments for frogs from each locality, using 9,999 permutations. The dependent variable for these models was either peptide presence/absence or the intensity of the mass signal for each peptide, and temperature treatment was the main effect. I did not run models containing other main effects or interaction terms because sample sizes were small.

To compare the total number of antimicrobial peptide species detected among frogs raised under different temperature treatments, I used a generalized linear model (Package MASS, function glm) with a Poisson distribution. The total number of peptide species was the dependent variable and temperature treatment was the main effect. Again, due to small sample sizes, models containing other main and interaction effects were not run.

2.2.8 White blood cell counts

The animals were euthanized at Vanderbilt University, after weighing and measuring them, with an overdose of 1% buffered tricaine methanosulfonate (MS-222). A cardiac puncture was used on euthanized frogs to collect blood samples in capillary tubes. This was done before dissecting the spleen and thymus. The white blood cells were stained with Trypan Blue (Sigma, T-6146), which permitted counting of only live cells. Splenocytes, thymocytes (see below) and white blood cells were counted from one group of animals at one-month post-metamorphosis and another set of animals at two months post-metamorphosis (11 - 24 animals per group, see Table 2.2). White blood cells were counted in whole blood diluted 50-fold with APBS, using a hemocytometer to estimate cells/ml. They divided the total white blood cell counts by the total animal body weight to estimate white blood cell concentrations as cells/ml.

2.2.9 White blood cell analyses

To compare the white blood cell concentrations among frogs from different temperature treatments I ran a linear model (package ‘nlme’, function ‘lm’) with white blood cell concentration as the response variable.

2.2.10 Lymphocyte counts

Splenocytes and thymocytes were counted at Vanderbilt University to compare lymphocyte activity among frogs from the current and future temperature treatments. The same two sets of animals were used, at one month and two months post-metamorphosis, that were used for the white blood cell counts described above (see Table 2.2). Spleens and thymuses were dissected and placed individually on autoclaved depression slides in 200 µl of complete L-15 medium (L-15 medium supplemented with 100 I.U./mL penicillin, 100 µg/mL streptomycin, 1% Tetracycline, 12.5 mM sodium bicarbonate, 50 µM 2-mercaptoethanol, 2 mM L-glutamine, and 1% heat inactivated fetal calf serum). Spleens and thymuses were disassociated separately using forceps and counted live (Trypan blue stained) lymphocytes using a hemocytometer. Lymphocytes were counted using the total sample volumes (whole organs). When only one thymus was found, (this happened for two animals from Pennsylvania and two from Louisiana), the number of cells found in the one thymus was multiplied by two for comparison with samples in which cells in both thymuses were counted. After counting, splenocytes were cultured to measure activity (see below).

2.2.11 Lymphocyte analyses

To compare thymocyte and splenocyte cell counts among frogs from the two temperature treatments, I log transformed the counts to meet the assumption of normality and ran linear models (package nlme, function lm). For both thymocytes and splenocytes, I used log transformed cell count as the response variable. Splenocyte counts were divided by animal body weight (gbw) for analysis.

2.2.12 T- and B-cell proliferation

To compare lymphocyte proliferation among frogs from the two temperature treatments, splenocyte proliferation was measured in response to a T-cell mitogen (Phytohemagglutinin, or PHA at 2 μg/ml) and a B-cell mitogen (heat-killed *E. coli* at 10^7/ml) using splenocyte samples collected from 5 - 12 animals per treatment at one month (T-cells) or two months (B-cells) post-metamorphosis (Table 2.2). Splenocytes were measured at a concentration of 10,000 cells/well in L-15 medium in the presence of one of these two mitogens at 26 °C in 5 % CO_2, 95 % air in a laminar flow hood. When it was not possible to obtain 10,000 splenocytes from a single animal (Louisiana samples: 27/40, Pennsylvania samples: 4/40, Vermont samples: 2/26 individuals), the sample was divided among two wells to compare proliferation in one well containing the mitogen to the background proliferation in the well containing splenocytes and L-15 medium only. T-cell and B-cell assays were cultured for 3 and 5 d, respectively, and pulsed with 0.5 μCi ^{3}H-thymidine (5 μCi/mL, specific activity 2 Ci/mmole) (Perkin Elmer, Waltham, MA, USA) 24 h before harvesting cells. Proliferation was measured by a scintillation counter (Beckman LS 6500) to quantify the uptake of ^{3}H-thymidine and recorded as counts per minute (CPM). Response was calculated as the average CPM in wells with PHA or *E. coli*, divided by the average CPM in wells with splenocytes only (no mitogen).

2.2.13 T- and B-cell proliferation analysis

For comparisons of T- and B-cell proliferation among frogs from different temperature treatments, I log transformed CPM ratios (mitogen present / mitogen absent) to achieve

normality, then ran linear models (package nlme, function lm) with log (CPM ratio) as the response variable.

2.2.14 Bd exposure and subsequent immune measurements

The group of 56 frogs (10 – 16 animals per temperature treatment, see Table 2.2) that I exposed to *Bd* was housed at 16 °C from metamorphosis until the end of the experiment. Fifteen to twenty days after metamorphosis, I haphazardly chose approximately half of these animals to expose to *Bd* and the remainder were sham-exposed (see Table 2.2). To prepare the *Bd* inoculate, I used one-week-old cultures of the "Section Line" isolate of *Bd* (passage # 12) grown in liquid TGhL broth (16 g tryptone, 4 g gelatin hydrolysate, 2 g lactose, 1000 ml distilled water; Longcore *et al*. 1999) to seed *Bd* growth on agar plates. The plates were inverted and incubated at 21 °C for one week before I flooded them with DI water to collect zoospores for inoculation. I exposed each frog individually to the same quantity of *Bd* zoospores (10^6 per inoculation) every two weeks for a period of 8 weeks (i.e., 4 inoculations). Animals were inoculated individually in 100 mL plastic containers containing 40 mL of inoculum for 24 h before being returned to their Ziplock containers. I sham-exposed control frogs following the same schedule and protocol but using inoculum I created by flooding blank (no *Bd*) agar plates with DI water.

Prior to each inoculation and at the end of the experiment (on days 0, 14, 28, 42 and 56), I measured each animal's SVL and mass and collected a skin swab to test for *Bd*. To estimate infection load, I swabbed (using a Medical Wire and Equipment #MW113 swab) each frog five times on each of the dorsal surface, ventral surface, each side of the body and each limb, making sure to rotate the swab while taking the samples. The swabs were stored at -20 °C prior to DNA extraction.

To quantify *Bd* DNA from swab samples, I extracted genomic DNA from each swab using the "animal tissue" protocol and the Qiagen DNeasy Extraction Kit with a final elution volume of 200 µl. I then ran a qPCR assay (Boyle *et al.* 2004) using a QuantStudio™ 3 Real Time PCR system. I used 25 µl reactions containing 12.5 µl of 2x SensiFast probe Lo-Rox Master Mix (Bioline, London UK), PCR primers at a concentration of 900 nM, the MGB probe at 240 nM, 400 ng/µl BSA, 3 µl water, and 5 µl of template DNA. Positive (known to contain *Bd* DNA) and negative (same master mix but with molecular grade water added instead of DNA template) amplification controls and a 6-fold dilution series of plasmid-based standards (Pisces Molecular, CO) were included on each qPCR reaction plate. I used the default QuantStudio software (V.1.4) conditions for amplification (2 min at 50 °C and 10 min at 95 °C, followed by 50 cycles of 15 s at 95 °C and 1 min at 60 °C). I report infection load in terms of *Bd* DNA copies (= plasmid equivalents). To estimate the *Bd* load on a swab, I multiplied the number of DNA copies detected in the qPCR reaction by 40 (since I used $1/40^{th}$ of the DNA extracted from the swab in each reaction).

2.2.15 Statistical analyses of infection and disease indicators

To test for differences in *Bd* infection load across temperature treatments, I built generalized linear mixed models (function 'glmer') using Template Model Builder (package 'glmmTMB'). The response variable in each analysis was the log-transformed *Bd* load (*Bd* DNA copies +1) detected on each skin swab sample and the fixed effects were temperature treatment and the interaction between temperature treatment and time since first exposure. Individual frog ID was included as random effect in each model. I used a Gaussian (function 'gaussian') distribution because the data was normally distributed. I also tested for differences in the

probability of infection among temperature treatments by coding individuals as positive/negative for *Bd* for a given sampling period based on whether (or not) *Bd* DNA was detected on their swab sample using qPCR. For this analysis, I used generalized linear mixed models (package 'lme4') with a binomial (function 'glmer') distribution, temperature treatment and the interaction between temperature treatment and time since first exposure were included as fixed effects and individual frog ID was included as a random effect.

I compared body condition between sham- and *Bd*-exposed and animals that developed as larvae under different temperature treatments using scaled mass index as the dependent variable. I calculated scaled mass index using the 'smatr' package, which tests for a common slope amongst several allometric lines and used the animal's mass just before the first exposure as a reference for the slope. To compare scaled mass index among *Bd*-exposed frogs from the two larval temperature treatments I used linear mixed models ('nlme' package function 'lme') with temperature treatment, time since first exposure, and their interaction as fixed effects. Individual frog ID was included as a random effect.

To compare survival among *Bd*-exposed frogs and among temperature treatment groups, I used a Cox proportional hazards model ('survival' package, 'coxph' function), with days surviving as the dependent variable and larval temperature treatment as the only factor.

2.2.16 Splenocyte counts

At the end of the exposure experiment (56 days after initial exposure, when the frogs were two and a half months post-metamorphosis), I weighed the frogs and euthanized them by bath in 1% buffered tricaine methanosulfonate (MS-222, Sigma-Adrich, St Louis, MO, USA) I then dissected spleens from 7 - 14 frogs per treatment group (Table 2.2) and placed the spleens

individually on autoclaved depression slides in 20 µl sterile amphibian phosphate buffered saline (APBS; 100 mL PBS with 25 mL water). I used a slightly different procedure for breaking open the spleen and counting the splenocytes than described above for newly metamorphosed frogs. This time, I disassociated the spleens using 25-gauge needles and added 20 µl of Trypan blue stain (Sigma/Alrich, St. Louis, MO, USA) to each sample. I then used a hemocytometer to estimate live cell densities. I counted cells using the hemocytometer, counting cells in two to three 10 µl volumes and averaging those values. Following the hemocytometer's instructions, I divided that count by the number of grid squares from which I counted cells and multiplied by 10,000 to convert the volume to ml. I then divided by frog mass to yield the number of spleen cells per ml per gram body weight (cells/gbw).

2.2.17 Post-exposure splenocyte analysis

To test for differences in splenocyte concentrations between frogs from the two exposure and two temperature treatment groups, I log transformed the cell counts (cells/ml/gbw) to meet the normality assumption. To compare these counts between temperature treatments, I ran a linear model (package 'nlme', function 'lm') with log splenocyte cells/ml/gbw as the response variable.

2.2.18 Mucosome collection

I collected skin mucus from the *Bd*-exposed and sham-exposed frogs (Table 2.2) from each temperature treatment after two weeks of *Bd* (or sham) exposure to test for differences in the ability of the "mucosome" to kill *Bd in vitro* (Woodhams *et al*. 2014). The mucosome

includes secondary metabolites, AMPs, lysozymes, mucosal antibodies, and alkaloids. To collect the mucosome, each frog was rinsed in 10 ml of molecular grade water for 1 h in a 50 ml conical tube. The frog was then returned to its enclosure and the rinse water was immediately passed through a 0.22 μm filter to remove live bacterial cells. The filtered samples were then stored at -20 °C prior to growth challenge assays (described below).

2.2.19 Mucosome effects on *Bd* viability

To assess the effect of whole mucosome on *Bd* zoospore viability, cell proliferation was quantified by ATP detection by the Woodhams Lab at the University of Massachusetts, Boston. To begin, each mucosome sample was lyophilized until completely dry and resuspended in 1 ml of sterile molecular grade water. The concentration of a 4-day old culture of the "Section Line" *Bd* isolate (passage #15) was quantified using a hemocytometer and diluted to a concentration of 10^6 zoospores/ml. This process generally followed the mucosome viability assay setup of Woodhams *et al*. (2014), but the assay was slightly modified so that the CellTiter-Glo 2.0 (Promega) kit could be used to measure zoospore viability.

Each sample was run in five wells: 3 (triplicate) wells containing *Bd* plus media (1% tryptone) and 2 (duplicate) wells containing sterile media only. The duplicate media only wells were included to facilitate background correction, due to the potential for ATP presence in the mucosome. For each sample, 25 μl of *Bd* solution (or sterile medium alone) and 25 μl of the mucosome sample were added to each well. Each plate contained 6 positive control wells (containing 25 μl of *Bd* solution plus 25 μl of sterile MilliQ water, and 6 negative control wells (containing 25 μl of heat killed *Bd* plus 25 μl of sterile MilliQ water) for zoospore viability. Three nutrient background wells (to account for the potential presence of ATP in the water and

media) were also included on each plate. These contained 25 µl of media plus 25 µl of sterile MilliQ water.

After setup was complete, each plate was incubated for 1 h at 21 ºC, then in a dark room, 50 µl of CellTiter-Glo 2.0 Reagent was added to each well to make a 1:1 solution, and the plate was covered with a foil sealing film. The plates were then placed on a shaker for 3 min at 200 rpm, then removed and incubated at 21 ºC for 15 min to lyse the cells and release ATP. Plates were then read using a luminescent channel of a POLARstar Omega microplate reader. To calculate percent zoospore viability, the average media control (media plus MilliQ water) luminescent reading value was subtracted from each positive and negative zoospore viability control. The background luminescent readings (duplicate wells containing media plus mucosome) were averaged for each sample and this value was subtracted from each of the triplicate sample replicates that contained mucosome and *Bd*. The readings were averaged for replicates of negative *Bd* viability control wells, and this value was subtracted from each of the other wells (mucosome and positive control wells) to remove the ATP value of dead *Bd*. Finally, the resulting values were averaged for the positive control replicates the background-corrected sample well values were divided by the average positive control value to get a proportional cell viability. These triplicate proportional cell viability values were then averaged for each sample prior to statistical analysis.

To test for a difference in the viability of *Bd* zoospores following exposure to mucosome from frogs that developed under current and future temperature treatments, and among exposure groups, I log transformed the proportional cell viability values to meet the normality assumption. To compare these values among *Bd*- and sham-exposed frogs from the two temperature

treatments, I ran linear models (package ‘nlme’, function ‘lm’) with log (proportion viable cells) as the response variable.

2.3 Results

2.3.1 Survival

In each population and temperature treatment, fewer than half of all tadpoles survived to metamorphosis. Survival to metamorphosis was observed in 34/152 (22 %) current temperature and 53/148 (35.82 %) future temperature treatment *R. pipiens* tadpoles from Vermont and in 57/190 (30 %) current temperature and 78/184 (42 %) future temperature treatment *R. pipiens* tadpoles from Pennsylvania. For *R. sphenocephala*, tadpoles from Tennessee experienced 0 % (0/190 animals) survival in both temperature treatments whereas 73/135 (42 %) current and 44/145 (33 %) future temperature animals from Louisiana survived to metamorphosis. I saw differences among populations and species in terms of which temperature treatment experienced greater survival. For *R. pipiens*, survival to metamorphosis did not differ significantly between temperature groups for animals from Vermont (COXPH: $\chi^2_1 = 0.4633$, $p = 0.496$; Figure 2.3A), but animals from Pennsylvania had significantly greater survival in the future temperature treatment (COXPH: $\chi^2_1 = 6.0257$, $p = 0.014$; Figure 2.3B). None of the *R. sphenocephala* animals from Tennessee survived to metamorphosis, but tadpoles in future temperature treatment survived longer (COXPH: $\chi^2_1 = 53.789$, $p < 0.001$; Figure 2.3C). Only for the *R. sphenocephala* from Louisiana was survival to metamorphosis reduced in the future temperature treatment (COXPH: $\chi^2_1 = 15.255$, $p < 0.001$; Figure 2.3D), as we had predicted it would be.

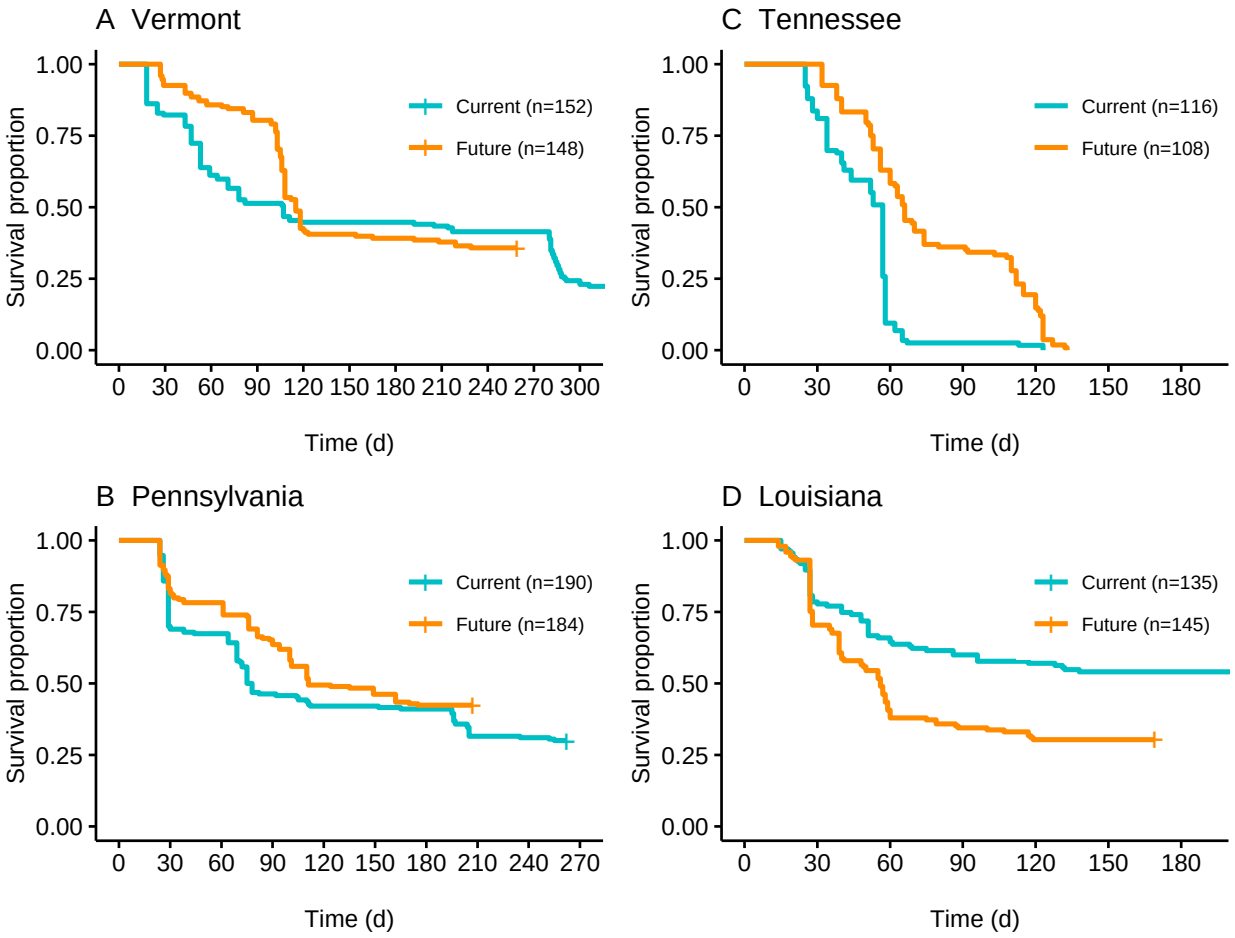

Figure 2.3 Larval survival curves.

A.) Vermont *R. pipiens* (COXPH: p = 0.496), B.) Pennsylvania *R. pipiens* (COXPH: p = 0.014), C.) Tennessee *R. sphenocephala* (COXPH: p < 0.001), and D.) Louisiana *R. sphenocephala* (COXPH: p < 0.001). Day zero is the day when the tadpoles were placed inside the temperature treatments (at Gosner stage 25).

2.3.2 Larval period

Larval periods for animals from Vermont, Pennsylvania and Louisiana populations were shorter in the future temperature treatment than in the current temperature treatment (COXPH: $\chi^2_1 \geq 38.752$, $p < 0.001$; Figure 2.4). The shortest larval periods we observed for Vermont, Pennsylvania and Louisiana were similar across species and populations (range: 127 – 153 d) for animals from the future temperature treatments whereas the longest larval periods (range 241 – 321 d) for animals from the current temperature treatments differed more dramatically, with some *R. pipiens* individuals from Vermont taking more than 300 d to metamorphose.

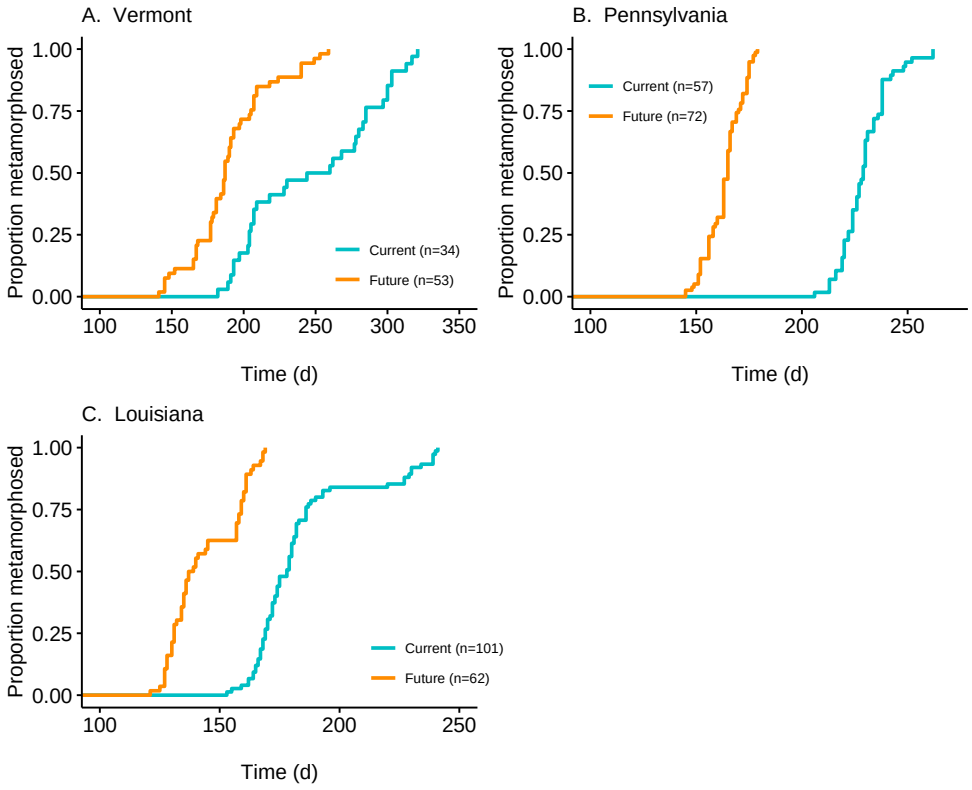

Figure 2.4 The proportion of individuals that successfully metamorphosed (tail fully absorbed, Gosner stage 46) from each temperature treatment, from the Vermont and Pennsylvania R. pipiens and the Louisiana R. sphenocephala populations.

For *R. pipiens* from Vermont, larval period ranged from 141 – 321 d (current temperature mean: 248 d, range 182 to 321 d; future temperature mean: 190 d, range 141 – 259 d; COXPH: $p < 0.001$). For *R. pipiens* from Pennsylvania, larval period ranged from 145 – 262 d (current temperature mean: 230 d, range 206 - 262 d; future temperature mean: 164 d, range 145 – 207 d; COXPH: $p < 0.001$). For *R. sphenocephala* from Louisiana, larval period ranged from 153 – 241 d (current temperature mean: 184 d, range 153 – 241 d; future temperature mean 144 d, range 127 - 169 d (COXPH: $p < 0.001$).

2.3.3 Mass at metamorphosis

Regardless of population of origin, *R. pipiens* that developed in the future temperature treatment had lower mass at metamorphosis than animals that developed in the current temperature treatment (LM: Vermont $F_{1,84} = 62.778$, $p < 0.001$; Pennsylvania $F_{1,133} = 134.39$, $p < 0.001$; Figure 2.5). However, for *R. sphenocephala* from Louisiana there was not a significant difference in mass between metamorphs from the current and future temperature treatments (LM: $F_{1,97} = 0.396$ $p = 0.531$).

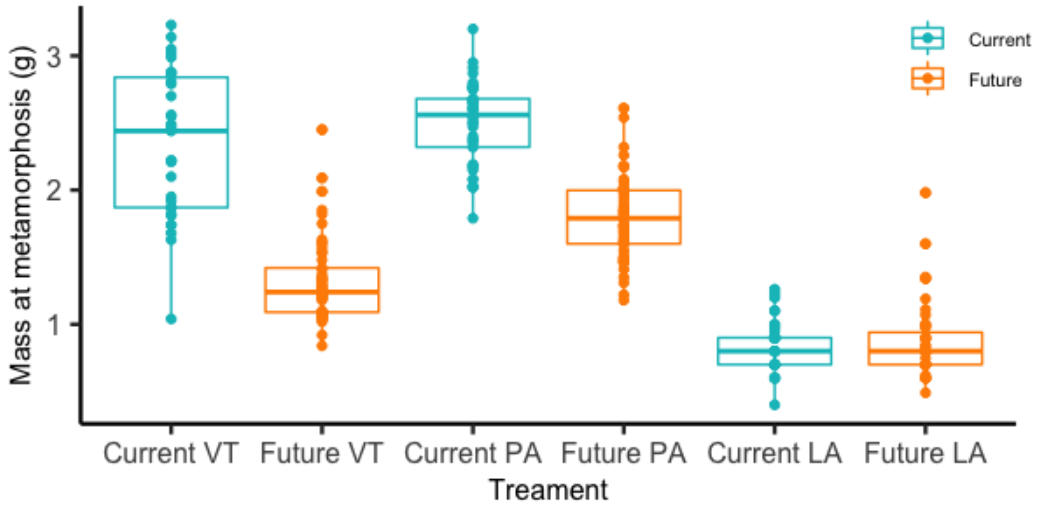

Figure 2.5 Box plots showing mass at metamorphosis (g).

For frogs reared in current and future temperature treatments from Vermont (VT), Pennsylvania (PA), and Louisiana (LA). For Vermont *R. pipiens*: current temperature treatment, mean = 2.35 g, range = 1.04 to 3.23 g; future temperature treatment mean = 1.32 g, range = 0.84 to 2.45 g. For *R. pipiens* from Pennsylvania, current temperature treatment mean = 2.50 g, range = 1.79 to 3.20 g; future temperature mass mean = 1.79 g, range = 1.18 to 2.61 g. For *R. sphenocephala* from Louisiana, current temperature treatment mean = 0.84 g, range = 0.40 to 1.26 g; future temperature mean = 0.87 g, range = 0.49 – 1.98 g. The middle line corresponds to the median. The lower and upper

hinges correspond to the first and third quartiles (the 25th and 75th percentiles). The upper whisker extends from the hinge to the largest value no further than 1.5 times the inter-quartile range.

2.3.4 Body size (SVL)

For all three populations that survived to metamorphosis, animals from the future temperature treatment were smaller in size at metamorphosis, as determined by SVL, than animals from the current temperature treatment (ANOVAs: Vermont *R. pipiens*: $F_{1,85} = 83.469$, $p < 0.001$; Pennsylvania *R. pipiens:* $F_{1,133} = 187.83$, $p < 0.001$; Louisiana *R. sphenocephala:* $F_{1,97} = 4.602$ $p = 0.034$; Figure 2.6).

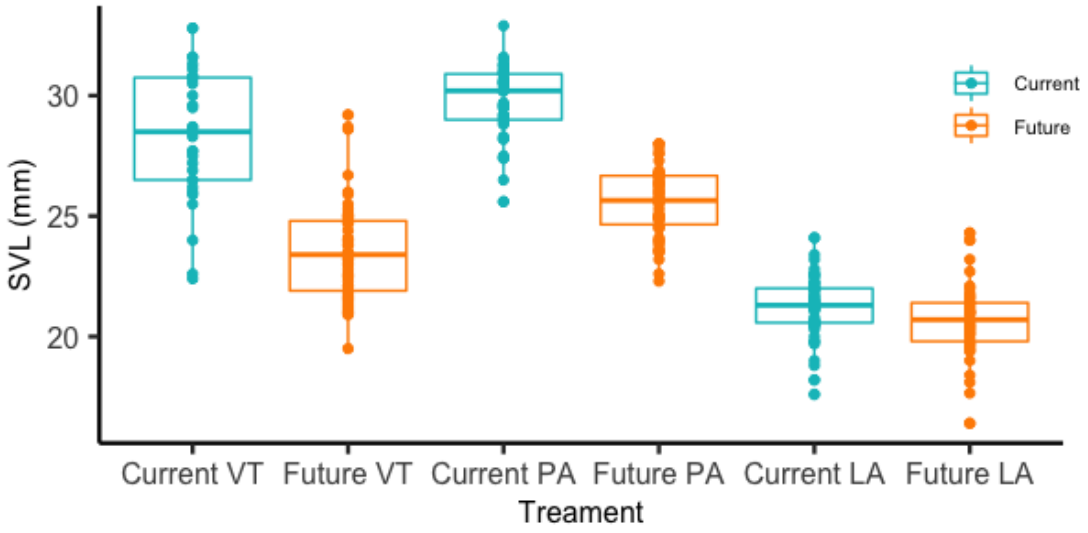

Figure 2.6 Box plots showing snout-vent length (SVL) at metamorphosis for frogs from current and future treatments.

For Vermont *R. pipiens* from the current temperature treatment mean = 28.4 mm, range = 22.4 to 32.8 mm; future temperature treatment mean = 23.519 mm, range = 19.5-29.2 mm. For *R. pipiens* from Pennsylvania, current temperature treatment mean = 29.8 mm, range = 25.6 to 33.9 mm; future temperature treatment mean = 25.6 mm, range = 19.5 to 29.2 mm). For *R. sphenocephala* from Louisiana, current temperature treatment mean = 21.3 mm,

range = 17.6-24.1 mm; future temperature treatment mean = 20.7 mm, range = 19.5 – 29.2 mm. The middle line corresponds to the median. The lower and upper hinges correspond to the first and third quartiles (the 25th and 75th percentiles). The upper whisker extends from the hinge to the largest value no further than 1.5 times the inter-quartile range.

2.3.5 Total peptides in skin secretions

For *R. pipiens* from Vermont at both one-month and two-months post-metamorphosis, the best model for variation in total peptides secreted was the simplest one, which included temperature treatment as a main effect but did not include any other main effects or interactions with temperature treatment (one-month: AIC = 9.867, ΔAIC = 1.591; two-months: AIC = 3.759, ΔAIC = 0.795; Table 2.3). At both time points, Vermont frogs that developed in the current temperature treatment secreted more peptides than the frogs from the future temperature treatment (LMs: one-month $F_{1,10} = 5.735$, $p = 0.038$; two-months $F_{1,10} = 10.840$, $p = 0.008$; Figures 2.7A, 2.7B).

For Pennsylvania *R. pipiens*, at one-month and two-months post-metamorphosis, I chose the simplest model (with only temperature treatment as a main effect) one-month: AIC = 1.301, ΔAIC = 0.265; two-months: AIC = 14.010, ΔAIC = 1.846; Table 2.3). However, at neither time point was there a significant effect of temperature treatment on the amount of peptides secreted (LMs: one-month $F_{1,16} = 0.700$, $p = 0.416$; two-months $F_{1,16} = 0.622$, $p = 0.442$). Frogs that developed in the current temperature treatment secreted a mean of 1.805 (range: 1.472 – 2.208) log (ug/gbw) at one month and a mean of 2.147 (range: 1.289 – 2.485) log (ug/gbw) peptides at two months post-metamorphosis. Frogs that developed in the future temperature treatment

secreted a mean of 1.711 (range: 1.424 – 2.087) log (ug/gbw) at one month and a mean of 2.020 (range: 1.660 – 2.351) log (ug/gbw) peptides at two months post-metamorphosis.

For Louisiana *R. sphenocephala*, the model with the lowest AIC at one-month post-metamorphosis included an interaction between temperature treatment and growth rate (from metamorphosis to one month old) (AIC = -4.917, ΔAIC = 4.001; Table 2.3). The model with the lowest AIC at two-months post-metamorphosis included an interaction between temperature treatment and time to metamorphosis (AIC = 1.242, ΔAIC = 5.308; Table 2.3). At both time points, frogs that developed as larvae in the current temperature treatment secreted more peptides than frogs from the future temperature treatment (LMs: one-month $F_{1,13} = 5.990$, $p = 0.030$; two-months $F_{1,10} = 8.334$, $p = 0.017$; (Figure 2.7C, 2.7D). Growth rate (one-month: $F_{1,13} = 1.710$, $p = 0.214$) and time to metamorphosis (two-months: $F_{1,10} = 0.083$, $p = 0.780$) did not have significant main effects on total peptides. At the one-month time point, frogs that had a faster growth rate in the future chamber secreted a lower quantity of peptides (LM, temperature treatment x growth rate interaction: $F_{1,13} = 28.714$, $p < 0.001$, $\beta = -185.522$, Figure 2.7C). At two-months post-metamorphosis, frogs that took longer to metamorphose in the future chamber secreted lower quantities of peptides (LM, temperature x time to metamorphosis interaction: $F_{1,10} = 9.195$, $p = 0.013$, $\beta = -0.058$, Figure 2.7D). The number of samples for this population at two months post metamorphosis was very small ($n = 5$), so these results should be interpreted with caution.

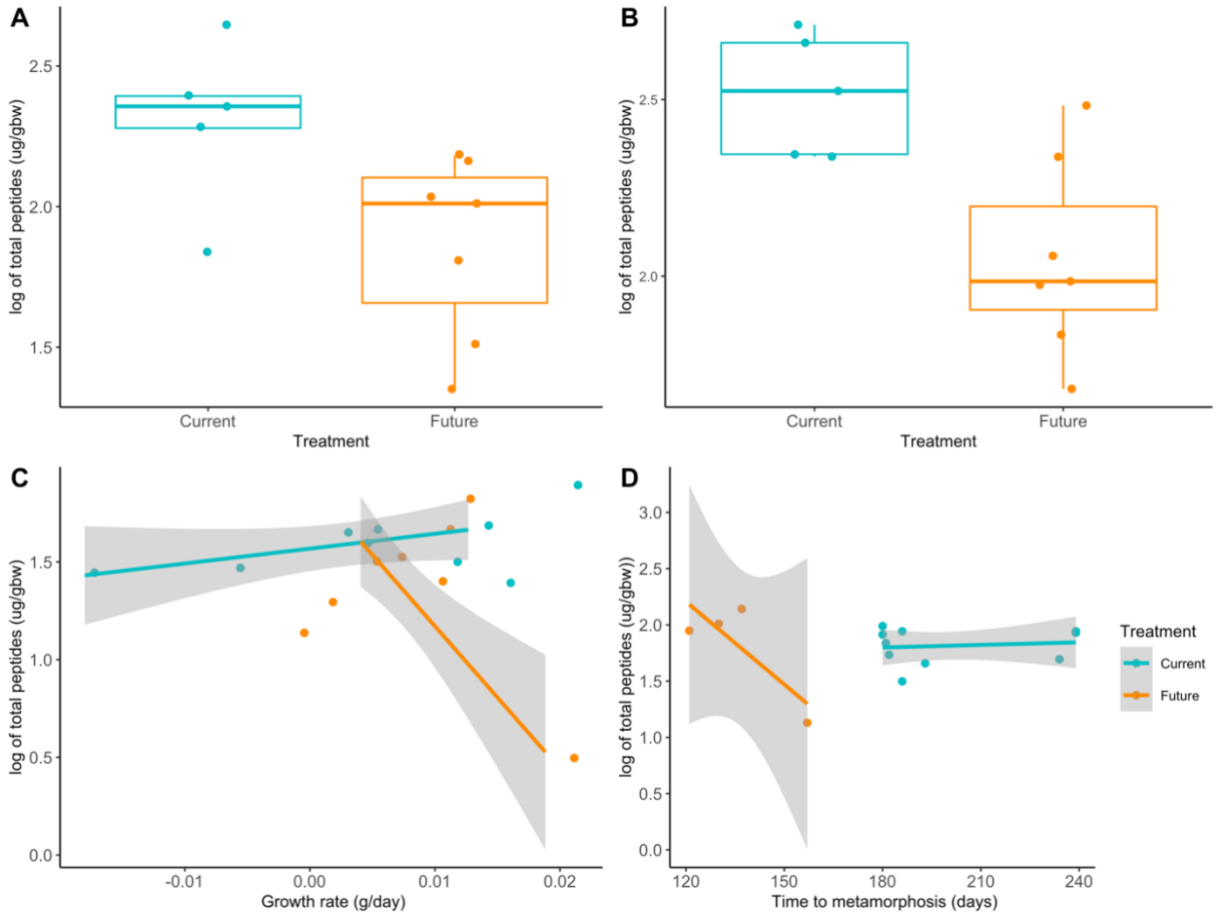

Figure 2.7 Box plots showing total peptides secreted (in µg per g body weight, or µg/gbw) for R. pipiens from Vermont.

(A) one month post-metamorphosis: current temperature treatment mean = 2.303, range = 1.844 to 2.642 log (µg/gbw); future temperature treatment mean = 1.867, range = 1.355 – 2.180 log (µg/gbw), and (B) two months post-metamorphosis: current temperature treatment mean = 2.516, range = 2.338 – 2.711 log (µg/gbw); future temperature treatment mean = 2.050, range = 1.681 – 2.483 log (µg/gbw). In (C), the scatter plot and lines of best fit are for the relationships between total peptides, in log (µg/gbw), and growth rate (g/day) for R. sphenocephala from Louisiana at one month post metamorphosis. (D) scatter plot and lines of best fit for the relationships between total peptides, in log (µg/gbw), and time to metamorphosis (days) for R. sphenocephala from Louisiana at two months post-metamorphosis. Each point represents one individual and the shaded area represents 95 % confidence intervals. In the boxplots, the middle line corresponds to the median. The lower and upper hinges correspond to the first and third quartiles (the 25th and 75th percentiles). The upper whisker extends from the hinge to the largest value no further than 1.5 times the inter-quartile range.

2.3.6 Secretion of antimicrobial peptides

I found 14 out of the 19 peptides described by Tennessen (2009) for *R. pipiens* in different parts of the United States in our samples from Vermont frogs. The best model to describe variation in the number of AMPs present in skin secretion samples from this population included the interaction between temperature treatment and time to metamorphosis for frogs at both one months (AIC = 48.302, ΔAIC = 2.643; Table 2.3) and two months (AIC = 51.865, ΔAIC = 4.555; Table 2.3) post-metamorphosis. At both time points, frogs reared under the current temperature treatment had a greater number of AMPs present in their secretions (GLM; one-month: $\chi^2_1 = 5.132$, $p = 0.024$, two-months: $\chi^2_1 = 11.995$, $p < 0.001$; Figure 2.8A, 2.8B) but the main effect of time to metamorphosis was not significant (GLM: one-month: $\chi^2_1 = 0.037$, $p = 0.847$, two-months: $\chi^2_1 = 0.185$, $p = 0.668$). There was also a significant interaction between temperature treatment and time to metamorphosis at one and two months old. At both time points, frogs in the future temperature treatment that took longer to reach metamorphosis had a greater number of AMPs present in their secretions, but for frogs in the current temperature treatment the number of peptides we recovered did not appear to be correlated with developmental timing (GLM; one month: $\chi^2_1 = 4.643$, $p = 0.031$; two months: $\chi^2_1 = 9.515$, $p < 0.001$; Figure 2.8A, 2.8B). However, given the small sample sizes per month for this population ($n = 4 - 6$ per temperature treatment) these results should be interpreted with caution.

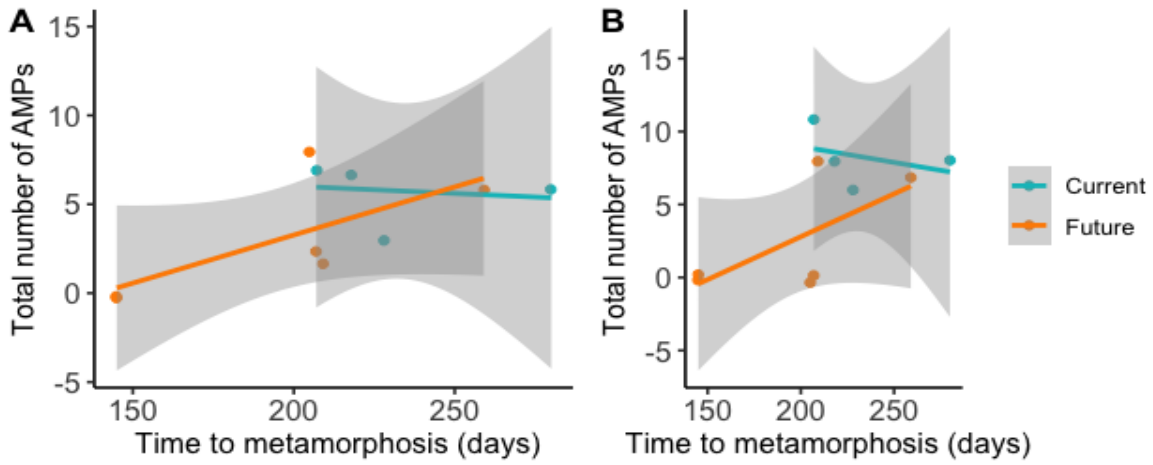

Figure 2.8 Scatter plot and lines of best fit for the relationships between the number of antimicrobial peptides (AMPs) detected and time to metamorphosis (days) for R. pipiens from Vermont reared in current and future temperature treatments.

At one (A) and two (B) months post-metamorphosis. Each point represents one individual, and the shaded area represents 95 % confidence intervals.

I found 13 out of the 19 peptides described by Tennessen (2009) for *R. pipiens* in different parts of the United States in our samples from Pennsylvania frogs. The best model to describe variation in the number of AMPs present from this population at one-month post-metamorphosis included temperature and mass at metamorphosis as main effects (AIC = 36.991, ΔAIC = 1.788; Table 2.3). At two months post-metamorphosis, the best model included the main effects of temperature and growth rate (AIC = 92.875, ΔAIC = 0.455; Table 2.3). At one-month post-metamorphosis, there was not a significant difference in the number of AMPs present in skin secretions for Pennsylvania frogs from different temperature treatments (GLM: $\chi^2_1 = 0.188$, $p = 0.665$), nor was there a significant main effect of mass at metamorphosis $\chi^2_1 = 3.458$, $p = 0.063$. At the two-month time point, there was not a significant effect temperature or growth rate

on the number of AMPs detected (GLM: $\chi^2_1 \leq 2.949$, $p \geq 0.086$). Frogs tended to secrete fewer AMPs at one-month post-metamorphosis (current temperature treatment mean = 1, range 0 to 3; future temperature treatment mean = 0.417, range 0 to 2) than at two months post-metamorphosis (current temperature treatment mean = 4.167, range: 0 to 7; future temperature treatment mean = 1.667, range 0 to 7).

Table 2.3 AIC values for models compared for each immune variable.

Sample	Temp.	Temp. + Mass at metamorphosis	Temp. + Growth rate	Temp. + Time to metamorphosis	Temp. * Mass at metamorphosis	Temp. * Growth rate	Temp. * Time to metamorphosis	ΔAIC
White Blood Cell Counts								
VT1	9.636	11.306	10.475	7.351	9.833	4.662	**-3.669**	8.331
VT2	**11.137**	12.739	12.965	11.704	14.290	12.378	13.620	0.567
PA1	-7.510	-5.713	-5.969	**-9.736**	-5.077	-6.247	-7.755	1.981
PA2	**-4.790**	-3.624	-3.239	-2.890	-5.642	-3.095	-2.890	1.166
LA1	**-1.332**	-0.099	0.281	-0.581	1.572	2.260	-1.327	0.005
LA2	2.348	3.128	**-1.350**	3.818	5.056	0.328	5.804	1.678
Thymocyte Counts								
VT1	19.670	21.658	20.885	19.992	20.998	19.296	**15.484**	3.812
VT2	20.299	**14.377**	22.103	18.429	16.246	23.765	19.970	1.869
PA2	13.545	15.530	12.455	**9.450**	15.443	8.703	10.502	1.052
PA2	**-7.187**	-6.474	-5.652	-7.224	-5.850	-8.714	-5.232	0.713
LA2	36.668	37.567	**28.044**	35.456	28.882	29.952	32.681	0.838
LA2	3.083	**-1.991**	4.381	4.270	-0.398	3.835	4.687	-2.389
Splenocyte counts								
VT1	16.020	17.466	17.291	13.280	18.128	15.412	**9.564**	3.717
VT2	**5.948**	7.945	7.881	6.743	7.993	9.641	8.388	0.795
PA1	32.169	33.348	**23.869**	29.626	32.717	25.154	25.839	1.285
PA2	9.499	8.456	**-7.181**	10.857	10.453	-6.775	5.696	0.407
LA1	29.184	30.701	**26.030**	31.184	30.676	27.331	30.992	1.301
LA2	**20.449**	21.680	22.334	22.447	21.093	22.089	24.054	0.643

Table 2.3 (continued)

B-cell proliferation								
VT2	-4.411	**-7.653**	-2.418	-3.741	-6.270	-0.987	-2.623	1.3825
PA2	**-3.846**	-2.121	-5.258	-1.846	-0.317	-3.279	-3.689	-1.412
LA2	9.018	10.501	9.870	10.740	12.435	**-1.215**	10.528	10.233
T-cell proliferation								
VT1	22.565	24.536	24.516	22.935	26.443	23.496	**20.387**	2.1779
PA1	30.956	32.722	32.587	**28.084**	33.573	33.621	27.934	2.8711
LA1	22.670	**19.278**	22.639	24.485	21.146	24.638	23.742	1.868
BCA (Mucosal peptides)								
VT1	**9.867**	11.458	11.575	12.112	13.036	12.111	12.708	1.591
PA1	**1.301**	3.142	3.276	1.566	3.490	2.746	3.010	0.265
LA1	11.531	9.344	12.903	13.171	0.916	**-4.917**	10.793	4.001
VT2	**3.759**	8.239	4.554	5.261	6.809	5.202	5.450	0.795
PA2	**14.010**	15.856	15.241	15.884	17.353	16.280	17.410	1.846
LA2	6.551	7.915	7.394	8.371	9.799	9.367	**1.242**	5.308
Total AMPs								
VT1	59.51915	55.70955	55.43057	50.94563	57.05001	52.443	**48.3024**	2.64323
PA1	41.1108	**36.991**	38.779	40.25659	38.986	38.926	42.9522	1.788
LA1	24.71222	24.251	23.938	**23.691**	26.13	25.548	25.662	0.247
VT2	66.70279	63.927	62.01169	59.3802	64.989	56.42	**51.865**	4.555
PA2	97.30482	93.33	**92.875**	97.693	95.22	91.711	95.747	0.455
LA2	**14.81899**	15.238	15.049	15.673	17.238	17.049	17.673	0.23001

Bolded values indicate best fit models. Sample abbreviations indicate population (VT, PA or LA) and developmental time point (1 = 1 month and 2 = 2 months post-metamorphosis).

The Louisiana *R. sphenocephala* population was not included in this analysis because we were only able to detect a small number of AMPs in a few individuals. There are only four AMPs that have been described for *R. sphenocephala* (Holden *et al.* 2015) and among my 38 samples taken from Louisiana frogs at one- and two-months post-metamorphosis I only detected two of these, and only 6 animals had any detectible AMPs.

The PERMANOVA (taking into account the 19 peptides from *R. pipiens* from across the United States) considering peptide presence/absence only, did not show any significant differences between the AMP communities in secretions collected from *R. pipiens* that developed in current vs. future temperature treatments. This was true at both one month (Bray–Curtis distances; Vermont: $F_{1,6} = 2.381$, $p = 0.176$; Pennsylvania: $F_{1,5} = 0.485$, $p = 0.760$) and two months (Bray–Curtis distances; Vermont: $F_{1,6} = 3.057$, $p = 0.072$; Pennsylvania: $F_{1,7} = 1.468$, $p = 0.218$) after metamorphosis. The results were very similar when intensity of the mass signal for each peptide (i.e., peptide relative abundances) was considered (Bray–Curtis distances: Vermont one month: $F_{1,6} = 0.905$, $p = 0.519$; Vermont two months: $F_{1,6} = 1.284$, $p = 0.242$; Pennsylvania one month: $F_{1,5} = 1.065$, $p = 0.343$). The only exception was for Pennsylvania *R. pipiens* at two months where there was a significant difference in number and intensity of AMPs detected between the two temperature treatments (Bray-Curtis distance: $F_{1,7} = 2.346$, $p = 0.048$; Figure 2.9) such that frogs that developed in the current temperature treatment had AMP communities that were more tightly clustered than frogs that developed in the future temperature treatment. However, due to the small sample sizes for each population and time point, all of these results should be interpreted with caution.

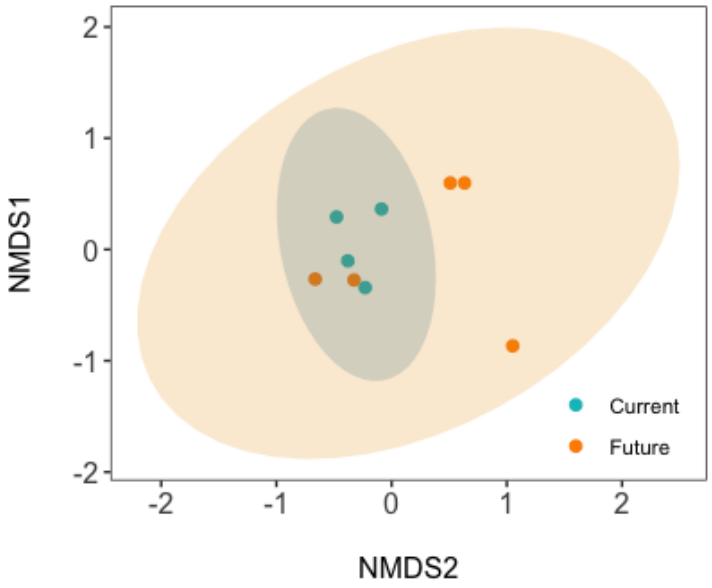

Figure 2.9 Non-multidimensional scaling (NMDS) plot of Bray-Curtis distances between AMP communities from R. pipiens from Pennsylvania at two months post-metamorphosis.

Distances were calculated using both presence/absence and relative intensity information for each AMP, as measured by MALDI mass spectrometry. The ellipses are 95 % confidence intervals.

I repeated the same analysis but this time using only using the seven AMPs previously described from Vermont *R. pipiens* (Tennessen 2009) for both the Vermont and Pennsylvania samples even though the AMPs for Pennsylvania *R. pipiens* have not previously been described. I found six of the seven peptides previously described from Vermont in both populations. However, in Pennsylvania at one month post-metamorphosis, only three of them were detected (Temporin 1P, Brevinin 1 Pa, and Brevinin 1Pe). The PERMANOVA considering peptide presence/absence only did not show any significant differences between the AMP communities in secretions collected from *R. pipiens* that developed in current vs. future temperature treatments. This was true at both one month (Bray–Curtis distances: Vermont one month $F_{1,7}$ = 1.848, p = 0.329, two months $F_{1,7}$ = 2.176, p = 0.124). For Pennsylvania there were too few

samples to run this analysis. For AMP intensities I also didn't find a significant difference between *R. pipiens* that developed in current vs. future temperature treatments. This was true at both one month (Bray–Curtis distances: Vermont one month $F_{1,7} = 0.457$, $p = 0.907$, two months $F_{1,7} = 0.939$, $p = 0.578$).

2.3.7 White blood cell counts

For *R. pipiens* from Vermont, the best model to describe variation in white blood cell counts at one-month post-metamorphosis included the interaction between temperature treatment and time to metamorphosis (AIC = -3.669, ΔAIC = 8.331; Table 2.3). At two-months post-metamorphosis, the best model included only the main effect of temperature treatment (AIC = 11.137, ΔAIC = 0.567; Table 2.3). At one-month post-metamorphosis, frogs that developed in the current temperature treatment had more white blood cells than frogs from the future temperature treatment (LM: $F_{1,8} = 15.094$, $p = 0.005$). However, the interaction between temperature treatment and time to metamorphosis was also significant (LM: $F_{1,8} = 15.675$, $p = 0.004$, $\beta = 0.010$), such that frogs from the future temperature treatment that had spent more time as larvae had more white blood cells, but frogs from the current temperature treatment with longer larval periods had similar white blood cell counts no matter how long their larval period was (Figure 2.10A). At two months post-metamorphosis there were no differences in white blood cell counts between the two temperature treatments (LM: $F_{1,9} = 1.740$, $p = 0.220$). Current temperature mean: 7.556, range: 7.267 – 8.311 log (cells/ml); future temperature mean: 7.276, range: 6.845 – 7.488 log (cells/ml) (Table 2.4).

For *R. pipiens* from Pennsylvania, the best model to describe variation in white blood cell counts at one-month post-metamorphosis included the main effect of temperature treatment and

time to metamorphosis (AIC = -9.736, ΔAIC = 1.981: Table 2.3). At two months, it included only temperature treatment as a main effect (AIC = -4.790, ΔAIC = 1.166; Table 2.3). At one month, the effects of temperature treatment and time to metamorphosis on white blood cell count were not significant (LM: $F_{1,13} \leq 3.951$, $p \geq 0.067$). At two months post-metamorphosis, the effect of temperature treatment on white blood cell counts was not significant (LM: $F_{1,16} = 0.037$, $p = 0.851$). Current temperature mean at one month: 7.027, range: 6.829 – 7.217 log (cells/ml); future temperature mean: 7.041 range: 6.628 – 7.317 log (cells/ml). Current temperature mean at two months: 7.104, range: 6.903 – 7.337 log (cells/ml); future temperature mean: 7.124, range: 6.653 – 7.415 log (cells/ml) (Table 2.4).

For *R. sphenocephala* from Louisiana, the model that best fit the data at one month included only the main effect of temperature (AIC = -1.332, ΔAIC = 0.005: Table 2.3). At two months post-metamorphosis the best model included temperature treatment and growth rate as main effects (AIC = -1.350, ΔAIC = 1.678; Table 2.3). At one-month post-metamorphosis, there was no significant effect of temperature treatment on white blood cell counts (LM: $F_{1,17} = 0.360$, $p = 0.557$). Current temperature mean at one month: 6.935, range: 6.544 – 7.176 log (cells/ml); future temperature mean: 6.873 range: 6.544 – 7.154 log (cells/ml). At two months, there was no significant effect of temperature treatment (LM: $F_{1,8} = 1.972$, $p = 0.198$) but there was a significant positive effect of growth rate on white blood cell count (LM: $F_{1,8} = 5.429$, $p = 0.048$) (Figure 2.10B). Current temperature mean at two months: 6.843, range: 6.699 - 7.041 log (cells/ml); future temperature mean: 6.772, range: 6.398 - 7.106 log (cells/ml) (Table 2.4).

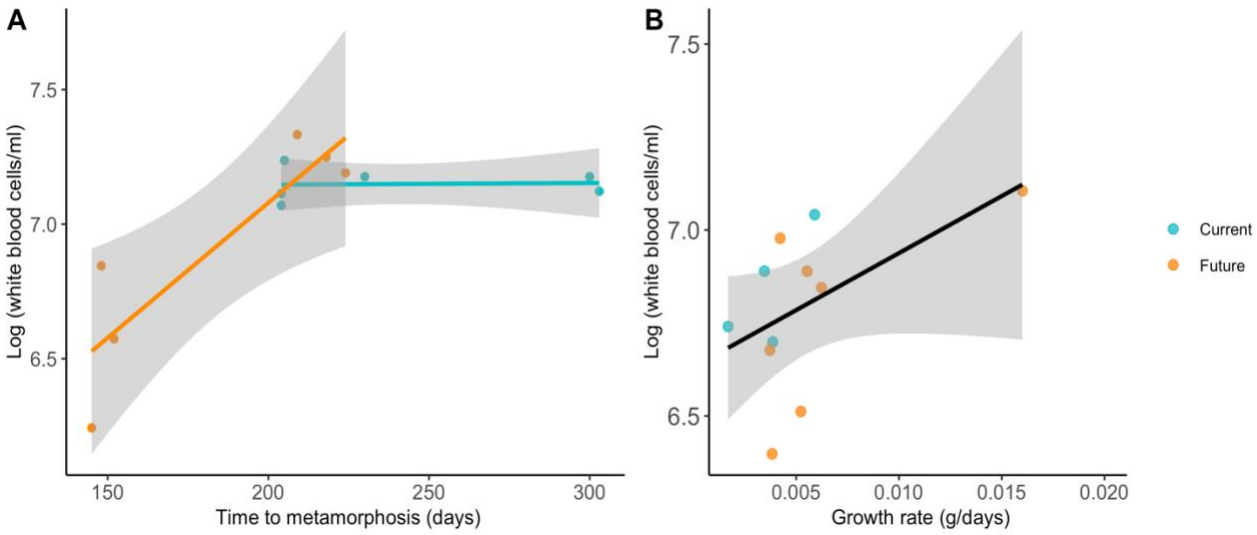

Figure 2.10 Scatter plot and lines of best fit for the relationships between log-transformed white blood cell counts (cells/ml).

and (A) time to metamorphosis (days) for *R. pipiens* from Vermont at one month post-metamorphosis, or (B) growth rate (g/days) at two month post-metamorphosis for *R. pipiens* from Louisiana. Each point represents one individual, and the shaded areas represent 95 % confidence intervals.

Table 2.4 Table showing the mean and log10 transformed mean of immune measures at one- and two-months post-metamorphosis in frogs reared in current and future temperature treatments.

	Current 1 month		**Future 1 month**		**Current 2 months**		**Future 2 months**	
	Mean	Log_{10} mean	Mean	Log_{10} mean	Mean	Log_{10} mean	Mean	Log_{10} mean
White blood cells, Vermont	14,208,333	7.149	11,208,333	6.906	66,375,000	7.555	20,500,000	7.276
White blood cells, Pennsylvania	11,100,000	7.027	11,812,500	7.041	13,700,000	7.104	14,312,500	7.124
White blood cells, Louisiana	9,326,923	6.935	8,541,667	6.872	7,312,500	6.842	6,785,714	6.772
Thymocytes, Vermont	74,886	4.678	64,564	4.617	245,630	5.183	216,509	5.176
Thymocytes, Pennsylvania	41,764	4.544	16,696	4.143	17,187	4.200	30,770	4.460
Thymocytes, Louisiana	138,215	4.960	197,717	5.172	82,458	4.859	312,913	5.441
Splenocytes, Vermont	30,098	4.411	36,797	4.350	29,851	4.429	38,914	4.525
Splenocytes, Pennsylvania	174,227	5.106	126,081	4.889	181,666	5.204	342,447	5.446
Splenocytes, Louisiana	15,758	4.059	17,120	4.085	10,203	3.769	12,843	3.976
B-cell proliferation, Vermont					1.151	0.043	1.609	0.163
B-cell proliferation, Pennsylvania					1.380	0.091	1.586	0.166
B-cell proliferation, Pennsylvania					3.126	0.321	1.130	0.033
T-cell proliferation, Vermont	7.474	0.736	17	0.874				
T-cell proliferation, Pennsylvania	107	1.908	45	1.345				
T-cell proliferation, Louisiana	10	0.862	12	0.858				
BCA (mucosal peptides), Vermont	234.563	2.303	89.896	1.866	349.159	2.516	134.729	2.050
BCA (mucosal peptides), Pennsylvania	74.566	1.805	57.239	1.711	192.507	2.147	118.878	2.020
BCA (mucosal peptides), Louisiana	39.519	1.57062	27.640	1.309	76.794	1.852	76.365	1.762

2.3.8 Thymocyte counts

For *R. pipiens* from Vermont, the best model to explain variation in thymocyte counts included the interaction between temperature treatment and time to metamorphosis (AIC = 15.484, ΔAIC = 3.812; Table 2.3). For two-months post-metamorphosis, the best model included the main effects of temperature treatment and mass at metamorphosis (AIC = 14.377, ΔAIC = 1.869; Table 2.3). The main effects of temperature treatment and time to metamorphosis were not significant (LMs: $F_{1,8} \leq 4.820$, $p \geq 0.059$). There was, however, a significant interaction between temperature treatment and time to metamorphosis (LM: $F_{1,8} = 5.761$, $p = 0.043$, $\beta = 0.013$). In the future temperature treatment, the thymocyte count tended to increase with time to metamorphosis whereas in the current temperature treatment, thymocyte counts were slightly lower for frogs that took longer to metamorphose. (Figure 2.11A). At two months post-metamorphosis, the main effect of temperature treatment was not significant (LM: $F_{1,11} = 2.866$, $p = 0.118$). There was, however, a positive effect of mass at metamorphosis on thymocyte counts (LM: $F_{1,11} = 8.369$, $p = 0.015$, $\beta = 0.617$) (Figure 2.11B).

For *R. pipiens* from Pennsylvania, the best model at one-month post-metamorphosis included the main effects of temperature and time to metamorphosis (AIC = 9.450, ΔAIC = 1.052; Table 2.3). At two months, the best model included only temperature treatment as a main effect (AIC = -7.187, ΔAIC = 0.713: Table 2.3). For this population at one month, there was no significant difference between thymocyte counts in frogs from current and future temperature treatments (LM: $F_{1,15} = 2.209$, $p = 0.158$). However, there was a significant positive effect of time to metamorphosis on thymocyte count (LM: $F_{1,15} = 0.460$, $p = 0.027$; Figure 2.11C). At two

months post-metamorphosis, frogs from the future temperature treatment had more thymocytes than frogs from the current temperature treatment (LM: $F_{1,20} = 10.435$, $p = 0.004$; Figure 2.11D).

For *R. sphenocephala* from Louisiana, the model that best fit our data for frogs at one-month post-metamorphosis was the one with temperature treatment and growth rate as main effects (AIC = 28.044, ΔAIC = 0.838; Table 2.3). At two months post-metamorphosis, the best model included temperature treatment and mass at metamorphosis as main effects (AIC = -1.991, ΔAIC = -2.389: Table 2.3). At one month, there was a significant positive effect of growth rate on (LM: $F_{1,22} = 11.650$, $p = 0.002$, $\beta = 50.041$, Figure 2.11E) but the main effect of temperature treatment was not significant (LM: $F_{1,22} = 3.920$, $p = 0.060$). At two months, frogs that developed in the future temperature treatment had more thymocytes than frogs from the current temperature treatment (LM: $F_{1,11} = 16.951$, $p = 0.002$). Across both temperature treatments, frogs with a greater mass at metamorphosis also had more thymocytes (LM: $F_{1,11} = 7.233$, $p = 0.021$, $\beta = 0.756$, Figure 2.11F).

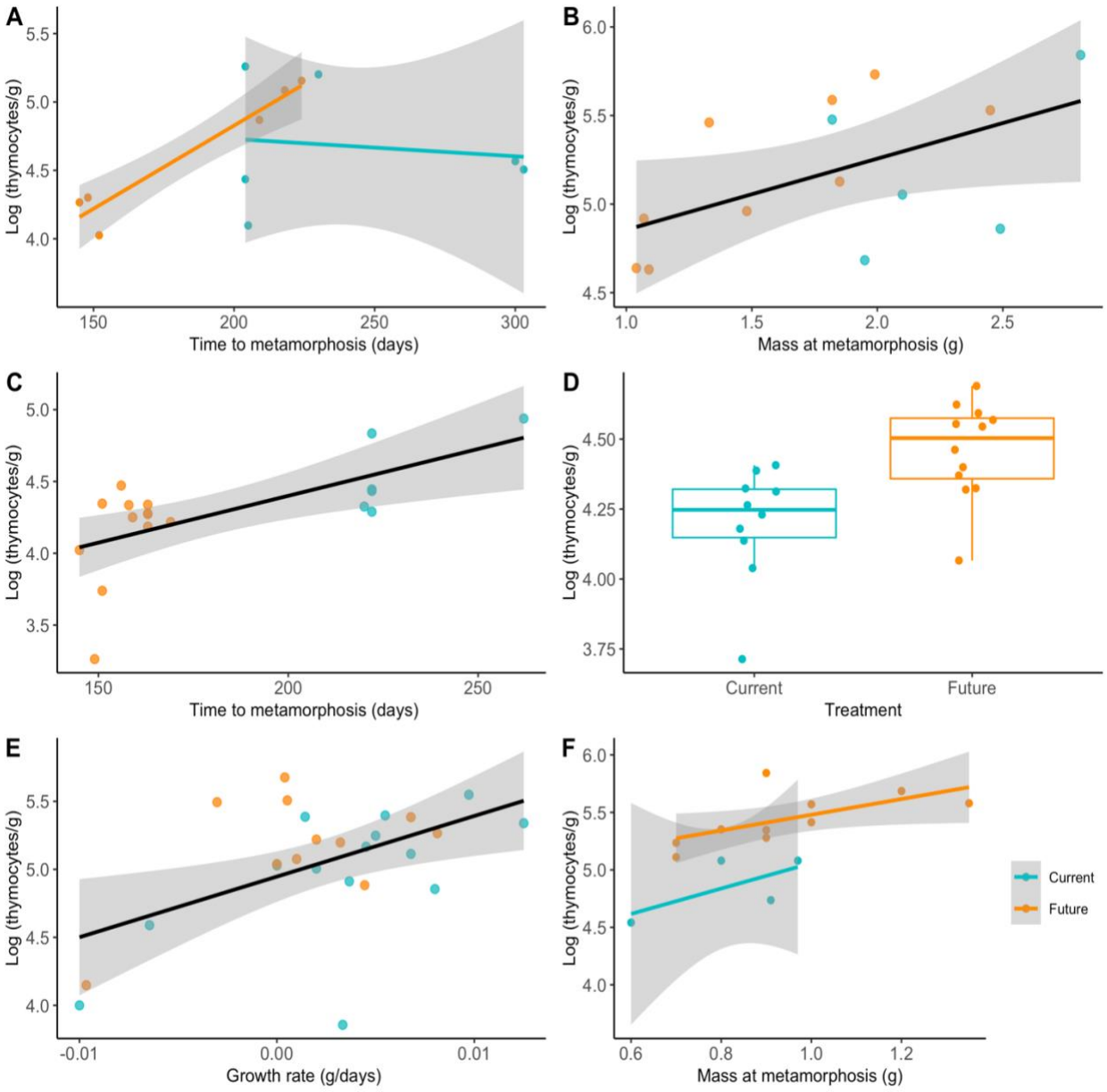

Figure 2.11 Scatter plot and lines of best fit for the relationships between log-transformed thymocyte counts (cells /g).

and (A) time to metamorphosis (days) for *R. pipiens* from Vermont at one month post-metamorphosis, (B) mass at metamorphosis (g) for *R. pipiens* from Vermont at two months, and (C) time to metamorphosis (days) for *R. pipiens* from Pennsylvania at one month post-metamorphosis. Plot (D) shows box plots of log-transformed thymocyte counts (cells/g) for *R. pipiens* from Pennsylvania at two months post-metamorphosis. Plot (E) shows growth rate (g/day) for *R. sphenocephala* from Louisiana at one month and (F) show mass at metamorphosis (g) for *R. sphenocephala* from Louisiana at two months post-metamorphosis. Each point represents one individual and the

shaded areas represent 95 % confidence intervals. In the boxplots, the middle line corresponds to the median. The lower and upper hinges correspond to the first and third quartiles (the 25th and 75th percentiles). The upper whisker extends from the hinge to the largest value no further than 1.5 times the inter-quartile range.

2.3.9 Splenocyte counts

For *R. pipiens* from Vermont, the best model to describe variation in splenocyte counts at one-month post-metamorphosis included the interaction between temperature treatment and time to metamorphosis (AIC = 9.564, ΔAIC = 3.717; Table 2.3). For two-month-old frogs, the best model included only the main effect of temperature treatment (AIC = 5.948, ΔAIC = 0.795; Table 2.3). At one-month post-metamorphosis, none of the main or interaction effects in the model were significant (LMs: $F_{1,8} \leq 4.882$, $p \geq 0.058$) though small sample sizes (n = 6 current, 6 future temperature treatment) likely impacted my power to detect anything but a very large effect size. The mean splenocyte count for all frogs at one-month post-metamorphosis was 4.381 log/ml/g (range: 3.769 to 4.951 log/g). At two months post-metamorphosis, with a slightly larger sample size (n = 5 current, n = 9 future), the main effect of temperature was also not significant, (LM: $F_{1,12} = 0.436$, $p = 0.522$). The mean splenocyte count for all frogs at two months was 4.491 log/ml/g (range: 4.041 to 4.808) log cells/g (Table 2.4).

For *R. pipiens* from Pennsylvania at one- and two-months post-metamorphosis the best model was the one that included the main effects of temperature treatment and growth rate (one month: AIC = 23.869, ΔAIC =1.285; two months: AIC = -7.181, ΔAIC = 0.407; Table 2.3). At one month, there was not a significant effect of temperature treatment (LM: $F_{1,15} = 2.596$, $p = 0.128$), however splenocyte counts were positively correlated with growth rate (LM: $F_{1,15} = 11.582$, $p = 0.004$; Figure 2.12A). At two months, with a slightly larger sample size, frogs from

the future temperature treatment had greater splenocyte counts (LM: $F_{1,19} = 12.867$, $p = 0.002$) and splenocyte counts were again positively correlated with growth rate (LM: $F_{1,19} = 25.413$, $p < 0.001$; Figure 2.12B).

For *R. sphenocephala* from Louisiana at one-month post-metamorphosis, the best fitting model included temperature treatment and growth rate as main effects (AIC = 26.030, ΔAIC = 1.301; Table 2.3). At two months old, the best model included only temperature treatment (AIC = 20.449, ΔAIC = 0.642; Table 2.3). At one-month post-metamorphosis, splenocyte counts were not significantly different between frogs from the two temperature treatments (LM: $F_{1,23} = 0.244$ $p = 0.626$) but frogs that grew faster after metamorphosis had more splenocytes (LM: $F_{1,23} = 5.043$, $p = 0.034$, $\beta = 115.223$; Figure 2.12C). At two months post-metamorphosis there was again no difference in splenocyte counts between frogs from the current and future temperature treatments (LM: $F_{1,12} = 0.640$, $p = 0.439$).

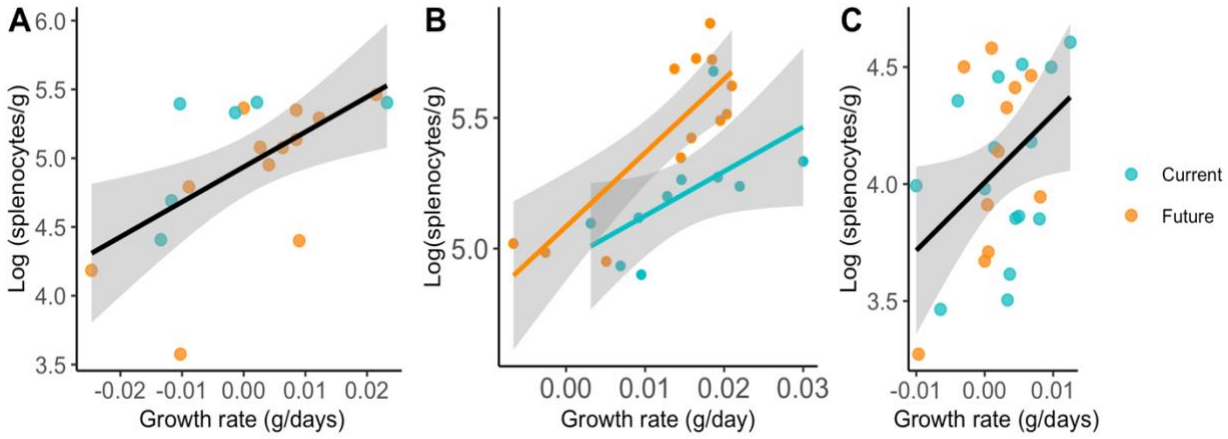

Figure 2.12 Scatter plots and lines of best fit for the relationships between log-transformed splenocyte counts (cells/g).

and growth rate (g/day) for *R. pipiens* from Pennsylvania at one month (A) and two months (B) post-metamorphosis, and for (C) *R. sphenocephala* from Louisiana at one-month post-metamorphosis. Each point represents one individual, and the shaded areas represent 95 % confidence intervals.

2.3.10 T-lymphocyte proliferation

For T-lymphocyte proliferation the assay was only performed at one-month post-metamorphosis. The best model for *R. pipiens* from Vermont included the interaction between time to metamorphosis and temperature treatment (AIC = 20.387, ΔAIC = 2.178; Table 2.3). For Pennsylvania, the best model was the one with temperature treatment and time to metamorphosis as main effects (AIC = 28.084, ΔAIC = 2.871: Table 2.3). For *R. sphenocephala* from Louisiana, the best model included temperature and mass at metamorphosis as main effects (AIC = 19.278, ΔAIC = 1.868; Table 2.3). At one-month post-metamorphosis, none of the main effects or interactions in the model were significant (LM: $F_{1,8} \leq 3.687$, $p \geq 0.091$; current temperature mean: 1.694, range: 0.601- 2.879 log (fold T-lymphocyte proliferation); future temperature mean: 2.011, range: 0.008 - 4.170 log (fold T-lymphocyte proliferation) (Table 2.5). However, small sample sizes (n = 6 current, 6 future temperature treatment) would have precluded detection of all but the largest effect sizes.

For the *R. pipiens* frogs from Pennsylvania, T-lymphocyte proliferation was not significantly different among frogs from the two temperature treatments ($F_{1,15} = 1.799$, $p = 0.200$). However, time to metamorphosis had a significant positive relationship with T-lymphocyte proliferation ($F_{1,15} = 4.663$, $p = 0.047$, $\beta = 0.052$, Figure 2.13A). For *R. sphenocephala* from Louisiana, the main effect of temperature treatment was not significant ($F_{1,12} = 0.231$, $p = 0.640$) but there was a significant negative relationship between T-cell proliferation and mass at metamorphosis ($F_{1,12} = 5.191$, $p = 0.042$, $\beta = -2.219$, Figure 2.13B).

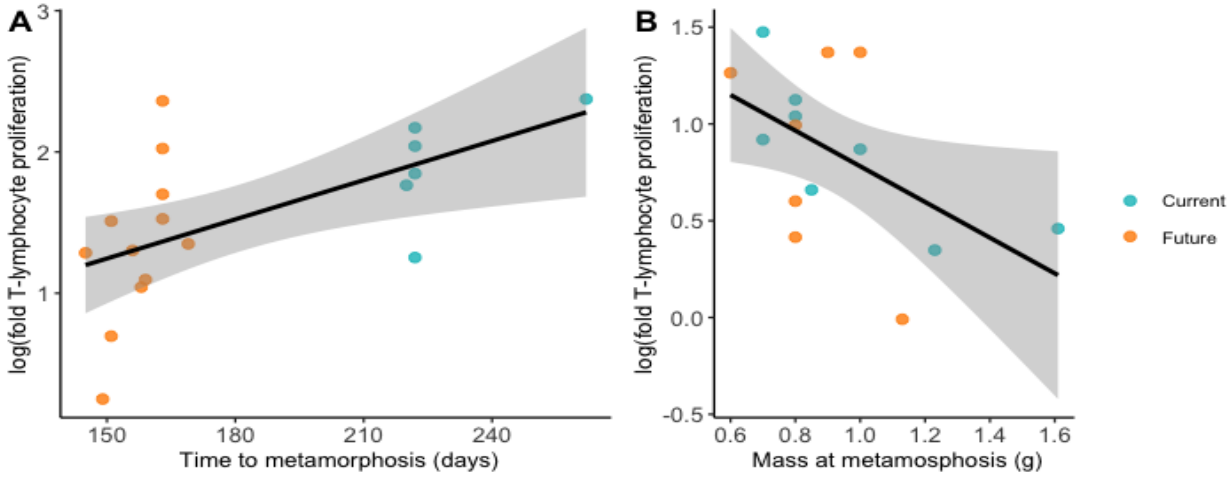

Figure 2.13 Scatter plot and lines of best fit for the relationships between log-transformed T-lymphocyte proliferationat one-month post-metamorphosis.

and (A) time to metamorphosis (days) in *R. pipiens* from Pennsylvania and (B) mass at metamorphosis (g) in *R. sphenocephala* from Louisiana. Each point represents one individual, and the shaded area represents 95 % confidence intervals.

2.3.11 B-lymphocyte proliferation

The B-lymphocyte proliferation assay was only performed at two months post metamorphosis. For *R. pipiens* from Vermont, the best model to describe B-lymphocyte proliferation had temperature treatment and mass at metamorphosis as main effects (AIC = -7.653, ΔAIC = 1.3825; Table 2.3). Frogs from this population that were reared in the future temperature treatment had greater B-cell proliferation than frogs from the current temperature treatment (LM: $F_{1,11} = 5.941$, $p = 0.033$). However, there was also a positive correlation between B-cell proliferation and mass at metamorphosis (LM: $F_{1,11} = 4.995$, $p = 0.048$, $\beta = 0.499$, Figure 2.14A). For *R. pipiens* frogs from Pennsylvania, the best model to describe B-lymphocyte proliferation had only temperature treatment as main effect (AIC = -3.846, ΔAIC = -1.412; Table

2.3). B-lymphocyte proliferation did not differ significantly among frogs from the two temperature treatments for this population (LM: $F_{1,20} = 0.746$, $p = 0.398$). Current temperature mean: 0.091, range: -0.356- 0.482 log (fold proliferation); future temperature mean: 0.166, range: -0.164 - 0.470 log (fold proliferation) (Table 2.4).

For *R. sphenocephala* from Louisiana, the best model contained the interaction between growth rate and temperature treatment (AIC = -1.215, ΔAIC = 10.233). For this population, the main effect of temperature treatment was not significant (LM: $F_{1,15} = 0.085$, $p = 0.775$) but there was a significant positive relationship between B-lymphocyte proliferation and growth rate (LM: $F_{1,15} = 15.853$, $p = 0.002$, $\beta = 171.748$). The interaction between temperature treatment and growth rate was also significant for Louisiana frogs (LM: $F_{1,15} = 14.867$, $p = 0.002$, $\beta = -197.624$), such that frogs reared in the current temperature treatment had a strong positive correlation between growth rate and B-lymphocyte proliferation whereas for frogs from the future temperature treatment, B-cell proliferation was slightly negatively correlated with growth rate after metamorphosis (Figure 2.14B).

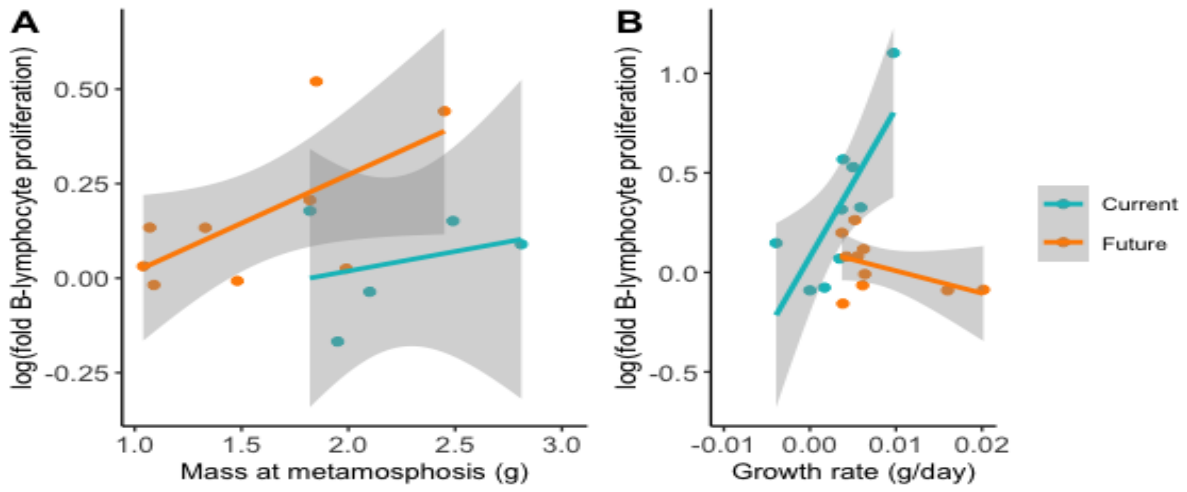

Figure 2.14 Scatter plot and lines of best fit for the relationships between log-transformed B-lymphocyte proliferation at two months post-metamorphosis.

and (A) mass at metamorphosis (g) for *R. pipiens* from Vermont, and (B) growth rate (g/day) for *R. sphenocephala* from Louisiana. Each point represents one individual, and the shaded areas represent 95 % confidence intervals.

2.3.12 *Bd* infections

I compared the *Bd* infection load ($\log_{10}$ *Bd* DNA copies per swab) and the probability that a frog was infected (yes/no) among treatment groups during the four weeks of the *Bd* exposure experiment using skin swabs and a qPCR assay. I also compared scaled mass index (a measure of body condition) and survival among frogs reared under the two temperature treatments. For infection load, probability of infection, and scaled mass index, I tested for main and interaction effects of time since first exposure and the temperature treatment in which the frogs were reared. For *Bd*-exposed *R. pipiens* from Vermont, none of these main or interaction effects were significant for *Bd* infection load (GLMM: $\chi^2_1 \leq 1.100$, $p \geq 0.294$), probability of infection (GLMM: $\chi^2_1 \leq 0.002$, $p \geq 0.951$, or scaled mass index (LME: $\chi^2_1 \leq 2.176$, $p \geq 0.151$). However,

Bd-exposed frogs reared in the current temperature treatment had greater survival after exposure to *Bd* than frogs from the future temperature treatment (Cox regression: $\chi^2_1 = 5.146$, $p = 0.023$, n =10 current, n=15 future temperature treatment; Figure 2.15).

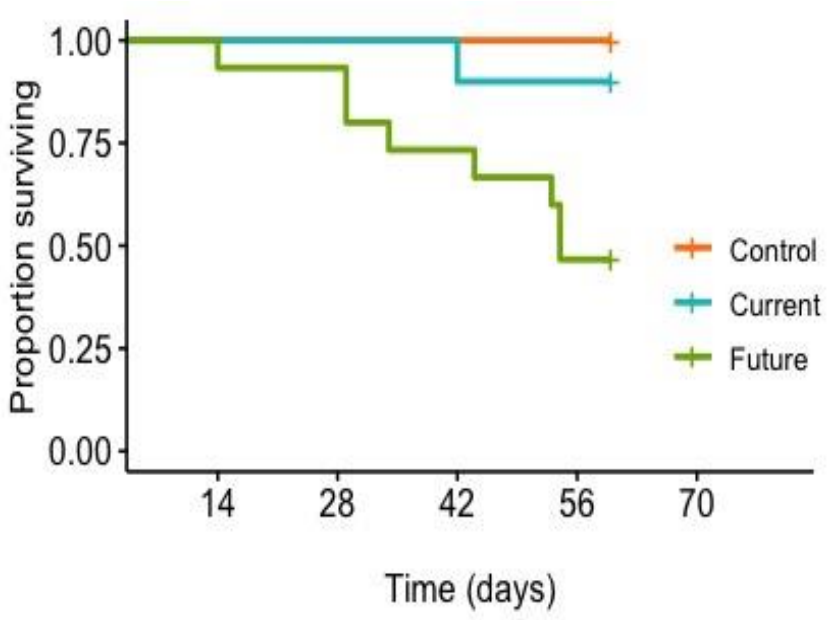

Figure 2.15 Survival curves for R. pipiens from Vermont that were exposed to Bd.

Labelled by temperature treatment and for all frogs (regardless of temperature treatment) in the control (sham exposure) group from week one after metamorphosis (Gosner stage 46) until day sixty after the first *Bd* exposure (COXPH: $p = 0.023$).

For *Bd*-exposed *R. pipiens* from Pennsylvania, frogs from the future temperature treatment experienced a lower *Bd* infection load (GLMM: $\chi^2_1 = 17.383$, $p \leq 0.001$, Figure 2.16 n =15 current, n= 15 future temperature treatment). Overall, infection load decreased with time since first exposure to *Bd* (GLMM: $\chi^2_1 = 18.645$, $p \leq 0.001$), but there was also a significant interaction between temperature treatment and time since first exposure (GLMM: $\chi^2_1 = 11.666$, $p \leq 0.001$); frogs from the current temperature treatment decreased in *Bd* load over time while

frogs from the future temperature saw their infection loads increase slightly (Figure 2.16). There was also a difference in infection probability among frogs reared under the two temperature treatments (GLMM: $\chi^2_1 = 4.172$, $p = 0.041$) such that Pennsylvania frogs reared in the current temperature treatment were more likely to become infected after exposure to *Bd* than frogs from the future temperature treatment (Figure 2.17). However, the main effect of time since first exposure and the interaction between time and temperature treatment were not significant (GLMM: $\chi^2_1 \leq 1.922$, $p \geq 0.166$). There was a significant main effect of temperature treatment on scaled mass index during the exposure experiment (LMER: $\chi^2_1 = 19.430$, $p < 0.001$, Figure 2.18) such that frogs reared in the future temperature treatment had a greater scaled mass index. However, this difference existed at the start of the exposure experiment and there was no significant effect of time since first *Bd*-exposure or interaction between time and temperature treatment on body mass index ($\chi^2_1 \leq 2.770$, $p \geq 0.103$), which suggests that the difference among temperature treatments was a holdover from development under those temperatures and not generated by exposure to *Bd*. There was no difference in survival after *Bd* exposure between Pennsylvania frogs from the two temperature treatments (Cox regression: $\chi^2_1 = 1.386$, $p = 0.239$). Most of the *Bd*-exposed frogs survived until the end of the experiment mean was 58.533 days (range: 16 – 60 days). For the *Bd*-exposed frogs in the current temperature treatment, the survival mean was 57 days (range: 16 – 60 days) and for the exposed frogs in the future temperature treatment, all frogs survived until the end of the experiment (60 days).

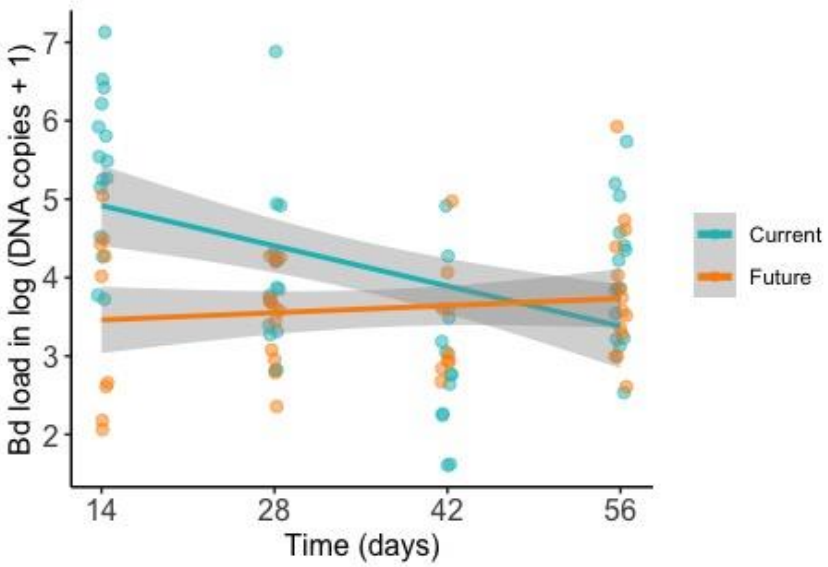

Figure 2.16 Scatter plot and lines of best fit for the relationship between Bd infection load, in log (DNA copies + 1), and since first exposure for Bd-exposed R. pipiens from Pennsylvania that were reared in current and future temperature treatments.

Each dot represents one individual, and the shaded areas represent 95 % confidence intervals.

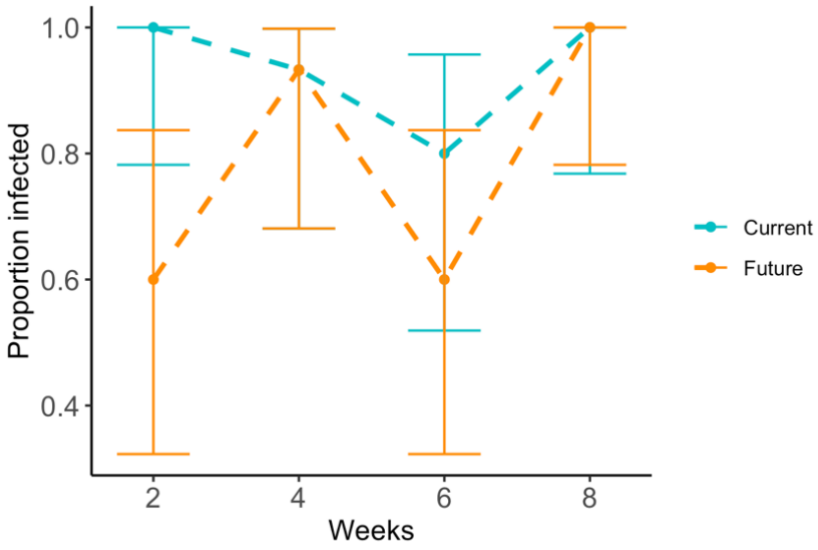

Figure 2.17 Relationship between the mean proportion of frogs infected with Bd, as determined by qPCR, and time since first exposure for Bd-exposed R. pipiens from Pennsylvania reared in current and future temperature treatments.

Error bars represent 95% confidence intervals calculated using the Clopper-Pearson method (Clopper 1934).

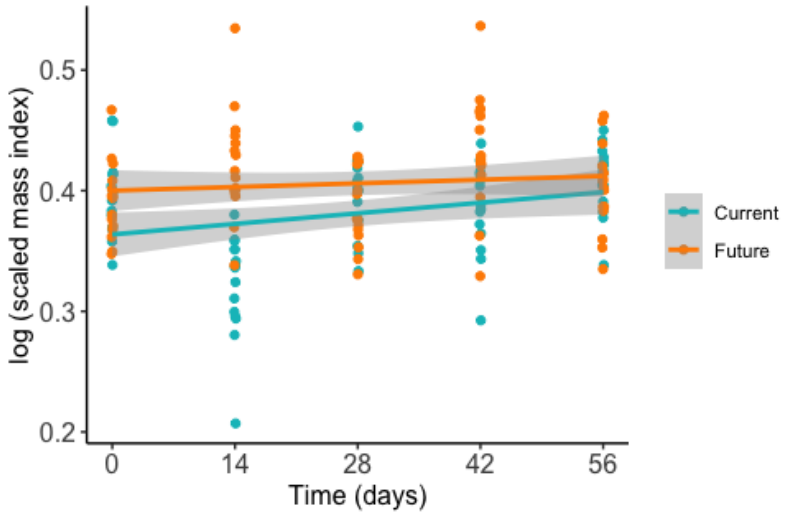

Figure 2.18 Scatter plot and lines of best fit for the relationship between body condition, measured as scaled mass index, and time since first exposure for Bd-exposed R. pipiens from Pennsylvania reared under current and future temperature treatments.

Each point represents one individual, and the shaded areas represent 95 % confidence intervals.

For *Bd*-exposed *R. sphenocephala* from Louisiana, there were no significant main or interaction effects of temperature treatment or time since first exposure on *Bd* infection load (GLMM: $\chi^2_1 \leq 1.891$, $p \geq 0.169$; n = 15 current, n = 16 future temperature treatment; mean: 3.765, range 2.089 to 7.143 log (DNA copies +1). For probability of infection, the main effect of temperature treatment and the interaction between temperature treatment and time since first exposure were not significant (GLMM: $\chi^2_1 \leq 1.562$, $p \geq 0.211$; n =15 current, n =16 future temperature treatment) but there was a significant main effect of time since first exposure (GLMM: $\chi^2_1 = 8.272$, $p = 0.004$, $\beta = 0.266$) such that frogs from the future temperature treatment were more likely to become infected later in the experiment and the current temperature treatment tended to lose infections over the course of the experiment (Figure 2.19). Scaled mass index differed among frogs from the two temperature treatments (LM: $\chi^2_1 = 13.105$, $p \leq 0.001$) and frogs from both temperature treatments increased in body mass index over the course of the exposure experiment (LM: $\chi^2_1 = 9.381$, $p = 0.003$, Figure 2.20). However, similar to the Pennsylvania population, there was no significant interaction between temperature treatment and time since first *Bd* exposure (LM: $\chi^2_1 = 0.007$, $p = 0.936$) suggesting that the main effect of temperature treatment on body condition was a result of their rearing conditions and not an effect of *Bd* exposure. There was no difference in survival after *Bd* exposure between frogs from the two temperature treatments for this population (Cox regression: $\chi^2_1 = 0.144$, $p = 0.7041$). Most of the *Bd*-exposed frogs survived until the end of the experiment (mean 57 days, range: 19 – 60 days survived). For the exposed frogs in the current temperature treatment the survival mean was 57 days (range: 19 – 60 days) and for the exposed frogs in the future temperature treatment the survival mean was 58 days (range: 27 – 60 days).

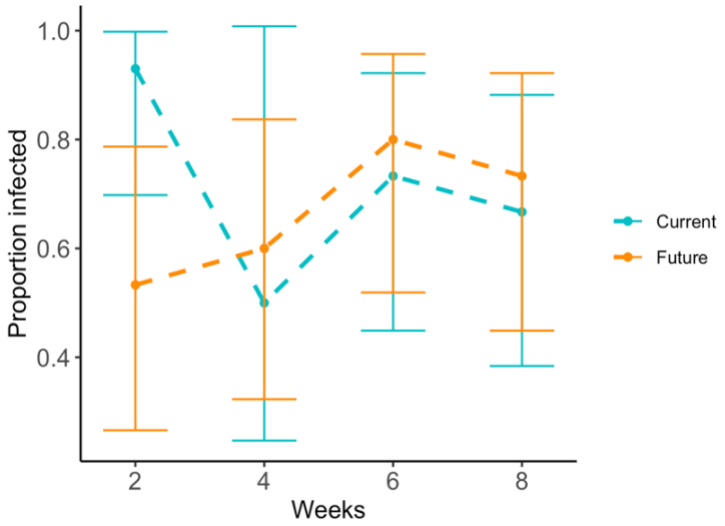

Figure 2.19 Relationship between the mean proportion of frogs infected with Bd, as determined by qPCR, and time since first exposure for Bd-exposed R. sphenocephala from Louisiana reared in current and future temperature treatments.

Error bars represent 95% confidence intervals calculated using the Clopper-Pearson method (Clopper 1934).

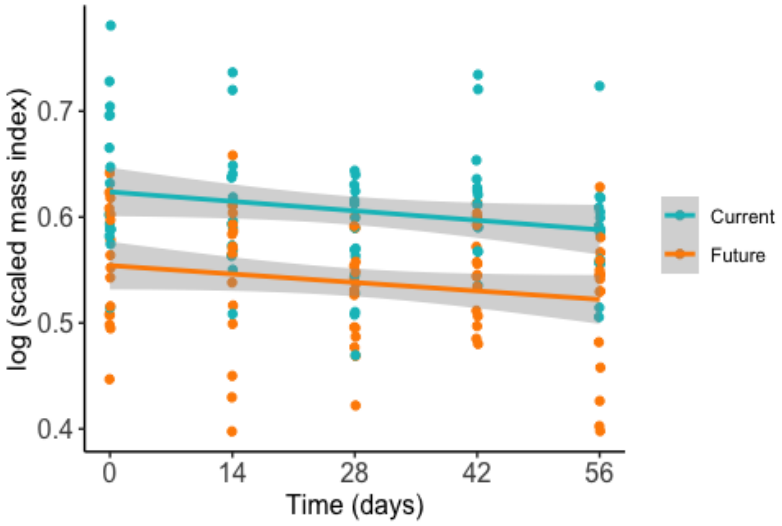

Figure 2.20 Scatter plot and lines of best fit for the relationship between body condition, measured as scaled mass index, and time since exposure for Bd-exposed R. sphenocephala from Louisiana reared in current and future temperature treatments.

Each point represents one individual and the shaded areas represent 95 % confidence intervals.

2.3.13 Splenocyte counts after *Bd* exposure

I compared splenocyte counts among frogs from the two temperature treatments and two *Bd* exposure treatments (*Bd* vs. sham exposed) one week after the end of the *Bd* exposure experiment. The model that best fit the data for *R. pipiens* from Vermont included the interaction between temperature treatment and *Bd* exposure group and the main effect of growth rate (AIC = -11.581, ΔAIC = 1.649, Table 2.5). There were significant main effects of temperature treatment (LM: $F_{1,30} = 9.787$, $p = 0.004$, Figure 2.21) and growth rate (LM: $F_{1,30} = 5.569$, $p = 0.025$, $\beta = -11.670$) on splenocyte counts. Frogs from the future temperature treatment had more splenocytes and the faster the frogs grew after metamorphosis, the lower the number of splenocytes (Figure 2.22 A). There was not a significant effect of exposure group, or interaction between temperature treatment and exposure group for Vermont frogs (LM: $F_{1,30} \leq 2.063$, $p \geq 0.162$).

For *R. pipiens* from Pennsylvania, the best model to explain variation in splenocyte counts after the *Bd* exposure experiment only included the interaction between temperature treatment and *Bd* exposure group (AIC = -14.185, ΔAIC = 1.859, Table 2.5). Here I found a significant difference between frogs reared in the current and future temperature treatments (LM: $F_{1,48} = 10.374$, $p = 0.003$, Fig 21); the frogs from the future temperature treatment had more splenocytes than the ones from the current temperature treatment (Figure 2.21). However, there was no significant difference in splenocyte counts between frogs that had been exposed to *Bd* and sham exposed frogs (LM: $F_{1,48} = 0.034$, $p = 0.855$) and the interaction between *Bd*-exposure group and temperature treatment was also not significant (LM: $F_{1,48} = 1.199$, $p = 0.280$) (Table 2.6)

For *R. sphenocephala* from Louisiana, the best model for splenocyte counts after *Bd* exposure contained two- and three-way interactions between temperature treatment, *Bd* exposure

group, and mass at metamorphosis (AIC = -33.767, ΔAIC = 5.242; Table 2.5). There was a significant main effect of mass at metamorphosis (LM: $F_{1,35} = 6.623$, $p = 0.015$, $\beta = -0.226$, Figure 2.22 B) such that the frogs that metamorphosed with a greater body mass had fewer splenocytes. The[r]e was also a significant difference in the number of splenocytes between frogs reared in the current and future chambers ($F_{1,35} = 7.065$, $p = 0.012$, Figure 2.21) with frogs from the future temperature treatment having more splenocytes. There was also a significant interaction between temperature treatment and mass at metamorphosis ($F_{1,35} = 7.501$, $p = 0.010$, $\beta = -0.391$) such that splenocyte counts from frogs reared in the future temperature treatment decreased faster with mass at metamorphosis than did the counts for frogs from the current temperature treatment (Figure 2.22 B). There was not a significant effect of exposure group and none of the other two-or three-way interactions in the model were significant (LM: $F_{1,30} \leq 0.786$, $p \geq 0.382$) (Table 2.6).

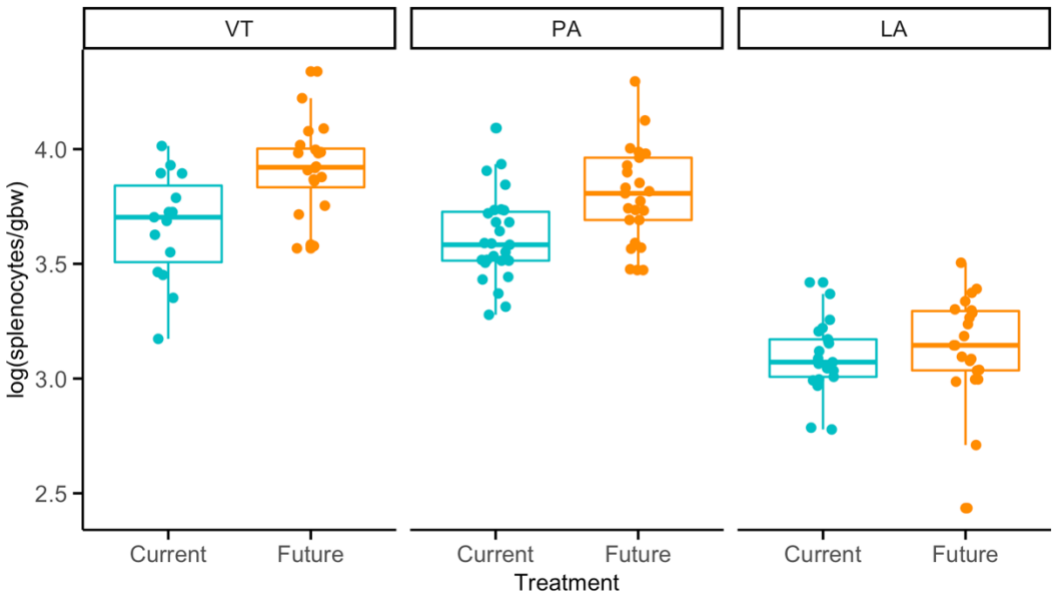

Figure 2.21 Box plots showing the relationship between log-transformed splenocyte counts (cells/gbw)for R. pipiens from Vermont and Pennsylvania, and R. sphenocephala from Louisiana at one week after the last exposure to Bd.

Each point represents one individual. The middle line corresponds to the median. The lower and upper hinges correspond to the first and third quartiles (the 25th and 75th percentiles). The upper whisker extends from the hinge to the largest value no further than 1.5 times the inter-quartile range.

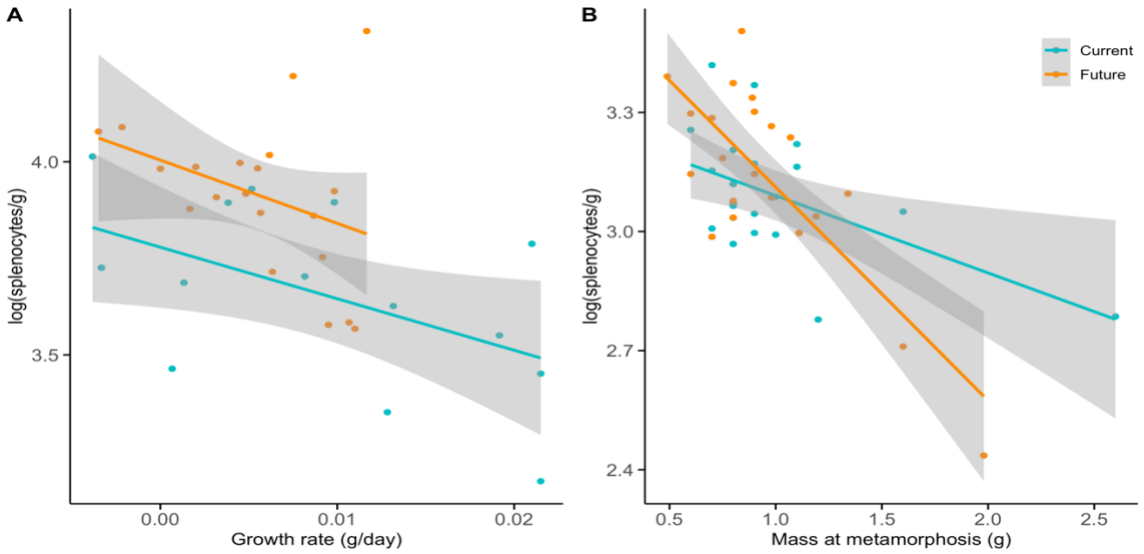

Figure 2.22 Scatter plots and lines of best fit for the relationship between log-transformed splenocyte counts (cells/gbw).

and (A) growth rate (day/g) for *R. pipiens* from Vermont and (B) mass at metamorphosis in *R. sphenocephala* from Louisiana. Each point represents one individual, and the shaded areas represent 95 % confidence intervals.

2.3.14 Inhibition of *Bd* growth by mucosome samples

After the *Bd* exposure experiment, I compared the ability of mucosome samples collected from frogs in my two exposure groups and the two temperature treatments to inhibit the growth of *Bd in vitro*. The model that best fit the data for *R. pipiens* from Vermont included the main and interactive effects of temperature treatment and exposure group and also included mass at

metamorphosis as a main effect (AIC = 239.546, ΔAIC = 0.076, Table 2.5). For this population, there was a significant main effect of temperature treatment (LM: $F_{1,21} = 7.395$ $p = 0.013$, Figure 2.23 A) such that the mucosome of frogs reared in the current temperature treatment was more inhibitive of *Bd* growth than the mucosome of frogs from the future temperature treatment. There was not a significant main effect of exposure group, or mass at metamorphosis, nor an interaction between temperature treatment and exposure group (LM: $F_{1,21} \leq 2.562$, $p \geq 0.124$).

Table 2.5 AIC values for models compared for each immune variable after Bd exposure.

	Temp. * Exposure	Temp. * Exposure + Mass at metamorphosis	Temp. * Exposure + Growth rate	Temp. * Exposure + Time to metamorphosis	Temp. * Exposure * Mass at metamorphosis	Temp. * Exposure * Growth rate	Temp.* Exposure * Time to metamorphosis	ΔAIC
				Mucosome				
VT	255.754	**239.546**	257.698	239.622	241.685	260.071	244.769	0.076
PA	251.432	**243.473**	249.804	250.303	248.144	254.830	250.855	4.671
LA	239.136	232.934	**223.204**	231.302	237.902	223.476	235.945	0.272
				Spleen				
VT	-7.621	-5.622	**-11.581**	-7.340	-3.677	-13.230	-2.886	3.96
PA	**-14.185**	-12.326	-12.248	-12.275	-7.531	-7.152	-7.072	1.859
LA	-9.304	-28.524	-7.316	-9.929	**-33.767**	-8.237	-9.042	5.243

Table 2.6 Table showing the mean and log10 mean of splenocyte counts from exposed and sham exposed frogs from current and future temperature treatments.

	Current sham-exposed		Future sham-exposed		Current *Bd*-exposed		Future *Bd*-exposed	
	Mean	Log_{10} mean	Mean	Log_{10} mean	Mean	Log_{10} mean	Mean	Log_{10} mean
Splenocytes, Vermont	5080.055	3.642	10719.33	4.001	5402.877	3.691	5962.976	3.747
Splenocytes, Pennsylvania	4537.472	3.603	7926.385	3.847	4463.719	3.617	5977.512	3.739
Splenocytes, Louisiana	1274.18	3.071	1419.042	3.081	1381.251	3.123	1600.263	3.169

For *R. pipiens* from Pennsylvania, the model that best fit the mucosome inhibition data included the main and interactive effects of temperature treatment and exposure group and also included mass at metamorphosis as a main effect (AIC = 243.473 ΔAIC = 4.671, Table 2.5). For this population there were significant main effects of temperature treatment (LM: $F_{1,23} = 21.851$, $p < 0.001$) and exposure group (LM: $F_{1,23} = 7.035$, $p < 0.014$) and a significant interaction between temperature treatment and exposure group ($F_{1,23} = 8.233$, $p = 0.009$, $\beta = 37.905$); frogs reared in the future temperature treatment had more effective mucosome against *Bd* when they had been previously exposed to that pathogen, whereas in the current temperature treatment, *Bd*-exposed frogs had mucosome with a lower capacity to inhibit *Bd* growth (Figure 2.23 B). There was also a significant main effect of mass at metamorphosis (LM: $F_{1,23} = 9.824$, $p = 0.005$, $\beta = -25.861$) such that inhibition of *Bd* growth by mucosome decreased with mass at metamorphosis (Figure 2.23C).

For *R. sphenocephala* from Louisiana, the best model to explain variation in mucosome inhibition of *Bd* growth after the exposure experiment included the main and interactive effects of temperature treatment and exposure group along with growth rate as a main effect (AIC = 223.204, ΔAIC = 0.272, Table 2.5). For this population only temperature treatment was significant ($F_{1,23} = 5.006$, $p = 0.035$), with frogs in the future temperature treatment having more inhibitive mucosome than frogs from the current temperature treatment (Figure 2.23D). The main effect of exposure group and all interaction effects in the model were not significant (LM: $F_{1,23} \leq 1.970$, $p \geq 0.174$).

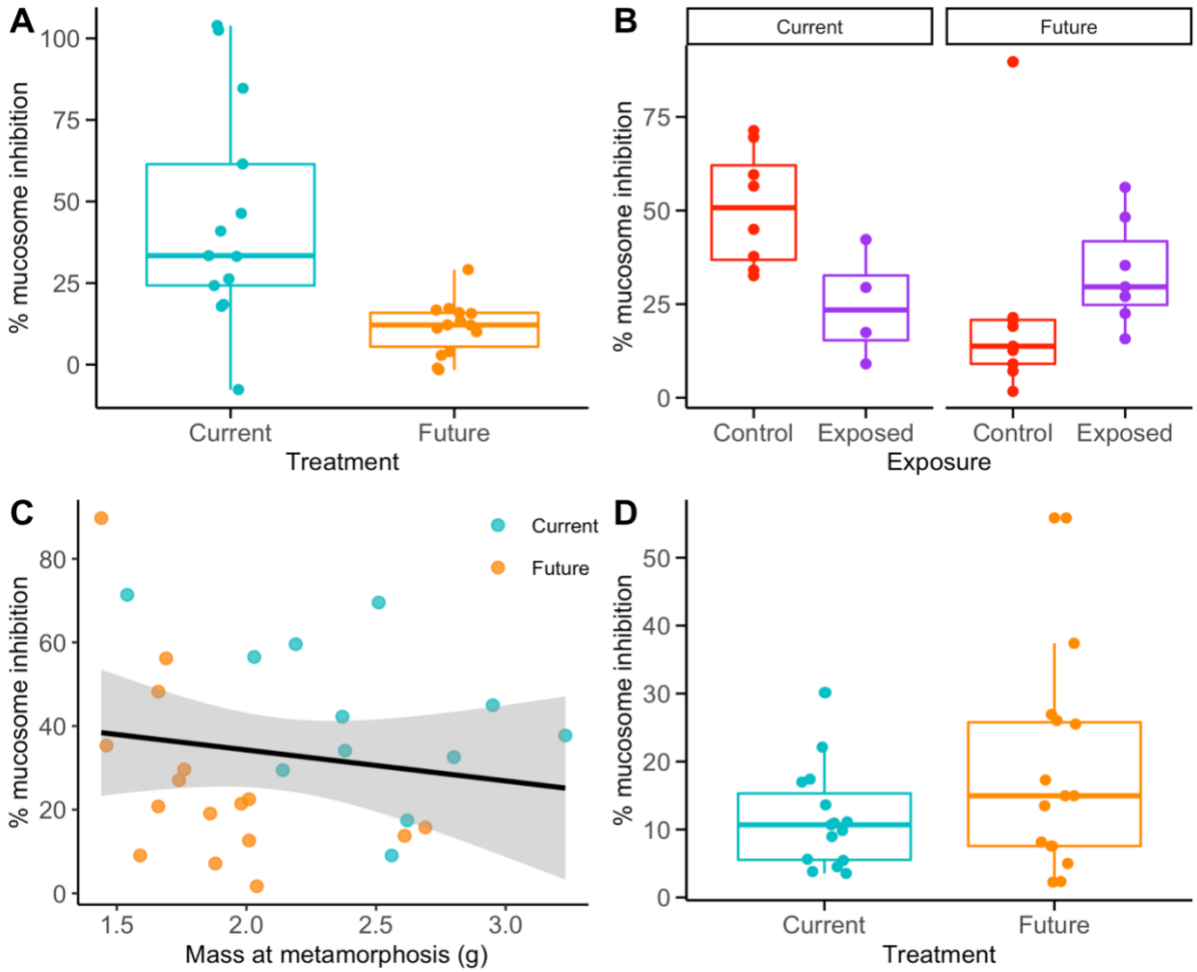

Figure 2.23 Boxplots showing the relationship between inhibition (%) of Bd growth by mucosome.

(A) *Bd*- and sham-exposed *R. pipiens* from Vermont from current and future temperature treatments: current temperature treatment mean = 45.0373 % (range = -7.693 to 103.904 %) and future temperature treatment mean = 11.258 % (range = -1.621 to 29.085 %) and (B) *Bd*- and sham-exposed *R. pipiens* from Pennsylvania from the current and future temperature treatments: current temperature treatment mean for sham-exposed = 50.803 % (range = 32.578 to 71.372 %) and for *Bd*-exposed 24.547 % (range = 9.046 to 42.256 %), future temperature treatment mean for sham-exposed = 21.698 % (range = 1.697 to 89.726 %) and for *Bd*-exposed 33.525 % (range = 15.750 – 56.184 %). Plot (C) is a scatter plot and line of best fit for the relationship between inhibition (%) of *Bd* growth by mucosome and mass at metamorphosis (g) for *R. pipiens* from Pennsylvania, with shaded areas representing 95% confidence intervals. Plot D shows boxplots of the relationship between inhibition (%) of *Bd* growth by mucosome from *Bd*- and sham-exposed *R. sphenocephala* from Louisiana from the current and future temperature treatments:

current temperature treatment mean = 11.652 % (range = 3.536 – 30.154 %) and future temperature treatment mean = 17.687 % (range = 2.258 –55.854 %). For all plots, each point equals one individual. In the boxplots the middle line corresponds to the median. The lower and upper hinges correspond to the first and third quartiles (the 25th and 75th percentiles). The upper whisker extends from the hinge to the largest value no further than 1.5 times the inter-quartile range.

2.4 Discussion

I measured the direct and indirect effects of developing as larvae under simulated climate change temperatures on Northern and Southern leopard frogs' immune systems. For nearly all of the aspects of development and immune function that I measured, the patterns with temperature treatment differed among populations and species. From what I observed, each population did respond to the stressor of elevated developmental temperature, but they did so through changes to different suites of factors, each of which may affect their fitness (both overall and in the face of pathogens). Other studies investigating the effects of stressors on immune function have found similarly inconsistent results among populations and species. For example, fish exposed to heavy metals, such as copper, often show a decrease in lymphocytes (Dick and Dixon 1985, Dethloff 1998). However, one study done in tilapia found more lymphocytes in fish exposed to higher levels of copper (Nussey 1995). Plasticity in response to developmental stressors (*e.g.*, temperature, water level, predators) at the larval stage have been well documented in amphibians (Gervasi and Foufopuolos 2008, Brannelly *et al*. 2019). However, the carry-over effects of those stressors in later life stages, and especially on the immune system, have rarely been studied.

Let's first consider the developmental aspects of elevated temperature, like larval survival, time to metamorphosis, size and mass at metamorphosis, on the animals in my experiment. Survival was very low in all the populations compared to the experiment in Chapter 1 where animals were reared in mesocosms outside. In this experiment, more than half the tadpoles in each environmental chamber died prior to metamorphosis. The low survival in this study could be due to a negative effect of frequent water changes on development of a beneficial microbiome (as compared with more natural conditions in our mesocosm study). The artificial lighting conditions, the noise inside the working chambers, and the diet I fed the tadpoles could have affected tadpole survival as well. Based on what has been seen in other frog species, I predicted that the tadpoles developing at a higher temperature would metamorphose faster, at a smaller size, and would have lower survival to metamorphosis. In the Northern leopard frog, larvae in the future temperature treatment developed faster and metamorphosed at a smaller size but there was no difference in survival to metamorphosis. In the Southern leopard frogs from Louisiana (the only population of this species where animals survived to metamorphosis), animals from the future temperature treatment developed faster, but there was no difference in size at metamorphosis. In these frogs, survival to metamorphosis was lower in the future temperature than in the current temperature treatment.

It seems logical that toward the southern part of their range, northern hemisphere temperate zone species would be better adapted to tolerate higher-than-average temperatures and more northern populations would be better adapted to colder and shorter summers (Conover and Schlutz 1995). However, in my experiment, the only population showing reduced survival to metamorphosis in the future temperature treatment was the *R. sphenocephala* population from Louisiana. Survival was similar between both temperature treatments in both of the *R. pipiens*

populations. This could be explained by the Louisiana *R. sphenocephala* larvae, which live closer to the southern edge of their species range, having a narrower range of thermal tolerance than the more northern *R. pipiens* populations I studied. Recent comparisons have found support for this pattern in comparisons between tadpoles of tropical and temperate amphibian species (Gutiérrez-Pesquera *et al*. 2016).

As predicted, the frogs exposed to the future temperatures metamorphosed faster in all the populations studied. The frogs that developed as larvae in my future temperature treatments were also smaller body length and mass after metamorphosis. This pattern, where tadpoles reared in warmer water metamorphose faster but at a smaller size, has been observed in many amphibians (Uhlenuth 1919, Etkin 1964, Gilbert 2020) and may be a general pattern for ectotherms (Howe 1967, Lock and McLaren 1970). The impacts of these plastic responses to elevated temperature may have lingering consequences later in life. Larger juveniles often grow to be larger adults, and smaller juveniles can take longer to reach sexual maturity (Berven 1990, Cabrera-Guzmán *et al*. 2013). A larger body size at the time that metamorphosis is complete has been correlated with greater terrestrial survival since, as reported for *Bufo calamita* (Reques and Tejedo 1997), *Pelohylax lessonae* and *P. esculentus* (Altwegg and Reyer 2003), larger frogs are better able to cope with different stressors, such as predation and desiccation, in their terrestrial habitats. Elevated temperature is just one of many aspects of climate change that can cause morphological and physiological stresses on amphibian larvae. But do these effects include negative impacts on the immune system?

Stressors can have more dramatic negative effects on health when experienced during formative stages of life. In this study and in previous work (Morey and Reznick 2001; Van Buskirk and Saxer 2001; Relyea and Hoverman 2003) it has been shown that the quality of a

tadpole's environment early in development has post-metamorphic effects on survival, growth, and morphology. Here I examined the carry-over effects of elevated temperature on multiple measures of both the innate and adaptive immune function in newly-metamorphosed leopard frogs. I hypothesized that elevated temperature is a stressor that will have a negative impact on immune response. The few other studies that have examined the effects of environmental stressors on immune response in amphibians have found support for this hypothesis. For example, adult southern leopard frogs forced to metamorphose faster due to drying and warming, developed antimicrobial peptides (AMPs) much later than animals that did not experience these stressors (Holden *et al*. 2015). In this study, as predicted, Vermont and Louisiana animals reared in the future temperature treatment secreted lower quantities of hydrophobic peptides in their mucus. The number of AMPs secreted was also lower in animals from Vermont that developed in the future temperature treatment. This suggests that developing as a tadpole in a warmer than normal environment, as is expected under climate change, could compromise this aspect of the amphibian innate immune system. Mucosal peptides are the first line of defense against the amphibian chytrid fungus, *Bd* (Carey *et al.* 1999). When I compared aspects of the adaptive immune system among temperature treatments, however, I saw a different pattern.

For the adaptive immune system, I hypothesized that the production of white blood cells, thymocytes, splenocytes, and T and B cells would be lower for frogs that developed under the stress of elevated temperatures. This is because under acute stress, non-essential processes such as immune function are inhibited by the hormonal stress response (Sapolsky *et al*. 2000). I found, as predicted, that the *R. pipiens* from Vermont that developed in the current temperature treatment had more white blood cells. However, this pattern was not seen in frogs from the other populations studied. Contrary to my predictions, the *R. pipiens* from Pennsylvania that developed

in the future temperature treatment produced more thymocytes and splenocytes than the current temperature and the *R. sphenocephala* from Louisiana that developed in the future temperature treatment also produced more thymocytes. There were no differences in T-lymphocyte proliferation between the temperature treatments, however the Vermont *R. pipiens* from the future temperature treatment had greater B-lymphocyte proliferation than frogs from the current temperature treatment. Another potential explanation might be that the immune system undergoes a major reorganization during metamorphosis and the greater number of lymphocytes might be due to a catch-up phenomenon experienced by frogs that developed in more stressful larval conditions. Taken together, these studies suggest that developing as larvae under elevated temperatures might actually stimulate the immune system, potentially creating an advantage for protection against infectious diseases. A strong between-season temperature dependence of circulating lymphocytes and eosinophils has been documented in Red-Spotted Newts (Raffel *et al*. 2006). However, the impacts of smaller changes in temperature on the adaptive immune system, as in this study, have never been investigated before in amphibians. It is possible that in this study, an increase of two or three degrees Celsius might not have been enough for temperature to act as a stressor on the leopard frog immune system. Other studies have found that higher temperatures within an amphibian's optimal temperature range usually stimulate the immune system whereas at temperatures near the bottom end of the optimal temperature range the immune system slows down, perhaps due to low energy supply (Rollins-Smith and Woodhams 2012).

In many of the immune parameters I measured, instead of temperature during development having a direct effect on later-life immune parameters, I found that growth rate, mass at metamorphosis and time to metamorphosis, which were themselves affected by

temperature, had carry over effects on different aspects of the immune system. These measurements could also reflect how relatively costly the developmental responses to elevated temperature were (i.e., how much energy was left for immune development), or perhaps, different strategies for mitigating the stressor. Phenotypic plasticity is often costly, and trade-offs exist between the benefits given by plasticity in one trait and the consequences of that plasticity on other traits that affect fitness (Newman 1992, Roff 1992). I hypothesized that there would be a positive correlation between time to metamorphosis and immune parameters because frogs with shorter larval periods have less time to acquire the resources they need to build their immune system. Frogs that are smaller at metamorphosis, I hypothesized, would have lower immune defenses because they have invested more energy into metamorphosing faster. For frogs with a fast growth rate after metamorphosis, I predicted a negative relationship with immune function since fast growers are likely prioritizing putting resources into growing large over investment in the immune system.

While the developmental temperature did not directly affect some aspects of the immune system, I found that, in the Northern population (Vermont) of *R. pipiens*, mass at metamorphosis was positively correlated with thymocyte counts and B-lymphocyte proliferation. This matched my prediction because the higher the mass at metamorphosis, the more reserves they would have had available to build the immune system. As predicted, at one-month post-metamorphosis, Vermont frogs from the future temperature treatment that took longer to metamorphose had more white blood cells. Perhaps this is because they had ample time to build the immune system. However, in frogs from the current temperature treatment, the amount of white blood cells was not correlated with larval period. Perhaps when not under temperature stress even animals with shorter larval periods have enough resources to build up ample white blood cells.

In the other population of *R. pipiens* (Pennsylvania), the faster the frogs grew after metamorphosis the greater the number of splenocytes, regardless of the temperature. During the rapid climax of metamorphosis, the lymphocyte numbers in circulation and in the thymus and spleen decrease (Rollins-Smith *et al*. 1984). But soon after, there is a burst of lymphocyte development (Du Pasquier and Weiss 1973). This burst seemed to happen more quickly for frogs with a faster growth rate after metamorphosis. In the future temperature treatment for this population, frogs that spent more time as a tadpole secreted more peptides. T-lymphocyte proliferation also increased with larval period both in current and future temperature treatments. Perhaps animals that spend longer periods as tadpoles and metamorphose larger do not have to spend as much time investing in energetically demanding life-history processes (such as foraging for food) after metamorphosis, and as a result, they can invest more energy into the immune system (Lochmiller & Deerenberg 2000; Norris & Evans 2000).

For the southern leopard frogs from Louisiana from the future temperature treatment, animals that grew faster during their first month after metamorphosis secreted less peptides and had lower B-lymphocyte proliferation. However, those correlations were not seen in animals from the current temperature treatment, suggesting that developing under elevated temperature, which often leads to smaller metamorphs that have to quickly catch up in growth in order to compete with their peers, can result in lower innate immune function. It seems logical that these frogs are investing more in growth, than in immune system development. However, for this population, as for the Northern leopard frogs, the faster animals grew after metamorphosis the greater their white blood cell and splenocyte counts, regardless of the temperature. In this population, greater mass at metamorphosis also was also correlated with greater thymocyte counts at two months post-metamorphosis. This matched my prediction, possibly because the

higher the mass at metamorphosis, the more reserves an animal may have available to build the immune system. However, as in *R. pipiens*, a higher mass at metamorphosis was associated with lower T- lymphocyte proliferation. Since this assay was done when the frogs were only one month old, most of them were less than one 1 g in body weight. It is possible that by this point they simply hadn't had enough time or resources to develop this aspect of the adaptive immune system. For this population, contrary to what we saw in the Pennsylvania *R. pipiens*, the longer an animal from the future temperature treatment spent as tadpole the less mucosal peptides it secreted. Taken together, my results suggest that developing in an elevated, future temperature can have indirect effects on the immune system that act through differences in size and growth rate after metamorphosis but that the aspects of the immune system that are affected often differs among populations and species.

Most of the *Bd*-exposed frogs in my exposure experiment did not exhibit clinical signs of chytridiomycosis, even though they maintained infections for the duration of the experiment with moderately heavy infection loads. Developmental temperature seemed to affect the course of infection after exposure, however. For example, in my Pennsylvania *R. pipiens*, *Bd* exposed frogs from the future temperature treatment increased in *Bd* load and prevalence throughout the exposure experiment whereas frogs from the current temperature treatment decreased in load and prevalence. These results suggest that the larval developmental temperature impacts a frog's susceptibility to *Bd*, perhaps through effects on pathogen resistance. Similarly, the scaled mass index, a measure of body condition, increased more quickly in Pennsylvania frogs from the current temperature treatment. This suggests that even in the absence of clinical signs of chytridiomycosis, developing as a tadpole in warmer than average conditions can lead to greater sub-lethal effects of *Bd* infection later in life. In Louisiana *R. sphenocephala*, however, body

mass index decreased at the same rate frogs from the current and future temperature treatments, suggesting that this effect may be species and/or population specific. In Vermont *R. pipiens, Bd*-exposed frogs from the future temperature treatment had significantly lower survival than *Bd*-exposed frogs from the current temperature treatment and control (sham exposed) animals. This, it appears that developing in elevated, future temperature conditions as a tadpole made these frogs more susceptible to lethal effects of *Bd* infection after metamorphosis.

In addition to effects of developmental temperature, I also hypothesized that exposure to *Bd* might affect the immune system of juvenile leopard frogs. To test this hypothesis, I compared splenocytes counts one week after the last *Bd* exposure in my exposure experiment. However, I did not find any effects of prior infection with *Bd* on splenocyte counts. This could be because the animals didn't develop heavy enough infections to trigger an increase in this type of adaptive immune response or because the splenocyte response was not playing an important role in fighting *Bd* infection. In a study in *Xenopus lae*vis with low level *Bd* infections splenocyte counts were also found not to differ between *Bd*- and sham-exposed frogs (Fites *et al*. 2014). However, studies of the highly susceptible frog *Atelopus zeteki* late in infection, when animals had heavy *Bd* loads, supports that idea that fungal products from the skin infection can decrease splenic lymphocyte numbers (Ellison *et al*. 2014). While I did not find an effect of *Bd* exposure on splenocytes, after the *Bd* exposure experiment I did see an effect of developmental temperature on splenocytes; the frogs from the future temperature treatments had more splenocytes than the ones from the current temperature treatments. This could be due to higher metabolic rates during development at elevated temperatures (Rollins-Smith and Woodhams, 2012). However, this effect of temperature, like others we observed in animals prior to the

exposure experiment, was only seen in some populations (in this case in both populations of *Rana pipiens*).

After the *Bd*-exposure experiment, as in the younger froglets sampled prior to the exposure experiment, faster growth rate after metamorphosis and greater mass at were negatively correlated with splenocyte counts. After the exposure experiment, the ability of the mucosome, which includes bacterial products as well as inhibitory proteins and peptides and possibly lysozymes (Woodhams *et al.* 2014), to inhibit *Bd* seemed to have been affected by developmental temperatures in different ways for the two leopard frog species. In *R. pipiens* from Vermont, as I predicted, frogs that developed in the current temperature treatment had mucus that was more effective at inhibiting *Bd* growth than frogs from the future temperature treatment. However, in *R. sphenocephala* the opposite pattern with temperature was seen. In Pennsylvania *R. pipiens*, there was an effect of *Bd* exposure on mucosome inhibition. However, the pattern ran counter to my predictions. The mucosome of sham exposed frogs from the current temperature treatment inhibited *Bd* growth more than that of the *Bd* exposed frogs, however the mucosome of frogs from the future temperature treatment was more effective at inhibiting *Bd* growth if the animal had been exposed to *Bd*. Contrary to my predictions, the magnitude of *Bd* growth inhibition by mucosome decreased with an animal's mass at metamorphosis. Without a more detailed analysis of changes in different components of the mucosome it is difficult to understand what may be driving these patterns. Perhaps under some sets of conditions inhibitory bacteria are more dominant and actively secret more *Bd*-inhibitory products? In general, despite finding several significant differences in immune parameters among temperature treatments and *Bd* exposure groups, the complex results I found suggests that more work needs to be done to

tease apart what is happening with the immune system after exposure to the stressors of elevated temperatures and *Bd*.

It is striking to see so many significant differences among the many immune parameters between frogs that developed in my two temperature treatments, especially considering that the frogs reared as tadpoles under these different temperatures had all been treated the same for months after metamorphosis. Taken together, my study's results suggest that the combined threats of temperature and infectious disease across life stages may interact to put amphibians at a greater risk of mortality than would be expected from one of these threats alone. Temperature had direct effects on development, size, and the innate immune system. There were also indirect effects of temperature and carry-over effects of temperature on either later life stages or on development, which also generated differences in immune measures. Because temperature impacts development in different ways for different populations, the impacts of temperature stress can be many and varied and really challenging to predict. This study shows that different impacts to the innate and adaptive immune system are there, and they are likely impacting many aspects of fitness, especially given the risk that emerging infectious diseases pose to amphibians and other taxa.

3.0 Understanding the landscape-level movement of an emerging wildlife pathogen

3.1 Introduction

As infectious diseases emerge with increasing frequency and impact on wildlife populations (Johnson and Paull 2011) it becomes ever more critical to understand the links between environment, host-pathogen biology, and disease dynamics (Raffel *et al*. 2013). Fungal pathogens such as white nose syndrome in bats (Foley *et al*. 2011), colony collapse disorder in bees (Bromenshenk *et al.* 2010), and chytridiomycosis in amphibians (Berger *et al*. 1998; Casadevall *et al.* 2005) have been important drivers of recent wildlife declines and extinctions (Fisher *et al.* 2009). Although we have learned a lot about the biology of these host-pathogen systems in recent years, important questions remain elusive, including how pathogens move across the landscape. The goal of this study was to better understand the dynamics and movement of *Batrachochytrium dendrobatidis* (*Bd*), the chytrid fungal pathogen that causes the sometimes-lethal skin disease chytridiomycosis in amphibians, across a landscape where amphibian hosts inhabit both ephemeral and permanent ponds. My study was designed to answer three key questions: (1) how does pathogen load and prevalence change across the amphibian active season in ephemeral versus permanent ponds, and (2) which amphibian hosts play the largest role in moving *Bd* across the landscape, and (3) how is genetic variation in *Bd* structured across the landscape? To answer these questions, I conducted a field study in Northwest Pennsylvania, though due to the nearly global distribution and impact of *Bd* on amphibians, my findings are likely to shed light on the mechanisms that underlie *Bd* dynamics and spread in other areas of the world as well.

The infectious life stage of *Bd* is the zoospore, which is motile in aquatic environments and has the potential to transmit to new hosts (Longcore *et al*. 1999; Greenspan *et al*. 2012). As a consequence of the aquatic nature of the fungus, which cannot survive desiccation, frog species associated with permanent ponds (Kriger and Hero, 2007) and streams (Hero *et al*. 2005; Gründler *et al*. 2012) are significantly more likely to be infected with *Bd* than more terrestrial species and those associated with ephemeral waterbodies, which dry out each year. The proportion of individuals infected can also differ among species and life stages. While the factors that underlie a species' susceptibility to *Bd* remain unclear, variation in skin defenses appear to be important. The skin mucus of many amphibian hosts contains antimicrobial peptides (AMPs), which the amphibians produce and store in granular glands in the skin (Rollins-Smith 2009). Additionally, amphibian skin is home to a diverse microbiota, which can be an important component of the defense against *Bd* and other skin pathogens (Kruger 2020). Habitat use may also be an important factor in determining the likelihood of infection with *Bd*. Post-metamorphic hosts can move between aquatic habitats (Regosin *et al*. 2003), potentially spreading the pathogen, but tadpoles are generally restricted to their natal aquatic environment (Hoff *et al*. 1999) and as a result, the likelihood of infection on new metamorphs emerging from their natal pond likely depends on the zoospore pool in that pond environment. For example, in Eastern North America, leopard frogs (*Rana pipiens*), green frogs (*R. clamitans*) and bullfrogs (*R. catesbeiana*) overwinter and/or reproduce in permanent ponds but migrate to ephemeral ponds in late spring/early summer, making them potential vectors for *Bd*.

The zoospore pool in a pond, and hence the *Bd* prevalence and load on infected hosts, may also depend on abiotic factors like pH, temperature, canopy cover, or depth, and any non-amphibian species that act as reservoirs for *Bd* (Raffel *et al*. 2010). Johnson and Speare (2003)

suggested that *Bd* can persist in aquatic environments for long periods of time (7 weeks in a pond) probably using the high level of nutrients and the nonliving organic substrate given by algae in the absence of amphibian hosts. The growth of *Bd* in vitro is strongly temperature dependent, suggesting that temperature may be an important predictor of *Bd* infections on hosts as well. In culture, *Bd* grows well at cool temperatures and can even withstand freezing, whereas maximum growth occurs between 17 °C and 25 °C (Piotrowski *et al*. 2004). The pathogen appears to grow more slowly in temperatures exceeding 26°C, and it dies after 5 minutes at 60 °C (Johnson *et al*. 2003). *Bd* growth in culture also appears to depend on pH. In one study, *Bd* grew and reproduced at pHs between 4 and 8 while growth was greatest at pH 6 to 7 (Piotrowsky *et al*. 2004). In a study with newts (*Notophthalmus viridescens*), *Bd* load was higher, and animals were less able to clear infections, when ponds were more completely covered by canopy vegetation. The shade this vegetation provides appears to reduce the ability of ponds to warm up, and warmer temperatures help the newts to clear their infections (Raffel *et al*. 2010). Seasonal variation in both temperature and humidity have both been suggested to control the prevalence of *Bd* infections, and the timing of chytridiomycosis outbreaks, in the wild (Berger *et al*. 2004; Retallick *et al*. 2004). However, *Bd* dynamics may also depend on the presence of amphibian and/or non-amphibian reservoir host species in the pond.

There are a few *Bd* reservoir taxa that could act as vectors of the pathogen between ponds. *Bd* infects the keratinized skin of post-metamorphic amphibians and the keratinized mouthparts of amphibian larvae, but it also survives in parts of other animal taxa that contain keratin. For example crustaceans, which contain keratin in their digestive tract, may serve as reservoir hosts. *Bd* has been shown to survive and even complete its life cycle in crayfish (McMahon *et al*. 2013) and Brannelly *et al.* (2015) found that crayfish (*Procambarus* spp. and

Orconectes spp.) can be infected with *Bd* in the wild. Crayfish can also transmit *Bd* to tadpoles under laboratory conditions (McMahon *et al.* 2013). In the laboratory, some studies have shown that certain fish could serve as reservoirs, with samples taken from zebrafish displaying various stages of *Bd* development, including discharged mature zoosporangia (Liew *et al*. 2017). It seems most likely, however, that the most important reservoirs for *Bd* are probably amphibian species, like the North American bullfrog (*Rana catesbeiana*, Daszak *et al*. 2004), and the Pacific treefrog (*Pseudacris regilla*, Padgett-Flohr and Hopkins 2009) which can harbor large *Bd* loads and do not usually develop disease symptoms.

Bd's aquatic zoospores cannot survive extended dry periods (Johnson *et al.* 2003), thus, I hypothesize that the multi-year persistence of *Bd* in ephemeral ponds, must be dependent upon infected animals bringing zoospores back to the pond each spring. Ephemeral ponds are a unique, often predator-free habitat that support the reproduction and early development of a suite of species depend upon them, including a number of invertebrates and amphibians (Hopey and Petranka 1994). In contrast, permanent ponds are larger habits that hold water throughout the year and also often contain predatory fish and a diverse community of small-bodied invertebrates and vertebrates (Wellborn *et al.* 1996). Because they do not freeze solid all they way to their bottoms, many species overwinter in permanent ponds, including larval and adult amphibians, which can act as reservoir hosts for aquatic pathogens like *Bd*, allowing them to persist across years (McDonald and Alford, 1999).

In Eastern North America, some amphibian hosts, like leopard frogs (*R. pipiens*) and green frogs (*R. clamitans*) overwinter and/or reproduce in permanent ponds (Neill, 1948) but migrate to ephemeral ponds in late spring/early summer, making these species potential vectors for *Bd* to ephemeral pond communities. Other species, like wood frogs (*R. sylvatica*) and spring

peepers (*Pseudacris crucifer*), use only ephemeral ponds. These species, which overwinter terrestrially (Storey and Storey, 1984) and reproduce very early in spring, could also bring *Bd* to ephemeral ponds if they emerge infected from hibernation. Understanding how pathogens spread to and from ephemeral ponds, and how both types of pond communities contribute to the landscape-level dynamics of host-pathogen interactions, will be important for predicting disease risk and developing mitigation strategies.

Thus far, five lineages of *Bd* have been described worldwide (*Bd*CAPE, *Bd*Asia1, *Bd*Asia2/Brazil, *Bd*Asia3 and *Bd* GPL; O'Hanlon *et al*. 2018). The *Bd* lineage associated with amphibian declines, the Global Pandemic Lineage (GPL; Farrer *et al*. 2011; Rosenblum *et al*. 2013), appears to have spread worldwide within the last 100 years, and is thought to have reached North America in 1980s-1990s (O'Hanlon *et al*. 2018). The phylogenetic relationships among the lineages suggest that *Bd*Asia is the most basal lineage and that *Bd*GPL is the most recent lineage (Farrer *et al*. 2011, O'Hanlon *et al*. 2018). The GPL has been divided in two genetic groups *Bd*GPL-1, which is primarily found in North America and Europe, and *Bd*GPL-2, which is distributed worldwide (Rosenblum *et al*. 2013). The arrival of *Bd*-GPL-1 caused declines in North America and *Bd*-GPL-2 in Central America (Schloegel *et al*. 2012). Our recent work suggests that several groups belonging to the GPL strain are infecting amphibians in Northwest Pennsylvania, and that many are shared across ponds and host species (Byrne *et al*. unpublished). Using a new genomic assay, I was able to distinguish which amphibian hosts are bringing which strains into ephemeral ponds, which strains end up dominating the community, and which are carried out of the pond in this region. This information is novel and will aid in predicting the dynamics and spread of *Bd* across landscapes.

Here I test six hypotheses about the dynamics and spread of *Bd* at my study sites:

(H1) At the start of each amphibian active season, ephemeral pond host communities will have little to no *Bd* whereas permanent pond host communities, where many host species hibernate, will have more *Bd*.

(H2) *Bd* load (number of zoospores per host) and prevalence (proportion of hosts infected in a population) in both types of pond will fluctuate with host temperature and pond pH.

(H3) *Bd* moves from permanent to ephemeral ponds each year via hosts that overwinter and breed in permanent ponds but occasionally visit ephemeral ponds.

Alternatively (H4), *Bd* is primarily brought to ephemeral ponds by ephemeral pond specialist species that emerge infected from terrestrial hibernacula and breed in ephemeral ponds soon thereafter. In this case, I predict that *Bd* load and prevalence in ephemeral ponds will be high on ephemeral pond species as they enter the pond

(H5) New metamorphs emerging from ephemeral ponds will have infection prevalences and loads similar to the adult amphibians using the pond at the same time.

(H6) The genetic variation present in *Bd* at my field sites will be structured by pond, host species, and time of year.

To test these hypotheses, I surveyed ephemeral and permanent ponds during three years and tested for differences in infection load and probability of infection. I used drift fences (fences surrounding each pond that amphibians cannot pass through or over without my help) and pitfall traps (i.e., buckets buried in the ground which amphibians trying to pass through the fence fall into) to sample all amphibians entering and leaving two ephemeral ponds from the start of the breeding season until the pond dried.

3.2 Methods

3.2.1 Surveys at permanent and ephemeral ponds

I sampled field sites in the spring, summer, and fall across 3 different years. I conducted this research from 2017 to 2019 in Northwestern Pennsylvania, near the Pymatuning Lab of Ecology (PLE). Sampling was conducted at ten sites (Table 3.1): five ephemeral ponds and five permanent sites that are separated from one another by from 1 km to 15 km. Each site was sampled once per month from March to September in 2017 and 2018. In 2019 the ponds were sampled twice per season. I attempted to collect data from 20 individuals from each amphibian species present at each site during each survey.

Table 3.1 Field site names, locations, and pond types

Field site code and name	Coordinates	Pond Type
PA01 Wood lab	41.569722 N -80.452500 W	Ephemeral
PA02 RV	41.691933 N -80.500450 W	Permanent
PA03 Sanctuary lake	41.644136 N -80.429444 W	Ephemeral
PA04 Cow Pit	41.672083 N -80.513067 W	Permanent
PA06 Tuttle	41.638883 N -80.495116 W	Permanent
PA07 Beaver	41.665167 N -80.514650 W	Permanent
PA09 David's pond	41.621208 N -80.469131 W	Permanent
PA10 Phelps	41.690883 N -80.512467 W	Ephemeral
PA11 Church	41.650494 N -80.423694 W	Ephemeral
PA12 Black Jack	41.665733 N -80.511781 W	Ephemeral

At each field site I placed data loggers to record air temperature and humidity (Onset HOBO U23-001) in full sun and in shade and water temperature (Onset HOBO UA-002-64, 5 cm below surface) every hour. A soil temperature logger (Onset HOBO UA-001-64) was also buried in a hole next to each pond (5 cm deep) to record every hour.

At the start of each field survey, a handheld weather meter (Kestrel 3000) was placed 2 meters above the ground in a tree and allowed to adjust to the air temperature. When it was stable, I recorded the air temperature, wind speed, barometric pressure, and humidity. Using a calibrated water quality meter (Oakton waterproof double junction pH Meter I-1000), I measured water temperature, conductivity, TDS and pH, 5 cm below the surface and 3 m (or as close as safely possible) from the water's edge. To look for amphibians, I waded into the pond and walked around the perimeter to look for amphibians. For the fences, I used the same method, but I didn't wade into the pond, I only walked along the fence looking inside the buckets or around the fence. When an amphibian was sighted, I used a non-contact infrared thermometer (Dual laser IR thermometer, Model EC400L2) to measure surface body temperature and the surface temperature of their microhabitat (the site where the frog was located). I then attempted to catch the amphibian and if successful, recorded its time of capture. Most of the amphibians were caught by hand using a fresh pair of nitrile gloves to reduce pathogen transmission (Phillot *et al*. 2010). If nets were used, they were cleaned between sites with F10 SC (a veterinary disinfectant that has been shown to kill *Bd* (Van Rooij *et al*. 2017). I also disinfected my waders with F10SC between ponds. Captured amphibians were placed individually in Ziploc plastic bags for processing and handling. Bags were discarded after one use.

At the end of a sampling night, I weighed, measured, and swabbed each animal that had been captured. A dial caliper was used to measure the snout-to-vent length (SVL) as a measure

of body size. The tail length was measured separately for salamanders. To record body mass, I used a Pesola scale and first recorded the total mass of the frog inside the plastic bag. Then, I recorded the mass of the bag alone and subtracted this from the mass of the animal and bag. I also recorded the animal's sex (when possible) and life-stage. To collect skin swab samples for *Bd* diagnostics, I swabbed adult and juvenile amphibians five times on dorsal, ventral, right, and left sides, and feet with a sterile swab (Medical Wire MW113). For tadpoles, I swabbed the mouthparts only, five times. For salamanders, I swabbed five times on the dorsal and ventral surfaces, right and left sides, each foot, and the dorsal and ventral surface of the tail for a total of 45 strokes. After the swabbing was complete, the swab was placed into a labeled 1.5 mL tube and frozen at -20˚C. Once all measures were taken, the animals were released near the location where they were collected.

3.2.2 Surveys at fenced ephemeral ponds

I conducted surveys at the two fenced ephemeral pond sites (Wood Lab and Sanctuary Lake, Table 3-1) from March to August 2019. The hydroperiod of these ephemeral ponds depends on localized precipitation and recharge from groundwater. The Sanctuary Lake pond usually holds water for eight months of the year and Wood Lab pond for ten months of the year. The maximum recorded depth was 80 cm for both sites. I installed the drift fences 1-3 m from the edge of the pond to intercept all amphibians moving to and from the pond. I installed the fences in the fall preceding the study and left them open until the early spring, just before the first amphibians began to emerge from hibernation, to allow animals to go to and from the pond. The drift fences were made from 35 cm wide fine aluminum mesh buried 7-10 cm in the ground and held in place with wooden stakes every 1.5 m. The fences, when closed, entirely surrounded

each pond. I buried 1-gallon buckets as pitfall traps along the inside and outside of each fence to capture amphibians moving along the fence. The lids of the buckets each had a 12 x 8 cm hole to allow the amphibians to fall in the bucket. In the bottom of each bucket I punched four holes to allow water to drain. Into each bucket I also placed a plastic bag liner with two holes in its bottom to avoid cross contamination among sampling nights. The liner was replaced with a clean one each time an amphibian was found in a bucket. I placed these pitfall traps every 4 m outside and every 5 m inside along each fence for a total of 18 buckets inside and 25 buckets outside at the Sanctuary Lake pond and 22 buckets inside and 31 buckets outside at the Wood Lab pond. The fence total circumference of the fence was 131 m at the Sanctuary Lake site and 156 m at the Wood Lab site.

I sampled at the fenced ephemeral ponds for 40 nights between March 14 and August 8 of 2019. During each survey, I checked each pitfall trap by removing the bucket lid and searching through any organic material that may have accumulated in the trap. All animals captured were processed as described below and released approximately 4 m from the trap on the opposite side of the fence from where they were collected. I checked pitfall traps, on average, for three nights per week, prioritizing rainy nights, between 1900 and 0200 h. On days when the pitfall traps were not checked lids without holes were placed on the buckets to prohibit amphibians from falling in. During the breeding season and when new metamorphs were emerging from the ponds, I checked the pitfall traps one to two times per day. When animals were not breeding or metamorphosing, I checked the ponds two or three times a week. Mostly when it was raining.

At the fenced ponds, I only sampled amphibians from along the fences and in the pitfall traps. I did not wade into the ponds or use nets to capture animals in the ponds. Each animal was

handled using a clean pair of nitrile gloves. I placed each animal individually in a plastic Ziploc bag until the entire length of the fence and all pitfall traps had been searched. Then, I recorded sex and life stage of each animal, as well as whether it was captured on the outside or inside of the fence or in one of the pitfall traps. I also recorded instances where multiple amphibians were captured in the same bucket. Animals captured on the outside of the fence were processed before the ones that were captured inside the fence (water side). I weighed, measured, and swabbed the animals using the methods previously described. Amphibians captured from the fenced ponds were then marked by toe-clipping the same single digit on all the adult animals using a nail clipper (model 5X-3GPL-MUFZ) that had been sterilized in 100% ethanol prior to each use. The toes were clipped and stored individually in 100% ethanol.

3.2.3 DNA extraction and qPCR protocol

Bd-DNA was extracted from each swab using the "animal tissue" protocol and the Qiagen DNeasy Extraction Kit with a final elution volume of 200 µL. I then ran a qPCR assay (Blooi et al. 2013) using a QuantStudio™ 3 Real Time PCR system. I used 25 µL reactions containing 12.5 µL of 2x SensiFast probe Lo-Rox Mix, PCR primers at a concentration of 900 nM, the MGB probe at 240 nM, 400 ng/µL BSA, 3 µL water per well and 5 µL of template DNA (diluted 1:10 in DI water). The negative controls had the same master mix but with water added instead of a DNA template. The default QuantStudio amplification (V.1.4) software conditions (2 min at 50°C and 10 min at 95°C, followed by 40 cycles of 15 s at 95°C and 1 min at 60°C) were used (Boyle et al. 2004; Hyatt et al. 2007). Each swab sample was run once and each qPCR run contained a positive and negative control, and a series of plasmid dilution standards (Pisces Molecular, CO). Samples were run in singlicate and whole-swab Bd load was calculated by

multiplying results by 40. I excluded from analysis any wells where the internal positive control DNA did not amplify. I also excluded data from any qPCR runs where the negative extraction control was positive.

3.2.4 Isopropanol precipitation of samples containing *Bd* DNA

For samples that tested positive for Bd by qPCR, I used an isopropanol precipitation to prepare the remaining volume of the 200 µl DNA extraction for genotyping. To each sample I added 250 µL low TE, 50µl 3M Sodium Acetate (NaOAc), 2.5µl glycogen. I then added 500 µL of isopropanol and inverted the sample 10 times. I placed the samples at 4°C overnight and then spun them at 13,000 g for 10 min, after which I decanted the supernatant without disturbing the pellet. I then dislodged the pellet using 500 µL of cold 70% ethanol by inverting the sample a couple of times. The samples were then spun for 1 min at 13,000 g to get the pellet to the bottom of the tube. The ethanol was then decanted with a pipette, and I let the pellet dry before resuspending the pellet in 15 µL of low TE. These samples were stored at 4°C.

3.2.5 Sequencing and cleaning

The *Bd* DNA samples were genotyped from 110 swab samples collected from the two ephemeral pond sites that had fences using a custom genotyping assay (see Byrne *et al*. 2017). However only 57 amplified. Briefly, this assay uses the Fluidigm Access Array platform to perform microfluidic multiplex PCR on 191 regions of the *Bd* genome and one diagnostic locus for the closely related fungus *Batrachochytrium salamandrivorans* (*Bsal*). Each target locus is 150-200 base pairs long and the targets are distributed across the *Bd* nuclear and mitochondrial

genomes. All samples were pre-amplified in two separate PCR reactions, each containing 96 primer pairs, at a final concentration of 500nM. For each preamplification PCR reaction the FastStart High Fidelity PCR System (Roche) was used at the following concentrations: 1x FastStart High Fidelity Reaction Buffer with $MgCl_2$, 4.5mM $MgCl_2$, 5% DMSO, 200 µM PCR Grade Nucleotide Mix, 0.1 U/µL FastStart High Fidelity Enzyme Blend. 1 µL of DNA was added to each preamplification reaction and used the following thermocycling profile: 95˚C for 10 min, 15 cycles of 95˚C for 15 sec and 60˚C for 4 min. Pre-amplified products were treated with 4 µL of 1:2 diluted ExoSAP-it (Affymetrix Inc.) and incubated for 15 min at 30˚C, then 30 min at 80˚C. Treated products were diluted 1:5 in PCR-grade water. The diluted products from each of the two preamplification reactions were combined in equal proportions and used for downstream amplification and sequencing.

Each preamplified sample was loaded into the Fluidigm Access Array IFC (Fluidigm, Inc.) for amplification. All samples were barcoded and amplified, then pooled for sequencing on an Illumina MiSeq lane using the 300 bp paired-end kits at the University of Idaho IBEST Genomics Resources Core. All sequencing data was pre-processed as described in Byrne *et al.* (2017) and generated consensus sequences for all variants present for each sample at each locus using IUPAC ambiguity codes for multiple alleles. Reads were filtered by selecting sequence variants that were present in at least five reads and represented at least 5% of the total number of reads for that sample/locus using dbcAmplicons (https://github.com/msettles/dbcAmplicons).

3.2.6 Statistical analysis

All statistical analyses were performed using R Studio 2019 (RStudio 2019) and R version 1.1.5019 (R Core team 2019). To do the figures I used ggplot2 Wickham (2009). Tables of statistical model outputs can be found in Appendix C (Tables C1-C10).

To test for differences in *Bd* infection load across ephemeral and permanent ponds sampled between 2017-2019, I built generalized linear mixed models (function 'lme') using Template Model Builder (package 'lme4'). The response variable in each analysis was the log-transformed *Bd* load [log (*Bd* DNA copies +1)] detected on each skin swab sample and the fixed effects were pond type (ephemeral or permanent), pond pH and amphibian body temperature. Frog species and site were included as random effects in each model. I also tested for differences in *Bd* infection (yes/no) among ephemeral and permanent ponds by coding individuals as positive/negative for *Bd* for a given sampling period based on whether (or not) *Bd* DNA was detected on their swab sample using qPCR. For this analysis, I used generalized linear mixed models (package 'lme4') with a binomial (function 'glmer') distribution, the pond type, pond pH and amphibian body temperature were the fixed effects. Frog species and site were included as random effects in each model.

For the fenced ponds, to determine whether *Bd* load was higher in species hibernating in permanent ponds relative to those hibernating in soil, I analyzed a subset of data that included only amphibians that were captured outside the fences (on their way to the pond). I used a linear mixed model ('nlme' package, function 'lme') with hibernation type (terrestrial vs. permanent pond), pond, and their interaction. Species was included as a random effect. To compare *Bd* infection (yes/no) between the two hibernation types, I used a generalized linear mixed model

(package ‘lme4’, function ‘glmer’) with a binomial distribution including hibernation type, site, and their interaction as fixed effects. Species was included as a random effect.

To test whether tadpoles metamorphosing in the fenced ephemeral ponds left the pond *Bd* loads similar to other frogs inside the pond I used linear models (nlme package, function ‘lm’) with the categories of metamorph vs. all other amphibians present as a fixed effect. I ran the linear models for the three species that metamorphosed in these ponds (northern leopard frog *Rana pipiens*, wood frog *Rana sylvatica*, and spotted salamander *Ambystoma maculatum*) separately.

I used a gene-tree to species-tree approach to construct a phylogeny to explore the relationship of the *Bd* collected for this study to previously-published *Bd* samples representing all known *Bd* lineages (N=13, Byrne *et al*. 2019, Rosenblum *et al*. 2013). First, I trimmed the consensus sequence dataset to eliminate loci that had more than 50% missing data, resulting in 117 loci. Next, I individually aligned all loci using the MUSCLE package (Edgar 2004) in R (v.3.4.3), checked the alignments for errors in Geneious v.10.2.3 (Kearse *et al*. 2012), and used the RAxML plugin in Geneious to search for the best scoring maximum likelihood tree for each locus using rapid bootstrapping (100 replicates). I then collapsed all branches in all trees with <10 bootstrap support and used Astral III to generate a consensus tree. Astral generates an unrooted species tree given a set of unrooted gene trees (Zhang *et al*. 2018).

To further explore the genetic variation of *Bd* sampled from amphibians at the two fenced ponds, I used a principal components analysis (PCA). First, I aligned all reads for all samples to a reference FASTA with target sequences from *Bd* isolate JEL423 using bwa mem (Li and Durbin, 2009). I then used freebayes to call variants based on haplotypes (Garrison and Marth, 2012). I called variants using the following flags to ensure high quality: --0 --min-coverage 5. A

total of 166 variants were then used to calculate a PCA using the R package adegenet (v.2.1.1) (Jombart 2008). I plotted the first two PCs, which together explain 20.3% of the variation in our data. I compared the PCA data between the two ponds, between animals captured inside vs. outside the fences, between seasons (spring vs. summer) and between amphibian species.

3.3 Results

More than one third (37.5%) of the 4,898 amphibians we swabbed in Pennsylvania tested positive by qPCR for the presence of *Bd*. To test for correlations between the independent variables of pond type (ephemeral vs permanent), pond pH, and amphibian body temperature and the dependent variable of *Bd* infection (yes/no) over the three years of sampling I used a generalized linear mixed model (GLME). In this model there were no significant main effects of pond type or pH and the interactions between pH and pond type and between body temperature and pond type were also non-significant (GLME: $t \leq 0.857$, $p \geq 0.392$). However, body temperature was correlated with *Bd* infection (GLME: $t = -5.497$, $p < 0.001$, Figure 3.1), with the probability of infection increasing with body temperature in both permanent and ephemeral ponds until ~12 -17 ºC and decreasing with body temperature above that point. I also did not find a significant effect of pond type, pond pH or a significant interaction between pH and pond type when considering *Bd* load as the dependent variable (LMM: $t \leq 1.846$, $p \geq 0.065$). However, *Bd* load was significantly correlated with animal body temperature (LMM: $t = -7.404$, $p < 0.001$) and the interaction between pond type and body temperature was also significant (LMM: $t = -2.820$, $p = 0.005$). In permanent ponds, *Bd* load decreased with increasing body temperature (β = -

10.018, p = 0.005, Figure 3.2) while in ephemeral ponds and *Bd* load decreased only very slightly as body temperatures increased.

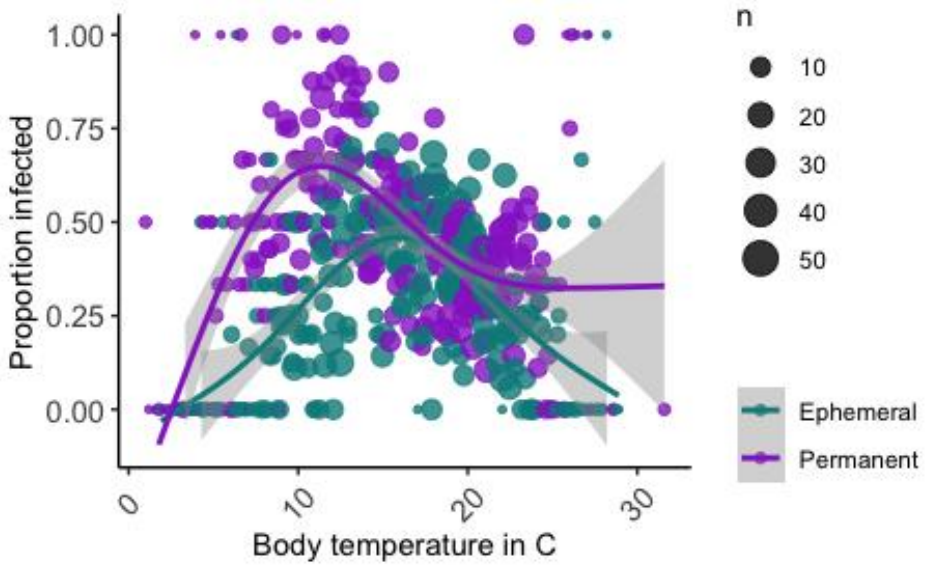

Figure 3.1 Relationship between the proportion of sampled animals that tested positive for Bd (via skin swab) and body temperature for amphibians sampled from ephemeral and permanent ponds.

The lines represent smoothed generalized additive model regressions, and the shaded areas are 95% confidence intervals. The size of the dot indicates the number of frogs from each pond type that were captured with a particular body temperature (to within 0.1 ºC).

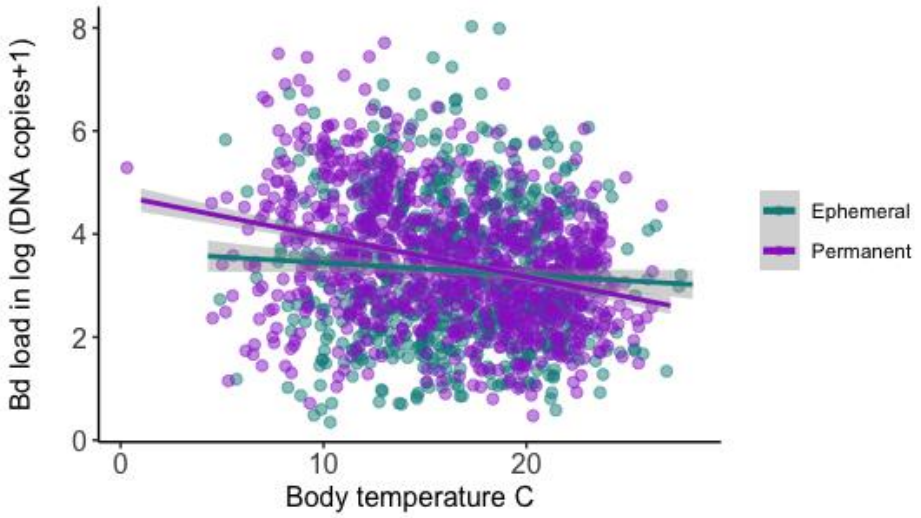

Figure 3.2 Relationship between amphibian body temperature and Bd infection load in ephemeral and permanent ponds.

The lines represent linear model fit between body temperature and *Bd* load and the shaded areas are 95% confidence intervals.

At the end of winter, when amphibians emerged from hibernation, both *Bd* infection loads and the proportion of infected individuals were lower in ephemeral ponds than in permanent ponds (Figure 3-3). To isolate the cause of these differences, I focused on data from the two ephemeral ponds that had been surrounded by drift fences and pitfall traps and asked which species were the first to enter the ponds with *Bd* infections.

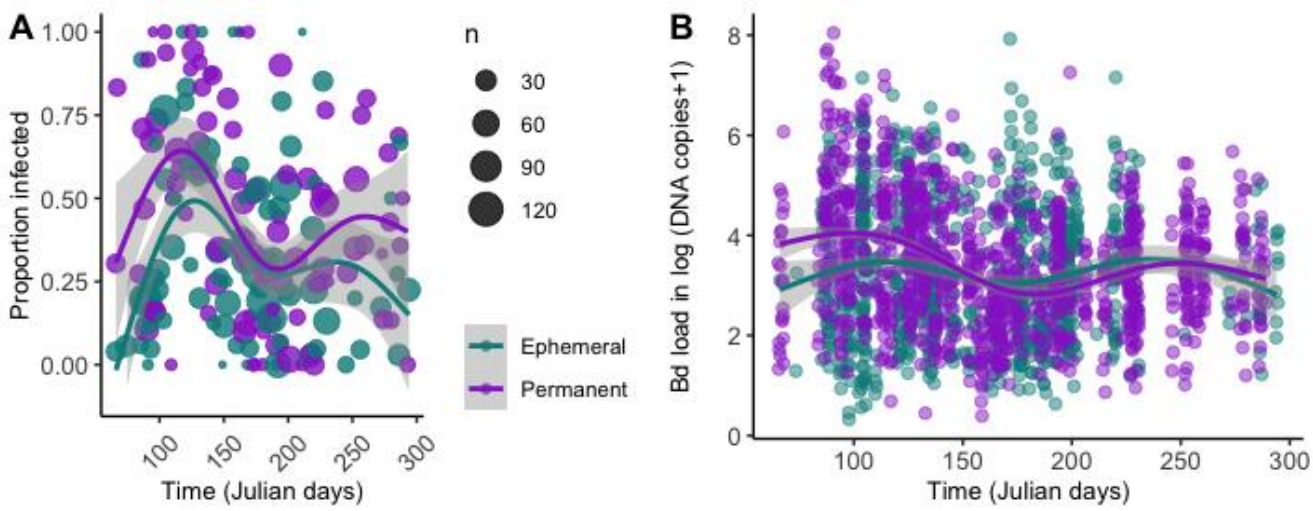

Figure 3.3 Relationship between time in Julian days for frogs collected from ephemeral and permanent ponds. and (A) the proportion of animals infected with *Bd*, and (B) *Bd* infection load. The lines represent smoothed generalized additive model regressions, and the shaded areas are 95% confidence intervals. The size of the dot indicates the number of animals sampled in a given survey.

I started sampling in Wood Lab pond, on March 14 of 2019, ten days after the ice covering the pond had completely melted. On the first night of sampling, I found Wood frogs (*Rana Sylvatica*), red-backed salamanders (*Plethodon cinereus)* and spotted salamanders (*Ambystoma maculatum*) along the fence and in the traps. None of the wood frogs or red-backed salamanders sampled were infected that night, however two of 21 spotted salamanders were infected. Amphibians did not start arriving at Sanctuary Lake pond until April and the first species to enter the pond infected with *Bd* was the Spring peeper (*Pseudacris crucifer*). On April 5 of 2019, three of five *P. crucifer* captured were infected, as were the single bullfrog (*Rana* catesbeiana) and American toad (*Anaxyrus americanus*) I captured.

The leopard frog (*Rana pipiens*), green frog (*Rana clamitans*) and bullfrog (*Rana catesbeiana*) are considered permanent pond hibernating species whereas the wood frog (*Rana sylvatica*), the spring peeper (*Pseudacris crucifer*), the American toad (*Anaxyrus americanus*),

the red-backed salamander (*Plethodon cinereus*) and the spotted salamander (*Ambystoma maculatum*) usually hibernate in the soil or under logs close to the pond (Neil 1948, Willis *et al*. 1956). To test the hypothesis that species which hibernate in permanent ponds bring more *Bd* into ephemeral ponds than the terrestrially hibernating species do, I compared the *Bd* infection load ($\log_{10}$ *Bd* DNA copies per swab) and the probability that an animal was infected (yes/no) at the time when it entered a fenced pond among the hibernation types. The *Bd* load on infected animals was significantly correlated with hibernation type (LMM: $t = -2.760$, $p = 0.028$). I did not find any significant main effect of pond (Wood Lab pond vs. Sanctuary Lake pond) or a significant interaction between hibernation type and pond (LMM: $t \leq 1.334$, $p \geq 0.185$). However, the *Bd* load on infected animals entering the fenced ephemeral ponds was greater for species that hibernate in permanent ponds than for species that hibernate terrestrially (LMM: $t = -2.760$, $p = 0.028$) (Figure 3.4). For *Bd* infection (yes/no) there was also a significant effect of hibernation type (GLME: $t = -6.084$, $p < 0.001$) (Figure 3.5) such that animals that hibernate in permanent ponds had a greater probability of entering the fenced ephemeral pond infected. There was also a significant main effect of pond (Wood Lab vs. Sanctuary Lake, GLME: $t = -3.794$, $p < 0.001$) and a significant interaction between hibernation type and pond (GLME: $t = 3.848$, $p < 0.001$). In Wood lab pond, frogs that hibernated in a permanent pond before entering were much more likely to be infected than frogs that hibernated in the soil (Figure 3.5). However, in Sanctuary Lake pond the proportion of animals entering the pond infected was similar regardless of where they had hibernated.

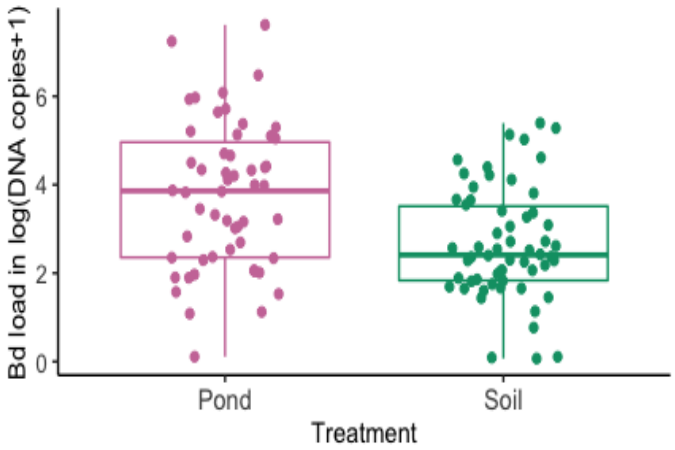

Figure 3.4 Box plots showing the relationship between Bd infection load, in log (DNA copies + 1), for animals entering the two fenced ponds and the hibernation typefor their species (permanent pond vs. terrestrial).

Each dot represents one individual.

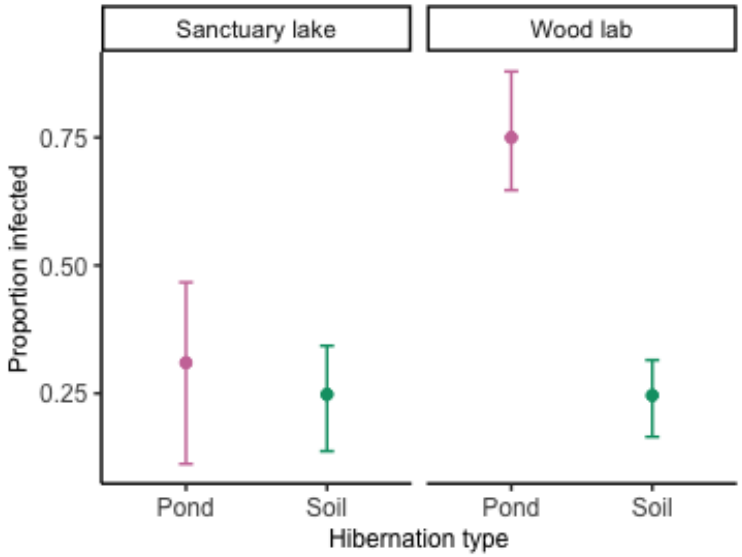

Figure 3.5 Proportion of individuals infected with Bd, upon arrival to (but before entering) the fenced ephemeral ponds, by hibernation type.

Error bars represent 95% confidence intervals on the proportions calculated using the Clopper-Pearson method (Clopper 1934).

The two species that bred and emerged as juveniles from Wood Lab pond were wood frogs and spotted salamanders. For the wood frogs, 29 of 131 individuals captured emerging from the pond after metamorphosis tested positive for *Bd* (mean DNA copies per swab = 17,324, range = 1 – 330,629). For spotted salamanders, two of 10 metamorphs emerged infected (mean DNA copies per swab = 173, range = 125 - 220]. Leopard frogs were the only species that bred and emerged as juveniles from Sanctuary Lake pond and 16 of 44 individuals were found to infected when leaving the pond (mean DNA copies per swab = 1,871, range = 34 - 15,136). For the leopard frogs metamorphosing in the Sanctuary Lake pond, there was no difference in *Bd* infection load between these metamorphs and the rest of the infected amphibians captured leaving the pond (LM: t = -0.755, p = 0.458; leopard frog metamorphs mean *Bd* DNA copies per swab =1,871, range = 34 - 15,136; other amphibians mean DNA copies per swab = 20,423, range = 1 – 162,112). There was also no difference in the probability of infection between leopard frog metamorphs and all other animals leaving that pond (GLME: t = 0.011, p = 0.991; leopard frog metamorphs mean proportion infected = 0.531, Clopper Pearson CI = 0.347- 0.709 other amphibians mean proportion infected = 0.667, Clopper Pearson CI = 0.348 – 0.901) for proportion infected. Similarly, there was also no difference in *Bd* load between spotted salamanders emerging from the Wood Lab pond and all other animals leaving that pond (LM: t = 1.753, p = 0.097; spotted salamander metamorphs mean *Bd* DNA copies per swab = 173, range = 125 - 220; other amphibians mean DNA copies per swab = 921,308, range = 116 - 15,661,890). However, the spotted salamander metamorphs had a lower probability of being infected with *Bd* than did other animals leaving that pond (GLME: t = 2.996, p = 0.003, Figure 3.6). The wood frogs emerging as metamorphs from the Wood Lab pond had both lower *Bd* loads (LMM: t =

3.852, p < 0.001) (Figure 3.7) and a lower probability of infection (GLME: t = 4.709, p < 0.001) than the rest of the animals leaving that pond (Figure 3.8).

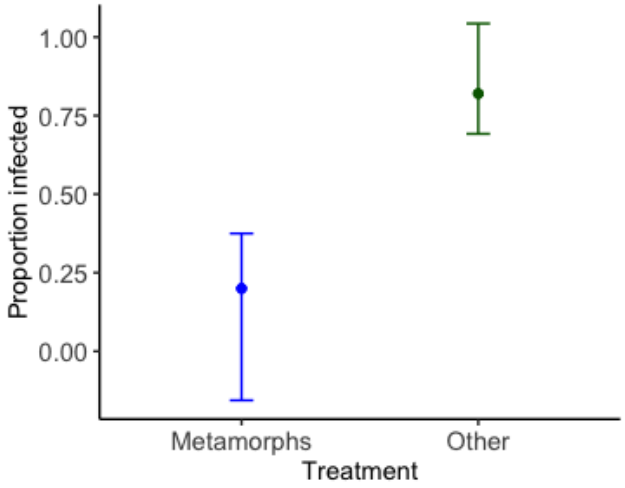

Figure 3.6 Proportion of individuals infected comparing spotted salamander (Ambystoma maculatum) metamorphs to all other animals leaving the Wood Lab pond.

Error bars represent 95% confidence intervals calculated using the Clopper-Pearson method (Clopper 1934).

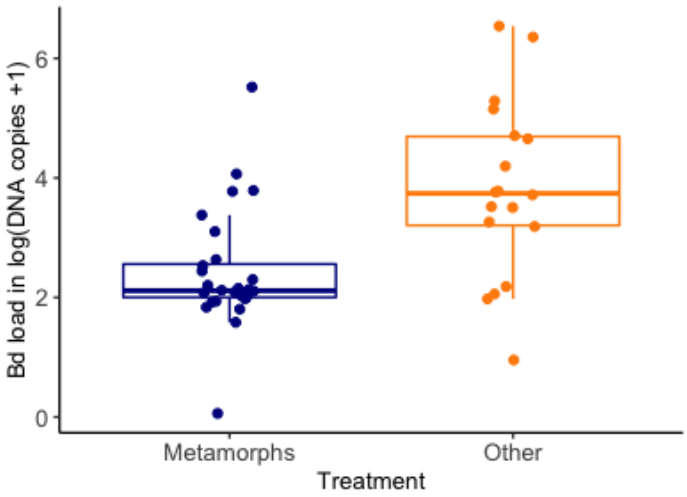

Figure 3.7 Box plots showing the relationship between Bd infection load, in log (DNA copies + 1), for leopard frog (Rana sylvatica) metamorphs and for all other animals captured leaving the Sanctuary Lake.

Each dot represents one individual. The middle line corresponds to the median. The lower and upper hinges correspond to the first and third quartiles (the 25th and 75th percentiles). The upper whisker extends from the hinge to the largest value no further than 1.5 times the inter-quartile range.

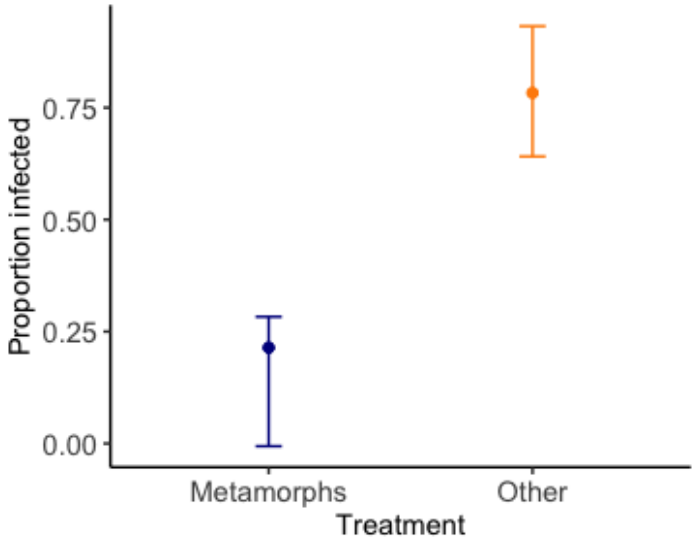

Figure 3.8 Proportion of individuals infected comparing wood frog (Rana sylvatica) metamorphs to all other animals leaving the Sanctuary Lake pond.

Error bars represent 95% confidence intervals on the proportion calculated using the Clopper-Pearson method (Clopper 1934).

3.3.1 Genetic variation in the fenced ponds

For the PCA analysis of *Bd* genetic variation in the two fenced ephemeral ponds, the first two principal components (PCs) together explained 21.3% of the total variance in haplotypes. To visualize how the genetic variation was distributed, I plotted the first two principal components by pond (Figure 3.9), by whether animals were sampled going into or out of the pond (Figure 3.10), by species (Figure 3.11), or by season spring vs. summer (Figure 3.12). In all cases there was significant overlap in haplotype variation among the sample categories.

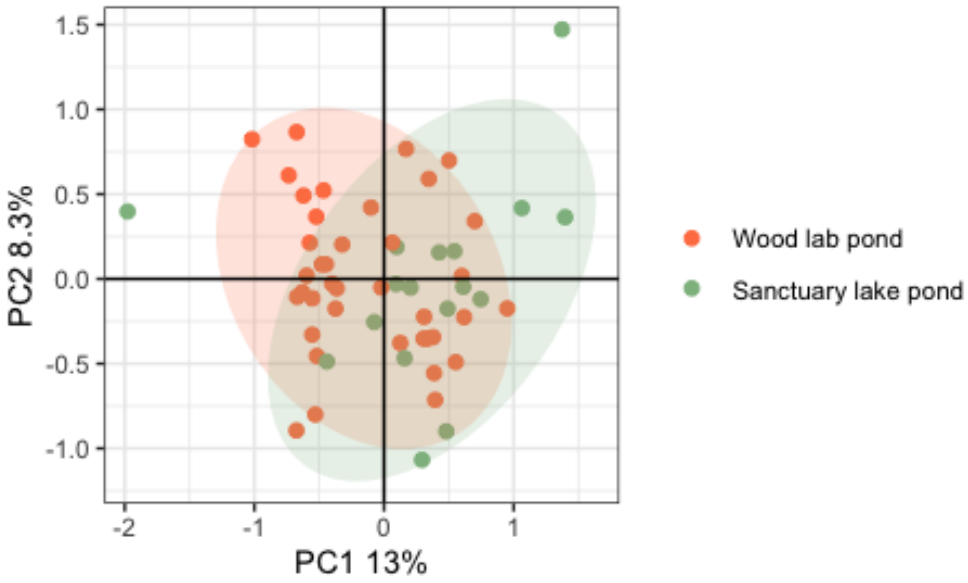

Figure 3.9 Scatter plot of PC1 versus PC2 showing variance among Bd haplotypes from the two fenced ponds.

The shaded ovals represent 95% confidence intervals.

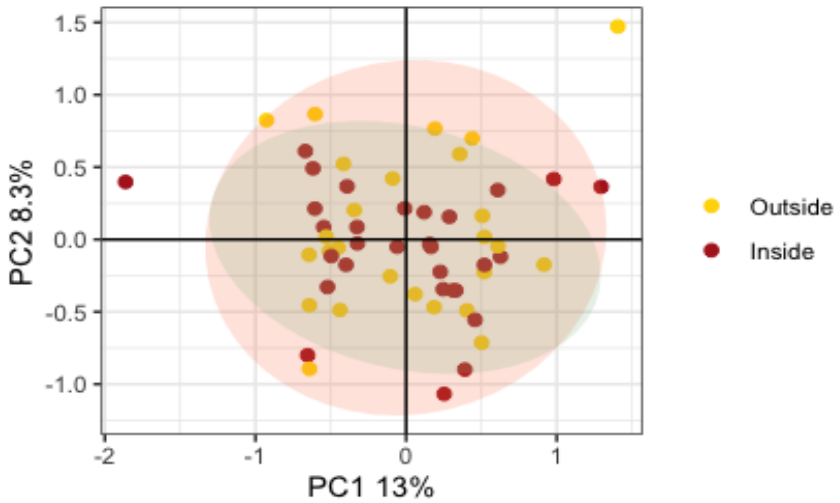

Figure 3.10 Scatterplot of PC1 versus PC2 showing variance among Bd haplotypes from animals entering (outside) vs. leaving (inside) the fenced ponds.

The shaded ovals represent 95% confidence intervals.

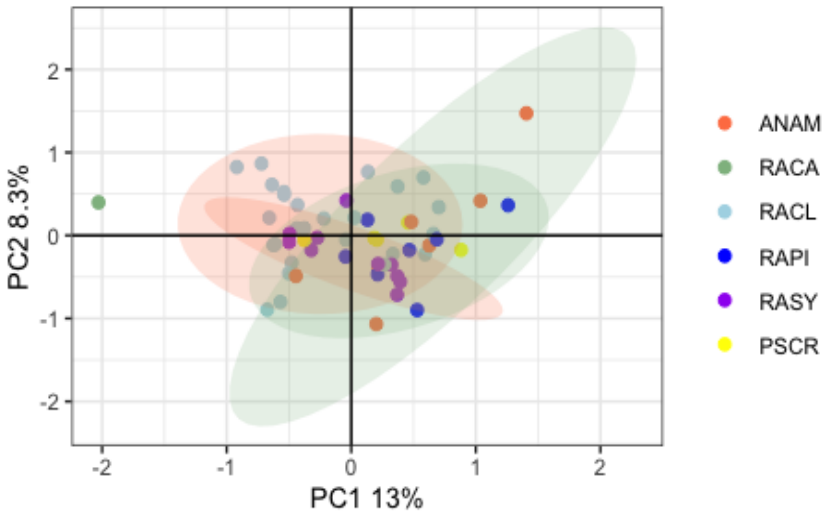

Figure 3.11 Scatterplot of PC1 versus PC2 showing variance among Bd haplotypes from different amphibian species in the two fenced ponds.

Anaxyrus americanus (ANAM, or the American toad), *Rana catesbeiana* (RACA, or the bullfrog), *Rana clamitans* (RACL, or the green frog), *Rana pipiens* (RAPI, or the northern leopard frog), *Rana sylvatica* (RASY, or the wood frog), *Pseudacris crucifer* (PSCR, or the spring peeper). The shaded ovals represent 95% confidence intervals.

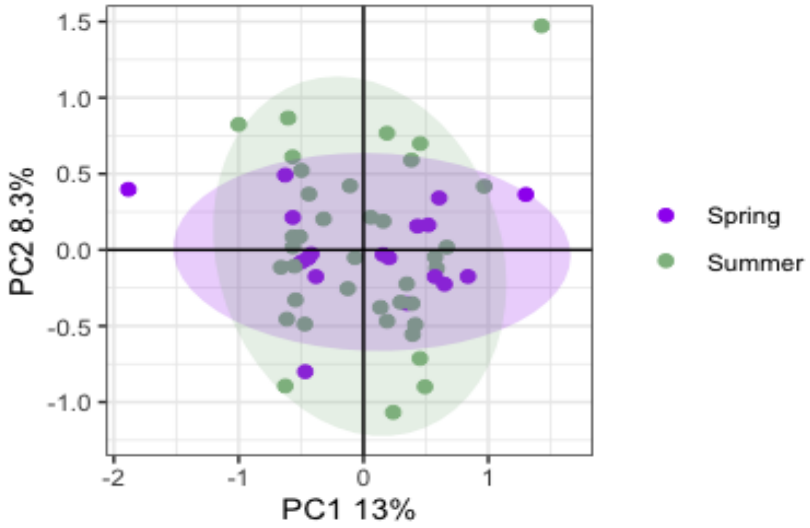

Figure 3.12 Scatterplot of PC1 versus PC2 showing variance among Bd haplotypes from animals collected in the spring vs. summer from the fenced ponds.

The shaded ovals represent 95% confidence intervals.

When looking at the phylogeny of *Bd* genotypes, I can see structure within the samples collected from animals in the fenced ponds. Some samples fell within the *Bd* GPL1 clade and others fell within *Bd* GPL2. Surprisingly, many of the samples seem to have haplotypes that look like a mix between both clades (GPL1 and the GPL2). Most of the sampled species were found to harbor both GPL1 and GPL2, as well as the "mixed" lineage suggesting the possibility of either recombination among lineages or co-infections with multiple lineages of *Bd*. I did not find any phylogenetic structure among samples from the two ponds or among samples from animals entering vs. leaving the ponds (Figure 3.13)

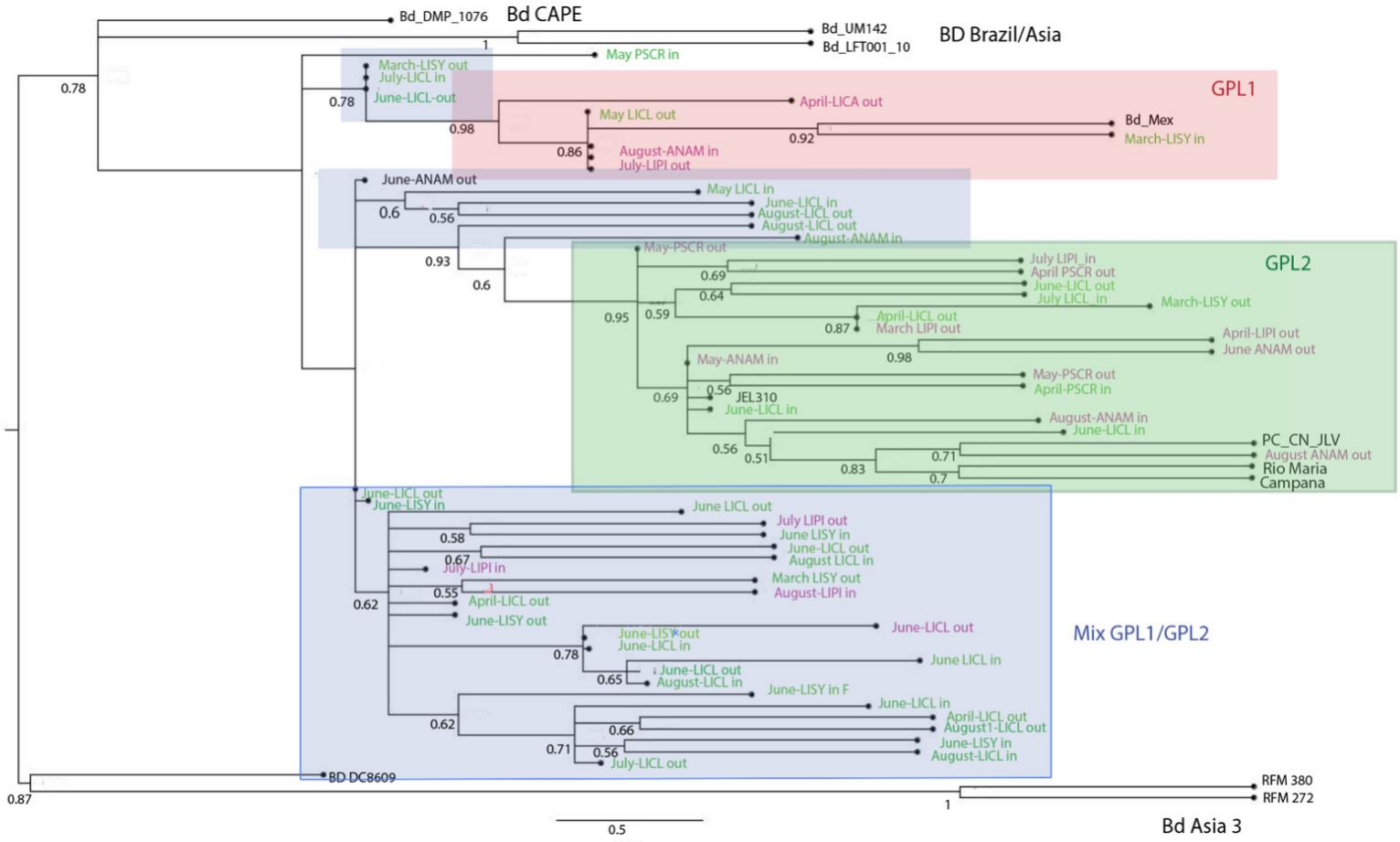

Figure 3.13 Phylogeny of Bd haplotypes inferred from ASTRAL and RAxML analyses.

The numbers denote ASTRAL local posterior probability values. The names in green represent the samples collected in Wood Lab pond and the names in pink denote the samples collected in Sanctuary Lake pond. Shading indicates clade (pink for GPL1, green for GPL2, blue for "mixed")

3.4 Discussion

Amphibians exhibit a diverse range of breeding (Duellman and Trueb 1986; McDiarmid and Altig 1999) and hibernating (Neil 1948) strategies that can influence their susceptibility to water-borne pathogens as well as their potential to act as reservoir hosts. Species that spend a large proportion of their life in or near permanent water may be more affected by waterborne pathogens like *Batrchochytrium dendrobatidis* and more likely to suffer declines because of them (Lips, 1998). The presence of various life stages of amphibian hosts in permanent ponds year-round may also play an important role in maintaining pathogens in the landscape as infected tadpoles and post-metamorphic amphibians that overwinter in ponds can act as pathogen reservoirs. For *Bd*, both amphibian and non-amphibian hosts may play important roles in pathogen maintenance in permanent ponds. For example, crayfish (*Procambarus* spp. and *Orconectes* spp.) can be infected with *Bd* in the wild and can transmit the fungus to tadpoles under laboratory conditions (McMahon *et al*. 2013, Brannelly *et al*. 2015). In the laboratory, some studies have shown that certain fish could act as reservoirs for *Bd* as well, with samples taken from zebrafish displaying various stages of development, including discharged mature zoosporangia (Liew *et al*. 2017). However, little is known about the relative importance of amphibian and non-amphibian reservoirs for *Bd* in the wild. In contrast, because the *Bd* fungus has aquatic, flagellated zoospores (Longcore *et al.* 1999) and cannot survive desiccation (Johnson *et al*. 2003) for it to be present in ephemeral ponds, which dry out each summer to fall, it must be brought there anew each spring, most likely by amphibians that make use of those ponds for breeding and larval development.

3.4.1 *Bd* prevalence and load in Pennsylvania

To better understand the factors that influence *Bd* dynamics across a landscape, I surveyed for *Bd* prevalence and load on amphibians in five ephemeral ponds and five permanent ponds near the Pymatuning Lab of Ecology in Northwest Pennsylvania. I detected *Bd* infections on amphibians in all of the sampled ponds no matter the time of the year and across all ponds and sampling periods, more than one third of the amphibians sampled were infected with *Bd*. However, none of them showed clear clinical signs of chytridiomycosis, the disease that *Bd* infection can cause, which can include skin sloughing, abnormal posture, lethargy, and loss of righting reflex (Nichols *et al.* 1998; Nichols *et al*. 2001). This pattern appears typical for the United States as, for example, previous field studies have found similar *Bd* prevalences in Illinois (31%; 55 of 180 samples positive), in California (26%; 5 of 19 samples positive), and in Virginia (25%; 15 of 60 samples positive) without clinical signs of disease (Lannoo *et al*. 2011). It has been hypothesized that this pattern of high prevalence without disease is a result of *Bd* having been present in this region for over 100 years, giving hosts and pathogens time to evolve ways of coexisting (Talley *et al*. 2015).

3.4.2 *Bd* infections in ephemeral vs permanent ponds

Because they are home to different suites of species, and because ephemeral ponds dry up each year, I hypothesized that there were going to be differences in *Bd* dynamics between ephemeral and permanent ponds. Because ephemeral ponds usually dry completely over the summer and do not fill up again until the fall (Colburn 2004) it seems unlikely that *Bd* zoospores would be able to survive from year to year in the pond. Instead, I hypothesize that *Bd* is brought

anew to ephemeral ponds each year after they refill. In the northern United States, even in years when ephemeral ponds do not dry completely, because they are shallow, they tend to freeze solid the winter (Colburn *et al*. 2008). This also prohibits amphibians from hibernating in ephemeral ponds and means that the species that use these ponds for breeding usually hibernate terrestrially by burrowing in soil or under logs. In deeper permanent ponds, however, only the top layer of the ice freezes completely and the water underneath that layer stays above freezing (Burn, 2005). In the northern parts of North America most frogs in the genus *Rana,* which includes many of the large pond-associated frogs, hibernate in the deep water of permanent ponds (Neil, 1948). *Bd* can survive for weeks in the water (Johnson and Speare, 2003), even at temperatures near freezing. Therefore, I hypothesized that the risk of maintaining infection over the winter is much higher for these species and that hibernating frogs, as well as tadpoles that overwinter in the water of permanent ponds may be important reservoirs for *Bd*.

I found that in the early spring, just after amphibians in Northwest Pennsylvania emerge from hibernation, *Bd* prevalence (the proportion of amphibians infected) and load are lower in ephemeral ponds than in permanent ponds. For the rest of the year, animals sampled from both ephemeral and permanent ponds followed a similar pattern of infection. In both pond types *Bd* prevalence and load peaked in the spring, declined in the summer, then increased again to reach a second peak in the fall. I hypothesize that the greater prevalence and load of *Bd* in permanent ponds in the spring results from infected animals shedding zoospores throughout the winter in these ponds. The larval stage of amphibians breeding in permanent waterbodies can last up to several years (Bury and Adams, 1999) and the keratinized mouthparts of these tadpoles have ample opportunity to become infected with the waterborne zoospores of *Bd* (Woodhams and Alford 2005; Narayan *et al*. 2014). These tadpoles, in addition to post-metamorphic life stages of

amphibians that hibernate within these ponds (Russell *et al*. 2010), are a likely source of shed zoospores, which can be transmitted to uninfected individuals (Rachowicz and Vredenburg 2004) increasing prevalence, or can reinfect the same host increasing *Bd* loads. I hypothesize that the similar pattern of *Bd* prevalence and load during the rest of the year in permanent vs. ephemeral ponds is a product of other abiotic environmental factors.

I hypothesized that pH and temperature are important abiotic influences on *Bd* dynamics in both permanent and ephemeral ponds in Northwest Pennsylvania. However, the pH of pond water was not a significant predictor of *Bd* infection probability or *Bd* load in either pond type in this study. My pH measurements were similar for both pond types; in permanent ponds, pH ranged from 5.61 to 10.3 (mean 7.245) and in ephemeral ponds from 4.41 to 10.44 (mean 7.41). Previous in vitro studies have shown that *Bd* survives from pH 4 to 8 but with an optimum between pH 6 and 7 (Piotrowsky *et al*. 2004). The fact that the pH values I measured span and exceed this range but yet I still found no correlation with *Bd* infections on amphibians inhabiting those ponds suggests that when on amphibian hosts, *Bd* may not be as sensitive to pH as it is in vitro. It is also possible that the long history of *Bd* in ponds of varying pH in the northeastern US might have influenced the relationship between pH and growth/survival for the lineages that inhabit this region.

Temperature, on the other hand, was a significant predictor of *Bd* infection in both ephemeral and permanent ponds. In both pond types *Bd* load decreased with amphibian body temperature, though it did so more markedly in permanent ponds. The weaker correlation with temperature in ephemeral ponds may be caused by shallow nature of these ponds, which causes temperatures to fluctuate more rapidly (Griffiths 1997*). Bd* prevalence, on the other hand, was lowest at the extremes of amphibian body temperature and reached a peak in the middle of the

range of body temperatures I measured. In permanent ponds, *Bd* infections reached a peak at a lower temperature (~12 ºC) than in ephemeral ponds (~ 17 ºC). It is not clear why the temperature of peak infection might differ between the two pond types if temperature is the main driver of *Bd* dynamics. Possible explanations might include differences in the thermal physiology of distinct *Bd* lineages in these pond types (see below) or differences in the thermal sensitivity of the defenses of hosts that inhabit these two pond types. Previous studies have attributed higher *Bd* prevalence in the spring to the fact that *Bd* survives well at cool temperatures (Piotrowski *et al.* 2004; Woodhams *et al.* 2008; Voyles *et al*. 2012; Martel *et al.* 2013) whereas the immune defenses of amphibians tend to be sluggish (Matutte *et al*. 2000; Robak *et al*. 2019).

I used drift fences to investigate which species bring *Bd* into ephemeral ponds each spring and to test alternative hypotheses about the source(s) of genetic variation in *Bd*. I hypothesized that permanent pond hibernating species that visit ephemeral ponds in the spring might be an important source of *Bd* zoospores and genetic variation for ephemeral ponds. Alternatively, the ephemeral pond breeders, which hibernate terrestrially, may emerge from hibernation infected and bring *Bd* to ephemeral ponds each spring. I found that the spotted salamander, *Ambystoma maculatum,* an ephemeral pond breeding species that hibernates in moist upland forest burrows next to ephemeral ponds (Stebbins and Cohen 1995; Petranka 1998), was the first species to enter one of my fenced ponds infected with *Bd.* The American toad, *Anaxyrus americanus*, which breeds in ephemeral ponds and hibernates in burrows one to two feet into the ground (Wright and Wright, 1949) and the spring peepers (*Pseudacris crucifer*), another ephemeral pond breeder that hibernates beneath debris on the forest floor (Layne and Kefauver, 1997) were the first species to enter the other fenced pond with *Bd* infections. This

suggests that ephemeral pond breeding species, despite hibernating terrestrially, may be an important source of *Bd* zoospores for ephemeral ponds each spring and that transmission from permanent to ephemeral ponds is not needed to sustain *Bd* in ephemeral pond communities over the long term. However, both the prevalence and load of *Bd* on ephemeral pond breeders in the early spring was low, suggesting that stochastic variation could be important to the dynamics of *Bd* in ephemeral ponds. Low prevalence in frogs inhabiting ephemeral waterbodies has been seen in other regions as well. For example, in a study that took place along the Nerang River in Australia, *Bd* was detected in only one individual (of the pouched frog *Assa darlingtoni*) of 117 that were found at ephemeral ponds, ephemeral streams, or terrestrial sites (Kriger and Hero, 2007). Little is known about how hibernation affects the course or outcome of *Bd* infections in amphibian hosts. In vitro, *Bd* grows more slowly, but with longer periods of zoospore activity, at temperatures near freezing than it does near its thermal optimum of 23 ºC (Voyles *et al*. 2012). It appears that some of the terrestrial hibernating animals in our study emerged infected, which suggests they were able to survive with infection over the long winter, however whether their *Bd* loads increased or decreased during this time remains unknown. It may also be possible for species hibernating underground to contract *Bd* infections while hibernating. *Bd* has been shown to be able to persist in moist sand for extended periods of time (12 weeks, Johnson and Speare 2005) and soil in which amphibians hibernate might remain moist at deeper levels due to plant roots (Van Leeuwen 2010). If so, this could explain how *Bd* makes it to ephemeral ponds each year. It could also be possible that visiting the ponds in fall before they froze (and before the fences were closed) left the zoospores in the pond that survived there until spring.

While they breed, develop, and hibernate in more permanent water, some amphibian species in my study area, like bullfrogs, green frogs, and leopard frogs, often spend time in and around

ephemeral ponds. I also hypothesized that these species, due to their time spent in permanent ponds, may bring more *Bd* into ephemeral ponds than the terrestrially hibernating species do. Kinney *et al*. (2011) saw this pattern in Indiana where *Bd* prevalence was greater in amphibians living in deeper, cooler, permanent pools than in shallow, warmer, semi-permanent systems. In this study, I found that both the probability of infection and the load of *Bd* on animals entering the fenced ephemeral ponds were greater for amphibian species that hibernate in permanent ponds than for species that hibernate terrestrially. This supports the idea that species associated with permanent ponds, while only transient visitors, play an important role in the dynamics of *Bd* in ephemeral ponds. It also suggests that permanent ponds, and the species associated with them, have a large influence on the distribution of this pathogen across the landscape.

In the summer, before they dry up, ephemeral ponds, too, may be a source of *Bd* movement across the landscape if animals leave these ponds infected. Since new metamorphs are often the life stage that is most susceptible to *Bd* (Sauer *et al*. 2020), and assuming that the likelihood of transmission is high, I hypothesized that the tadpoles that develop in ephemeral ponds would emerge from those ponds with similar infection loads and prevalences to other amphibian species and life stages present in the ponds. However, the tadpoles that developed in the fenced ponds metamorphosed with lower *Bd* loads than the other species and life stages present, and presumably responsible for creating the pool of zoospores in those ponds. Even though many studies in the tropics, like in Australia, Brazil, and Peru, have suggested that tadpoles are potential reservoirs for *Bd* (Narayan *et al*. 2014, Ruggeri *et al*. 2018, das Neves-da-Silva *et al*. 2021, Catenazzi *et al*. 2013), in the ephemeral ponds I studied, the tadpoles rarely got infected with *Bd*. Across three years of sampling in Northwest Pennsylvania, out of the 590 tadpoles sampled from six species, I only found eight individuals to be infected with *Bd*. For

comparison, at the Savannah River Site in South Carolina, *Bd* was identified in 64% of the *R. catesbeiana* tadpoles sampled and no *R. sphenocephala* tadpoles from this site (n = 50) were infected (Peterson *et al*. 2007). My swabbing technique might also have missed infections in tadpoles, as one previous study found that there is 1 in 2 chance of detecting *Bd* using oral swabs of infected tadpoles (Retallick *et al.* 2006).

3.4.3 Genotyping *Bd* in and out of the ponds

Genotyping *Bd* from skin swab samples allowed me to test hypotheses about the distribution of *Bd* lineages across a landscape and over time, something that until recently has not been possible. I hypothesized that genetic variation in *Bd* across the landscape I studied would be structured among the two ephemeral ponds since the ponds are too far apart (9 km) to expect amphibians to be able to move between them. I also hypothesized that genetic variation might be structured among species if there has been coevolution between particular *Bd* strains or lineages and the immune systems of particular amphibian hosts. However, despite finding a surprising amount of genetic diversity in *Bd* across the two ponds, there was a large amount of overlap between ponds and among the amphibian species from which the *Bd* samples were taken. I also hypothesized that, given the shifts in environmental conditions and the species and life stages of hosts that make use of ephemeral ponds throughout the time they hold water each year that we might see differences in the *Bd* lineages present on hosts entering versus leaving the pond and across seasons. For example, if certain strains or lineages were more virulent or transmissible than others we might see greater genetic diversity of *Bd* on animals entering the pond in early spring than on those leaving it, often in late summer, who have had time to contract new infections from the pond's zoospore pool. However, there was a large amount of overlap in

the *Bd* genetic variants found on animals entering vs. leaving the ponds and also across the spring and summer seasons when the ponds were full.

In both ponds we found a diversity of genotypes from within the globally invasive panzootic lineage (GPL), which has been divided in 2 sublineages (Schloegel *et al.* 2012). One of these, GPL-1, is often thought of as a North American lineage and is proposed to be ancestral to GPL-2, which is globally distributed and is the lineage responsible for declines in Central America (James *et al.* 2015). My findings support previous work reporting the presence of two sublineages of *Bd*-GPL in the United States (Schloegel *et al*. 2012). However, surprisingly, I also evidence for a clade with less than 0.7 posterior support that has a genotype that appears to be a mix of *Bd* GPL1 and GPL2. This finding could be explained by a large number of the animals we swabbed having been coinfected with *Bd* strains belonging to both sublineages. Alternatively, it could indicate recombination has been occurring among the two sublineages. Lab experiments have demonstrated the potential for coinfection. For example, in a coinfection experiment between *Bd* GPL1 and *Bd* Brazil in the African dwarf frog (*Hymenochirus curtipes*), *Bd* GPL1 was found to have a competitive advantage in spore production over *Bd* Brazil, especially and on frogs that eventually succumbed to *Bd* infection (Jenkinson *et al*. 2018).

Hybrids between clades of *Bd* have been reported as well. For example, a hybrid lineage between *Bd* Brazil and *Bd* GPL has been described from Brazil and in some host species, infection by this hybrid lineage has been associated with increased mortality (Greenspan *et al.* 2018).

In summary, my results show that all of the sampled host species in Northwest Pennsylvania have some prevalence of *Bd* infection and that the prevalence and severity of these infection tends to differ between ephemeral and permanent ponds. The difference is more

pronounced in the beginning of the amphibian breeding season in the springtime when hosts that hibernate terrestrially and breed in ephemeral ponds are less often, and less heavily, infected. This initial difference lessens as the amphibian active season progresses and the dynamics of *Bd* infections for the remainder of this time seem to be largely explained by temperature. While it is not common, species that hibernate terrestrially appear to occasionally enter ephemeral ponds to breed already infected with *Bd*. This suggests that movement of infected animals from permanent pond reservoirs to ephemeral ponds is not necessary for *Bd* to reach ephemeral pond communities each spring. The permanent pond hibernating species who often visit ephemeral ponds, however, often arrive there infected with *Bd*, and with greater loads than the species that use the ephemeral pond for breeding and larval development. Surprisingly, the tadpoles of ephemeral pond breeders, which coexist for several months with infected hosts of many species and life stages in ephemeral ponds, do not often contract infections themselves suggesting that this life stage does not act as an important reservoir for *Bd* in this region. Whether new metamorphs emerge from ephemeral ponds with a similar or lower prevalence and intensity of *Bd* infection to the rest of the host community appears to differ by species, though in no case were metamorphs found to be more infected than the rest of the host community. And finally, I found a wealth of genetic variation but little evidence of structure in *Bd* on hosts from two ephemeral ponds, including both the GPL1 and GPL2 sublineages and a third sublineage that appears to be a mix of both. Further study is needed to better understand what this mixed lineage represents. The combination of field and molecular techniques implemented in this study, including drift fences to monitor host movement and genotyping of pathogen samples from non-invasive skin swabs, has enabled a new and more detailed window into biotic and abiotic factors that shape the dynamics of this host-pathogen interaction across a landscape.

4.0 Conclusion

Effects of environmental variation on immunity, and the ability of hosts to regulate immune activity in the context of other physiological demands, may play important roles in shaping disease risk for wildlife. Because they are threatened globally by the fungal pathogen *Batrachochytrium dendrobatidis* (*Bd*), amphibians are an ideal taxon in which to study the effects of climate change on susceptibility to emerging infectious diseases. In North America, many amphibians develop and undergo metamorphosis in ephemeral ponds that are sporadically filled with rainwater and then desiccate at differing rates each year. Global climate change is predicted to alter temperature, precipitation, and humidity patterns, which will ultimately alter the conditions amphibians experience in these ephemeral ponds. Prior research has shown that decreases in water level and increases in pond temperature, as are predicted to occur more frequently under global climate change, are two of a handful of environmental stressors that can cause amphibians to accelerate larval development and metamorphosis. This can allow amphibians to metamorphose and escape harsh aquatic conditions faster, but little is known about how environmental stress experienced during larval development impacts the immune system later in life. Given the threat posed by chytridiomycosis (the disease caused by *Bd*) and other emerging infectious diseases, impacts on immunity may be an important yet often overlooked consequence of global climate change for amphibians. In this dissertation, I used experiments to investigate how pond drying and an increase in pond temperature impact not only the timing of metamorphosis, but also the development of immune defenses in North American leopard frog species. To better understand the dynamics and spread of *Bd*, I also conducted a

field study comparing infection among amphibian communities that inhabit permanent vs. ephemeral ponds.

In my experiments, accelerated pond drying and elevated pond temperatures, which are predicted to happen more frequently under global climate change, had direct effects on the survival, time to metamorphosis, size, and immune function of leopard frogs. In general, even when they did not exhibit developmental plasticity (i.e., did not speed development in response to the stressor), frogs that developed as larvae in the more stressful environments (fast drying and elevated temperature) had lower survival to, and size at, metamorphosis. Previous work has shown that small size at metamorphosis can have long-term negative consequences for frogs. For example, juvenile size is often positively correlated with adult survival (Berven 1990, Cabrera-Guzmán et al. 2013). Larger juveniles often grow to be larger adults, and smaller juveniles can take longer to reach sexual maturity (Berven, 1990), all of which suggests that developing in ponds affected by climate change may have impacts on fitness throughout an amphibian's lifetime.

In my study, individuals that developed in a faster-drying pond were not only smaller at metamorphosis, but they also often exhibited more rapid growth during their first months after metamorphosis. While I did find some direct effects of drying, I also saw indirect effects of size at metamorphosis, and the fast rate of post-metamorphic "catch up" growth these small frogs exhibited, on immune defenses and susceptibility to *Bd*. For example, the probability of a *Bd*-exposed frog becoming infected increased with a faster growth rate after metamorphosis and frogs that were larger at metamorphosis had skin mucus that was better able to inhibit the growth of *Bd*. The *Bd*-exposed frogs that experienced fast drying during development also expressed fewer antimicrobial peptides (AMPs, an important part of the innate immune defense against *Bd*)

and exhibited the lowest survival of all treatment groups when exposed to *Bd*. In summary, experiencing the stress of rapid pond drying during development appears to have negatively impacted the fitness of leopard frogs and their ability to fight infection later in life. Similar studies in other species are needed to determine how generalizable these findings are. However, the results of this study do suggest that management actions aimed at preventing the early drying of ephemeral ponds may produce benefits for the health and survival of at-risk amphibian populations.

When I exposed leopard frog tadpoles (two populations from each of two species) to elevated temperatures, simulating the warming of ponds under a moderate climate change scenario, I also saw both direct and indirect effects of this stressor on immune defenses and susceptibility to *Bd*. However, each population's immune system seemed to have responded to the temperature difference in a different way. The direct effects of increased temperature I observed most often included faster metamorphosis, smaller size at metamorphosis, lower innate immune function and higher adaptive immune function. My study was the first, to my knowledge, to investigate the effects of small (2 - 3ºC, as predicted under climate change) on amphibian immune function, and also the first to include multiple populations and species, making comparisons with past studies is difficult. However, this pattern, where various parts of the immune system differ in their directionality of change in response to shifts in temperature, has been seen in other studies. For example, during periods of low temperature (e.g., hibernation), amphibians often decrease the production of AMPs (Matutte *et al*. 2000), T and B-lymphocytes (Maniero and Carey, 1997), and antibodies (Cooper *at al.* 1992). However, some aspects of immune activity appear to be robust to shifts in temperature, including phagocytic activity, respiratory burst (Hardie *et al.* 1994), and the number of circulating neutrophils (Raffel

et al. 2013). One take away from this experiment, since the innate and adaptive branches of the immune system seemed to respond differently to changes in temperature, is the importance of taking into account both the aspects of immunity when studying the impacts of climate change. My finding that responses to small temperature shifts differed among species, and even among populations within species, was unexpected but suggests that the effects of climate change on complex traits like immune function may themselves be very complex, and likely hard to predict.

The indirect effects of increased temperature in my pond warming experiment, as with the pond drying experiment, often acted through effects on larval period, size at metamorphosis, and growth rate after metamorphosis. The most consistent patterns I saw were for immune parameters to be higher in frogs that had longer larval periods, were larger at metamorphosis, and grew more slowly after metamorphosis, though instances of other relationships were also seen. Interestingly, after exposure to the *Bd* pathogen, there was no difference in the probability of infection or in *Bd* load among temperature treatments. However, frogs reared in warmer water exhibited more mortality after *Bd* exposure. These frogs were dying at *Bd* loads where frogs reared in current temperature conditions were not, which suggests that climate change may impact how tolerant hosts are to infection. My finding that small increases in temperature can affect immune function and disease susceptibility in amphibians seems like an important one, though additional research that considers the impacts of climate-change relevant shifts in temperature on the immune system and disease susceptibility is needed to determine whether there are predictable patterns across populations and species. Unlike for pond drying, the most obvious management response, regulating pond temperatures in the face of rising air temperatures, unfortunately seems like a difficult prospect.

My field sampling, conducted over four years at the Pymatuning Lab of Ecology, showed that amphibians in this region often have a high prevalence of *Bd* but usually have low to intermediate infection loads. I did not detect *Batrachochytrium salamandrivorans* (*Bsal*) or observe clinical signs of chytridiomycosis in any of the amphibians sampled for this study. Non-detection of *Bsal* is good news, as the arrival of this pathogen could threaten the future of amphibian (and in particular salamander) diversity in North America. Not finding signs of disease is also good news, as it suggests that amphibians in this region are largely able to coexist, despite infection, with the now endemic *Bd* pathogen.

The proportion of individuals infected with *Bd* at my study sites increased with body temperature until ~16°C and decreased with increasing temperature after that. Interestingly, the proportion of individuals infected and pathogen load was lower in ephemeral pond associated amphibian species than in permanent pond associated species. This finding motivated me to ask which species bring *Bd* into to ephemeral ponds; specifically, what is the first species that brings the infection to the pond and where does it hibernate? Since *Bd* cannot tolerate desiccation I assumed that it must need to be brought to ephemeral ponds anew once they fill each spring and I predicted that species that hibernate in permanent ponds (where they can sustain infections more easily) might be the ones to bring it there. Interestingly, the a few individuals of the ephemeral pond breeding species that hibernate on land emerge infected with *Bd* and were the first to bring the pathogen to ephemeral ponds. When I compared the *Bd* genotypes on animals entering and leaving the ponds I found little evidence of genetic structure among ponds, among species, or among animals entering in spring vs. leaving in fall. However, I did find a surprisingly large amount of genetic variation in the *Bd* infecting amphibians at my field sites, including genotypes belonging to both sublineages of the global pandemic lineage of *Bd* (*Bd*-GPL1 and *Bd*-GPL2)

and genotypes that appeared to be a mix of both lineages that I hypothesize was due to coinfection of individual hosts with genotypes of Bd from both subclades. Overall, the lack of structure in the large amount of genetic variation I found suggest that *Bd* has likely been coexisting with amphibian hosts in Northwest Pennsylvania for some time and that strains are easily moved from one place to another. Future studies comparing virulence among genotypes, especially those including the mixed lineage, will be important to provide a management context to this finding of high pathogen genetic diversity.

In this dissertation, I focused on how two aspects of climate change, pond drying and pond warming, will affect the future of interactions between amphibians and their pathogens. However, amphibians are just one of many taxa threatened by the intersection of climate change and disease and my hope is that my findings and approach may be useful to inform studies on other taxa as well. As the climate changes, wildlife pathogens are emerging with increasing frequency and having increasingly dire consequences for biodiversity (Cunningham *et al*. 2017). Fungal pathogens, for example white nose syndrome in bats (Foley *et al.* 2011) and colony collapse disorder in bees (Bromenshenk *et al.* 2010), are especially sensitive to temperature have been important drivers of recent wildlife declines and extinctions (Casadevall 2005, Fisher *et al.* 2012). By applying the experimental techniques used here with *Bd* in amphibians to interactions between other hosts and pathogens we could learn more about how these other disease systems may be impacted by climate change. Furthermore, the application of non-invasive pathogen genotyping, as I did in my field study, to other disease systems could help to shed light on how other emerging fungal diseases spread across a landscape to colonize new habitats and host species. Using these techniques to resolve the links between climate and the outcomes of

host/fungal interactions will provide direction for effective management of threatened populations.

In this study I specifically considered the impacts of climate change on immune development and disease susceptibility in two semi-aquatic amphibian species, the northern and the southern leopard frogs (*Rana pipiens* and *R. clamitans*, respectively). I chose these species because the immunological resources had already been developed. However, going forward, it would be beneficial to include amphibian species with a greater diversity of ecologies (e.g., more aquatic and more terrestrial species) and with a greater taxonomic diversity (e.g., toads and salamanders) in studies of this nature as it is unclear whether the patterns, I observed in leopard frogs would be found across these species as well.

My experiments focused on climate as an early life stressor, and therefore after metamorphosis animals from all treatments were held under the same climate conditions. This, however, is unrealistic to what amphibians would experience as the climate warms in nature. For this reason, I would suggest that future studies consider continuing to observe the effects of climate stress experienced after metamorphosis on immune function and disease susceptibility. These results would yield a more accurate prediction of the effects of climate change pre- and post-metamorphosis. However, a tradeoff with this approach is that it would not allow the researcher to for carry-over and indirect effects of *Bd* exposure and climate from direct effects experienced during later life stages. Another approach could be to test for direct and indirect effects of temperature on the immune system and disease susceptibility by applying climate stress only during the post-metamorphic life stages. These results could be completely different from what we observed by applying the stressors during the larval stage. Though it is clear that the moderate climate change scenarios I considered had some significant impacts on amphibian

immunity and susceptibility to Bd, future studies might also consider using a more accelerated climate change scenario (generating a larger magnitude of climate stress) as this may result in effect sizes that are more amenable to detection using laboratory-scale experiments.

To follow up on the findings from my field study, it would be very interesting to use a similar approach but, in a location where *Bd* diversity is much lower. For example, in sites like the one where my Tennessee leopard frogs came from, where only one of the *Bd* GPL lineages seems to be present, it would be easier to estimate when particular *Bd* haplotypes enter the pond and what host species brings it. At my study site, the North American bullfrog, *Rana catesbeiana,* only appeared to carry *Bd* GPL-1, despite *Bd* GPL-2 being present at the same time in the ponds where bullfrogs coexist with other species. Using studies like this we can begin to understand the properties of host species that may inhibit colonization by particular *Bd* lineages, like *Bd* GPL-2. To follow up on my finding that some species that hibernate in soil burrows or under logs emerge infected with *Bd* after hibernation, it would be exciting to sample amphibians for *Bd* during hibernation to track changes in infection over time. This could be logistically challenging but very informative as little is known about how *Bd* infections proceed during hibernation.

In conclusion, my dissertation research demonstrated that larval development under stressful climate conditions, including pond drying and elevated temperatures, often has a cost in terms of reduced fitness of amphibians up to and shortly after metamorphosis. However, I also documented negative impacts of climate stressors experienced during the larval stage on different aspects of the innate and adaptive immune system, as well as on disease susceptibility, several months after metamorphosis. While my field studies suggest that amphibians are currently coexisting with the *Bd* pathogen in Northwest Pennsylvania, my experiments suggest

that this may change as the climate puts more stress on amphibian host populations. My research suggests that as ponds dry faster and reach warmer temperatures, effects of these changes on the ability of hosts to develop their immune defenses could result more mortality and a greater risk of disease-related declines. More work on other amphibian hosts, and across a broader range of wildlife disease systems, is needed to determine how the interaction between climate change and disease may impact biodiversity more generally.

Appendix A

Table A.1 Output from a linear mixed-effect model examining the variation in larval period across drying treatments.

	Dependent variable:
	log (Larval Period)
Drying Treatment	$\chi^2 = 0.650$ p = 0.722
Moderate Drying	0.009 (-0.018, 0.036)
	t = 0.630
	p = 0.537
No Drying	0.010 (-0.017, 0.037)
	t = 0.749
	p = 0.464
Constant	1.921^{***} (1.902, 1.941)
	t = 196.985
	p < 0.001
Observations	645
Log Likelihood	779.129
Akaike Information Criterion	-1548.258
Bayesian Information Criterion	-1525.935
Note:	*p < 0.05; **p < 0.01; ***p < 0.001

Coefficient estimates and standard errors (in parentheses) are shown for each factor. Mesocosm number was included as a random effect.

Table A.2 Output from a generalized linear model (quasi-binomial link) examining the number of animals that survived through metamorphosis versus the number of animals that did not per mesocosm as a concatenated variable.

	Dependent variable:
	log (Survival to Metamorphosis)
Drying Treatment	$\chi^2 = 0.388$ p = 0.824
Moderate Drying	-0.095 (-0.403, 0.213)
	t = -0.606
	p = 0.552
No Drying	-0.028 (-0.338, 0.281)
	t = -0.180
	p = 0.859
Constant	1.570^{***} (1.349, 1.791)
	t = 13.928
	p < 0.0001
Observations	21
Residual Deviance	8.920 (df = 18)
Null Deviance	9.112 (df = 20)
Note:	*p < 0.05; **p < 0.01; ***p < 0.001

Coefficient estimates and standard errors (in parentheses) are shown for each factor.

Table A.3 Output from a Cox proportional hazards model examining survival across the three drying treatments from metamorphosis to 42 d post-metamorphosis, clustered by mesocosm.

	Dependent variable:
	Survival (0 to 42 d Post-metamorphosis)
Drying Treatment	$\chi^2 = 6.042$ p = 0.049
Moderate Drying	-0.107 (0.289)
	z = -0.407
	p = 0.685
No Drying	-0.803* (0.399)
	z = -2.379
	p = 0.018
Body size (SVL)	$\chi^2 = 5.856$ p = 0.016
	-0.247* (0.090)
Observations	611
R^2	0.029
Maximum Possible R^2	0.695
Log Likelihood	-354.070
Wald Test	13.680** (df = 3) (p = 0.004)
Likelihood Ratio Test	17.788*** (df = 3) (p = 0.0005)
Log Rank Test	15.780** (df = 3) (p = 0.002)
Note:	*p < 0.05; **p < 0.01; ***p < 0.001

SVL (mm) was included as a covariate. Coefficient estimates and their standard errors (in parentheses) are shown for each factor.

Table A.4 Output from a linear model examining body mass at metamorphosis across the three drying treatments, clustered by mesocosm.

	Dependent variable:
	log (Body Mass)
Drying Treatment	$\chi^2 = 1.571$ p = 0.455
Moderate Drying	0.018 (-0.090, 0.125)
	t = 0.325
	p = 0.749
No Drying	-0.048 (-0.150, 0.055)
	t = -0.913
	p = 0.373
Time to metamorphosis	$\chi^2 = 22.886$ p < 0.001
	0.002^{***} (0.001, 0.002)
Drying Treatment : Time to metamorphosis	$\chi^2 = 10.774$ p = 0.005
Moderate Drying : Time to metamorphosis	-0.0003 (-0.001, 0.001)
	t = -0.652
	p = 0.515
No Drying : Time to metamorphosis	0.001^{*} (0.0003, 0.002)
	t = 2.532
	p = 0.012
Constant	-0.284^{***} (-0.356, -0.212)
	t = -7.731
	p < 0.001
Observations	644
Log Likelihood	716.465
Akaike Information Criterion	-1416.930
Bayesian Information Criterion	-1381.263
Note:	*p < 0.05; **p < 0.01; ***p < 0.001

Coefficient estimates and their standard errors (in parentheses) are shown for each factor.

Table A.5 Output from a linear model examining body length (SVL) at metamorphosis across the three drying treatments, clustered by mesocosm.

	Dependent variable:
	log (Body Length)
Drying Treatment	$\chi^2 = 5.477$ p = 0.064
Moderate Drying	-0.015 (-0.054, 0.024)
	t = -0.763
	p = 0.455
No Drying	-0.043* (-0.079, -0.006)
	t = -2.302
	p = 0.034
Larval Period	$\chi^2 = 2.5016$ p = 0.116
	0.0002 (-0.0001, 0.0005)
Drying Treatment : Larval Period	$\chi^2 = 15.163$ p= 0.001
Moderate Drying: Larval Period	0.0001 (-0.0003, 0.0005)
	t = 0.406
	p = 0.685
No Drying : Larval Period	0.001*** (0.0003, 0.001)
	t = 3.594
	p < 0.001
Constant	1.320*** (1.294, 1.346)
	t = 100.584
	p < 0.001
Observations	643
Log Likelihood	1351.914
Akaike Information Criterion	-2687.829
Bayesian Information Criterion	-2652.100
Note:	*p < 0.05; **p < 0.01; ***p < 0.001

Coefficient estimates and their standard errors (in parentheses) are shown for each factor.

Table A.6 Generalized linear mixed model with a binomial distribution of the probability of Bd infection across the three drying treatments.

	Dependent variable:
	Bd Infection (yes/no)
Drying Treatment	$\chi^2 = 4.708$ p = 0.095
Fast Drying	-0.416 (-0.897, 0.065)
	t = -1.695
	p = 0.090
Moderate Drying	0.078 (-0.383, 0.540)
	t = 0.333
	p = 0.739
Days Post-exposure	-0.266 (-0.559, 0.026)
	$\chi^2 = 3.195$ p = 0.074
Mass at Metamorphosis (g)	-0.109 (-0.468, 0.250)
	$\chi^2 = 0.355$ p = 0.552
Growth Rate (g/day)	0.301* (0.013, 0.589)
	χ^2=4.191 p = 0.041
Drying Treatment : Days Post-exposure	$\chi^2 = 7.889$ p = 0.019
Fast Drying : Days Post-exposure	0.189 (-0.248, 0.626)
	t = 0.848
	p = 0.396
Moderate Drying : Days Post-exposure	0.589** (0.171, 1.008)
	t = 2.763
	p = 0.006
Drying Treatment : Mass at Metamorphosis	$\chi^2 = 4.807$ p = 0.090
Fast Drying : Mass at Metamorphosis	0.490* (0.023, 0.958)
	t = 2.055
	p = 0.040
Moderate Drying : Mass at Metamorphosis	0.473 (-0.067, 1.013)
	t = 1.717
	p = 0.086
Drying Treatment: Growth Rate	$\chi^2 = 0.657$ p = 0.720
Fast Drying : Growth Rate	0.049 (-0.431, 0.528)
	t = 0.198
	p = 0.843
Moderate Drying : Growth Rate	-0.150 (-0.602, 0.302)

	t = -0.651
	p = 0.515
Constant	-0.416* (-0.749, -0.083)
	t = -2.450
	p = 0.015
Observations	593
Log Likelihood	-374.910
Akaike Information Criterion	775.821
Bayesian Information Criterion	832.829
Note:	*p < 0.05; **p < 0.01; ***p < 0.001

Days post exposure, mass at metamorphosis and post-metamorphic growth rate were independent factors and frog ID was included as a random effect. Coefficient estimates and their standard errors (in parentheses) are shown for each factor.

Table A.7 Linear mixed model of Bd infection load with drying treatment.

	Dependent variable:
	Bd load [log (DNA copies + 1)]
Drying Treatment	$\chi^2 = 1.465$ p = 0.481
Fast Drying	0.159 (-0.158, 0.475)
	t = 0.983
	p = 0.339
Moderate Drying	0.182 (-0.131, 0.495)
	t = 1.138
	p = 0.270
Days Post-exposure	$\chi^2 = 4.771$ p = 0.031
	-0.264* (-0.501, -0.027)
Pre-exposure Body Mass (g)	$\chi^2 = 9.870$ p = 0.002
	-0.242** (-0.393, -0.091)
Growth Rate (g/day)	$\chi^2 = 1.512$ p = 0.223
	0.078 (-0.047, 0.203)
Drying Treatment : Days Post-exposure	$\chi^2 = 6.949$ p = 0.031
Fast Drying : Days post-exposure	-0.083 (-0.413, 0.247)
	t = -0.492
	p = 0.624
Moderate Drying : Days Post-exposure	0.284 (-0.014, 0.583)
	t = 1.867
	p = 0.064
Constant	3.008*** (2.769, 3.247)
	t = 24.660
	p < 0.001
Observations	212
Log Likelihood	-284.070
Akaike Information Criterion	590.140
Bayesian Information Criterion	626.640
Note:	*p < 0.05; **p < 0.01; ***p < 0.001

Days post exposure, mass at metamorphosis and post-metamorphic growth rate as fixed effects and frog ID nested within mesocosm as random effects. Coefficient estimates and their standard errors (in parentheses) are shown for each factor.

Table A.8 Linear mixed model of body condition [measured as log (scaled mass index), or log SMI)].

	Dependent variable:
	Body Condition (log SMI)
Exposure Group (Sham vs. *Bd*-exposed)	$\chi^2 = 3.126$ p = 0.077
	0.016 (-0.002, 0.034)
Drying Treatment	$\chi^2 = 4.085$ p = 0.130
Moderate Drying	-0.015 (-0.033, 0.002)
	t = -1.684
	p = 0.110
No Drying	-0.017 (-0.034, 0.001)
	t = -1.817
	p = 0.086
Days Post-exposure	$\chi^2 = 8.763$ p = 0.003
	0.0003^{**} (0.0001, 0.0005)
Exposure Group : Drying Treatment	$\chi^2 = 0.447$ p = 0.800
Bd Exposed : Moderate Drying	0.008 (-0.017, 0.033)
	t = 0.643
	p = 0.521
Bd Exposed : No Drying	0.006 (-0.019, 0.031)
	t = 0.483
	p = 0.630
Exposure Group : Days Post-exposure	$\chi^2 = 37.562$ p < 0.001
Drying treatment : Days Post-exposure	$\chi^2 = 0.021$ p = 0.989
Moderate Drying : Days Post-exposure	0.00002 (-0.0002, 0.0003)
	t = 0.120
	p = 0.905
No Drying : Days Post-exposure	0.00002 (-0.0002, 0.0003)
	t = 0.134
	p = 0.894
Exposure Group : Drying Treatment : Days Post-exposure	$\chi^2 = 0.410$ p = 0.814
Bd Exposed : Moderate Drying : Days Post-exposure	0.0001 (-0.0003, 0.0005)
	t = 0.556
	p = 0.579
Bd Exposed : No Drying : Days Post-exposure	0.0001 (-0.0003, 0.0005)
	t = 0.556
	p = 0.579
Constant	0.208^{***} (0.195, 0.221)

	t = 32.056
	p = 0.000
Observations	1758
Log Likelihood	2462.216
Akaike Information Criterion	-4894.432
Bayesian Information Criterion	-4812.353

Note: $^{*}p < 0.05$; $^{**}p < 0.01$; $^{***}p < 0.001$

Exposure group, drying treatment, and days post-exposure as the main and interacting effects and frog ID nested within mesocosm as random effects. Coefficient estimates and their standard errors (in parentheses) are shown for each factor.

Table A.9 Output from a Cox proportional hazards model examining survival after Bd exposure.

	Dependent variable:
	Survival Post-*Bd* exposure
Drying Treatment : Exposure Group	χ^2 =11.061 p = 0.050
Fast Drying : Sham Exposed	0.515 (-1.293, 2.322)
	z = 0.576
	p = 0.565
Moderate Drying : Sham Exposed	0.676 (-1.022, 2.373)
	z = 1.000
	p = 0.317
Fast Drying : *Bd* Exposed	1.803* (0.265, 3.341)
	z = 2.475
	p = 0.013
Moderate Drying : *Bd* Exposed	1.572* (0.025, 3.120)
	z = 2.061
	p = 0.040
No Drying : *Bd* Exposed	1.281 (-0.307, 2.869)
	z = 1.650
	p = 0.100
Larval Period (d)	0.005 (-0.009, 0.019)
	z = 0.971
	p = 0.332
	χ^2 = 0.942
Observations	231
R^2	0.048
Maximum Possible R^2	0.803
Log Likelihood	-182.062
Wald Test	11.770 (df = 6) (p = 0.068)
Likelihood Ratio Test	11.366 (df = 6) (p = 0.078)
Log Rank Test	11.153 (df = 6) (p = 0.084)
Note:	*p < 0.05; **p < 0.01; ***p < 0.001

Larval period and the interaction between drying treatment and exposure group were the fixed effects and mesocosm was included as a random effect. Coefficient estimates and their standard errors (in parentheses) are shown for each factor.

Table A.10 Output from a linear model examining total mucosal peptides after Bd exposure across exposure groups and drying treatments.

	Dependent variable:
	Total mucosal peptides (peptides/ml/gbw)
Drying Treatment	F = 2.225 p = 0.118
Moderate Drying	0.320 (-50.562, 51.201)
	t = 0.012
	p = 0.991
No Drying	47.589 (-3.292, 98.471)
	t = 1.833
	p = 0.073
Exposure Group	F = 0.691 p = 0.410
	24.466 (-33.228, 82.161)
Drying Treatment : Exposure Group	F = 1.721, p = 0.189
Moderate Drying : *Bd* Exposed	-55.664 (-133.427, 22.099)
	t = -1.403
	p = 0.167
No Drying: *Bd* Exposed	-72.507 (-152.526, 7.512)
	t = -1.776
	p = 0.082
Constant	108.597*** (72.619, 144.576)
	t = 5.916
	p < 0.001
Observations	58
R^2	0.158
Adjusted R^2	0.077
Residual Standard Error	60.883 (df = 52)
F Statistic	1.946 (df = 5; 52) (p = 0.103)
Note:	*p < 0.05; **p < 0.01; ***p < 0.001

Coefficient estimates and their standard errors (in parentheses) are shown for each factor.

Table A.11 Output from a linear model examining Bd inhibition by peptides after Bd exposure across the three drying treatments and two exposure groups.

	Dependent variable:
	Bd Growth Index
Drying Treatment	F = 0.258, p = 0.773
Moderate Drying	0.112 (-0.291, 0.514)
	t = 0.545
	p = 0.589
No Drying	-0.071 (-0.460, 0.318)
	t = -0.360
	p = 0.721
Exposure group	F = 0.258, p = 0.721
Drying treatment : Exposure Group	F = 0.046, p = 0.830
Moderate Drying : *Bd* Exposed	-0.046 (-0.608, 0.516)
	t = -0.161
	p = 0.874
No Drying: *Bd* Exposed	-0.144 (-0.696, 0.408)
	t = -0.511
	p = 0.613
Constant	1.079*** (0.804, 1.354)
	t = 7.689
	p < 0.001
Observations	48
R^2	0.072
Adjusted R^2	-0.039
Residual Standard Error	0.397 (df = 42)
F Statistic	0.649 (df = 5; 42) (p = 0.664)
Note:	*p < 0.05; **p < 0.01; ***p < 0.001

Coefficient estimates and their standard errors (in parentheses) are shown for each factor.

Table A.12 General linear model for presence/absence of AMPs after Bd exposure across the three drying treatments.

	Dependent variable:
	count of AMPs detected
Exposure Group (Sham vs. *Bd*-exposed)	$\chi^2 = 6.3256$ p = 0.021
	-0.815* (-1.484, -0.145)
Drying Treatment	$\chi^2 = 2.9324$ p = 0.2308
Moderate Drying	-0.473 (-1.030, 0.084)
	t = -1.664
	p = 0.102
No Drying	-0.140 (-0.646, 0.366)
	t = -0.541
	p = 0.591
Drying Treatment * Exposure Group	$\chi^2 = 1.4962$, p = 0.4733
Moderate Drying : *Bd* Exposed	0.144 (-0.880, 1.169)
	t = 0.276
	p = 0.784
No Drying : *Bd* Exposed	0.529 (-0.357, 1.415)
	t = 1.170
	p = 0.247
Constant	1.836*** (1.491, 2.181)
	t = 10.426
	p < 0.001
Observations	62
Residual Deviance	152.785 (df = 56)
Null Deviance	185.784 (df = 61)
Note:	*p < 0.05; **p < 0.01; ***p < 0.001

Coefficient estimates and their standard errors (in parentheses) are shown for each factor.

Table A.13 Output of a PERMANOVA for AMP presence/absence after Bd exposure.

	Df	Sum of squares	R^2	F	p
Exposure Group (Sham vs. *Bd* Exposed)	1	1.0035	0.22831	14.087	< 0.001
Drying Treatment	2	0.1385	0.03151	0.972	0.426
Exposure Group : Drying Treatment	2	0.190	0.0432	1.335	0.257
Residuals	43	3.0631			
Total	48	4.3954	1.000		

Table A.14 Output of a PERMANOVA for AMP relative intensities after Bd exposure

	Df	Sum of Squares	R^2	F	p
Exposure Group (Sham vs. *Bd*-exposed)	1	1.037	0.134	7.160	0.0005
Drying Treatment	2	0.205	0.026	0.709	0.629
Exposure Group : Drying Treatment	2	0.294	0.038	1.016	0.399
Residual	43	6.225	0.802		
Total		48	7.7611	1	

Table A.15 Output of an ANOVA for Shannon diversity index comparing the AMP relative intensities between exposed and control frogs in the three drying treatments.

	Df	Sum of Squares	R^2	F	p
Exposure Group (Sham vs. *Bd*-exposed)	1	1.534	1.534	14.935	0.0004
Drying Treatment	2	0.021	0.026	0.102	0.903
Exposure Group : Drying Treatment	2	0.387	0.194	1.886	0.164
Residual	43	4.416	0.103		

Table A.16 Similarity percentage (simper) analysis results based on the decomposition of the Bray-Curtis dissimilarity index based on presence/absence of AMPs.

AMP	Brevinin 1 Pa	Brevinin 1 Pb	Brevinin 1 Pc	Brevinin 1 Pd	Brevinin 1 Pe	Brevinin 1 Pla
Simper Index	0.1471043	0.7325010	0.6763092	0.2927123	0.4293444	0.5549669

Values show the contribution of individual peptides to the overall Bray-Curtis dissimilarity.

Table A.17 Similarity percentage (simper) analysis results based on the decomposition of the Bray-Curtis dissimilarity index based on AMP relative intensities.

AMP	Brevinin 1 Pg	Brevinin 1 Pk	Brevinin 1 Pe
Simper Index	0.3200824	0.6118018	0.7864296

Values show the contribution of individual peptides to the overall Bray-Curtis dissimilarity.

Table A.18 Output from a linear model examining inhibition of Bd growth by mucosome samples in Bd-exposed and naïve (control) frogs.

	Dependent variable:
	Scaled Inhibition
Exposure Group	$\chi^2 = 0.074$ p = 0.788
	0.674 (-4.171, 5.520)
Drying Treatment	$\chi^2 = 0.6634$ p = 0.728
Moderate drying	-1.078 (-5.532, 3.376)
	t = -0.474
	p = 0.642
No drying	-2.003 (-6.847, 2.841)
	t = -0.810
	p = 0.430
log (Mass at Metamorphosis)	$\chi^2 = 7.146$ p = 0.013
	24.854* (6.631, 43.077)
Exposure Group : Drying Treatment	$\chi^2 = 1.969$ p = 0.374
Bd Exposed : Moderate Drying	0.533 (-5.939, 7.005)
	t = 0.161
	p = 0.873
Bd Exposed : No Drying	-3.699 (-10.375, 2.977)
	t = -1.086
	p = 0.287
Constant	6.802** (2.588, 11.017)
	t = 3.163
	p = 0.004
Observations	51
Log Likelihood	-136.850
Akaike Information Criterion	291.701
Bayesian Information Criterion	307.759
Note:	*p < 0.05; **p < 0.01; ***p < 0.001

Coefficient estimates and their standard errors (in parentheses) are shown for each factor.

Table A.19 Output from a linear model examining the correlation between Bd load and inhibition of Bd growth by mucosome samples.

	Dependent variable:
	Bd Load [log (DNA copies + 1)]
Scaled Inhibition	-0.105 (-2.680, 2.471)
	t = -0.080
	p = 0.930
Constant	1.265 (-1.472, 4.002)
	t = 0.906
	p = 0.381
Observations	21
Log Likelihood	-62.770
Akaike Information Criterion	133.540
Bayesian Information Criterion	137.317
Note:	*p < 0.05; **p < 0.01; ***p < 0.001

Coefficient estimates and their standard errors (in parentheses) are shown for each factor.

Appendix B

Table B.1 Output from a Cox proportional hazards model examining survival after metamorphosis between the two temperature treatments for VT.

	Dependent variable:
	Survival to metamorphosis VT
Chamber (Future)	-0.101 (-0.391, 0.189) t = -0.681 p = 0.496 χ^2 = 0.4633
Observations	300
R^2	0.002
Maximum Possible R^2	0.999
Log Likelihood	-1088.390
Wald Test	0.460 (df = 1) (p = 0.496)
LR Test	0.463 (df = 1) (p = 0.497)
Score (Logrank) Test	0.464 (df = 1) (p = 0.496)
Note:	*p<0.05; **p<0.01; ***p<0.001

Coefficient estimates and their standard errors (in parentheses) are shown for each factor.

Table B.2 Output from a Cox proportional hazards model examining survival after metamorphosis between the two temperature treatments for PA.

	Dependent variable:
	Survival to metamorphosis in PA
Chamber (Future)	-0.321* (-0.578, -0.064)
	z = -2.447
	p = 0.015
	χ^2 = 6.026
Observations	374
R^2	0.016
Maximum Possible R^2	0.999
Log Likelihood	-1309.428
Wald Test	5.990* (df = 1) (p = 0.015)
LR Test	6.026* (df = 1) (p = 0.015)
Score (Logrank) Test	6.037* (df = 1) (p = 0.015)
Note:	*p<0.05; **p<0.01; ***p<0.001

Coefficient estimates and their standard errors (in parentheses) are shown for each factor.

Table B.3 Output from a Cox proportional hazards model examining survival after metamorphosis between the two temperature treatments for TN.

	Dependent variable:
	Survival in TN
Chamber (Future)	-1.104^{***} (-1.400, -0.808) z = -7.317 p = 0.000 $\chi^2 = 53.789$
Observations	224
R^2	0.213
Maximum Possible R^2	1.000
Log Likelihood	-964.939
Wald Test	53.540^{***} (df = 1) (p = 0.000)
LR Test	53.789^{***} (df = 1) (p = 0.000)
Score (Logrank) Test	56.943^{***} (df = 1) (p = 0.000)
Note:	*p<0.05; **p<0.01; ***p<0.001

Coefficient estimates and their standard errors (in parentheses) are shown for each factor.

Table B.4 Output from a Cox proportional hazards model examining survival after metamorphosis between the two temperature treatments for LA.

	Dependent variable:
	Survival to metamorphosis LA
Chamber (Future)	0.623^{***} (0.305, 0.940)
	t = 3.840
	p = 0.0002
	χ^2=15.255
Observations	280
R^2	0.053
Maximum Possible R^2	0.998
Log Likelihood	-850.375
Wald Test	14.750^{***} (df = 1) (p = 0.0002)
LR Test	15.255^{***} (df = 1) (p = 0.0001)
Score (Logrank) Test	15.216^{***} (df = 1) (p = 0.0001)
Note:	*p<0.05; **p<0.01; ***p<0.001

Coefficient estimates and their standard errors (in parentheses) are shown for each factor.

Table B.5 Output from a Cox proportional hazards model examining time to metamorphosis between the two temperature treatments for VT.

	Dependent variable:
	Metamorphosis time VT
Chamber (Future)	1.652^{***} (1.082, 2.222) t = 5.679 p = 1.36×10^{-8} χ^2 = 38.752
Observations	87
R^2	0.359
Maximum Possible R^2	0.999
Log Likelihood	-285.311
Wald Test	32.250^{***} (df = 1) (p = 0.000)
LR Test	38.752^{***} (df = 1) (p = 0.000)
Score (Logrank) Test	38.577^{***} (df = 1) (p = 0.000)
Note:	*p<0.05; **p<0.01; ***p<0.001

Coefficient estimates and their standard errors (in parentheses) are shown for each factor.

Table B.6 Output from a Cox proportional hazards model examining time to metamorphosis between the two temperature treatments for PA.

	Dependent variable:
	Metamorphosis time PA
Chamber (Future)	5.750^{***} (3.723, 7.777) t = 5.560 p = 2.7 x10^{-8} χ^2 = 173.05
Observations	135
R^2	0.722
Maximum Possible R^2	1.000
Log Likelihood	-444.060
Wald Test	30.910^{***} (df = 1) (p = 0.00000)
LR Test	173.049^{***} (df = 1) (p = 0.000)
Score (Logrank) Test	145.892^{***} (df = 1) (p = 0.000)
Note:	*p<0.05; **p<0.01; ***p<0.001

Coefficient estimates and their standard errors (in parentheses) are shown for each factor.

Table B.7 Output from a Cox proportional hazards model examining time to metamorphosis between the two temperature treatments for LA.

	Dependent variable:
	Metamorphosis time LA
Chamber (Future)	2.944^{***} (2.361, 3.527) t = 9.904 $p = 2x10^{-16}$ χ^2=119.03
Observations	132
R^2	0.594
Maximum Possible R^2	1.000
Log Likelihood	-456.378
Wald Test	98.090^{***} (df = 1) (p = 0.000)
LR Test	119.026^{***} (df = 1) (p = 0.000)
Score (Logrank) Test	144.972^{***} (df = 1) (p = 0.000)
Note:	*p<0.05; **p<0.01; ***p<0.001

Coefficient estimates and their standard errors (in parentheses) are shown for each factor.

Table B.8 Output from a linear model examining body mass at metamorphosis across the two temperatures in VT.

	Dependent variable:
	Mass (g)
Treatment (Future)	-1.591*** (-1.984, -1.197)
	t = -7.923
	p = 0.000
	F = 62.778
Constant	3.426*** (3.120, 3.732)
	t = 21.945
	p = 0.000
Observations	86
R^2	0.428
Adjusted R^2	0.421
Residual Standard Error	0.910 (df = 84)
F Statistic	62.778*** (df = 1; 84) (p = 0.000)
Note:	*p<0.05; **p<0.01; ***p<0.001

Coefficient estimates and their standard errors (in parentheses) are shown for each factor.

Table B.9 Output from a linear model examining body mass at metamorphosis across the two temperatures in PA.

	Dependent variable:
	Mass (g)
Treatment (Future)	-0.335*** (-0.391, -0.278)
	t = -11.592
	p = 0.000
	F = 134.39
Constant	0.879*** (0.836, 0.922)
	t = 40.021
	p = 0.000
Observations	135
R^2	0.503
Adjusted R^2	0.499
Residual Standard Error	0.166 (df = 133)
F Statistic	134.386*** (df = 1; 133) (p = 0.000)
Note:	*p<0.05; **p<0.01; ***p<0.001

Coefficient estimates and their standard errors (in parentheses) are shown for each factor.

Table B.10 Output from a linear model examining body mass at metamorphosis across the two temperatures in LA.

	Dependent variable:
	Mass (g)
Treatment (Future)	0.029 (-0.061, 0.119)
	t = 0.629
	p = 0.531
	F = 0.396
Constant	0.839*** (0.780, 0.899)
	t = 27.603
	p = 0.000
Observations	99
R^2	0.004
Adjusted R^2	-0.006
Residual Standard Error	0.227 (df = 97)
F Statistic	0.396 (df = 1; 97) (p = 0.531)
Note:	*p<0.05; **p<0.01; ***p<0.001

Coefficient estimates and their standard errors (in parentheses) are shown for each factor.

Table B.11 Output from a linear model examining body length (mm) at metamorphosis across the two temperatures in VT.

	Dependent variable:
	SVL (mm)
Treatment (Future)	-4.952*** (-6.014, -3.890)
	t = -9.136
	p = 0.000
	F = 83.469
Constant	28.471*** (27.642, 29.300)
	t = 67.298
	p = 0.000
Observations	87
R^2	0.495
Adjusted R^2	0.490
Residual Standard Error	2.467 (df = 85)
F Statistic	83.469*** (df = 1; 85) (p = 0.000)
Note:	*p<0.05; **p<0.01; ***p<0.001

Coefficient estimates and their standard errors (in parentheses) are shown for each factor.

Table B.12 Output from a linear model examining body length (mm) at metamorphosis across the two temperatures in PA.

	Dependent variable:
	SVL (mm)
Treatment (Future)	-0.142*** (-0.162, -0.121)
	t = -13.705
	p = 0.000
	F = 187.83
Constant	3.394*** (3.379, 3.410)
	t = 431.859
	p = 0.000
Observations	135
R^2	0.585
Adjusted R^2	0.582
Residual Standard Error	0.059 (df = 133)
F Statistic	187.832*** (df = 1; 133) (p = 0.000)
Note:	*p<0.05; **p<0.01; ***p<0.001

Coefficient estimates and their standard errors (in parentheses) are shown for each factor.

Table B.13 Output from a linear model examining body length (mm) at metamorphosis across the two temperatures in LA.

	Dependent variable:
	SVL (mm)
Treatment (Future)	-0.604* (-1.156, -0.052)
	t = -2.145
	p = 0.035
	F = 4.602
Constant	21.257*** (20.894, 21.621)
	t = 114.577
	p = 0.000
Observations	99
R^2	0.045
Adjusted R^2	0.035
Residual Standard Error	1.388 (df = 97)
F Statistic	4.602* (df = 1; 97) (p = 0.035)
Note:	*p<0.05; **p<0.01; ***p<0.001

Coefficient estimates and their standard errors (in parentheses) are shown for each factor.

Table B.14 Output from a linear model examining mucosal peptides at one month across the two temperatures in VT.

	Dependent variable:
	Peptide counts/gbw (1 month)
Treatment (Future)	-1.005* (-1.827, -0.182)
	t = -2.393
	p = 0.038
	F = 5.735
Constant	5.303*** (4.674, 5.931)
	t = 16.537
	p = 0.000
Observations	12
R^2	0.364
Adjusted R^2	0.300
Residual Standard Error	0.717 (df = 10)
F Statistic	5.725* (df = 1; 10) (p = 0.038)
Note:	*p<0.05; **p<0.01; ***p<0.001

Coefficient estimates and their standard errors (in parentheses) are shown for each factor.

Table B.15 Output from a linear model examining mucosal peptides at two months across the two temperatures in VT.

	Dependent variable:
	Peptide counts/gbw (2 months)
Treatment (Future)	-1.072** (-1.710, -0.434)
	t = -3.292
	p = 0.008
	F = 10.84
Constant	5.793*** (5.306, 6.280)
	t = 23.301
	p = 0.000
Observations	12
R^2	0.520
Adjusted R^2	0.472
Residual Standard Error	0.556 (df = 10)
F Statistic	10.840** (df = 1; 10) (p = 0.009)
Note:	*p<0.05; **p<0.01; ***p<0.001

Coefficient estimates and their standard errors (in parentheses) are shown for each factor

Table B.16 Output from a linear model examining mucosal peptides at one month across the two temperatures in PA.

	Dependent variable:
	Peptide counts/gbw (1 month)
Treatment (Future)	-0.217 (-0.725, 0.291)
	t = -0.837
	p = 0.415
Constant	4.157*** (3.742, 4.572)
	t = 19.632
	p = 0.000
Observations	18
R^2	0.042
Adjusted R^2	-0.018
Residual Standard Error	0.519 (df = 16)
F Statistic	0.700 (df = 1; 16) (p = 0.416)
Note:	*p<0.05; **p<0.01; ***p<0.001

Coefficient estimates and their standard errors (in parentheses) are shown for each factor.

Table B.17 Output from a linear model examining mucosal peptides at two months across the two temperatures in PA.

	Dependent variable:
	Peptide counts/gbw (2 months)
Treatment (Future)	-0.291 (-1.015, 0.432)
	t = -0.789
	p = 0.442
Constant	4.943*** (4.352, 5.533)
	t = 16.400
	p = 0.000
Observations	18
R^2	0.037
Adjusted R^2	-0.023
Residual Standard Error	0.738 (df = 16)
F Statistic	0.622 (df = 1; 16) (p = 0.442)
Note:	*p<0.05; **p<0.01; ***p<0.001

Coefficient estimates and their standard errors (in parentheses) are shown for each factor

Table B.18 Output from a linear model examining mucosal peptides at one month across the two temperatures in LA.

	Dependent variable:
	Peptide counts/gbw (1 month)
Treatment (Future)	0.767^{*} (0.153, 1.381)
	t = 2.447
	p = 0.030
	F =5.990
Growth rate	17.517 (-8.754, 43.789)
	t = 1.307
	p = 0.214
	F = 1.710
Treatment (future) : Growth.rate	-185.522^{***} (-253.379, -117.664)
	t = -5.359
	p = 0.0002
	F = 28.714
Constant	3.611^{***} (3.333, 3.889)
	t = 25.456
	p = 0.000
Observations	17
R^2	0.738
Adjusted R^2	0.678
Residual Std. Error	0.411 (df = 13)
F Statistic	12.215^{***} (df = 3; 13) (p = 0.0005)
Note:	*p < 0.05; **p < 0.01; ***p < 0.001

Coefficient estimates and their standard errors (in parentheses) are shown for each factor.

Table B.19 Output from a linear model examining mucosal peptides at two months across the two temperatures in LA.

	Dependent variable:
	Peptide counts/gbw (2 months)
Treatment (Future)	8.032* (2.579, 13.486)
	t = 2.887
	p = 0.017
	F=8.334
Time to metamorphosis	0.002 (-0.010, 0.014)
	t = 0.288
	p = 0.780
	F=0.083
Treatment (future)* Time to metamorphosis	-0.058* (-0.096, -0.021)
	t = -3.032
	p = 0.013
	F=9.195
Constant	3.823* (1.389, 6.257)
	t = 3.079
	p = 0.012
Observations	14
R^2	0.493
Adjusted R^2	0.341
Residual Standard Error	0.482 (df = 10)
F Statistic	3.240 (df = 3; 10) (p = 0.069)
Note:	*p<0.05; **p<0.01; ***p<0.001

Coefficient estimates and their standard errors (in parentheses) are shown for each factor.

Table B.20 Output of a Permanova for AMPs presence/absence between temperature treatments in Vermont at 1 month.

	Df	Sum of Sqs	R^2	F	p
Temperature treatment	1	0.253	0.284	2.381	0.176
Residuals	6	0.638	0.716		
Total	7	0.891	1.000		
notes:			$^{*}p<0.05$; $^{**}p<0.01$; $^{***}p<0.001$		

Table B.21 Output of a Permanova for AMPs presence/absence between temperature treatments in Vermont at 2 months.

	Df	Sum of Sqs	R^2	F	p
Temperature treatament	1	0.257	0.338	3.057	0.072
Residuals	6	0.504	0.662		
Total	7	0.762	1.000		
notes:			$^{*}p<0.05$; $^{**}p<0.01$; $^{***}p<0.001$		

Table B.22 Output of a Permanova for AMPs presence/absence between temperature treatments in Pennsylvania at 1 month.

	Df	Sum of Sqs	R^2	F	p
Temperature treatment	1	0.173	0.088	0.485	0.760
Residuals	5	1.787	0.912		
Total	6	1.960	1.000		
notes:			$^{*}p<0.05$; $^{**}p<0.01$; $^{***}p<0.001$		

Table B.23 Output of a Permanova for AMPs presence/absence between temperature treatments in Pennsylvania at 2 months.

	Df	Sum of Sqs	R^2	F	p
Temperature treatment	1	0.272	0.173	1.468	0.218
Residuals	7	1.295	0.827		
Total	8	1.567	1.000		
notes:			$^{*}p<0.05$; $^{**}p<0.01$; $^{***}p<0.001$		

Table B.24 Output of a Permanova for AMPs intensities between temperature treatments in Vermont at 1 month.

	Df	Sum of Sqs	R^2	F	p
Temperature treatment	1	0.241	0.131	0.905	0.519
Residuals	6	1.598	0.869		
Total	7	1.839	1.000		
notes:			$^{*}p<0.05$; $^{**}p<0.01$; $^{***}p<0.001$		

Table B.25 Output of a Permanova for AMPs intensities between temperature treatments in Vermont at 2 months.

	Df	Sum of Sqs	R^2	F	p
Temperature treatment	1	0.305	0.175	1.284	0.242
Residuals	6	1.439	0.825		
Total	7	1.745	1.000		
notes:			$^{*}p<0.05$; $^{**}p<0.01$; $^{***}p<0.001$		

Table B.26 Output of a Permanova for AMPs intensities between temperature treatments in Pennsylvania at 1 month.

	Df	Sum of Sqs	R^2	F	p
Temperature treatment	1	0.456	0.176	1.065	0.343
Residuals	5	2.155	0.824		
Total	6	2.614	1.000		
notes:			$^{*}p<0.05$; $^{**}p<0.01$; $^{***}p<0.001$		

Table B.27 Output of a Permanova for AMPs intensities between temperature treatments in Pennsylvania at 2 month.

	Df	Sum of Sqs	R^2	F	p
Temperature treatment	1	0.553	0.251	2.346	0.048
Residuals	7	1.649	0.749		
Total	8	2.202	1.000		
notes:			$^{*}p<0.05$; $^{**}p<0.01$; $^{***}p<0.001$		

Table B.28 Output of a Permanova for AMPs presence/absence between temperature treatments with seven known peptides for Vermont at 1 month.

	Df	Sum of Sqs	R^2	F	p
Temperature treatment	1	0.168	0.235	1.848	0.329
Residuals	6	0.547	0.764		
Total	7	0.715	1.000		
notes:			$^{*}p<0.05$; $^{**}p<0.01$; $^{***}p<0.001$		

Table B.29 Output of a Permanova for AMPs presence/absence between temperature treatments with seven known peptides in Vermont at 2 months.

	Df	Sum of Sqs	R^2	F	p
Temperature treatment	1	0.135	0.2661	2.176	0.124
Residuals	6	0.734	0.734		
Total	7	0.507	1.000		
notes:			$^{*}p<0.05$; $^{**}p<0.01$; $^{***}p<0.001$		

Table B.30 Output of a Permanova for AMPs intensities between temperature treatments with seven known peptides for Vermont at 1 month.

	Df	Sum of Sqs	R^2	F	p
Temperature treatment	1	0.122	0.235	0.457	0.907
Residuals	6	1.600	0.764		
Total	7	1	1.000		
notes:			$^{*}p<0.05$; $^{**}p<0.01$; $^{***}p<0.001$		

Table B.31 Output of a Permanova for AMPs intensities between temperature treatments with seven known peptides in Vermont at 2 months.

	Df	Sum of Sqs	R^2	F	p
Temperature treatament	1	0.246	0.135	0.939	0.578
Residuals	6	1.572	0.865		
Total	7	1.818	1.000		
notes:			$^{*}p<0.05$; $^{**}p<0.01$; $^{***}p<0.001$		

Table B.32 Output of a generalized linear model with a Poisson distribution for VT at 1 month.

	LR Chisq	Df	p
Treatment	5.132	1	0.024*
Time to metamorphosis	0.037	1	0.847
Treatment time to metamorphosis	4.643	1	0.031*
notes:		$^{*}p<0.05$; $^{**}p<0.01$; $^{***}p<0.001$	

Table B.33 Output of a generalized linear model with a Poisson distribution for VT at 2 months.

	LR Chisq	Df	p
Treatment	11.995	1	$5.334x10^{-4}$***
Time to metamorphosis	0.185	1	0.668
Treatment time to metamorphosis	9.515	1	$2.038x10^{-3}$**
notes:		$^{*}p<0.05$; $^{**}p<0.01$; $^{***}p<0.001$	

Table B.34 Output of a generalized linear model with a Poisson distribution for PA at 1 month.

	LR Chisq	Df	p
Treatment	0.188	1	0.665
Mass meta	3.458	1	0.063
notes:		$^{*}p<0.05$; $^{**}p<0.01$; $^{***}p<0.001$	

Table B.35 Output of a generalized linear model with a Poisson distribution for PA at 2 months

	LR Chisq	Df	p
Treatment	2.662	1	0.103
Growth rate	2.949	1	0.086
notes:		$^{*}p<0.05$; $^{**}p<0.01$; $^{***}p<0.001$	

Table B.36 Output of a generalized linear model with a Poisson distribution for LA at 1 month.

	LR Chisq	Df	p
Treatment	0.320	1	0.572
Time to metamorphosis	1.692	1	0.193
notes:		$^{*}p<0.05$; $^{**}p<0.01$; $^{***}p<0.001$	

Table B.37 Output of a generalized linear model with a Poisson distribution for LA at 2 months.

	LR Chisq	Df	p
Treatment	1.499	1	0.221
notes:		$^{*}p<0.05$; $^{**}p<0.01$; $^{***}p<0.001$	

Table B.38 Output from a linear model examining total white blood cell counts at 1 month across the two temperatures in VT.

	Dependent variable:
	White blood cell counts cells/ml
Time to metamorphosis (days)	0.0001 (-0.003, 0.003)
	t = 0.039
	p = 0.970
	F = 0.0015
Treatment (Future)	-2.062** (-3.102, -1.022)
	t = -3.885
	p = 0.005
	F = 15.094
Time to metamorphosis : Treatment (Future)	0.010** (0.005, 0.015)
	t = 3.959
	p = 0.004
	F = 15.675
Constant	7.135*** (6.383, 7.886)
	t = 18.613
	p < 0.001
Observations	12
R^2	0.801
Adjusted R^2	0.726
Residual Standard Error	0.168 (df = 8)
F Statistic	10.721** (df = 3; 8) (p = 0.004)
Note:	*p<0.05; **p<0.01; ***p<0.001

Coefficient estimates and their standard errors (in parentheses) are shown for each factor.

Table B.39 Output from a linear model examining total white blood cell counts at 2 months across the two temperatures in VT.

	Dependent variable:
	White blood cell counts cells/ml
Treatment (Future)	-0.279 (-0.694, 0.136)
	t = -1.319
	p = 0.220
	F = 1.740
Constant	7.556*** (7.224, 7.887)
	t = 44.725
	p = 0.000
Observations	11
R^2	0.162
Adjusted R^2	0.069
Residual Standard Error	0.338 (df = 9)
F Statistic	1.740 (df = 1; 9) (p = 0.220)
Note:	*p<0.05; **p<0.01; ***p<0.001

Coefficient estimates and their standard errors (in parentheses) are shown for each factor.

Table B.40 Output from a linear model examining total white blood cell counts at 1 month across the two temperatures in PA.

	Dependent variable:
	White blood cell counts cells/ml
Time to metamorphosis (days)	0.013 (0.0002, 0.026)
	t = 1.988
	p = 0.067
	F = 3.951
Treatment (Future)	0.855 (0.008, 1.701)
	t = 1.980
	p = 0.068
	F = 3.919
Constant	4.118* (1.246, 6.990)
	t = 2.811
	p = 0.014
Observations	17
R^2	0.221
Adjusted R^2	0.110
Residual Standard Error	0.158 (df = 14)
F Statistic	1.988 (df = 2; 14) (p = 0.174)
Note:	*p<0.05; **p<0.01; ***p<0.001

Coefficient estimates and their standard errors (in parentheses) are shown for each factor.

Table B.41 Output from a linear model examining total white blood cell counts at 2 months across the two temperatures in PA.

	Dependent variable:
	White blood cell counts cells/ml
Treatment (Future)	0.019 (-0.176, 0.215)
	t = 0.192
	p = 0.851
	F = 0.037
Constant	7.104*** (6.940, 7.269)
	t = 84.704
	p = 0.000
Observations	17
R^2	0.002
Adjusted R^2	-0.064
Residual Standard Error	0.188 (df = 15)
F Statistic	0.037 (df = 1; 15) (p = 0.851)
Note:	*p<0.05; **p<0.01; ***p<0.001

Coefficient estimates and their standard errors (in parentheses) are shown for each factor.

Table B.42 Output from a linear model examining total white blood cell counts at 1 month across the two temperatures in LA.

	Dependent variable:
	White blood cell counts cells/ml
Treatment (Future)	-0.062 (-0.267, 0.142)
	t = -0.600
	p = 0.557
	F = 0.360
Constant	6.935*** (6.821, 7.050)
	t = 118.555
	p = 0.000
Observations	19
R^2	0.021
Adjusted R^2	-0.037
Residual Standard Error	0.211 (df = 17)
F Statistic	0.360 (df = 1; 17) (p = 0.557)
Note:	*p<0.05; **p<0.01; ***p<0.001

Coefficient estimates and their standard errors (in parentheses) are shown for each factor.

Table B.43 Output from a linear model examining total white blood cell counts cells/ml at 2 months across the two temperatures in LA.

	Dependent variable:
	White blood cell counts cells/ml
Treatment (Future)	-0.175 (-0.419, 0.069)
	t = -1.404
	p = 0.198
	F = 1.972
Growth rate (g/day)	39.159* (6.219, 72.099)
	t = 2.330
	p = 0.048
	F = 5.429
Constant	6.697*** (6.477, 6.916)
	t = 59.842
	p = 0.000
Observations	11
R^2	0.420
Adjusted R^2	0.275
Residual Standard Error	0.186 (df = 8)
F Statistic	2.898 (df = 2; 8) (p = 0.114)
Note:	*p < 0.05; **p < 0.01; ***p < 0.001

Coefficient estimates and their standard errors (in parentheses) are shown for each factor.

Table B.44 Output from a linear model examining log Thymocyte counts cells/g at 1 month across the two temperatures in VT.

	Dependent variable:
	log (Thymocyte counts cells/g)
Time to metamorphosis (days)	-0.001 (-0.008, 0.006)
	t = -0.365
	p = 0.725
	F = 0.133
Treatment (Future)	-2.588 (-4.899, -0.278)
	t = -2.195
	p = 0.059
	F = 4.820
Time to metamorphosis : Treatment (Future)	0.013* (0.002, 0.024)
	t = 2.400
	p = 0.043
	F = 5.761
Constant	4.983*** (3.314, 6.652)
	t = 5.853
	p = 0.0004
Observations	12
R^2	0.497
Adjusted R^2	0.308
Residual Standard Error	0.372 (df = 8)
F Statistic	2.635 (df = 3; 8) (p = 0.122)
Note:	*p<0.05; **p<0.01; ***p<0.001

Coefficient estimates and their standard errors (in parentheses) are shown for each factor.

Table B.45 Output from a linear model examining log Thymocyte counts cells/g at 2 months across the two temperatures in VT.

	Dependent variable:
	log (Thymocyte counts cells/g)
Treatment (Future)	0.403 (-0.064, 0.870)
	t = 1.693
	p = 0.119
	F = 2.867
Mass at metamorphosis (g)	0.617* (0.199, 1.035)
	t = 2.893
	p = 0.015
	F = 8.369
Constant	3.806*** (2.825, 4.786)
	t = 7.607
	p = 0.00002
Observations	14
R^2	0.432
Adjusted R^2	0.329
Residual Standard Error	0.343 (df = 11)
F Statistic	4.185* (df = 2; 11) (p = 0.045)
Note:	*p<0.05; **p<0.01; ***p<0.001

Coefficient estimates and their standard errors (in parentheses) are shown for each factor.

Table B.46 Output from a linear model examining log Thymocyte counts cells/g at 1 month across the two temperatures in PA.

	Dependent variable:
	log (Thymocyte counts cells/g)
Time to metamorphosis (days)	0.015* (0.003, 0.028)
	t = 2.459
	p = 0.027
	F = 6.044
Treatment (Future)	0.692 (-0.221, 1.604)
	t = 1.486
	p = 0.158
	F = 2.209
Constant	1.022 (-1.795, 3.839)
	t = 0.711
	p = 0.488
Observations	18
R^2	0.491
Adjusted R^2	0.424
Residual Standard Error	0.276 (df = 15)
F Statistic	7.247** (df = 2; 15) (p = 0.007)
Note:	*p<0.05; **p<0.01; ***p<0.001

Coefficient estimates and their standard errors (in parentheses) are shown for each factor.

Table B.47 Output from a linear model examining log Thymocyte counts cells/g at 2 months across the two temperatures in PA.

	Dependent variable:
	log (Thymocyte counts cells/g)
Treatment (Future)	0.260** (0.102, 0.418)
	t = 3.230
	p = 0.004
	F = 10.435
Constant	4.200*** (4.083, 4.316)
	t = 70.616
	p = 0.000
Observations	22
R^2	0.343
Adjusted R^2	0.310
Residual Standard Error	0.188 (df = 20)
F Statistic	10.435** (df = 1; 20) (p = 0.005)
Note:	*p<0.05; **p<0.01; ***p<0.001

Coefficient estimates and their standard errors (in parentheses) are shown for each factor.

Table B.48 Output from a linear model examining log Thymocyte counts cells/g at 1 month across the two temperatures in LA.

	Dependent variable:
	Log (Thymocyte counts cells/g)
Treatment (Future)	0.313 (0.003, 0.623)
	t = 1.980
	p = 0.060
	F = 3.920
Growth rate (g/day)	50.041** (21.306, 78.775)
	t = 3.413
	p = 0.002
	F = 11.650
Constant	4.796*** (4.573, 5.019)
	t = 42.203
	p = 0.000
Observations	25
R^2	0.380
Adjusted R^2	0.324
Residual Standard Error	0.385 (df = 22)
F Statistic	6.752** (df = 2; 22) (p = 0.006)
Note:	*p<0.05; **p<0.01; ***p<0.001

Coefficient estimates and their standard errors (in parentheses) are shown for each factor.

Table B.49 Output from a linear model examining log Thymocyte counts cells/g at 2 months across the two temperatures in LA.

	Dependent variable:
	Log (Thymocyte counts cells/g)
Mass at metamorphosis (g)	0.756* (0.205, 1.307)
	t = 2.689
	p = 0.021
	F = 7.232
Treatment (Future)	0.487** (0.255, 0.719)
	t = 4.117
	p = 0.002
	F = 16.951
Constant	4.239*** (3.750, 4.729)
	t = 16.986
	p = 0.000
Observations	14
R^2	0.754
Adjusted R^2	0.709
Residual Standard Error	0.191 (df = 11)
F Statistic	16.867*** (df = 2; 11) (p = 0.0005)
Note:	*p<0.05; **p<0.01; ***p<0.001

Coefficient estimates and their standard errors (in parentheses) are shown for each factor.

Table B.50 Output from a linear model examining log Splenocyte count (cells/g) at 1 month across the two temperatures in VT.

	Dependent variable:
	Log (Splenocyte counts cells/g (1 month))
Treatment (Future)	-3.991 (-8.148, 0.166)
	t = -1.882
	p = 0.097
	F = 3.541
Time to metamorphosis (days)	0.004 (-0.009, 0.016)
	t = 0.585
	p = 0.575
	F = 0.343
Treatment (Future) : Time to metamorphosis	0.022 (0.003, 0.042)
	t = 2.209
	p = 0.059
	F = 4.8818
Constant	9.275*** (6.273, 12.277)
	t = 6.055
	p = 0.0004
Observations	12
R^2	0.585
Adjusted R^2	0.429
Residual Standard Error	0.670 (df = 8)
F Statistic	3.752 (df = 3; 8) (p = 0.060)
Note:	*p<0.05; **p<0.01; ***p<0.001

Coefficient estimates and their standard errors (in parentheses) are shown for each factor.

Table B.51 Output from a linear model examining log Splenocyte count (cells/g) at 2 months across the two temperatures in VT.

	Dependent variable:
	Log (Splenocyte counts cells/g (2 months))
Treatment (Future)	0.221 (-0.435, 0.878)
	t = 0.660
	p = 0.522
	F = 0.436
Constant	10.198*** (9.671, 10.724)
	t = 37.962
	p = 0.000
Observations	14
R^2	0.035
Adjusted R^2	-0.045
Residual Standard Error	0.601 (df = 12)
F Statistic	0.436 (df = 1; 12) (p = 0.522)
Note:	*p<0.05; **p<0.01; ***p<0.001

Coefficient estimates and their standard errors (in parentheses) are shown for each factor.

Table B.52 Output from a linear model examining log Splenocyte count (cells/g) at 1 month across the two temperatures in PA.

	Dependent variable:
	Log (Splenocyte counts cells/g (1 month))
Treatment (Future)	-0.775 (-1.718, 0.168)
	t = -1.611
	p = 0.128
	F = 2.596
Growth rate (g/days)	63.618** (26.981, 100.256)
	t = 3.403
	p = 0.004
Constant	11.878*** (11.116, 12.641)
	t = 30.547
	p = 0.000
	F = 11.582
Observations	18
R^2	0.458
Adjusted R^2	0.386
Residual Standard Error	0.948 (df = 15)
F Statistic	6.346* (df = 2; 15) (p = 0.011)
Note:	*p<0.05; **p<0.01; ***p<0.001

Coefficient estimates and their standard errors (in parentheses) are shown for each factor.

Table B.53 Output from a linear model examining log Splenocyte count (cells/g) at 2 months across the two temperatures in PA.

	Dependent variable:
	Log (Splenocyte counts cells/g (2 months))
Treatment (Future)	0.656^{**} (0.297, 1.014)
	t = 3.587
	p = 0.002
	F = 12.867
Growth rate (g/days)	55.054^{***} (33.650, 76.459)
	t = 5.041
	p = 0.0001
	F = 25.413
Constant	11.179^{***} (10.770, 11.587)
	t = 53.658
	p = 0.000
Observations	22
R^2	0.647
Adjusted R^2	0.610
Residual Standard Error	0.425 (df = 19)
F Statistic	17.424^{***} (df = 2; 19) (p = 0.0001)
Note:	*p<0.05; **p<0.01; ***p<0.001

Coefficient estimates and their standard errors (in parentheses) are shown for each factor.

Table B.54 Output from a linear model examining log Splenocyte count (cells/g) at 1 month across the two temperatures in LA.

	Dependent variable:
	Log (Splenocyte count (cells/g) (1 month))
Treatment (Future)	0.166 (-0.493, 0.825)
	t = 0.494
	p = 0.627
	F = 0.244
Growth (g/day)	69.234* (8.811, 129.658)
	t = 2.246
	p = 0.035
	F = 5.043
Constant	9.153*** (8.696, 9.609)
	t = 39.288
	p = 0.000
Observations	26
R^2	0.181
Adjusted R^2	0.110
Residual Standard Error	0.838 (df = 23)
F Statistic	2.537 (df = 2; 23) (p = 0.101)
Note:	*p<0.05; **p<0.01; ***p<0.001

Coefficient estimates and their standard errors (in parentheses) are shown for each factor.

Table B.55 Output from a linear model examining log Splenocyte count (cells/g) at 2 months across the two temperatures in LA.

	Dependent variable:
	Log (Splenocyte counts cells/g (2 months))
Treatment (Future)	0.477 (-0.692, 1.646)
	t = 0.800
	p = 0.439
	F = 0.640
Constant	8.679*** (7.691, 9.667)
	t = 17.215
	p = 0.000
Observations	14
R^2	0.051
Adjusted R^2	-0.028
Residual Standard Error	1.008 (df = 12)
F Statistic	0.640 (df = 1; 12) (p = 0.440)
Note:	*p<0.05; **p<0.01; ***p<0.001

Coefficient estimates and their standard errors (in parentheses) are shown for each factor.

Table B.56 Output from a linear model examining log T lymphocyte proliferation proportion at 1 month across the two temperatures in VT.

	Dependent variable:
	Log (T-lymphocyte proliferation)
Treatment (Future)	-5.324 (-11.850, 1.203)
	t = -1.599
	p = 0.149
	F = 2.556
Time to metamorphosis	-0.002 (-0.021, 0.018)
	t = -0.171
	p = 0.869
	F = 0.029
Treatment (Future) : Time to metamorphosis	0.030 (-0.001, 0.061)
	t = 1.920
	p = 0.092
	F = 3.6865
Constant	2.097 (-2.616, 6.811)
	t = 0.872
	p = 0.409
Observations	12
R^2	0.414
Adjusted R^2	0.195
Residual Standard Error	1.052 (df = 8)
F Statistic	1.887 (df = 3; 8) (p = 0.211)
Note:	*p<0.05; **p<0.01; ***p<0.001

Coefficient estimates and their standard errors (in parentheses) are shown for each factor.

Table B.57 Output from a linear model examining log T lymphocyte proliferation proportion at 1 month across the two temperatures in PA.

	Dependent variable:
	Log (T-lymphocyte proliferation)
Treatment (Future)	2.412 (-1.112, 5.936)
	t = 1.341
	p = 0.200
	F = 1.799
Time to metamorphosis (days)	0.052* (0.005, 0.100)
	t = 2.159
	p = 0.048
	F = 4.663
Constant	-7.559 (-18.441, 3.324)
	t = -1.361
	p = 0.194
Observations	18
R^2	0.413
Adjusted R^2	0.335
Residual Standard Error	1.066 (df = 15)
F Statistic	5.287* (df = 2; 15) (p = 0.019)
Note:	*p<0.05; **p<0.01; ***p<0.001

Coefficient estimates and their standard errors (in parentheses) are shown for each factor.

Table B.58 Output from a linear model examining log T lymphocyte proliferation proportion at 1 month across the two temperatures in LA.

	Dependent variable:
	Log (T-lymphocyte proliferation)
Treatment (Future)	-0.231 (-1.170, 0.709)
	t = -0.481
	p = 0.640
	F = 0.231
Mass at metamorphosis (g)	-2.219* (-4.127, -0.310)
	t = -2.278
	p = 0.042
	F = 5.191
Constant	4.117** (2.178, 6.056)
	t = 4.161
	p = 0.002
Observations	15
R^2	0.302
Adjusted R^2	0.186
Residual Standard Error	0.907 (df = 12)
F Statistic	2.596 (df = 2; 12) (p = 0.116)
Note:	*p<0.05; **p<0.01; ***p<0.001

Coefficient estimates and their standard errors (in parentheses) are shown for each factor.

Table B.59 Output from a linear model examining log B lymphocyte proliferation proportion at 2 months across the two temperatures in VT.

	Dependent variable:
	Log (B-lymphocyte proliferation)
Treatment (Future)	0.608* (0.119, 1.097)
	t = 2.437
	p = 0.033
	F = 5.941
Mass at metamorphosis	0.499* (0.061, 0.937)
	t = 2.235
	p = 0.048
	F = 4.995
Constant	-1.017 (-2.045, 0.011)
	t = -1.938
	p = 0.079
Observations	14
R^2	0.385
Adjusted R^2	0.273
Residual Standard Error	0.359 (df = 11)
F Statistic	3.446 (df = 2; 11) (p = 0.069)
Note:	*p<0.05; **p<0.01; ***p<0.001

Coefficient estimates and their standard errors (in parentheses) are shown for each factor.

Table B.60 Output from a linear model examining log B lymphocyte proliferation proportion at 2 months across the two temperatures in PA.

	Dependent variable:
	Log (B-lymphocyte proliferation)
Treatment (Future)	0.173 (-0.219, 0.565)
	t = 0.864
	p = 0.399
	F = 0.746
Constant	0.210 (-0.080, 0.499)
	t = 1.420
	p = 0.171
Observations	22
R^2	0.036
Adjusted R^2	-0.012
Residual Standard Error	0.467 (df = 20)
F Statistic	0.746 (df = 1; 20) (p = 0.399)
Note:	*p<0.05; **p<0.01; ***p<0.001

Coefficient estimates and their standard errors (in parentheses) are shown for each factor.

Table B.61 Output from a linear model examining log B lymphocyte proliferation proportion at 2 months across the two temperatures in LA.

	Dependent variable:
	Log (B-lymphocyte proliferation)
Treatment (Future)	0.098 (-0.558, 0.753)
	t = 0.292
	p = 0.775
	F = 0.085
Growth rate (g/day)	171.748** (87.205, 256.292)
	t = 3.982
	p = 0.002
	F = 15.853
Treatment (Future) : Growth rate	-197.624** (-298.078, -97.169)
	t = -3.856
	p = 0.002
	F = 14.867
Constant	0.179 (-0.232, 0.590)
	t = 0.853
	p = 0.407
Observations	19
R^2	0.637
Adjusted R^2	0.564
Residual Standard Error	0.467 (df = 15)
F Statistic	8.762** (df = 3; 15) (p = 0.002)
Note:	*p<0.05; **p<0.01; ***p<0.001

Coefficient estimates and their standard errors (in parentheses) are shown for each factor.

Table B.62 Linear mixed model of Bd infection load with temperature treatment, time post exposure as fixed effects and their interaction for LA.

	Dependent variable:
	Bd infection intensity in LA
Treatment (Future)	
	Estimate = -0.676
	Std = 0.505
	z = -1.338
	p = 0.181
	χ^2= 1.790
Week	
	Estimate= 0.079
	Std = 0.057
	Z = 1.375
	p = 0.169
	χ^2= 1.891
Treatment (Future) : Week	
	Estimate= 0.079
	Std= 0.088
	z = 0.898
	p = 0.369
	χ^2= 0.807
Note:	*p<0.05; **p<0.01; ***p<0.001

Coefficient estimates and their standard errors (in parentheses) are shown for each factor.

Table B.63 Generalized linear mixed model with a binomial distribution of the probability of Bd infection across the two temperatures by week in LA.

	Dependent variable:
	Change *Bd* probability of infection post *Bd* exposure in LA
Treatment (Future)	-1.155 (-3.061, 0.752)
	t = -1.187
	p = 0.235
	χ^2 = 1.409
Week	0.266** (0.085, 0.447)
	t = 2.876
	p = 0.004
	χ^2 = 8.272
Treatment (Future) : Week	0.170 (-0.097, 0.437)
	t = 1.250
	p = 0.211
	χ^2 =1.562
Constant	-2.805*** (-4.251, -1.360)
	t = -3.804
	p = 0.0002
Observations	303
Log Likelihood	-143.292
Akaike Information Criterion	296.583
Bayesian Information Criterion	315.152
Note:	*p<0.05; **p<0.01; ***p<0.001

Coefficient estimates and their standard errors (in parentheses) are shown for each factor.

Table B.64 Linear mixed model of Bd infection load with temperature treatment, days post exposure as fixed effects and their interaction for PA.

	Dependent variable:
	Bd infection intensity in PA
Treatment (Future)	
	Estimate = -2.061
	Std = 0.494
	z = -4.169
	p = 3.06×10^{-5} ***
	χ^2 = 17.383
Week	
	Estimate = -0.256
	Std = 0.059
	Z = -4.318
	p = 1.57×10^{-5} ***
	χ^2= 18.645
Treatment (Future) : Week	
	Estimate= 0.302
	Std= 0.088
	z = 3.416
	p = 0.636×10^{-3} ***
	χ^2= 11.666
Constant	
	t = -3 .804
	p = 0.0002
Note:	*p<0.05; **p<0.01; ***p<0.001

Coefficient estimates and their standard errors (in parentheses) are shown for each factor.

Table B. 65 Generalized linear mixed model with a binomial distribution of the probability of Bd infection across the two temperatures by week in PA.

	Dependent variable:
	Change in probability of infection post *Bd* exposure
Treatment (Future)	-3.218* (-6.305, -0.130)
	t = -2.043
	p = 0.041
	χ^2=4.172
Week	-0.121 (-0.587, 0.345)
	t = -0.510
	p = 0.610
	χ^2 = 0.260
Treatment (Future) : Week	0.392 (-0.162, 0.945)
	t = 1.386
	p = 0.166
	χ^2 = 1.922
Constant	3.252* (0.513, 5.991)
	t = 2.327
	p = 0.020
Observations	119
Log Likelihood	-44.146
Akaike Information Criterion	98.291
Bayesian Information Criterion	112.187
Note:	*p<0.05; **p<0.01; ***p<0.001

Coefficient estimates and their standard errors (in parentheses) are shown for each factor.

Table B.66 Linear mixed model of Bd infection load with temperature treatment, days post exposure as fixed effects and their interaction for VT.

	Dependent variable:
	Bd infection intensity in VT
Treatment (Future)	
	Estimate= 0.669
	Std = 0.653
	z = 1.026
	p = 0.305
	χ^2= 0.031
Week	
	Estimate= 8.32 x10^{-3}
	Std = 0.013
	z= 0.642
	p = 0.521
	χ^2 = 0.055
Treatment (Future) : Week	
	Estimate= -0.018
	Std= 0.017
	z = -1.049
	p = 0.294
	χ^2= 1.100
Constant	
	t = -3.804
	p = 0.0002
Note:	*p<0.05; **p<0.01; ***p<0.001

Coefficient estimates and their standard errors (in parentheses) are shown for each factor.

Table B.67 Generalized linear mixed model with a binomial distribution of the probability of Bd infection across the two temperatures by week in VT.

	Dependent variable:
	Change in probability of infection post *Bd* exposure
Treatment (Future)	-17.066 (-765.683, 731.551)
	t = -0.045
	p = 0.964
	χ^2= 0.002
Week	-0.015 (-0.497, 0.467)
	t = -0.061
	p = 0.951
	χ^2= 0.003
Treatment (Future) : Week	7.873 (-366.435, 382.182)
	t = 0.041
	p = 0.967
	χ^2=0.002
Constant	2.546 (-0.435, 5.527)
	t = 1.674
	p = 0.095
Observations	94
Log Likelihood	-21.466
Akaike Information Criterion	52.931
Bayesian Information Criterion	65.648
Note:	*p<0.05; **p<0.01; ***p<0.001

Coefficient estimates and their standard errors (in parentheses) are shown for each factor.

Table B.68 Linear mixed model of Body condition (measured as log (scaled mass index), or log SMI) in VT and the interaction between Bd exposure and time of exposure.

	Dependent variable:
	Change in SMI post *Bd* exposure
Treatment (Future)	-0.029 (-0.127, 0.069)
	t = -0.579
	p = 0.568
	$\chi^2 = 0.3475$
Week	-0.009 (-0.022, 0.003)
	t = -1.449
	p = 0.151
	$\chi^2 = 2.1760$
Treatment (Future) : Week	0.011 (-0.005, 0.028)
	t = 1.363
	p = 0.176
	$\chi^2 = 1.9239$
Constant	0.574^{***} (0.498, 0.650)
	t = 14.834
	p = 0.000
Observations	116
Log Likelihood	67.676
Akaike Information Criterion	-123.351
Bayesian Information Criterion	-106.830
Note:	*p<0.05; **p<0.01; ***p<0.001

Coefficient estimates and their standard errors (in parentheses) are shown for each factor.

Table B.69 Linear mixed model of Body condition (measured as log (scaled mass index), or log SMI) in PA and the interaction between Bd exposure and time of exposure.

	Dependent variable:
	Change in SMI post *Bd* exposure
Treatment (Future)	0.133^{***} (0.073, 0.192)
	t = 4.348
	p = 0.0002
	$\chi^2 = 19.4301$
Week	0.007 (-0.001, 0.015)
	t = 1.641
	p = 0.103
	$\chi^2 = 2.7695$
Treatment (Future) : Week	-0.007 (-0.019, 0.004)
	t = -1.239
	p = 0.218
	$\chi^2 = 1.5771$
Constant	0.830^{***} (0.787, 0.872)
	t = 38.369
	p = 0.000
Observations	147
Log Likelihood	125.015
Akaike Information Criterion	-238.030
Bayesian Information Criterion	-220.087
Note:	*p<0.05; **p<0.01; ***p<0.001

Coefficient estimates and their standard errors (in parentheses) are shown for each factor.

Table B.70 Linear mixed model of Body condition (measured as log (scaled mass index), or log SMI) in LA and the interaction between Bd exposure and time of exposure.

	Dependent variable:
	Change in SMI post *Bd* exposure
Treatment (Future)	-0.158** (-0.245, -0.071)
	t = -3.573
	p = 0.001
	χ^2 = 13.105
Week	-0.010** (-0.016, -0.003)
	t = -3.023
	p = 0.003
	χ^2 = 9.3812
Treatment (Future) : Week	-0.0004 (-0.009, 0.009)
	t = -0.080
	p = 0.936
	χ^2 = 0.007
Constant	1.436*** (1.374, 1.497)
	t = 45.875
	p = 0.000
Observations	156
Log Likelihood	137.531
Akaike Information Criterion	-263.062
Bayesian Information Criterion	-244.763
Note:	*p<0.05; **p<0.01; ***p<0.001

Coefficient estimates and their standard errors (in parentheses) are shown for each factor.

Table B.71 Output from a Cox proportional hazards model examining survival across the two temperatures after Bd exposure in VT.

	Loglik	χ^2	Df	p
Null	-27.332			
Temperature	-24.759	5.146	1	0.023*
Note:		*p<0.05; **p<0.01; ***p<0.001		

Table B.72 Output from a Cox proportional hazards model examining survival across the two temperatures after Bd exposure in PA.

	Loglik	χ^2	Df	p
Null	-3.4012			
Temperature	-2.7081	1.3863	1	0.239
Note:		*p<0.05; **p<0.01; ***p<0.001		

Table B.73 Output from a Cox proportional hazards model examining survival across the two temperatures after Bd exposure in LA.

	Loglik	χ^2	Df	p
Null	-28.772			
Temperature	-28.700	0.1443	1	0.7041
Note:		*p<0.05; **p<0.01; ***p<0.001		

Table B.74 Output from a linear model examining log Splenocyte count (cells/g) after exposure across the two temperatures in VT.

	Dependent variable:
	Splenocyte counts/g
Exposure Group (Exposed)	-0.007 (-0.202, 0.188)
	t = -0.075
	p = 0.942
	F = 0.006
Temperature Treatment	0.282** (0.105, 0.458)
	t = 3.128
	p = 0.004
	F = 9.787
Growth rate (g/day)	-11.670* (-21.361, -1.978)
	t = -2.360
	p = 0.025
	F = 5.569
Exposure Group: Temperature Treatment	-0.198 (-0.468, 0.072)
	t = -1.436
	p = 0.162
	F = 2.063
Constant	3.768*** (3.602, 3.934)
	t = 44.440
	p = 0.000
Observations	35
R^2	0.494
Adjusted R^2	0.426
Residual Std. Error	0.187 (df = 30)
F Statistic	7.317*** (df = 4; 30) (p = 0.0004)
Note:	*p**p***p<0.001

Coefficient estimates and their standard errors (in parentheses) are shown for each factor.

Table B.75 Output from a linear model examining log Splenocyte count (cells/g) after exposure across the two temperatures in PA.

	Dependent variable:
	Splenocyte counts/g
Exposure Group (Exposed)	0.014 (-0.137, 0.165)
	t = 0.184
	p = 0.855
	F = 0.034
Temperature Treatment	0.243** (0.095, 0.391)
	t = 3.221
	p = 0.003
	F = 10.374
Exposure Group: Temperature Treatment	-0.122 (-0.340, 0.096)
	t = -1.095
	p = 0.280
	F = 1.199
Constant	3.604*** (3.499, 3.708)
	t = 67.555
	p = 0.000
Observations	52
R^2	0.219
Adjusted R^2	0.170
Residual Std. Error	0.200 (df = 48)
F Statistic	4.480** (df = 3; 48) (p = 0.008)
Note:	*p**p***p<0.001

Coefficient estimates and their standard errors (in parentheses) are shown for each factor.

Table B.76 Output from a linear model examining log Splenocyte count (cells/g) after exposure across the two temperatures in LA.

	Dependent variable:
	Splenocyte counts/g
Exposure Group (Exposed)	-0.139 (-0.512, 0.234)
	t = -0.730
	p = 0.470
	F = 0.533
Temperature Treatment	0.444* (0.117, 0.772)
	t = 2.658
	p = 0.012
	F = 7.065
Mass at metamorphosis (g)	-0.226* (-0.397, -0.054)
	t = -2.574
	p = 0.015
	F = 6.623
Exposure Group: Temperature Treatment	-0.145 (-0.726, 0.435)
	t = -0.491
	p = 0.627
	F = 0.241
Exposure Group : Mass at metamorphosis	0.171 (-0.207, 0.550)
	t = 0.887
	p = 0.382
	F = 0.786
Temperature Treatment : Mass at metamorphosis	-0.391** (-0.671, -0.111)
	t = -2.739
	p = 0.010
	F = 7.501
Exposure Group : Temperature Treatment : Mass at metamorphosis	0.099 (-0.498, 0.696)
	t = 0.325
	p = 0.748
	F = 0.106
Constant	3.310*** (3.110, 3.510)
	t = 32.452
	p = 0.000
Observations	43

R^2	0.550
Adjusted R^2	0.460
Residual Std. Error	0.147 (df = 35)
F Statistic	6.112^{***} (df = 7; 35) (p = 0.0002)
Note:	$^{*}p^{**}p^{***}p<0.001$

Coefficient estimates and their standard errors (in parentheses) are shown for each factor.

Table B.77 Output from a linear model examining total mucosal peptides after Bd exposure across exposure groups for VT

	Dependent variable:
	Log (Mucosome inhibition %)
Exposure group (Exposed)	-21.475 (-47.772, 4.821)
	t = -1.601
	p = 0.124
	F = 2.562
Temperature Treatment (Future)	-49.139* (-84.554, -13.723)
	t = -2.719
	p = 0.013
	F = 7.395
Mass at metamorphosis (g)	-3.846 (-26.706, 19.014)
	t = -0.330
	p = 0.745
	F = 0.109
Exposure Group : Temperature Treatment	23.961 (-11.161, 59.083)
	t = 1.337
	p = 0.195
	F = 1.788
Constant	64.403* (5.131, 123.675)
	t = 2.130
	p = 0.046
Observations	26
R^2	0.414
Adjusted R^2	0.303
Residual Standard Error	21.407 (df = 21)
F Statistic	3.712* (df = 4; 21) (p = 0.020)
Note:	*p<0.05; **p<0.01; ***p<0.001

Coefficient estimates and their standard errors (in parentheses) are shown for each factor.

Table B.78 Output from a linear model examining total mucosal peptides after Bd exposure across exposure groups for PA.

	Dependent variable:
	Log (Mucosome inhibition %)
Exposure group (Exposed)	-27.064* (-47.063, -7.064)
	t = -2.652
	p = 0.014
	F = 7.035
Temperature Treatment (Future)	-43.512*** (-61.755, -25.268)
	t = -4.675
	p = 0.0001
	F = 21.852
Mass at metamorphosis (g)	-25.861** (-42.032, -9.690)
	t = -3.134
	p = 0.005
	F = 9.824
Exposure Group : Temperature Treatment	37.905** (12.013, 63.798)
	t = 2.869
	p = 0.009
	F = 8.233
Constant	114.259*** (72.934, 155.585)
	t = 5.419
	p = 0.00002
Observations	28
R^2	0.512
Adjusted R^2	0.427
Residual Standard Error	16.658 (df = 23)
F Statistic	6.032** (df = 4; 23) (p = 0.002)
Note:	*p<0.05; **p<0.01; ***p<0.001

Coefficient estimates and their standard errors (in parentheses) are shown for each factor.

Table B.79 Output from a linear model examining total mucosal peptides after Bd exposure across exposure groups for LA.

	Dependent variable:
	Log (Mucosome inhibition %)
Exposure group (Exposed)	3.251 (-8.654, 15.155)
	t = 0.535
	p = 0.598
	F = 0.287
Temperature Treatment (Future)	14.502* (1.798, 27.206)
	t = 2.237
	p = 0.036
	F = 5.006
Mass at metamorphosis (g)	-348.389 (-954.128, 257.349)
	t = -1.127
	p = 0.271
	F = 1.271
Exposure Group : Temperature Treatment	-12.371 (-29.645, 4.904)
	t = -1.404
	p = 0.174
	F = 1.970
Constant	13.960* (4.045, 23.875)
	t = 2.760
	p = 0.012
Observations	28
R^2	0.202
Adjusted R^2	0.064
Residual Standard Error	11.599 (df = 23)
F Statistic	1.458 (df = 4; 23) (p = 0.248)
Note:	*p<0.05; **p<0.01; ***p<0.001

Coefficient estimates and their standard errors (in parentheses) are shown for each factor.


Vermont
Legend
Distance
4.25 Km
VT weather station
VT pond
Google Earth
5000 ft

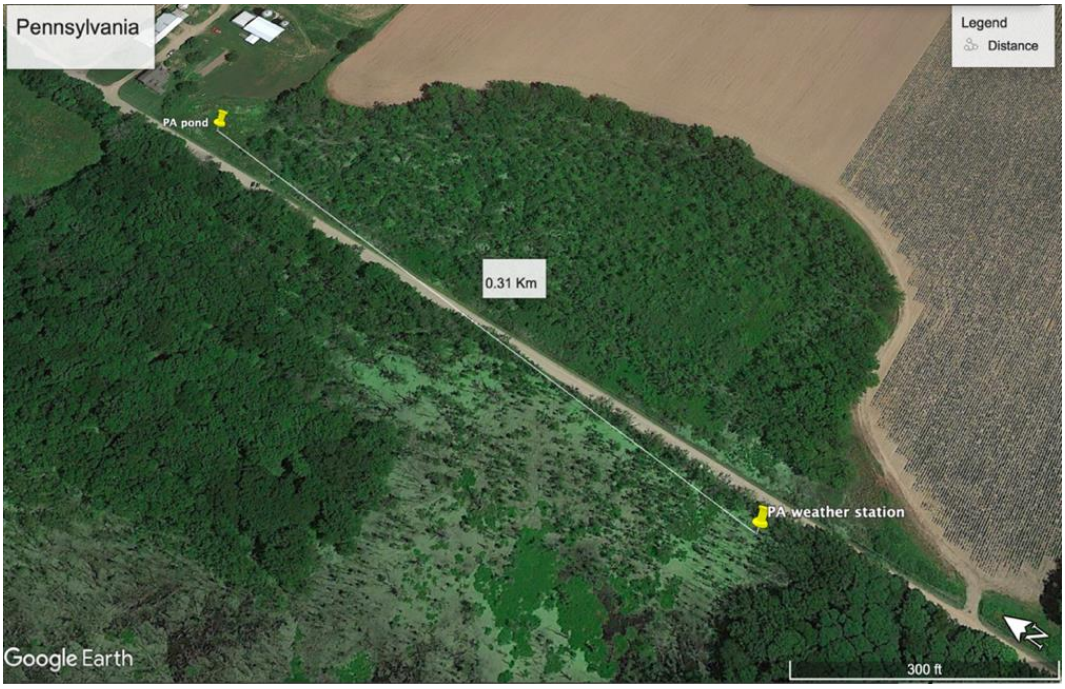
Pennsylvania
Legend
Distance
PA pond
0.31 Km
PA weather station
Google Earth
300 ft

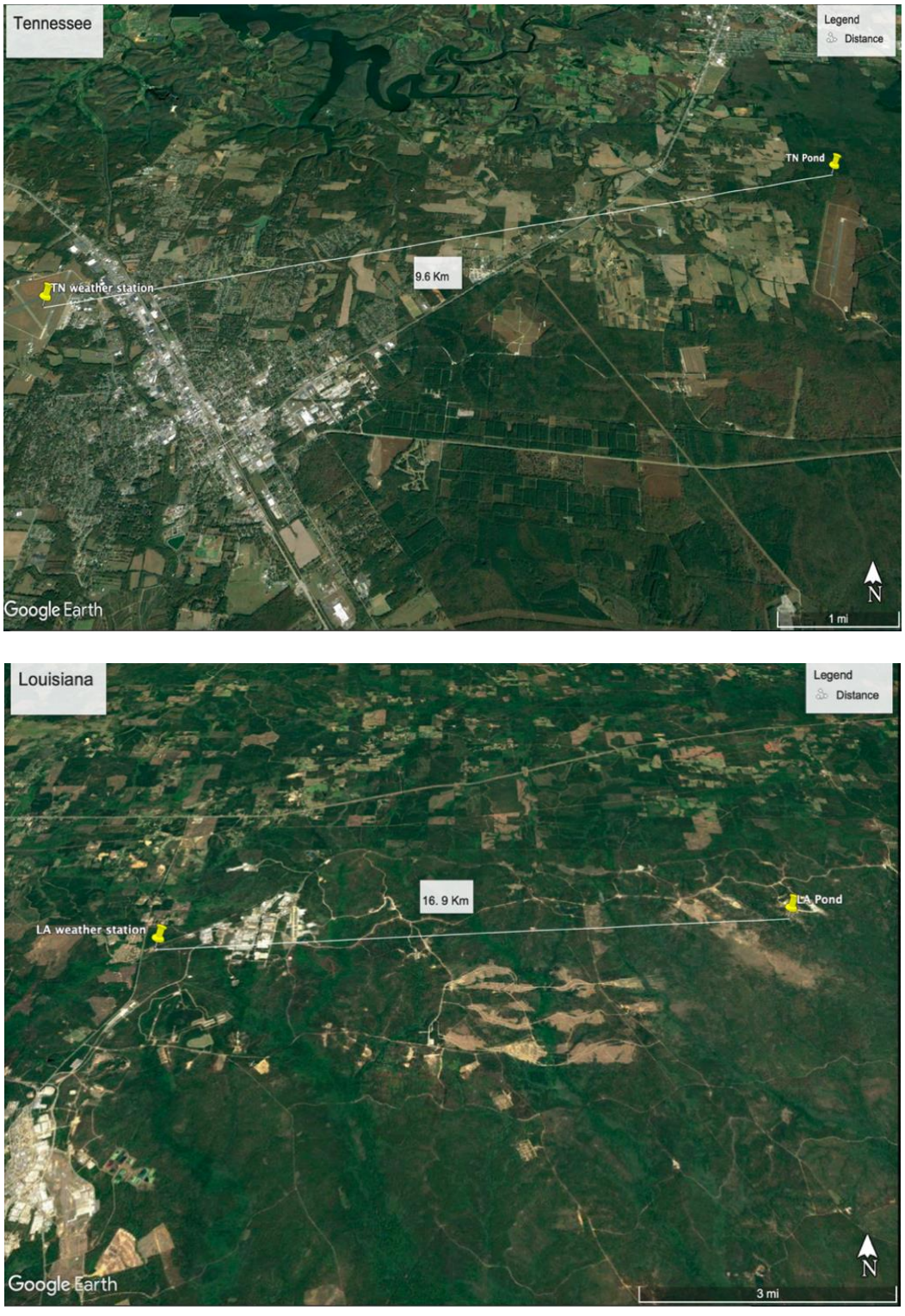

Figure B.1 Distance between each pond where the egg masses were collected, and the weather station used to collect the temperatures for the experiment.

Appendix C

Table C.1 Output from a generalized linear mixed model with a binomial distribution of the probability of Bd infection (yes/no) with pond type (ephemeral vs. permanent), pH and animal body temperature as factors.

	Dependent variable:
	Bd Infection
Pond Type (Ephemeral vs. Permanent)	-0.072 (-1.563, 1.419)
	t = -0.095
	p = 0.925
Pond pH	0.004 (-0.094, 0.101)
	t = 0.071
	p = 0.944
Animal Body Temperature	-0.075*** (-0.102, -0.048)
	t = -5.497
	p < 0.001
Pond Type : pH	0.017 (-0.148, 0.182)
	t = 0.203
	p = 0.839
Pond Type : Animal Body Temperature	-0.014 (-0.046, 0.018)
	t = -0.857
	p = 0.392
Constant	0.082 (-1.071, 1.235)
	t = 0.140
	p = 0.889
Observations	5176
Log Likelihood	-2015.081
Akaike Information Criterion	4046.162
Bayesian Information Criterion	4095.212
Note:	*p < 0.05; **p < 0.01; ***p < 0.001

Coefficient estimates and their standard errors (in parentheses) are shown for each factor.

Table C.2 Output from a linear mixed model of Bd load with pond type (ephemeral vs. permanent), pH and animal body temperature as factors.

	Dependent variable:
	Bd load in log (DNA copies + 1)
Pond Type (Ephemeral vs. Permanent)	-89.491 (-423.975, 244.994)
	t = -0.524
	p = 0.600
Pond pH	-16.280 (-37.111, 4.551)
	t = -1.532
	p = 0.126
Animal Body Temperature	-21.068*** (-26.644, -15.491)
	t = -7.404
	p < 0.001
Pond Type : pH	33.972 (-2.100, 70.045)
	t = 1.846
	p = 0.065
Pond Type : Animal Body Temperature	-10.018** (-16.982, -3.054)
	t = -2.820
	p = 0.005
Constant	675.873*** (413.949, 937.796)
	t = 5.058
	p < 0.001
Observations	5098
Log Likelihood	-25868.150
Akaike Information Criterion	51754.300
Bayesian Information Criterion	51809.480
Note:	*p < 0.05; **p < 0.01; ***p < 0.001

Coefficient estimates and their standard errors (in parentheses) are shown for each factor.

Table C.3 Output from a linear mixed model of Bd load on infected animals across the two hibernation types (permanent pond vs. terrestrial) in the two fenced ponds.

	Dependent variable:
	Bd load in log (DNA copies + 1)
Hibernation Type (pond vs. soil)	-1.674* (-2.863, -0.485)
	t = -2.760
	p = 0.028
Pond (Wood Lab vs. Sanctuary Lake)	-0.368 (-0.908, 0.173)
	t = -1.334
	p = 0.185
Hibernation Type : Pond	0.417 (-0.249, 1.083)
	t = 1.228
	p = 0.222
Constant	4.245*** (3.373, 5.116)
	t = 9.550
	p < 0.001
Observations	112
Log Likelihood	-201.944
Akaike Information Criterion	415.888
Bayesian Information Criterion	431.981
Note:	*p < 0.05; **p < 0.01; ***p < 0.001

Coefficient estimates and their standard errors (in parentheses) are shown for each factor.

Table C.4 Output from a generalized linear mixed model with a binomial distribution of the probability of Bd infection (yes/no) across the two hibernation types in the two ponds.

	Dependent variable:
	Bd infection
Hibernation Type (pond vs. soil)	-3.522*** (-4.657, -2.388)
	t = -6.084
	p < 0.001
Pond (Wood Lab vs. Sanctuary Lake)	-0.949*** (-1.439, -0.459)
	t = -3.794
	p < 0.001
Hibernation Type : Pond	1.132*** (0.555, 1.708)
	t = 3.848
	p < 0.001
Constant	2.047*** (1.086, 3.008)
	t = 4.176
	p < 0.001
Observations	338
Log Likelihood	-187.078
Akaike Information Criterion	384.156
Bayesian Information Criterion	403.256
Note:	*p < 0.05; **p < 0.01; ***p < 0.001

Coefficient estimates and their standard errors (in parentheses) are shown for each factor.

Table C.5 Output from a linear mixed model comparing Bd infection load on leopard frogs (Rana pipiens) that metamorphosed in the Sanctuary Lake pond to all other amphibians captured leaving the pond.

	Dependent variable:
	Bd load in log (DNA copies + 1)
Species (*Rana pipiens* vs. all other)	-0.360 (-1.295, 0.574)
	t = -0.755
	p = 0.458
Constant	2.569*** (2.111, 3.027)
	t = 10.996
	p < 0.001
Observations	25
R^2	0.024
Adjusted R^2	-0.018
Residual Standard Error	1.018 (df = 23)
Note:	*p < 0.05; **p < 0.01; ***p < 0.001

Coefficient estimates and their standard errors (in parentheses) are shown for each factor.

Table C.6 Output from a generalized linear mixed model with a binomial distribution comparing the probability of Bd infection on leopard frogs (Rana pipiens) that metamorphosed in the Sanctuary Lake pond to all other amphibians captured leaving the pond.

	Dependent variable:
	Bd infection
Species (*Rana pipiens* vs. all other)	18.148 (-3147.397, 3183.693)
	t = 0.011
	p = 0.991
Constant	-0.582* (-1.143, -0.021)
	t = -2.032
	p = 0.043
Observations	59
Log Likelihood	-34.585
Akaike Information Criterion	73.170
Residual Deviance	69.170 (df = 57)
Null Deviance	80.413 (df = 58)
Note:	*p < 0.05; **p < 0.01; ***p < 0.001

Coefficient estimates and their standard errors (in parentheses) are shown for each factor.

Table C.7 Output from a linear mixed model comparing Bd infection load on the spotted salamanders (Ambystoma maculatum) that metamorphosed in the Wood Lab pond to all other amphibians captured leaving the pond.

	Dependent variable:
	Bd load in log (DNA copies + 1)
Species (*Ambystoma maculatum* vs. all other)	1.655 (-0.195, 3.504)
	t = 1.753
	p = 0.097
Constant	2.223* (0.468, 3.978)
	t = 2.483
	p = 0.024
Observations	20
R^2	0.146
Adjusted R^2	0.098
Residual Standard Error	1.266 (df = 18)
Note:	*p < 0.05; **p < 0.01; ***p < 0.001

Coefficient estimates and their standard errors (in parentheses) are shown for each factor.

Table C.8 Generalized linear mixed model comparing the probability of Bd infection for the spotted salamanders (Ambystoma maculatum) that metamorphosed in the Wood Lab pond to all other amphibians captured leaving the pond.

	Dependent variable:
	Bd infection
Metamorphosis	2.890** (1.000, 4.781)
	t = 2.996
	p = 0.003
Constant	-1.386 (-2.936, 0.163)
	t = -1.754
	p = 0.080
Observations	32
Log Likelihood	-15.435
Akaike Information Criterion	34.870
Residual Deviance	30.870 (df = 30)
Null Deviance	42.340 (df = 31)
Note:	*p < 0.05; **p < 0.01; ***p < 0.001

Coefficient estimates and their standard errors (in parentheses) are shown for each factor.

Table C.9 Output from a linear mixed model comparing Bd infection load on the wood frogs (Rana sylvatica) that metamorphosed in the Wood Lab pond to all other amphibians captured leaving the pond.

	Dependent variable:
	Bd load in log (DNA copies + 1)
Species (*Rana sylvatica* vs. all other)	1.404^{***} (0.690, 2.118)
	t = 3.852
	p < 0.001
Constant	2.418^{***} (1.971, 2.865)
	t = 10.606
	p < 0.001
Observations	46
R^2	0.252
Adjusted R^2	0.235
Residual Standard Error	1.206 (df = 44)
Note:	*p < 0.05; **p < 0.01; ***p < 0.001

Coefficient estimates and their standard errors (in parentheses) are shown for each factor.

Table C.10 Output from a generalized linear mixed model with a binomial distribution of the probability comparing Bd infection on the wood frogs (Rana sylvatica) that metamorphosed in the Wood Lab pond to all other amphibians captured leaving the pond.

	Dependent variable:
	Bd infection
Species (*Rana sylvatica* vs. all other)	2.583^{***} (1.508, 3.659)
	t = 4.709
	p < 0.001
Constant	-1.303^{***} (-1.720, -0.885)
	t = -6.112
	p < 0.001
Observations	154
Log Likelihood	-80.015
Akaike Information Criterion	164.029
Residual Deviance	160.029 (df = 152)
Null Deviance	187.806 (df = 153)
Note:	*p < 0.05; **p < 0.01; ***p < 0.001

Coefficient estimates and their standard errors (in parentheses) are shown for each factor.

Bibliography

Adlard, R. D., & Nolan, M. J. (2015). Elucidating the life cycle of *Marteilia sydneyi*, the aetiological agent of QX disease in the Sydney rock oyster (Saccostrea glomerata). *International Journal for Parasitology*, *45*(6), 419-426.

Altwegg, R. & Reyer, H.U. (2003) Patterns of natural selection on size at metamorphosis in water frogs. *Evolution*, 57, 872–882.

Altizer, S., Ostfeld, R. S., Johnson, P. T., Kutz, S., & Harvell, C. D. (2013). Climate change and infectious diseases: from evidence to a predictive framework. *science*, *341*(6145), 514-519.

Amburgey, S., Funk, W. C., Murphy, M., & Muths, E. (2012). Effects of hydroperiod duration on survival, developmental rate, and size at metamorphosis in boreal chorus frog tadpoles (*Pseudacris maculata*). *Herpetologica*, *68*(4), 456-467.

Angilletta Jr, M. J., & Angilletta, M. J. (2009). Thermal adaptation: a theoretical and empirical synthesis.

Ardia, D. R., Pérez, J. H., & Clotfelter, E. D. (2010). Experimental cooling during incubation leads to reduced innate immunity and body condition in nestling tree swallows. *Proceedings of the Royal Society B: Biological Sciences*, *277*(1689), 1881-1888.

Babbitt K.J. (2005) The relative importance of wetland size and hydroperiod for amphibians in southern New Hampshire, USA. *Wetl Ecol Manag* 13:269–279

Baldwin, W. M., & Cohen, N. (1981). A giant cell with dendritic cell properties in spleens of the anuran amphibian *Xenopus laevis*. *Developmental & Comparative Immunology*, *5*(3), 461-473

Beaudry, A., Fortier, M., Masson, S., Auffret, M., Brousseau, P., & Fournier, M. (2016). Effect of Temperature on Immunocompetence of the Blue Mussel (*Mytilus Edulis*). *Journal of xenobiotics*, *6*(1), 5889

Becker, M. H., Walke, J. B., Murrill, L., Woodhams, D. C., Reinert, L. K., Rollins-Smith, L. A., L.A., Burzynski, E.A., Umile, T.P., Minbiole, K.P. & Belden, L. K. (2015). Phylogenetic distribution of symbiotic bacteria from Panamanian amphibians that inhibit growth of the lethal fungal pathogen *Batrachochytrium dendrobatidis*. *Molecular ecology*, *24*(7), 1628-1641.

Bell, S. C., Alford, R. A., Garland, S., Padilla, G., & Thomas, A. D. (2013). Screening bacterial metabolites for inhibitory effects against *Batrachochytrium dendrobatidis* using a spectrophotometric assay. *Diseases of Aquatic Organisms*, *103*(1), 77-85

Bellouin, N., Collins, W. J., Culverwell, I. D., Halloran, P. R., Hardiman, S. C., Hinton, T. J., Jones, C.D., McDonald, R.E., McLaren, A.J., O'Connor, F.M. and Roberts, M.J. & Wiltshire, A. (2011). The HadGEM2 family of met office unified model climate configurations. *Geoscientific Model Development*, *4*(3), 723-757.

Ben-Haim, Y., M. Zicherman-Keren, & E. Rosenberg. 2003. Temperature-regulated bleaching and lysis of the coral *Pocillopora damicornis* by the novel pathogen *Vibrio coralliilyticus*. *Applied and Environmental Microbiology* 69(7):4,236–4,242.

Benson, D. A., Clark, K., Karsch-Mizrachi, I., Lipman, D. J., Ostell, J., & Sayers, E. W. (2013). GenBank. *Nucleic acids research*, *42*(D1), D32-D37.

Berger, L., Speare, R., Daszak, P., Green, D. E., Cunningham, A. A., Goggin, C. L., Slocombe, R., Ragan, M.A., Hyatt, A.D., McDonald, K.R. and Hines, H.B.& Parkes, H. (1998). Chytridiomycosis causes amphibian mortality associated with population declines in the rain forests of Australia and Central America. *Proceedings of the National Academy of Sciences*, *95*(15), 9031-9036.

Berger, L., Speare, R., & Hyatt, A. (1999). Chytrid fungi and amphibian declines: overview, implications and future directions. *Declines and disappearances of australian frogs. Environment Australia, Canberra*, *1999*, 23-33.

Berger, L., Speare, R., Hines, H.B., Marantelli, G., Hyatt, A.D., McDonald, K.R., Skerratt, L.F., Olsen, V., Clarke, J.M., Gillespie, G. and Mahony, M., (2004). Effect of season and temperature on mortality in amphibians due to chytridiomycosis. *Australian Veterinary Journal*, *82*(7), pp.434-439.

Berven, K. A. (1990). Factors affecting population fluctuations in larval and adult stages of the wood frog (*Rana sylvatica*). *Ecology*, *71*(4), 1599-1608.

Berven, K. A., & Grudzien, T. A. (1990). Dispersal in the wood frog (*Rana sylvatica*): implications for genetic population structure. *Evolution*, *44*(8), 2047-2056.

Boyle DG, Boyle DB, Olsen V, Morgan JA, Hyatt AD (2004) Rapid quantitative detection of chytridiomycosis (*Batrachochytrium dendrobatidis*) in amphibian samples using real-time Taqman PCR assay. *Diseases of Aquatic Organisms* 60: 141–148.

Boyle, D. G., Hyatt, A. D., Daszak, P., Berger, L., Longcore, J. E., Porter, D., Hengstberger, S.G. & Olsen, V. (2003). Cryo-archiving of *Batrachochytrium dendrobatidis* and other chytridiomycetes. *Diseases of aquatic organisms*, *56*(1), 59-64.

Brannelly, L. A., McMahon, T. A., Hinton, M., Lenger, D., & Richards-Zawacki, C. L. (2015). Batrachochytrium dendrobatidis in natural and farmed Louisiana crayfish populations: prevalence and implications. *Diseases of aquatic organisms*, *112*(3), 229-235.

Brannelly, L. A., Ohmer, M. E., Saenz, V., & Richards-Zawacki, C. L. (2019). Effects of hydroperiod on growth, development, survival and immune defences in a temperate amphibian. *Functional Ecology*, *33*(10), 1952-1961.

Bromenshenk, J. J., Henderson, C. B., Wick, C. H., Stanford, M. F., Zulich, A. W., Jabbour, R. E., Deshpande S.V., McCubbin P.E., Seccomb R.A., Welch P.M., Williams T. & Cramer Jr, R. A. (2010). Iridovirus and microsporidian linked to honey bee colony decline. *PloS one*, *5*(10), e13181.

Burge, C.A., C.M. Eakin, C.S. Friedman, B. Froelich, P.K. Hershberger, E.E. Hofmann, L.E. Petes, K.C. Prager, E. Weil, B.L. Willis, and others. 2014. Climate change influences on marine infectious diseases: Implications for management and society. *Annual Review of Marine Science* 6:249–277.

Burn, C. R. (2005). Lake-bottom thermal regimes, western Arctic coast, Canada. *Permafrost and Periglacial Processes*, *16*(4), 355-367.

Bury, R.B. & Adams, M.J. (1999) Variation in age at metamorphosis across a latitudinal gradient for the tailed frog, *Ascaphus truei*. *Herpetologica*, 55, 283–291.

Byrne, A. Q., Rothstein, A. P., Poorten, T. J., Erens, J., Settles, M. L., & Rosenblum, E. B. (2017). Unlocking the story in the swab: A new genotyping assay for the amphibian chytrid fungus *Batrachochytrium dendrobatidis*. *Molecular Ecology Resources*. https://doi.org/10.1111/1755-0998.12675

Byrne, A. Q., Vredenburg, V. T., Martel, A., Pasmans, F., Bell, R. C., Blackburn, D. C., … Rosenblum, E. B. (2019). Cryptic diversity of a widespread global pathogen reveals expanded threats to amphibian conservation. *Proceedings of the National Academy of Sciences*, *116*(41), 20382 LP-20387. https://doi.org/10.1073/pnas.1908289116

Cabrera-Guzmán, E., Crossland, M. R., Brown, G. P., & Shine, R. (2013). Larger body size at metamorphosis enhances survival, growth and performance of young cane toads (*Rhinella marina*). *PloS one*, *8*(7), e70121.

Carey, C., Cohen, N., & Rollins-Smith, L. (1999). Amphibian declines: an immunological perspective. *Developmental & Comparative Immunology*, *23*(6), 459-472.

Casadevall, A. (2005). Fungal virulence, vertebrate endothermy, and dinosaur extinction: is there a connection?. *Fungal Genetics and Biology*, *42*(2), 98-106.

Catenazzi, A., von May, R., & Vredenburg, V. T. (2013). High prevalence of infection in tadpoles increases vulnerability to fungal pathogen in high-Andean amphibians. *Biological Conservation*, *159*, 413-421.

Clopper, C. J. and Pearson, E. S. (1934) 'The use of confidence or fiducial limits illustrated in the case of the binomial', *Biometrika*, 26, 404-41 3.

Cohen, J. M., Civitello, D. J., Venesky, M. D., McMahon, T. A., & Rohr, J. R. (2019). An interaction between climate change and infectious disease drove widespread amphibian declines. *Global change biology*, *25*(3), 927-937.

Colburn, E.A. (2004). Vernal Pools: Natural History and Conservation. McDonald and Woodward Publishing Company, Blacksburg, VA.

Colburn, E. A., Weeks, S. C., & Reed, S. K. (2008). Diversity and ecology of vernal pool invertebrates. *Science and conservation of vernal pools in northeastern North America. CRC Press, Boca Raton*, 105-126.

Collins, M., Knutti, R., Arblaster, J., Dufresne, J. L., Fichefet, T., Friedlingstein, P., P., Gao, X., Gutowski, W.J., Johns, T., Krinner, G. & Shongwe, M. (2013). Long-term climate change: projections, commitments and irreversibility. In *Climate Change 2013-The Physical Science Basis: Contribution of Working Group I to the Fifth Assessment Report of the Intergovernmental Panel on Climate Change* (pp. 1029-1136). Cambridge University Press.

Conover, D. O., & Schultz, E. T. (1995). Phenotypic similarity and the evolutionary significance of countergradient variation. *Trends in Ecology & Evolution*, *10*(6), 248-252.

Cooper, E.L., Wright R.K., Klempau, A.E., Smith, C.T. (1992). Hibernation alters the frog's immune system. Cryobiology 29: 616– 631.

Crespi, E. J., & Warne, R. W. (2013). Environmental conditions experienced during the tadpole stage alter post-metamorphic glucocorticoid response to stress in an amphibian. 989-1001.

Crump, M. L. (1989). Effect of habitat drying on developmental time and size at metamorphosis in *Hyla pseudopuma*. *Copeia*, *1989*(3), 794-797.

Cunningham, A. A., Daszak, P., & Wood, J. L. (2017). One Health, emerging infectious diseases and wildlife: two decades of progress?. *Philosophical Transactions of the Royal Society B: Biological Sciences*, *372*(1725), 20160167.

das Neves-da-Silva, D., Borges-Júnior, V. N. T., Branco, C. W. C., & de Carvalho, A. M. P. T. (2021). Effects of intrinsic and extrinsic factors on the prevalence of the fungus Batrachochytrium dendrobatidis (Chytridiomycota) in stream tadpoles in the Atlantic Forest domain. *Aquatic Ecology*, 1-12.

Daszak, P., Strieby, A., Cunningham, A. A., Longcore, J. E., Brown, C. C., & Porter, D. (2004). Experimental evidence that the bullfrog (*Rana catesbeiana*) is a potential carrier of chytridiomycosis, an emerging fungal disease of amphibians. *Herpetological Journal*, *14*, 201-208.

Demas, G., & Nelson, R. (Eds.). (2012). *Ecoimmunology*. Oxford University Press.

Denver, R. J., Mirhadi, N., & Phillips, M. (1998). Adaptive plasticity in amphibian metamorphosis: Response of *Scaphiopus Hammondii* tadpoles to habitat desiccation. *Ecology, 79*(6), 1859-1872.

Dethloff, G. M., & Bailey, H. C. (1998). Effects of copper on immune system parameters of rainbow trout (Oncorhynchus mykiss). *Environmental Toxicology and Chemistry: An International Journal, 17*(9), 1807-1814.

Deutsch, C. A., Tewksbury, J. J., Huey, R. B., Sheldon, K. S., Ghalambor, C. K., Haak, D. C., & Martin, P. R. (2008). Impacts of climate warming on terrestrial ectotherms across latitude. *Proceedings of the National Academy of Sciences*, *105*(18), 6668-6672.

Dick PT, Dixon DG (1985) Changes in circulating blood cell levels of rainbow trout, *Salmo gairdneri* Richardson, following acute and chronic exposure to copper. J *Fish Biology* 26:475–481.

Dowell, S. F. (2001). Seasonal variation in host susceptibility and cycles of certain infectious diseases. *Emerging infectious diseases*, *7*(3), 369.

Downs, C. J., & Stewart, K. M. (2014). A primer in ecoimmunology and immunology for wildlife research and management. *California Fish Game*, *100*, 371-395.

Duellman, W.E. & Trueb, L. (1986) Biology of amphibians. McGraw-Hill, New York.

Du Pasquier, L., & Weiss, N. (1973). The thymus during the ontogeny of the toad Xenopus laevis: growth, membrane-bound immunoglobulins and mixed lymphocyte reaction. *European journal of immunology*, *3*(12), 773-777.

Easterling, D. R., Evans, J. L., Groisman, P. Y., Karl, T. R., Kunkel, K. E., & Ambenje, P. (2000). Observed variability and trends in extreme climate events: a brief review. *Bulletin of the American Meteorological Society*, *81*(3), 417-426.

Edgar, R. C. (2004). MUSCLE: multiple sequence alignment with high accuracy and high throughput. *Nucleic Acids Research*, *32*(5), 1792–7. https://doi.org/10.1093/nar/gkh340

Edge, C. B., Houlahan, J. E., Jackson, D. A., & Fortin, M. J. (2016). The response of amphibian larvae to environmental change is both consistent and variable. *Oikos*, *125*(12), 1700-1711.

Ellison, A. R., Savage, A. E., DiRenzo, G. V., Langhammer, P., Lips, K. R., & Zamudio, K. R. (2014). Fighting a losing battle: vigorous immune response countered by pathogen suppression of host defenses in the chytridiomycosis-susceptible frog *Atelopus zeteki*. *G3: Genes, Genomes, Genetics*, *4*(7), 1275-1289.

Etkin, W. (1964). Metamorphosis. Pages 427-467 in J. A. Moore, editor. Physiology of the Amphibia. Academic Press, New York, New York, USA.

Farrer, R. A., Weinert, L. A., Bielby, J., Garner, T. W., Balloux, F., Clare, F., Bosch, J., Cunningham, A.A., Weldon, C., du Preez, L.H. and Anderson, L. & Fisher, M. C. (2011). Multiple emergences of genetically diverse amphibian-infecting chytrids include a globalized hypervirulent recombinant lineage. *Proceedings of the National Academy of Sciences*, *108*(46), 18732-18736.

Fick, S. E., & Hijmans, R. J. (2017). WorldClim 2: new 1-km spatial resolution climate surfaces for global land areas. *International journal of climatology*, *37*(12), 4302-4315.

Fisher, M. C., Garner, T. W., & Walker, S. F. (2009). Global emergence of Batrachochytrium dendrobatidis and amphibian chytridiomycosis in space, time, and host. *Annual review of microbiology*, *63*, 291-310.

Fisher, M. C., & Garner, T. W. (2020). Chytrid fungi and global amphibian declines. *Nature Reviews Microbiology*, *18*(6), 332-343.

Fites, J. S., Ramsey, J. P., Holden, W. M., Collier, S. P., Sutherland, D. M., Reinert, L. K., Gayek, A.S., Dermody, T.S., Aune, T.M., Oswald-Richter, K. & Rollins-Smith, L. A. (2013). The invasive chytrid fungus of amphibians paralyzes lymphocyte

Fites, J. S., Reinert, L. K., Chappell, T. M., & Rollins-Smith, L. A. (2014). Inhibition of local immune responses by the frog-killing fungus *Batrachochytrium dendrobatidis*. *Infection and Immunity*, *82*(11), 4698.

Flucher, B. E., Lenglachner-Bachinger, C., Pohlhammer, K., Adam, H., & Mollay, C. (1986). Skin peptides in Xenopus laevis: morphological requirements for precursor processing in developing and regenerating granular skin glands. *The Journal of cell biology*, *103*(6), 2299-2309.

Foley, J., Clifford, D., Castle, K., Cryan, P., & Ostfeld, R. S. (2011). Investigating and managing the rapid emergence of white-nose syndrome, a novel, fatal, infectious disease of hibernating bats. *Conservation biology*, *25*(2), 223-231.

Freitas, J. S., Felício, A. A., Teresa, F. B., & de Almeida, E. A. (2017). Combined effects of temperature and clomazone (Gamit®) on oxidative stress responses and B-esterase

activity of *Physalaemus nattereri* (Leiuperidae) and *Rhinella schneideri* (Bufonidae) tadpoles. *Chemosphere*, *185*, 548-562.

Garrison, E., & Marth, G. (2012). Haplotype-based variant detection from short-read sequencing. *arXiv Preprint arXiv:1207.3907*.

Gervasi, S. S., & Foufopoulos, J. (2008). Costs of plasticity: responses to desiccation decrease post-metamorphic immune function in a pond-breeding amphibian. *Functional Ecology*, *22*(1), 100-108.

Gilbert, D. J., Magrath, M. J., & Byrne, P. G. (2020). Warmer temperature and provision of natural substrate enable earlier metamorphosis in the critically endangered Baw Baw frog. *Conservation Physiology*, *8*(1), coaa030.

Goessling, J. M., Guyer, C., & Mendonça, M. T. (2017). More than fever: thermoregulatory responses to immunological stimulation and consequences of thermoregulatory strategy on innate immunity in Gopher Tortoises (Gopherus polyphemus). *Physiological and Biochemical Zoology*, *90*(4), 484-493.

Goldstein, J. A., Hoff, K. V. S., & Hillyard, S. D. (2017). The effect of temperature on development and behaviour of relict leopard frog tadpoles. *Conservation Physiology*, *5*(1), cow075.

Gomez-Mestre, I., Kulkarni, S., & Buchholz, D. R. (2013). Mechanisms and consequences of developmental acceleration in tadpoles responding to pond drying. *PLoS One*, *8*(12), e84266.

Gosner, K. L. (1960). A simplified table for staging anuran embryos and larvae with notes on identification. *Herpetologica*, *16*(3), 183-190.

Greenspan, S. E., Calhoun, A. J., Longcore, J. E., & Levy, M. G. (2012). Transmission of Batrachochytrium dendrobatidis to wood frogs (Lithobates sylvaticus) via a bullfrog (L. catesbeianus) vector. *Journal of wildlife diseases*, *48*(3), 575-582.

Greenspan, S. E., Lambertini, C., Carvalho, T., James, T. Y., Toledo, L. F., Haddad, C. F. B., & Becker, C. G. (2018). Hybrids of amphibian chytrid show high virulence in native hosts. *Scientific reports*, *8*(1), 1-10.

Greenspan, S. E., Longcore, J. E., & Calhoun, A. J. (2012). Host invasion by Batrachochytrium dendrobatidis: fungal and epidermal ultrastructure in model anurans. *Diseases of aquatic organisms*, *100*(3), 201-210.

Griffiths, R. A. (1997). Temporary ponds as amphibian habitats. *Aquatic Conservation: Marine and freshwater ecosystems*, *7*(2), 119-126.

Groner, M. L., Buck, J. C., Gervasi, S., Blaustein, A. R., Reinert, L. K., Rollins-Smith, L. A., Bier, M.E., Hempel, J.& Relyea, R. A. (2013). Larval exposure to predator cues alters immune function and response to a fungal pathogen in post-metamorphic wood frogs. *Ecological Applications*, *23*(6), 1443-1454.

Gründler, M.C., Toledo, L.F., Parra-Olea, G., Haddad, C.F., Giasson, L.O., Sawaya, R.J., Prado, C.P., Araujo, O.G., Zara, F.J., Centeno, F.C. and Zamudio, K.R., (2012.) Interaction between breeding habitat and elevation affects prevalence but not infection intensity of

Batrachochytrium dendrobatidis in Brazilian anuran assemblages. *Diseases of aquatic organisms*, *97*(3), pp.173-184.

Gustin, E. S., & Richter, S. C. (2014). Use of Genetic Markers to Verify the Distribution of Northern Leopard Frogs (*Lithobates pipiens*) and Southern Leopard Frogs (*Lithobates sphenocephalus*) in Kentucky. *Journal of the Kentucky Academy of Science*, *74*(1), 10-16.

Gutiérrez-Pesquera, L. M., Tejedo, M., Olalla-Tárraga, M. Á., Duarte, H., Nicieza, A., & Solé, M. (2016). Testing the climate variability hypothesis in thermal tolerance limits of tropical and temperate tadpoles. *Journal of Biogeography*, *43*(6), 1166-1178.

Hadji-Azimi, I., Coosemans, V., Canicatti, C., & Perrenot, N. (1987). Atlas of adult *Xenopus laevis laevis* hematology. *Developmental and comparative immunology*, *11*(4), 807-874.

Hardie, L.J., Fletcher, T.C., Secombes C.J. (1994). Effect of tcmperature on macrophage activation and the production of macrophage activating factor by rainbow trout (Oncorhynchus mykiss) leucocytes. *Developmental and comparative immunology* 18: 57-66

Harkey, G. A., & Semlitsch, R. D. (1988). Effects of temperature on growth, development, and color polymorphism in the ornate chorus frog *Pseudacris ornata*. *Copeia*, 1001-1007.

Harris, R. N., Brucker, R. M., Walke, J. B., Becker, M. H., Schwantes, C. R., Flaherty, D. C., Lam, B.A., Woodhams, D.C., Briggs, C.J., Vredenburg, V.T. & Minbiole, K. P. (2009). Skin microbes on frogs prevent morbidity and mortality caused by a lethal skin fungus. *The ISME journal*, *3*(7), 818.

Harvell, C. D., Mitchell, C. E., Ward, J. R., Altizer, S., Dobson, A. P., Ostfeld, R. S., & Samuel, M. D. (2002). Climate warming and disease risks for terrestrial and marine biota. *Science*, *296*(5576), 2158-2162.

Hero, J. M., Williams, S. E., & Magnusson, W. E. (2005). Ecological traits of declining amphibians in upland areas of eastern Australia. *Journal of Zoology*, *267*(3), 221-232.

Hillis, D. M., & Wilcox, T. P. (2005). Phylogeny of the New World true frogs (*Rana*). *Molecular Phylogenetics and Evolution*, *34*(2), 299-314.

Holden, W. M., Reinert, L. K., Hanlon, S. M., Parris, M. J., & Rollins-Smith, L. A. (2015). Development of antimicrobial peptide defenses of southern leopard frogs, *Rana sphenocephala*, against the pathogenic chytrid fungus, *Batrachochytrium dendrobatidis*. *Developmental & Comparative Immunology*, *48*(1), 65-75.

Houghton, R. A. (2007). Balancing the global carbon budget. *Annual Review Earth Planet. Sci.*, *35*, 313-347.

Howe, R. W. (1967). Temperature effects on embryonic development in insects. *Annual review of entomology*, *12*(1), 15-42.

Hopey, M. E., & Petranka, J. W. (1994). Restriction of wood frogs to fish-free habitats: how important is adult choice?. *Copeia*, *1994*(4), 1023-1025.

Hyatt, A.D., D. G. Boyle, V. Olsen, D. B. Boyle, L. Berger, D. Obendorf, A. Dalton, K. Krriger, M. Hero, H. Hines, R. Philott, R. Campbell, G. Marantelli, F. Gleason, & A. Colling.

2007. Diagnostic assays and sampling protocols for the detection of *Batrachochytrium dendrobatidis*. *Diseases of Aquatic Organisms*. Org. 73:175–192.

Hyatt, A.D Houghton, R. A. (2007). Balancing the global carbon budget. *Annual Review Earth Planet. Sci., 35,* 313-347.

Howe, R. W. (1967). Temperature effects on embryonic development in insects. *Annual review of entomology*, *12*(1), 15-42.

IPCC, 2014: Climate Change 2014: Synthesis Report. Contribution of Working Groups I, II and III to the Fifth Assessment Report of the Intergovernmental Panel on Climate Change [Core Writing Team, R.K. Pachauri and L.A. Meyer (eds.)]. IPCC, Geneva, Switzerland, 151 pp.

James, T.Y., Toledo, L.F., Rödder, D., da Silva Leite, D., Belasen, A.M., Betancourt-Román, C.M., Jenkinson, T.S., Soto-Azat, C., Lambertini, C., Longo, A.V., Ruggeri, J., Collins, J.P., Burrowes, P.A., Lips, K.R., Zamudio, K.R.& Longcore, J. E. (2015). Disentangling host, pathogen, and environmental determinants of a recently emerged wildlife disease: lessons from the first 15 years of amphibian chytridiomycosis research. *Ecology and evolution*, *5*(18), pp.4079-4097.

Jenkinson, Thomas S., David Rodriguez, Rebecca A. Clemons, Lucas A. Michelotti, Kelly R. Zamudio, L. Felipe Toledo, Joyce E. Longcore, and Timothy Y. James. (2018)."Globally invasive genotypes of the amphibian chytrid outcompete an enzootic lineage in coinfections." *Proceedings of the Royal Society B* 285, no. 1893 (2018): 20181894.

Johnson, M., Berger, L., Phillips, L. & Speare, R. (2003) Fungicidal effects of chemical disinfectants, UV light, desiccation and heat on the amphibian chytrid, Batrachochytrium dendrobatidis. Diseases of Aquatic Organisms, 57, 255–260.

Johnson, P. T., & Paull, S. H. (2011). The ecology and emergence of diseases in fresh waters. *Freshwater Biology*, *56*(4), 638-657.

Johnson, P. T., Rohr, J. R., Hoverman, J. T., Kellermanns, E., Bowerman, J., & Lunde, K. B. (2012). Living fast and dying of infection: host life history drives interspecific variation in infection and disease risk. *Ecology letters*, *15*(3), 235-242.

Johnson, M. & Speare, R. (2003) Survival of Batrachochytrium dendrobatidis in water: quarantine and control implications. *Emerging Infectious Diseases*, 9, 922–925.

Jombart, T. (2008). adegenet: a R package for the multivariate analysis of genetic markers. *Bioinformatics*, *24*(11), 1403–1405.

Jurd, R. D. (1994). "Not proper mammals": Immunity in monotremes and marsupials. *Comparative immunology, microbiology and infectious diseases*, *17*(1), 41-52.

Kanakambika, P., & Muthukkaruppan, V. R. (1972). Effect of splenectomy on the immune response in the lizard, Calotes versicolor. *Experientia*, *28*(10), 1225-1226.

Kearney, M. R., & Porter, W. P. (2017). NicheMapR–an R package for biophysical modelling: the microclimate model. *Ecography*, *40*(5), 664-674.

Kearney, M. R., Shamakhy, A., Tingley, R., Karoly, D. J., Hoffmann, A. A., Briggs, P. R., & Porter, W. P. (2014). Microclimate modelling at macro scales: a test of a general microclimate model integrated with gridded continental-scale soil and weather data. *Methods in Ecology and Evolution*, *5*(3), 273-286.

Kearse, M., Moir, R., Wilson, A., Stones-Havas, S., Cheung, M., Sturrock, S., … Drummond, A. (2012). Geneious Basic: An integrated and extendable desktop software platform for the organization and analysis of sequence data. *Bioinformatics* , *28*(12), 1647–1649. https://doi.org/10.1093/bioinformatics/bts199.

Kelly, C. D., Tawes, B. R., & Worthington, A. M. (2014). Evaluating indices of body condition in two cricket species. *Ecology and Evolution*, *4*(23), 4476-4487.

Kendell, K. (2002). *Survey protocol for the northern leopard frog*. Fish & Wildlife Division, Resource Status and Assessment Branch, Alberta Sustainable Resource Development.

Kiesecker, J. M., & Skelly, D. K. (2001). Effects of disease and pond drying on gray tree frog growth, development, and survival. *Ecology*, *82*(7), 1956-1963.

Kikuyama, S., Kawamura, K., Tanaka, S., & Yamamoto, K. (1993). Aspects of amphibian metamorphosis: hormonal control. *International review of cytology*, *145*, 105-148.

Kinney VC, Heemeyer JL, Pessier AP, Lannoo MJ (2011) Seasonal pattern of Batrachochytrium dendrobatidis infection and mortality in Lithobates areolatus:affirmation of Vredenburg's '10,000 Zoospore Rule.'. *PLoS ONE* 6: e16708.

Knapp, R. A., Fellers, G. M., Kleeman, P. M., Miller, D. A., Vredenburg, V. T., Rosenblum, E. B., & Briggs, C. J. (2016). Large-scale recovery of an endangered amphibian despite ongoing exposure to multiple stressors. *Proceedings of the National Academy of Sciences*, *113*(42), 11889-11894.

Kriger, K. M., & Hero, J. M. (2007). The chytrid fungus Batrachochytrium dendrobatidis is non-randomly distributed across amphibian breeding habitats. *Diversity and Distributions*, *13*(6), 781-788.

Kirk, J. T. O. (1984). Dependence of relationship betIen inherent and apparent optical properties of water on solar altitude. *Limnology and Oceanography*, *29*(2), 350-356.

Koprivnikar, J., Paull, S. H., & Johnson, P. T. (2014). Combined influence of hydroperiod and parasitism on larval amphibian development. *Freshwater Science*, *33*(3), 941-949.

Kruger, A. (2020). Frog skin microbiota vary with host species and environment but not chytrid infection. *Frontiers in microbiology*, *11*, 1330.

Kriger, K. M., Pereoglou, F., & HERO, J. M. (2007). Latitudinal variation in the prevalence and intensity of chytrid (*Batrachochytrium dendrobatidis*) infection in eastern Australia. *Conservation Biology*, *21*(5), 1280-1290.

Lacoursière-Roussel, A., Rosabal, M., & Bernatchez, L. (2016). Estimating fish abundance and biomass from eDNA concentrations: variability among capture methods and environmental conditions. *Molecular Ecology Resources*, *16*(6), 1401-1414.

Langwig, K. E., Frick, W. F., Reynolds, R., Parise, K. L., Drees, K. P., Hoyt, J. R., Cheng, T.L., Kunz, T.H., Foster, J.T. & Kilpatrick, A. M. (2015). Host and pathogen ecology drive the seasonal dynamics of a fungal disease, white-nose syndrome. *Proceedings of the Royal Society B: Biological Sciences*, *282*(1799), 20142335.

Lannoo, M. J., Petersen, C., Lovich, R. E., Nanjappa, P., Phillips, C., Mitchell, J. C., & Macallister, I. (2011). Do frogs get their kicks on Route 66? Continental US transect reveals spatial and temporal patterns of Batrachochytrium dendrobatidis infection. *PLoS One*, *6*(7), e22211.

Layne JR, Kefauver J (1997) Freeze tolerance and postfreeze recovery in the frog *Pseudacris crucifer*. Copeia 1997:260–264.

Li, H., & Durbin, R. (2009). Fast and accurate short read alignment with Burrows–Wheeler transform. *Bioinformatics*, *25*(14), 1754–1760. https://doi.org/10.1093/bioinformatics/btp324.

Liao, W., Atkinson, C. T., LaPointe, D. A., & Samuel, M. D. (2017). Mitigating future avian malaria threats to Hawaiian forest birds from climate change. *PloS one*, *12*(1), e0168880.

Liew, N., Moya, M.J.M., Wierzbicki, C.J., Hollinshead, M., Dillon, M.J., Thornton, C.R., Ellison, A., Cable, J., Fisher, M.C. and Mostowy, S., (2017). Chytrid fungus infection in zebrafish demonstrates that the pathogen can parasitize non-amphibian vertebrate hosts. *Nature Communications*, *8*(1), pp.1-10.

Lips, K.R. (1998) Decline of a tropical montane amphibian fauna. Conservation Biology, 12, 106–117.

Lochmiller, R. L., & Deerenberg, C. (2000). Trade-offs in evolutionary immunology: just what is the cost of immunity? *Oikos, 88*(1), 87-98.

Lock, A. R. and I. A. McLaren. (1970). The effect of varying and constant temperature on the size of a marine copepod. *Limnology and Oceanography*, *15*(4), 638-640.

Loman, J., & Claesson, D. (2003). Plastic response to pond drying in tadpoles *Rana temporaria*: tests of cost models. *Evolutionary Ecology Research*, *5*(2), 179-194.

Longcore, J. E., Pessier, A. P., & Nichols, D. K. (1999). *Batrachochytrium dendrobatidis* gen. et sp. nov., a chytrid pathogenic to amphibians. *Mycologia*, *91*(2), 219-227.

Maniero, G. D., & Carey, C. (1997). Changes in selected aspects of immune function in the leopard frog, *Rana pipiens*, associated with exposure to cold. *Journal of Comparative Physiology B, 167*(4), 256-263.

Martel, A., Spitzen-van der Sluijs, A., Blooi, M., Bert, W., Ducatelle, R., Fisher, M. C., Woeltjes, A., Bosman, W., Chiers, K., Bossuyt, F. & Pasmans, F. (2013). *Batrachochytrium salamandrivorans* sp. nov. causes lethal chytridiomycosis in amphibians. *Proceedings of the National Academy of Sciences*, *110*(38), 15325-15329.

Martin, L. B., Hopkins, W. A., Mydlarz, L. D., & Rohr, J. R. (2010). The effects of anthropogenic global changes on immune functions and disease resistance. *Annals of the New York Academy of Sciences, 1195*(1), 129.

Matutte, B., Storey, K. B., Knoop, F. C., & Conlon, J. M. (2000). Induction of synthesis of an antimicrobial peptide in the skin of the freeze-tolerant frog, *Rana sylvatica*, in response to environmental stimuli. *FEBS letters*, *483*(2-3), 135-138.

McArthur, J. V. (2006). Microbial ecology: an evolutionary approach. *Elsevier*.

McDiarmid, R.W. & Altig, R. (1999) Tadpoles: the biology of anuran larvae. University of Chicago Press, Chicago, IL.

McDonald, K., & Alford, R. A. (1999). A review of declining frogs in northern Queensland. *Declines and Disappearances of Australian Frogs, Canberra*, 14-22.

McMahon, T. A., Romansic, J. M., & Rohr, J. R. (2013). Nonmonotonic and monotonic effects of pesticides on the pathogenic fungus B*atrachochytrium dendrobatidis* in culture and on tadpoles. *Environmental science & technology*, *47*(14), 7958-7964.

Moore, M. P., & Martin, R. A. (2019). On the evolution of carry-over effects. *Journal of Animal Ecology*, *88*(12), 1832-1844.

Morey, S., & Reznick, D. (2001). Effects of larval density on postmetamorphic spadefoot toads (Spea hammondii). *Ecology*, *82*(2), 510-522.

Narayana, J. L., & Chen, J. Y. (2015). Antimicrobial peptides: possible anti-infective agents. *Peptides*, *72*, 88-94.

Narayan, E. J., Graham, C., McCallum, H., & Hero, J. M. (2014). Over-wintering tadpoles of Mixophyes fasciolatus act as reservoir host for *Batrachochytrium dendrobatidis*. *PLoS One*, *9*(3), e92499.

Neill, W. T. (1948). Hibernation of amphibians and reptiles in Richmond County, Georgia. *Herpetologica*, *4*(3), 107-114.

Newman, R. A. (1992). Adaptive plasticity in amphibian metamorphosis. *BioScience*, *42*(9), 671-678.

Nichols, D.K., Lamirande, E.W., Pessier, A.P. & Longcore, J.E. (2001) Experimental transmission of cutaneous chytridiomycosis in dendrobatid frogs. *Journal of Wildlife Diseases*, 37, 1–11.

Nichols, D.K., Pessier, A.P. & Longcore, J.E. (1998) Cutaneous chytridiomycosis: an emerging disease? *Proceedings of the American Association of Zoo Veterinarians*, 1998, 269–271.

Nicolas, P., & Mor, A. (1995). Peptides as weapons against microorganisms in the chemical defense system of vertebrates. *Annual review of microbiology*, *49*(1), 277-304.

Noland, R. & Ultsch, G. R. (1981). The Roles of Temperature and Dissolved Oxygen in Microhabitat Selection by the Tadpoles of a Frog (*Rana pipiens*) and a Toad (*Bufo terrestris*). *Copeia* 3, 645–652.

Norris, K., & Evans, M. R. (2000). Ecological immunology: life history trade-offs and immune defense in birds. *Behavioral Ecology*, *11*(1), 19-26.

Nussey, G., Vanvuren, J.H.J. & Dupreez, H.H. (1995) Effect of copper on the differential white blood cell counts of the Mozambique tilapia (*Oreochromis mossambicus*). Comparative Biochemistry and Physiology C, 111, 381–388.

O’Connor, C. M., Norris, D. R., Crossin, G. T., & Cooke, S. J. (2014). Biological carryover effects: Linking common concepts and mechanisms in ecology and evolution. Ecosphere, 5, 28.

O’hanlon, S. J., Rieux, A., Farrer, R. A., Rosa, G. M., Waldman, B., Bataille, A., Kosch, T.A., Murray, K.A., Brankovics, B., Fumagalli, M. Martin, M.D., Wales N, Alvarado-Rybak M, Bates KA, Berger L, Böll S, Brookes L, Clare F, Courtois EA, Cunningham AA, Doherty-Bone TM, Ghosh P, Gower DJ, Hintz WE, Höglund J, Jenkinson TS, Lin CF, Laurila A, Loyau A, Martel A, Meurling S, Miaud C, Minting P, Pasmans F, Schmeller DS, Schmidt BR, Shelton JMG, Skerratt LF, Smith F, Soto-Azat C, Spagnoletti M, Tessa G, Toledo LF, Valenzuela-Sánchez A, Verster R, Vörös J, Webb RJ, Wierzbicki C, Wombwell E, Zamudio KR, Aanensen DM, James TY, Gilbert MTP, Weldon C, Bosch J, Balloux F, Garner TWJ, & Fisher, M. C. (2018). Recent Asian origin of chytrid fungi causing global amphibian declines. *Science*, *360*(6389), 621-627.

Oksanen, J., Blanchet, F. G., Kindt, R., Legendre, P., Minchin, P. R., O’hara, R. B., Simpson, G.L., Solymos, P., Stevens, M.H.H. & Wagner, H. (2013). Vegan: community ecology package version 2.0-2. *R package*.

O'Regan, S. M., Palen, W. J., & Anderson, S. C. (2014). Climate warming mediates negative impacts of rapid pond drying for three amphibian species. *Ecology*, *95*(4), 845-855.

Padgett-Flohr, G. E., & Hopkins II, R. L. (2009). Batrachochytrium dendrobatidis, a novel pathogen approaching endemism in central California. *Diseases of Aquatic Organisms*, *83*(1), 1-9.

Peig, J., & Green, A. J. (2009). New perspectives for estimating body condition from mass/length data: the scaled mass index as an alternative method. *Oikos*, *118*(12), 1883-1891.

Phillott, A. D., Grogan, L. F., Cashins, S. D., McDonald, K. R., Berger, L. E. E., & Skerratt, L. F. (2013). Chytridiomycosis and seasonal mortality of tropical stream-associated frogs 15 years after introduction of *Batrachochytrium dendrobatidis*. *Conservation Biology*, *27*(5), 1058-1068.

Phillott, A. D., Speare, R., Hines, H. B., Skerratt, L. F., Meyer, E., McDonald, K. R., ... & Berger, L. (2010). Minimising exposure of amphibians to pathogens during field studies. *Diseases of Aquatic Organisms*, *92*(2-3), 175-185.

Peterson, D. F., & Keller, A. A. (1990). Effects of climate change on US irrigation. *Journal of irrigation and Drainage Engineering*, *116*(2), 194-210.

Peterson, J. D., Wood, M. B., Hopkins, W. A., Unrine, J. M., & Mendonça, M. T. (2007). Prevalence of Batrachochytrium dendrobatidis in American bullfrog and southern leopard frog larvae from wetlands on the Savannah River site, South Carolina. *Journal of Wildlife Diseases*, *43*(3), 450-460.

Pigliucci, M., C. J. Murren, & C. D. Schlichting. 2006. Phenotypic plasticity and evolution by genetic assimilation. J. Exp. Biol. 209:2362– 2367.

Pinheiro, J., Bates, D., DebRoy, S., Sarkar, D., Heisterkamp, S., Van Willigen, B., & Maintainer, R. (2017). Package 'nlme'. *Linear and nonlinear mixed effects models*, *version*, *3*(1).

Piotrowski, J. S., Annis, S. L., & Longcore, J. E. (2004). Physiology of Batrachochytrium dendrobatidis, a chytrid pathogen of amphibians. *Mycologia*, *96*(1), 9-15.

Peterson, D. F., & Keller, A. A. (1990). Effects of climate change on US irrigation. *Journal of irrigation and Drainage Engineering*, *116*(2), 194-210.

Petranka, JW (1998) Salamanders of the United States and Canada. Smithsonian Institution Press, Washington DC, 597.

R Core Team (2019). R: A language and environment for statistical computing. R Foundation for Statistical Computing, Vienna, Austria. URL http://www.R-project.org/

R Core Team (2020). R: A language and environment for statistical computing. R Foundation for Statistical Computing, Vienna, Austria. URL https://www.R-project.org.

Rachowicz, L. J., & V. T. Vredenburg. 2004. Transmission of *Batrachochytrium dendrobatidis* within and between amphibian life stages. *Diseases of Aquatic Organisms* 61:75–83.

Rachowicz, L.J., Knapp, R.A., Morgan, J.A.T., Stice, M.J., Vredenburg, V.T., Parker, J.M. & Briggs, C.J. (2006) Emerging infectious disease as a proximate cause of amphibian mass mortality. *Ecology*, 87, 1671–1683.

Raffel, T. R., Michel, P. J., Sites, E. W., & Rohr, J. R. (2010). What drives chytrid infections in newt populations? Associations with substrate, temperature, and shade. *EcoHealth*, *7*(4), 526-536.

Raffel, T. R., Rohr, J. R., Kiesecker, J. M., & Hudson, P. J. (2006). Negative effects of changing temperature on amphibian immunity under field conditions. *Functional Ecology*, *20*(5), 819-828.

Raffel, T. R., Romansic, J. M., Halstead, N. T., McMahon, T. A., Venesky, M. D., & Rohr, J. R. (2013). Disease and thermal acclimation in a more variable and unpredictable climate. *Nature Climate Change*, *3*(2), 146-151.

Ramsey, J. P., Reinert, L. K., Harper, L. K., Woodhams, D. C., & Rollins-Smith, L. A. (2010). Immune defenses against Batrachochytrium dendrobatidis, a fungus linked to global amphibian declines, in the South African clawed frog, *Xenopus laevis*. *Infection and immunity*, *78*(9), 3981-3992.

Reading, C. J., & Clarke, R. T. (1999). Impacts of climate and density on the duration of the tadpole stage of the common toad *Bufo bufo*. *Oecologia*, *121*(3), 310-315.

Regosin, J. V., Windmiller, B. S., & Reed, J. M. (2003). Terrestrial habitat use and winter densities of the wood frog (*Rana sylvatica*). *Journal of Herpetology*, *37*(2), 390-394.

Relyea, R. A., & Hoverman, J. T. (2003). The impact of larval predators and competitors on the morphology and fitness of juvenile treefrogs. *Oecologia*, *134*(4), 596-604.

Reques, R., & Tejedo, M. (1997). Reaction norms for metamorphic traits in natterjack toads to larval density and pond duration. *Journal of Evolutionary Biology*, *10*(6), 829-851.

Retallick, R. W., McCallum, H., & Speare, R. (2004). Endemic infection of the amphibian chytrid fungus in a frog community post-decline. *PLoS Biol*, *2*(11), e351.

Retallick, R. W., Miera, V., Richards, K. L., Field, K. J., & Collins, J. P. (2006). A non-lethal technique for detecting the chytrid fungus Batrachochytrium dendrobatidis on tadpoles. *Diseases of Aquatic Organisms*, *72*(1), 77-85.

Riha, V. F., & Berven, K. A. (1991). An analysis of latitudinal variation in the larval development of the wood frog (*Rana sylvatica*). *Copeia*, 209-221.

Robak, M. J. (2016). *Effects of Temperature on Amphibian Resistance and Susceptibility to Chytridiomycosis* (Doctoral dissertation, Tulane University School of Science and Engineering).

Robak, M. J., Reinert, L. K., Rollins-Smith, L. A., & Richards-Zawacki, C. L. (2019). Out in the cold and sick: Low temperatures and fungal infections impair a frog's skin defenses. *Journal of Experimental Biology*, *222*(18), jeb209445.

Robak, M. J., & Richards-Zawacki, C. L. (2018). Temperature-dependent effects of cutaneous bacteria on a frog's tolerance of fungal infection. *Frontiers in microbiology*, *9*, 410.

Roff, D.A. (1992) The Evolution of Life Histories: Theory and Analysis. Chapman & Hall, New York.

Rohr, J. R., & Raffel, T. R. (2010). Linking global climate and temperature variability to widespread amphibian declines putatively caused by disease. *Proceedings of the National Academy of Sciences*, *107*(18), 8269-8274.

Rohr, J. R., Raffel, T. R., & Sessions, S. K. (2009). Digenetic trematodes and their relationship to amphibian declines and deformities. *Amphibian biology*, *8*, 3067-3088.

Rollins-Smith, L. A. (1998). Metamorphosis and the amphibian immune system. *Immunological reviews*, *166*(1), 221-230.

Rollins-Smith, L. A. (2009). The role of amphibian antimicrobial peptides in protection of amphibians from pathogens linked to global amphibian declines. *Biochimica et Biophysica Acta (BBA)-Biomembranes*, *1788*(8), 1593-1599.

Rollins-Smith, L. A. (2020). Global amphibian declines, disease, and the ongoing battle between Batrachochytrium fungi and the immune system. *Herpetologica*, *76*(2), 178-188.

Rollins-Smith, L. A., & Conlon, J. M. (2005). Antimicrobial peptide defenses against chytridiomycosis, an emerging infectious disease of amphibian populations. *Developmental & Comparative Immunology*, *29*(7), 589-598.

Rollins-Smith, L. A., Doersam, J. K., Longcore, J. E., Taylor, S. K., Shamblin, J. C., Carey, C., & Zasloff, M. A. (2002). Antimicrobial peptide defenses against pathogens associated with global amphibian declines. *Developmental & Comparative Immunology*, *26*(1), 63-72.

Rollins-Smith, L. A., Parsons, S. C., & Cohen, N. (1984). During frog ontogeny, PHA and Con A responsiveness of splenocytes precedes that of thymocytes. *Immunology*, *52*(3), 491.

Rollins-Smith, L. A., & Woodhams, D. C. (2012). Amphibian immunity (pp. 92-143). New York: Oxford University Press.

Rollins-Smith, L. A., Woodhams, D. C., Reinert, L. K., Vredenburg, V. T., Briggs, C. J., Nielsen, P. F., & Conlon, J. M. (2006). Antimicrobial peptide defenses of the mountain

yellow-legged frog (*Rana muscosa*). *Developmental & Comparative Immunology*, *30*(9), 831-842.

Rosenblum, E. B., James, T. Y., Zamudio, K. R., Poorten, T. J., Ilut, D., Rodriguez, D., Eastman, J.M., Richards-Hrdlicka, K., Joneson, S., Jenkinson, T.S. and Longcore, J.E. Stajich, J. E. (2013). Complex history of the amphibian-killing chytrid fungus revealed with genome resequencing data. *Proceedings of the National Academy of Sciences of the USA*, *110*(23), 9385–90. https://doi.org/10.1073/pnas.1300130110.

Rowe, L., & Ludwig, D. (1991). Size and timing of metamorphosis in complex life cycles: time constraints and variation. *Ecology*, *72*(2), 413-427.

Ruggeri, J., Toledo, L. F., & de Carvalho-e-Silva, S. P. (2018). Stream tadpoles present high prevalence but low infection loads of *Batrachochytrium dendrobatidis* (Chytridiomycota). *Hydrobiologia*, *806*(1), 303-311.

Russell, D. M., Goldberg, C. S., Waits, L. P., & Rosenblum, E. B. (2010). Batrachochytrium dendrobatidis infection dynamics in the Columbia spotted frog *Rana luteiventris* in north Idaho, USA. *Diseases of Aquatic Organisms*, *92*(2-3), 223-230.

Ruthsatz, K., Peck, M. A., Dausmann, K. H., Sabatino, N. M., & Glos, J. (2018). Patterns of temperature induced developmental plasticity in anuran larvae. *Journal of thermal biology*, *74*, 123-132.

Sapolsky, R. M., Romero, L. M., & Munck, A. U. (2000). How do glucocorticoids influence stress responses? Integrating permissive, suppressive, stimulatory, and preparative actions. *Endocrine reviews*, *21*(1), 55-89.

Sauer, E. L., Cohen, J. M., Lajeunesse, M. J., McMahon, T. A., Civitello, D. J., Knutie, S. A., S.A., Nguyen, K., Roznik, E.A., Sears, B.F., Bessler, S. and Delius, B.K. & Rohr, J. R. (2020). A meta-analysis reveals temperature, dose, life stage, and taxonomy influence host susceptibility to a fungal parasite. *Ecology*, *101*(4), e02979.

Schindler, D. W., Bayley, S. E., Parker, B. R., Beaty, K. G., Cruikshank, D. R., Fee, E. J., Schindler, E.U. & Stainton, M. P. (1996). The effects of climatic warming on the properties of boreal lakes and streams at the Experimental Lakes Area, northwestern Ontario. *Limnology and Oceanography*, *41*(5), 1004-1017.

Scheele, B. C., Pasmans, F., Skerratt, L. F., Berger, L., Martel, A. N., Beukema, W. & De la Riva, I. (2019). Amphibian fungal panzootic causes catastrophic and ongoing loss of biodiversity. *Science*, *363*(6434), 1459-1463.

Shannon, C. E. (1948). A mathematical theory of communication. *The Bell system technical journal*, *27*(3), 379-423.

Schloegel, L. M., Hero, J. M., Berger, L., Speare, R., McDonald, K., & Daszak, P. (2006). The decline of the sharp-snouted day frog (*Taudactylus acutirostris*): the first documented case of extinction by infection in a free-ranging wildlife species? *EcoHealth*, *3*(1), 35-40.

Schloegel, L.M., Lisa M., Luis Felipe Toledo, Joyce E. Longcore, Sasha E. Greenspan, Conrado Augusto Vieira, Maria Lee, Serena Zhao, S., Wangen, C., Ferreira, C.M., Hipolito, M., Davies, A.J. Cuomo, C.A., Daszak, P. & James, T. Y. (2012). "Novel, panzootic and hybrid genotypes of amphibian chytridiomycosis associated with the bullfrog trade." *Molecular ecology* 21, no. 21 (2012): 5162-5177.

Schmid-Hempel, P. (2005). Evolutionary ecology of insect immune defenses. *Annual Review of. Entomology*, *50*, 529-551.

Simpkins, C. A., Kriger, K. M., & Hero, J. M. (2017). Prevalence of *Batrachochytrium dendrobatidis* on amphibians from low pH, oligotrophic waterbodies. *Herpetological Review*, *48*(4), 775-776.

Stebbins, R. C. (2003). *Western Reptiles and Amphibians, Third Edition.* Houghton Mifflin, Boston.

Stebbins RC, Cohen NW (1995) A Natural History of Amphibians. Princeton University Press, New Jersey.

Stevenson, L. A., Alford, R. A., Bell, S. C., Roznik, E. A., Berger, L., & Pike, D. A. (2013). Variation in thermal performance of a widespread pathogen, the amphibian chytrid fungus *Batrachochytrium dendrobatidis*. *PloS one*, *8*(9), e73830.

Storey, K. B., & Storey, J. M. (1984). Biochemical adaption for freezing tolerance in the wood frog, *Rana sylvatica*. *Journal of Comparative Physiology B*, *155*(1), 29-36.

Streicker, D. G., Lemey, P., Velasco-Villa, A., & Rupprecht, C. E. (2012). Rates of viral evolution are linked to host geography in bat rabies. *PLoS Pathogens*, *8*(5), e1002720.

Talley, B. L., Muletz, C. R., Vredenburg, V. T., Fleischer, R. C., & Lips, K. R. (2015). A century of Batrachochytrium dendrobatidis in Illinois amphibians (1888–1989). *Biological Conservation*, *182*, 254-261.

Tejedo, M., Marangoni, F., Pertoldi, C., Richter-Boix, A., Laurila, A., Orizaola, G., Nicieza, A.G., Álvarez, D. & Gomez-Mestre, I., (2010). Contrasting effects of environmental factors during larval stage on morphological plasticity in post-metamorphic frogs. *Climate research*, *43*(1-2), pp.31-39.

Tennessen, J. A., Woodhams, D. C., Chaurand, P., Reinert, L. K., Billheimer, D., Shyr, Y., Caprioli, R.M., Blouin, M.S. & Rollins-Smith, L. A. (2009). Variations in the expressed antimicrobial peptide repertoire of northern leopard frog (*Rana pipiens*) populations suggest intraspecies differences in resistance to pathogens. *Developmental & Comparative Immunology*, *33*(12), 1247-1257.

Turner, A. M., & Chislock, M. F. (2007). Dragonfly predators influence biomass and density of pond snails. *Oecologia*, *153*(2), 407-415.

Uhlenhuth, E. (1919). Relation between thyroid gland, metamorphosis, and growth. *The Journal of general physiology*, *1*(4), 473-482.

Van Buskirk, J. V., & Saxer, G. (2001). Delayed costs of an induced defense in tadpoles? Morphology, hopping, and development rate at metamorphosis. *Evolution*, *55*(4), 821-829.

Van Leeuwen, C. (2010). Terroir: the effect of the physical environment on vine growth, grape ripening and wine sensory attributes. In *Managing wine quality* (pp. 273-315). Woodhead Publishing.

Van Rooij, P., Pasmans, F., Coen, Y., & Martel, A. (2017). Efficacy of chemical disinfectants for the containment of the salamander chytrid fungus *Batrachochytrium salamandrivorans*. *PLoS One*, *12*(10), e0186269.

Voyles, J., Johnson, L. R., Briggs, C. J., Cashins, S. D., Alford, R. A., Berger, L, Skerratt, L.F, Speare, R. Rosenblum, E.B..(2012) . Temperature alters reproductive life history patterns in Batrachochytrium dendrobatidis, a lethal pathogen associated with the global loss of amphibians." *Ecology and evolution* 2, no. 9 (2012): 2241-2249.

Voyles, J., Woodhams, D. C., Saenz, V., Byrne, A. Q., Perez, R., Rios-Sotelo, G., G., Ryan, M.J., Bletz, M.C., Sobell, F.A., McLetchie, S. Reinert, L. & Richards-Zawacki C. L. (2018). Shifts in disease dynamics in a tropical amphibian assemblage are not due to pathogen attenuation. *Science*, *359*(6383), 1517-1519.

Voyles, J., Young, S., Berger, L., Campbell, C., Voyles, W. F., Dinudom, A., Cook, D., Webb, R., Alford, R.A., Skerratt, L.F. & Speare, R. (2009). Pathogenesis of chytridiomycosis, a cause of catastrophic amphibian declines. *Science*, *326*(5952), 582-585.

vS Hoff, K., Blaustein, A. R., McDiarmid, R. W., & Altig, R. (1999). Behavior: interactions and their consequences.

Willis, Y. L., Moyle, D. L., & Baskett, T. S. (1956). Emergence, breeding, hibernation, movements and transformation of the bullfrog, *Rana catesbeiana*, in Missouri. *Copeia*, *1956*(1), 30-41.

Wellborn, G. A., D. K. Skelly & E. E. Werner (1996). Mechanisms creating community structure across a freshwater habitat gradient. *Annual Review of Ecology and Systematics* 27: 337–363.

Wickham, H. (2009) ggplot2: elegant graphics for data analysis. Springer New York.

Wilk, J., & Hughes, D. A. (2002). Simulating the impacts of land-use and climate change on water resource availability for a large south Indian catchment. *Hydrological Sciences Journal*, *47*(1), 19-30.

Woodhams, D.C. & Alford, R.A. (2005) Ecology of chytridiomycosis in rainforest stream frog assemblages of tropical Queensland. *Conservation Biology*, 19, 1449–1459.

Woodhams, D.C., R.A. Alford, C.J. Briggs, M. Johnson, and L.A. RollinsSmith. (2008). Life-history trade-offs influence disease in changing climates: strategies of am amphibian pathogen. *Ecology* 89:1627–1639.

Woodhams, D. C., Bell, S. C., Bigler, L., Caprioli, R. M., Chaurand, P., Lam, B. A., Reinert, L.K., Stalder, U., Vazquez, V.M., Schliep, K., Hertz, A. & Rollins-Smith, L. A. (2016). Life history linked to immune investment in developing amphibians. *Conservation physiology*, *4*(1), cow025.

Woodhams, D. C., Brandt, H., Baumgartner, S., Kielgast, J., Küpfer, E., Tobler, U., Davis, L.R., Schmidt, B.R., Bel, C., Hodel, S., Knight, R. & McKenzie, V. (2014). Interacting symbionts and immunity in the amphibian skin mucosome predict disease risk and probiotic effectiveness. *PLoS One*, *9*(4), e96375.

Woodhams, D. C., Kenyon, N., Bell, S. C., Alford, R. A., Chen, S., Billheimer, D., D., Shyr, Y. & Rollins-Smith, L. A. (2010). Adaptations of skin peptide defenses and possible response to the amphibian chytrid fungus in populations of Australian green-eyed treefrogs, *Litoria genimaculata*. *Diversity and Distributions*, *16*(4), 703-712.

Woodhams, D. C., Rollins-Smith, L. A., Carey, C., Reinert, L., Tyler, M. J., & Alford, R. A. (2006). Population trends associated with skin peptide defenses against chytridiomycosis in Australian frogs. *Oecologia*, *146*(4), 531-540.

Woodhams, D.C., Rollins-Smith, L.A., Reinert, L.K., Lam, B.A., Harris, R.N., Briggs, C.J., Vredenburg, V.T., Patel, B.T., Caprioli, R.M., Chaurand, P. & Hunziker, P. (2020). Probiotics modulate a novel amphibian skin defense peptide that is antifungal and facilitates growth of antifungal bacteria. *Microbial ecology*, *79*(1), pp.192-202.

Woodhams, D. C., Voyles, J., Lips, K. R., Carey, C., & Rollins-Smith, L. A. (2006). Predicted disease susceptibility in a Panamanian amphibian assemblage based on skin peptide defenses. *Journal of Wildlife Diseases*, *42*(2), 207-218.

Wright, A. H., and A. A. Wright. (1949). Handbook of frogs and toads of the United States and Canada. Ithaca, New York: Comstock Publishing Associates, Cornell University Press.

Xie, G. Y., Olson, D. H., & Blaustein, A. R. (2016). Projecting the global distribution of the emerging amphibian fungal pathogen, *Batrachochytrium dendrobatidis*, based on IPCC climate futures. *PLOS one*, *11*(8), e0160746.

Yeh, S. W., Kug, J. S., Dewitte, B., Kwon, M. H., Kirtman, B. P., & Jin, F. F. (2009). El Niño in a changing climate. *Nature*, *461*(7263), 511-514.

Zapata, A., Leceta, J., & Villena, A. (1981). Reptilian bone marrow. An ultrastructural study in the Spanish lizard, *Lacerta hispanica*. *Journal of morphology*, *168*(2), 137-149.

Zhang, C., Rabiee, M., Sayyari, E., & Mirarab, S. (2018). ASTRAL-III: polynomial time species tree reconstruction from partially resolved gene trees. *BMC Bioinformatics*, *19*(6), 153. https://doi.org/10.1186/s12859-018-2129-y

Zhang, P., Zhang, J., & Chen, M. (2017). Economic impacts of climate change on agriculture: The importance of additional climatic variables other than temperature and precipitation. *Journal of Environmental Economics and Management*, *83*, 8-31.